

GEOLOGICAL REPORT
ON
RECONNAISSANCE SURVEY (G4) FOR GLAUCONITE AND ASSOCIATED
MINERALIZATION IN DHAMINI - PIPARWASI SIMLIYA AREA, SHEOPUR
DISTRICT,
MADHYA PRADESH

PREPARED FOR
NATIONAL MINERAL EXPLORATION AND DEVELOPMENT TRUST
MINISTRY OF MINES,
ROOM No. 325 & 326, WING-F, UDYOG BHAWAN, RAFI AHMED KIDWAI MARG,
RAJPATH AREA, CENTRAL SECRETARIAT
NEW DELHI-110011

MARCH -2026

| | |
|------------------------|------------------|
| PREPARED BY | |
| DR. SUNIL KUMAR PANDAY | SENIOR GEOLOGIST |
| AKHAND PRATAP SINGH | GEOLOGIST |
| SHRAVYA MEHTA | GEOLOGIST |



MMPL PRIVATE LIMITED
(FORMERLY MAHESHWARI MINING PVT. LTD.) FR 07 SHILPANGAN,
PLOT NO – LB 1, SECTOR III, SALT LAKE, KOLKATA, INDIA PIN:
700098

GEOLOGICAL REPORT
ON
RECONNAISSANCE SURVEY (G4) FOR GLAUCONITE AND ASSOCIATED
MINERALIZATION IN DHAMINI - PIPARWASI SIMLIYA AREA, SHEOPUR
DISTRICT, MADHYA PRADESH

(A Project under NMEDT, File No. 23/492/2024-NMET/ 283, dated, 21st Aug, 2024)

FOR SUBMISSION TO
NATIONAL MINERAL EXPLORATION AND DEVELOPMENT TRUST
MINISTRY OF MINES,
ROOM NO. 325 & 326, WING-F, UDYOG BHAWAN, RAFI AHMED KIDWAI MARG,
RAJPATH AREA, CENTRAL SECRETARIAT
NEW DELHI-110011

MARCH-2026

PREPARED BY

DR. SUNIL KUMAR PANDAY

SENIOR GEOLOGIST

AKHAND PRATAP SINGH

GEOLOGIST

SHRAVYA MEHTA

GEOLOGIST



Maheshwari

Global Technologies. Ecological Mining.

NABET/AEA/25/009,

Job No.: MMPL/GRNC/26/DPS/017

MMPL PRIVATE LIMITED
(FORMERLY MAHESHWARI MINING PVT. LTD.) FR 07 SHILPANGAN,
PLOT No – LB 1, SECTOR III, SALT LAKE, KOLKATA, INDIA PIN:
700098

CONTENTS

| | |
|--|----|
| List of Tables | 1 |
| List of Plates | 1 |
| List of Figures | 2 |
| List of Photographs | 2 |
| List of Photomicrograph | 3 |
| List of Annexures..... | 3 |
| अध्याय 1: कार्यकारी सारांश | 5 |
| Chapter 1. Executive Summary | 10 |
| Chapter 2. Details of the Qualified Person(s) / Exploration Agency | 14 |
| 2.1 Details of the Exploration Agency | 14 |
| 2.2 Details of the Qualified Persons | 15 |
| Chapter 3. Title and ownership | 16 |
| 3.1 Title and ownership..... | 16 |
| Chapter- 4. Details of the Area Under Study | 18 |
| 4.1 Village, District, State:..... | 18 |
| 4.2 Survey of India Toposheet No. & Coordinates:..... | 18 |
| 4.3 Cadastral details of the area: | 19 |
| 4.4 Mineral(s) under investigation or granted under licence or lease:..... | 19 |
| Chapter 5. Physiography and environment..... | 22 |
| 5.1 Relief and Drainage | 22 |
| 5.2 Accessibility and infrastructure - | 22 |
| 5.3 Local Demography- | 22 |
| 5.4 Forest and other land- | 23 |
| 5.5 Flora and Fauna within and nearby:..... | 23 |
| 5.6 Climatic conditions: | 24 |
| Chapter 6. Infrastructure | 26 |
| 6.1 Infrastructure and industrial environment in and around the block area | 26 |
| Chapter 7. Geology | 27 |
| 7.1 Regional geology of the area: | 27 |
| 7.2 Local geology of the block area..... | 29 |
| 7. 3 Descriptions of lithologies mapped in the area..... | 30 |
| 7.3.1. Sandstone | 30 |
| 7.3.2. Glauconitic Sandstone | 31 |
| 7.3.3. Intercalated Sandstone Shale | 32 |
| 7.4 Structural Details | 35 |
| 7.4 1 Primary Sedimentary Structures | 35 |

| | |
|--|----|
| 7.4.2 Secondary (Deformational) Structures | 36 |
| 7.5 Sedimentation and Provenance | 39 |
| 7.6 Trace Fossils?..... | 40 |
| 7.7 Mineral Prospect | 43 |
| 7.7.1 Surface indication of mineralization | 43 |
| 7.7.2 Mode of occurrence | 43 |
| 7.7.3 Details of Mineralization | 44 |
| 7.9.4 Genesis of glauconite formation | 44 |
| 7.9.5 Statistical correlation analysis: | 45 |
| Chapter -8: Previous Exploration..... | 51 |
| Chapter-9: Geochemical Data..... | 54 |
| 9.1 Geochemical data..... | 54 |
| 9.1.1 Surface geochemical analysis results and interpretations | 54 |
| 9.1.2 Borehole geochemical analysis and results..... | 56 |
| 10. Exploration undertaken during current investigation | 61 |
| 10.1 Introduction..... | 61 |
| 10.2 Objectives of exploration..... | 63 |
| 10.3 Basis of taking investigation..... | 63 |
| 2.4 Details of work approved vs achieved by MMPL..... | 64 |
| 10.5 Mode of operation of work components & associated agency | 67 |
| 10.6 Scheme of exploration | 67 |
| 10.7 Large Scale Geological Mapping..... | 69 |
| 10.8 Pitting..... | 70 |
| 10.9 Bedrock sampling | 70 |
| 10.10 Petrographic and Modal Analysis | 72 |
| 7.5.2 core samples petrographic study | 79 |
| 7.6. Mineral Phase analysis by XRD | 86 |
| 7.6.1 Results of three XRD analysis by GSI..... | 87 |
| 7.6.2 XRD analysis by Shiva Analyticals of one Sample..... | 89 |
| 11. Location of data point | 94 |
| 11.1 Location of data points: | 94 |
| 11. 2 Quality of Topographic Data: | 95 |
| Chapter-12. Sampling technique..... | 96 |
| 12.1 Bedrock Sampling:..... | 96 |
| 12.2 Pit Sampling:..... | 96 |
| 12.3 Petrological Samples..... | 97 |
| 12.4 Core Sampling: | 97 |

| | |
|--|-----|
| Chapter- 13. Exploratory Drilling..... | 99 |
| 13.1 Introduction..... | 99 |
| 13.2 Borehole Planning..... | 99 |
| 13. 3 Methodology of Drilling..... | 99 |
| 13.4 Drill Core Logging | 100 |
| 13.5 Core Recovery and RQD | 101 |
| 13.6 Sampling, Laboratory Procedure, and Quality of Assay | 107 |
| 13.6 .1 Core Sampling | 107 |
| 13.6 .2 Geochemical Analysis of Primary and External Check Samples | 108 |
| 13.6.3 Evaluation of Potash Zone | 109 |
| Chapter- 14. Sub-sampling techniques and sample preparation..... | 115 |
| 14.1 Sample Preparation | 115 |
| 14.2 Quality control procedure | 115 |
| Chapter- 15. Quality of assay data and laboratory tests..... | 117 |
| 15.1 Analytical laboratory and method..... | 117 |
| 15.2 Internal quality check analysis..... | 117 |
| 15.3 External Check Analysis..... | 117 |
| 10.3.1 Bed Rock Samples -XRF Primary Vs External Sample Result Comparison | 118 |
| 15.3.2 Bed rock samples ICPMS primary vs external sample result comparison | 121 |
| 15.3.3 Pit samples-XRF primary vs external sample result comparison | 123 |
| 15.3.4 BH Primary Vs External Check XRF Samples Comparision..... | 124 |
| Chapter 16. Bulk Density..... | 128 |
| 16.1 Introduction..... | 128 |
| 16.2 Interpretation..... | 128 |
| 16.3 Conclusion | 128 |
| Chapter 17. Resource estimation | 129 |
| 17.1 Introduction..... | 129 |
| 17.2 Methodology | 129 |
| 17.3 Tonnage Estimation | 130 |
| 17.4 Interpretation and Classification | 132 |
| 17.5 Stripping Ratio | 132 |
| Chapter -18 Summary and recommendations..... | 135 |
| 18.1 Conclusion | 135 |
| 18.2 Recommendations..... | 136 |
| REFERENCES | 137 |
| Reports | 137 |
| Books | 138 |

| | |
|-------------------------|-----|
| Websites..... | 138 |
| Research Articles | 138 |

List of Tables

| | |
|---|-----|
| Table 1 Details of the Exploration Agency | 14 |
| Table 2 Details of the Qualified Persons | 15 |
| Table 3 Showing Ownership of Reconnaissance Survey (G4) for Glauconite and associated mineralization in Dhamni-Piparwasi Simliya area, Sheopur district, Madhya Pradesh..... | 16 |
| Table 4 Timeline of Reconnaissance Survey (G-4) for Glauconitic Sandstone in Dhamni, Piparwasi, Simliya, Vijaypur, District- Sheopur, Madhya Pradesh Project..... | 17 |
| Table 5 Coordinates of the corner points block area | 18 |
| Table 6 Coordinates of Borehole Points..... | 18 |
| Table 7 Block Infrastructure details | 26 |
| Table 8 Stratigraphy of the Vindhyan Supergroup of rocks | 28 |
| Table 9 stratigraphy of the block area adopted from Jadia & Shrivastava, 1989–90; Shrivastava & Mehrotra, 1989–90..... | 30 |
| Table 10 Correlation Matrix Calculation of selected oxides of surface samples..... | 46 |
| Table 11 Potassium Oxide (K ₂ O) Distribution in surface samples | 55 |
| Table 12 Li Distribution in surface samples | 55 |
| Table 13Timeline of Reconnaissance Survey (G-4) for Glauconitic Sandstone in Dhamni, Piparwasi, Simliya, Vijaypur, District- Sheopur, Madhya Pradesh Project..... | 65 |
| Table 14 Quantum of work Proposed & Achieved by MMPL in Reconnaissance Survey (G-4) for Glauconitic Sandstone in Dhamni, Piparwasi, Simliya, Vijaypur, District- Sheopur, Madhya Pradesh..... | 66 |
| Table 15MODAL ANALYSIS OF SAMPLE ID: DPS04..... | 74 |
| Table 16 Details of Petrographic Sampling of Cores..... | 79 |
| Table 17Modal analysis of Sample ID: DPS-BH1-PG2 | 80 |
| Table 18 XRD Results of GSI lab with Geochemical Values..... | 87 |
| Table 19 XRD Results of XRD DPS-1 by Shiva Labs..... | 92 |
| Table 20Stoichiometric Comparison Table of XRD DPS-1 by shiva Labs | 92 |
| Table 21 Stoichiometric Oxide Table of XRD-DPS-1 By Shiva labs | 93 |
| Table 22 Location of Borehole Points | 94 |
| Table 23 General Information of Boreholes..... | 100 |
| Table 24 Core Recovery..... | 102 |
| Table 25 Core recovery and RQD | 102 |
| Table 26 Detailed Litholog of DPS/BH/01, | 104 |
| Table 27Detailed Litholog of DPS/BH/02..... | 105 |
| Table 28 Depth wise K ₂ O % and Mineralized Zone of >2% K ₂ O in DPS/BH/01 | 112 |
| Table 29 Depth wise K ₂ O % and Mineralized Zone of >2% K ₂ O in DPS/BH/02 | 113 |
| Table 30 Statistical Evaluation of External Assay XRF Precision of bedrock samples | 118 |
| Table 31 Showing Comparison of Primary and External Check of Bedrock Samples | 119 |
| Table 32 Showing Comparison of Primary and External Check of Bedrock Samples | 121 |
| Table 33 Statistical Evaluation of External Assay ICPMS Precision of bedrock samples..... | 121 |
| Table 34 Showing Comparison of Primary and External Check of PIT Samples | 123 |
| Table 35 Statistical Evaluation of External Assay XRF & ICPMS Precision of Boreholes samples | 124 |
| Table 36 Statistical Evaluation of External Assay XRF and ICPMS Precision of Borehole Samples | 125 |
| Table 37 Bulk Density Analysis of samples | 128 |
| Table 38 Parameters Considered for Inferred Resource (UNFC code 334) estimation of Reconnaissance Survey (G-4) for Glauconitic Sandstone Block | 130 |
| Table 39 Inferred Resource (UNFC code 334), of Reconnaissance Survey (G-4) for Glauconitic Sandstone in Dhamni, Piparwasi, Simliya Block..... | 131 |
| Table 40 Table presenting stripping ratio..... | 132 |

List of Plates

| | |
|---|-------------------------------------|
| PLATE I Location map of the block..... | 20 |
| PLATE II Location of the block on toposheet no 54G/05..... | 21 |
| PLATE III Drainage and contour map of the area | 25 |
| PLATE IV Outcrop Geological Map of Dhamini Piparwasi Simliya Area..... | 49 |
| PLATE V Interpreted Geological Map of Dhamini Piparwasi Simliya Area..... | 50 |
| PLATE VI Geochemical Map of K ₂ O % of Surface Samples Dhamini Piparwasi Simliya Glauconite G4 Block..... | 58 |
| PLATE VII Geochemical Map of K ₂ O and Li Enrichment Zone Based on Surface Sample Values | 59 |
| PLATE VIII Geochemical Contour map of K ₂ O% and Elevated Lithium Values of Dhamini Piparwasi Simliya Glauconite G4 Block..... | 60 |
| PLATE IX Pit Location Map with K ₂ O%..... | 71 |
| PLATE X Borehole Location Plan on Geological Map | 106 |
| PLATE XI Corelation of Boreholes..... | Error! Bookmark not defined. |

List of Figures

| | |
|--|-----|
| Figure 1 Location of the block in the Vindhyan Supergroup of rocks..... | 27 |
| Figure 2 Overlay of block boundary on regional geological map (1:50000 Map from NGDR) | 29 |
| Figure 3 Rose Diagram of Joints, in Dhamni-Piparwasi Simliya area, Sheopur district, Madhya Pradesh | 37 |
| Figure 4 Scatter Plot showing K ₂ O relationship with Al ₂ O ₃ , SiO ₂ , and Fe ₂ O ₃ in surface samples | 46 |
| Figure 5 Scatter Plot showing K ₂ O relationship with Al ₂ O ₃ , SiO ₂ , and Fe ₂ O ₃ in Borehole DPS BH-1 | 47 |
| Figure 6 Scatter Plot showing K ₂ O relationship with Al ₂ O ₃ , SiO ₂ , and Fe ₂ O ₃ in Borehole DPS BH-2 | 48 |
| Figure 7 K ₂ O% Values of NGCM Survey..... | 53 |
| Figure 8 XRD Plots of Phase identification by GSI labs | 88 |
| Figure 9 XRD Plots of Phase identification by Shiva Labs | 90 |
| Figure 10 Litholog of DPSBH1 | 110 |
| Figure 11 Litholog of DPS-BH2..... | 111 |
| Figure 12 Scatter Plots of Primary vs External Check samples Chemical analysis results of Selected Major Oxides of BRS samples | 120 |
| Figure 13 Scatter Plots of Primary vs External Check samples Chemical analysis results of Selected Trace Elements of BRS samples..... | 122 |
| Figure 14 Scatter Plots of Primary vs External Check samples Chemical analysis results of Selected Major Oxides of PIT samples | 123 |
| Figure 15 Scatter Plots of Primary vs External Check samples Chemical analysis results of Major oxides of Borehole samples..... | 125 |
| Figure 16 Scatter Plots of Primary vs External Check samples Chemical analysis results of Selected Trace Elements of Borehole samples | 126 |

List of Photographs

| | |
|---|----|
| Photograph 1 Showing Outcrop of bedded sandstone near Jhumkha, | 31 |
| Photograph 2 Showing Exposer of Glauconitic Bearing Sandstone Bed, near Barodakalan, | 33 |
| Photograph 3 Showing Intercaalted Sandstone shale sections near Khari Piparwas area, | 34 |
| Photograph 4. Left one Showing Laminations while right one Bedding in Dhamni-Piparwasi Simliya area, Sheopur district, Madhya Pradesh block..... | 35 |
| Photograph 5. Showing Asymmetrical Ripple marks in a outcrop in Dhamni-Piparwasi Simliya area, Sheopur district, Madhya Pradesh block, Hammer Head Oriented towards north. | 36 |
| Photograph 6 Showing Joint Patterns in rock exposer in in Dhamni-Piparwasi Simliya area, Sheopur district, Madhya Pradesh ,..... | 38 |
| Photograph 8 Fossils Impressions are observed near Jhumkha, | 41 |
| Photograph 9 Fossil Impressions are observed near Piparwasi, | 42 |

List of Photomicrograph

| | |
|---|----|
| Photomicrograph 1 of thin section DPS01 | 73 |
| Photomicrograph 2 Showing thin section DPS04 | 75 |
| Photomicrograph 3 Showing thin section DPS11 | 76 |
| Photomicrograph 4 Showing thin section DPS25 | 77 |
| Photomicrograph 5 Showing thin section DPS41 | 78 |
| Photomicrograph 6 Showing of thin section DPS-BH1-PG1 | 79 |
| Photomicrograph 7 Showing thin section DPS-BH1-PG2 | 81 |
| Photomicrograph 8 Showing thin section DPS-BH1-PG3 | 82 |
| Photomicrograph 9 Showing thin section DPS-BH2-PG4 | 82 |
| Photomicrograph 10 Showing thin section DPS-BH2-PG5 | 83 |

List of Annexures

| | |
|---|-----|
| Annexure 1 Statement showing details of Block boundary co-ordinates of Reconnaissance Survey (G-4) for Glauconitic Sandstone Block Dhamni-Piparwasi-Simliya area Vijaypur District Madhya Pradesh..... | 139 |
| Annexure 2 Showing co-ordinates & analyses results for major oxides (XRF analysis) of 150 bedrock samples | 140 |
| Annexure 3 Statement Showing co-ordinates & analyses results for REE and Trace Elements (ICPMS) of 75 bedrock samples | 144 |
| Annexure 4 Statement Showing co-ordinates & analyses results for major oxides (XRF analysis) of 50 Pit samples | 146 |
| Annexure 5 Statement Showing analyses results for major oxides (XRF analysis) of 53 Core samples | 148 |
| Annexure 6 Statement Showing co-ordinates & Comparison of analyses results for major oxides (XRF analysis) of 15 Bedrock External Check samples | 152 |
| Annexure 7 Statement Showing co-ordinates & Comparison of analyses results for REE & Trace Elements (ICPMS analysis) of 7 Bedrock External Check samples | 153 |
| Annexure 8 Statement Showing co-ordinates & Comparison of analyses results for major oxides (XRF analysis) of 5 Pit External Check samples | 153 |
| Annexure 9 Statement Showing co-ordinates & Comparison of analyses results for major oxides (XRF analysis) of 5 Core Check samples | 154 |
| Annexure 10 Statement Showing co-ordinates & Comparison of analyses results for REE & Trace Elements (ICPMS analysis) of 3 Core External Check samples | 154 |
| Annexure 11 Statement Showing Details of Boreholes Drilled by MMPL in the block..... | 155 |
| Annexure 12 Statement showing Run-wise Litholog of exploratory boreholes drilled by MMPL in the block. . | 155 |
| Annexure 13 Statement showing Run-wise Litholog of exploratory boreholes drilled by MMPL in the block . | 156 |
| Annexure 14 Statement Showing Borehole-wise intersection of Potassic Zone Reconnaissance Survey (G4) for Glauconite and associated mineralization in Dhamni-Piparwasi Simliya area, Sheopur district, Madhya Pradesh..... | 157 |
| Annexure 15 Statement Showing drillhole wise resource for $K_2O \geq 2\%$ in Reconnaissance Survey (G4) for Glauconite and associated mineralization in Dhamni-Piparwasi Simliya area, Sheopur district, Madhya Pradesh..... | 157 |
| Annexure 16 Statement showing X-Ray Diffraction studies carried out in Reconnaissance Survey (G4) for Glauconite and associated mineralization in Dhamni-Piparwasi Simliya area, Sheopur district, Madhya Pradesh..... | 158 |
| Annexure 17 Statement showing Bulk Density Determination of sample | 163 |
| Annexure 18 Minutes of 10th meeting of Technical-cum-Cost Committee - II (TCC - II) held on 23rd, 24th & 25th June 2025, the committee recommended to carry out the modal analysis of potash minerals and a certain mineral phase for potash content. The committee approved time extension of 3 months up to 20th November 2025 for submission of final geological report..... | 165 |
| Annexure 19 Minutes of 66th TCC Meeting held on 24th, 25th and 26th June, 2024, | 166 |
| Annexure 20- Modal Analysis report of Glauconite-Bearing Samples..... | 167 |
| Annexure 21 Petrography report of Dhamini Piparwasi Simliya glauconite block | 171 |
| Annexure 22 Report of Phase Identification using XRD carried out by GSI..... | 184 |

| | |
|---|------------|
| <i>Annexure 23 Compliance to Peer Review Comments</i> | <i>186</i> |
| <i>Annexure 24 Official Memorandum of NMET approval of Reconnaissance Survey (G4) in Dhamini Piparwasi Simliya area for glauconite and associated mineralization, Sheopur District Madhya Pradesh</i> | <i>187</i> |

अध्याय 1: कार्यकारी सारांश

1. 1. धमनी-पिपरवासी-सिमलिया क्षेत्र, श्योपुर जिला, मध्य प्रदेश में ग्लॉकोनाइट और संबंधित खनिजीकरण के लिए एक प्रारंभिक (G4-चरण) सर्वेक्षण किया गया, जिसकी आधिकारिक पुष्टि **फाइल नंबर 23/492/2024-NMET/ 283** के माध्यम से **21 अगस्त, 2024** को की गई थी। यह क्षेत्र सर्वे ऑफ इंडिया टोपोशीट नंबर 54G/05 के अंतर्गत आता है, कुल क्षेत्रफल **116 वर्ग किलोमीटर** है। ब्लॉक भौगोलिक रूप से अक्षांश 25°52'17.700" उ. अ. से 25°59'26.590" उ. अ. तथा देशांतर 77°18'48.981" पू. दे. से 77°24'59.923" पू. दे. (लगभग 136 वर्ग किमी बाउंडिंग बॉक्स) द्वारा परिभाषित है, जो विजयपुर तहसील, श्योपुर जिला, मध्य प्रदेश में स्थित है। परियोजना क्षेत्र में बिजईपुर तहसील के अंतर्गत धमनी, पिपरवासी, सिमलिया, खारी और चांदापुरा गाँव शामिल हैं। यह प्रस्ताव NMET की 66वीं तकनीकी समिति द्वारा अनुशंसित किया गया और 21 अगस्त 2024 को NMET की 36वीं कार्यकारी समिति (EC) द्वारा अनुमोदित किया गया।
1. 2. यह अनुशंसा भूवैज्ञानिक सर्वेक्षण ऑफ इंडिया (GSI) द्वारा मुरैना, शिवपुरी और श्योपुर जिलों में किए गए पूर्व भूवैज्ञानिक कार्यों पर आधारित थी, जहाँ विंध्यन सुपरग्रुप की ऊपरी रीवा बलुआ पत्थर संरचना में ग्लॉकोनाइटिक बलुआ पत्थरों की पहचान की गई थी। 1989-90 के क्षेत्रीय सत्र के दौरान, GSI की टीमों (जडिया और श्रीवास्तव; श्रीवास्तव और मेहरोत्रा; रामटेके और पटेल) ने 2,100 वर्ग किमी से अधिक क्षेत्र में विस्तृत भूवैज्ञानिक मानचित्रण किया। इन जांचों से विभिन्न स्थानों पर 5-10% ग्लॉकोनाइट और ऊपरी रीवा बलुआ पत्थर की महत्वपूर्ण मोटाई (~200 मीटर) का पता चला, जिसमें समुद्री निक्षेपण संकेतक मौजूद थे। न्यूनतम टेक्टोनिक गड़बड़ी और संरक्षित तलछटी विशेषताओं ने उथले समुद्री वातावरण में ग्लॉकोनाइट संचय का समर्थन किया। हाल ही में, 2020-21 में GSI अधिकारियों अरुण देव और मोहम्मद दानिश द्वारा किए गए NGCM ने K₂O मानों के साथ 1.45% से 3.30% तक ग्लॉकोनाइट की संभावना की पुष्टि की। महेश्वरी माइनिंग प्राइवेट लिमिटेड द्वारा नमूने लेने से K₂O मान 1.15% से 2.81% तक प्राप्त हुए, जो G-4 प्रस्ताव का आधार बने।
1. 3. पोटाश, उर्वरकों (N-P-K में K) का एक आवश्यक घटक, फसल की पैदावार, पौधों के पोषण और समग्र मृदा स्वास्थ्य को बढ़ाने के लिए व्यापक रूप से उपयोग किया जाता है। वैश्विक स्तर पर पोटाश गहरे जमावों से निकाला जाता है, लेकिन भारत अपनी कृषि मांग को पूरा

करने के लिए आयात पर निर्भर है। हालांकि, ग्लॉकोनाइटिक बलुआ पत्थर (ग्रीनसैंड्स) एक आशाजनक स्वदेशी विकल्प प्रदान करते हैं।

1. 4. ग्लॉकोनाइटिक बलुआ पत्थर/ग्रीनसैंड्स जमा पोटाश के लिए एक वैकल्पिक स्वदेशी संसाधन के रूप में उपयोग किए जा सकते हैं। ग्लॉकोनाइट मुख्य रूप से लोहा और पोटेशियम का एक जटिल हाइड्रस सिलिकेट है, जिसमें मुख्य रूप से फेरिक ऑक्साइड और आंशिक रूप से फेरस ऑक्साइड होता है। इसमें लगभग 4-7% K_2O होता है। इन संसाधनों का प्रमुख हिस्सा (91%) राजस्थान के नागौर जिले में, इसके बाद मध्य प्रदेश के पन्ना जिले (5%) और शेष उत्तर प्रदेश के सोनभद्र और चित्रकूट जिलों (4%) में स्थित है (इंडियन ब्यूरो ऑफ माइन्स, 2021)।
1. 5. धमनी-पिपरवासी-सिमलिया ब्लॉक, श्योपुर जिला, मध्य प्रदेश में 116 वर्ग किमी का बड़े पैमाने पर भूवैज्ञानिक मानचित्रण 1:12,500 के पैमाने पर किया गया, जो विंध्यन सुपरग्रुप के रीवा समूह की गोविंदगढ़ बलुआ पत्थर फॉर्मेशन (ऊपरी रीवा बलुआ पत्थर) को लक्षित करता था। यह फॉर्मेशन पूर्वी (सिमलिया, बेनीपुरा) और पश्चिमी (खारी, पिपरवासी) क्षेत्रों में अच्छी तरह से उजागर है, जिसमें ग्लॉकोनाइटिक बलुआ पत्थर और बलुआ पत्थर-शेल अंतर्वेशन, विशेष रूप से जामका खो सहायक नदी के साथ, मौजूद हैं। बलुआ पत्थर सफेद से धूसर-सफेद या हरा-धूसर, महीन से मध्यम दानेदार, पतली से मोटी परतों वाला, कठोर, संकुचित और मध्यम से अच्छी तरह छँटा हुआ है। यह क्षेत्र संरचनात्मक रूप से स्थिर है, जिसमें लगभग क्षैतिज परतें और ऑर्थोगोनल से उप-ऑर्थोगोनल ऊर्ध्वाधर जोड़ हैं, जो बिना किसी प्रमुख तह या भ्रंश के भंगुर विरूपण का संकेत देते हैं। जीपीएस, ब्रंटन कंपास और भूवैज्ञानिक उपकरणों का उपयोग करके एकत्र किए गए क्षेत्र डेटा को QGIS में डिजिटलाइज किया गया ताकि क्षेत्रीय अवलोकन, उपग्रह चित्रण और टोपोशीट्स को एकीकृत करके एक भूवैज्ञानिक मानचित्र बनाया जा सके।
1. 6. पांच चयनित बेडरॉक नमूनों के पेट्रोग्राफिक विश्लेषण से पता चला कि केवल दो में महत्वपूर्ण ग्लॉकोनाइट सामग्री (70-80%) थी, जबकि अन्य में यह विरल या अनुपस्थित थी। यह दर्शाता है कि ग्लॉकोनाइट पृथक स्ट्रैटिग्राफिक पैकेट्स में होता है, न कि समान रूप से वितरित, संभवतः स्थानीय निक्षेपण और भू-रासायनिक परिस्थितियों के तहत जो ग्लॉकोनाइटिकरण के लिए अनुकूल थीं।
1. 7. कुल 253 नमूने एकत्र किए गए, जिनमें 150 बेडरॉक, 50 गड्ढा और 53 बोरहोल कोर नमूने शामिल थे। सभी 253 नमूनों पर K_2O , Fe_2O_3 , Al_2O_3 और SiO_2 जैसे प्रमुख ऑक्साइड्स

निर्धारित करने के लिए XRF विश्लेषण किया गया। इसके अतिरिक्त, 111 नमूनों का ICP-MS द्वारा विश्लेषण किया गया, जिसमें 75 बेडरॉक नमूने और 53 में से 36 बोरहोल कोर नमूने शामिल थे।

1. 8. प्रमुख ऑक्साइड विश्लेषण (XRF) से 50 गड्ढा और 150 बेडरॉक नमूनों में रासायनिक रूप से विविध तलछटी चट्टानों का पता चला। सिलिका (SiO_2) सामग्री 49-97% तक है, जो क्वार्ट्ज-समृद्ध लिथोलॉजी को दर्शाता है। एल्यूमिना (Al_2O_3) 0.5-7% और Fe_2O_3 0.5-6.9% तक है, जो लोहा-युक्त खनिजों की उपस्थिति का संकेत देता है। उच्च CaO (0.06-36%) और MgO (<0.05-15%) मान कार्बोनेट-समृद्ध घटकों को दर्शाते हैं। K_2O 0.1-3.65% तक भिन्न है, जो संभवतः ग्लाकोनाइट से संबंधित है, जबकि निम्न Na_2O (0.08-0.44%) न्यूनतम फेल्डस्पार को दर्शाता है। मामूली ऑक्साइड्स में MnO (0.05-0.8%), TiO_2 (<0.05-0.34%), और $\text{P}_2\text{O}_5/\text{V}_2\text{O}_5$ (<0.05-0.54%) शामिल हैं। SO_3 1.8% तक पहुँचता है, SrO और BaO 0.4% से नीचे हैं, और LOI व्यापक (0.2-40%) है, जो परिवर्तनशील कार्बोनेट या हाइड्रस सामग्री को दर्शाता है। कुल मिलाकर यह प्रोफाइल क्वार्ट्जोज, कैल्केरियस और ग्लाकोनाइटिक तलछटी चट्टानों का समर्थन करती है।
1. 9. K_2O मान दर्शाते हैं कि 75% से अधिक बेडरॉक नमूने 0.5% से अधिक, लगभग 20% 1.5% से अधिक, और केवल 3 नमूने 3% से ऊपर हैं।
1. 10. ICP-MS विश्लेषण से लिथियम (Li) 2.2-383.9 ppm तक है, जिसमें अधिकांश नमूने 10-60 ppm की सीमा में हैं। हालांकि, कुछ नमूने (उदाहरण के लिए, DPS-1 से DPS-5, DPS-63, DPS-S-114) उच्च Li (>220 ppm) और इसके साथ उच्च K_2O (>2%, कुछ >3.4%) दर्शाते हैं, जो K_2O -Li के बीच मजबूत सहसंबंध का संकेत देता है। यह सुझाव देता है कि Li पोटेशियम-युक्त चरणों, जैसे ग्लाकोनाइट, मिट्टी, या डेट्राइटल माइका में हो सकता है, हालांकि महत्वपूर्ण Li खनिजीकरण के लिए कोई सुसंगत लिथोलॉजिकल समर्थन नहीं है।
1. 11. अन्य ट्रेस तत्व मध्यम रूप से भिन्न हैं: Co (0.7-22.9 ppm), Ga (1.0-26.6 ppm), Rb (10.6-125 ppm), Cu (10-232 ppm), Ni (<5-69 ppm), Pb (<5-453 ppm)। उच्च क्षेत्र शक्ति तत्व जैसे Y (1.5-20.9 ppm), Zr (8-482 ppm), Th (<0.5-18 ppm), और U (<0.5-46 ppm) परिवर्तनशील स्रोत चट्टानों को दर्शाते हैं।
1. 12. REEs हल्के REE (LREE) संवर्धन और भारी REE (HREE) कमी को दर्शाते हैं: La (~24.8 ppm), Ce (~60 ppm), Nd (~46 ppm), Sm (~11.9 ppm), Eu (~2.8 ppm) प्रमुख हैं, जबकि HREEs (Tb, Tm, Lu) अधिकतर <0.5 ppm हैं। मध्यवर्ती REEs (Gd ~9 ppm, Dy

~3.7 ppm, Er ~1.7 ppm, Yb ~1.6 ppm) मध्यम रूप से मौजूद हैं। यह REE पैटर्न स्रोत और डायजेनेसिस से प्रभावित तलछटी उत्पत्ति का समर्थन करता है।

1. 13. कुल 64 मीटर की ड्रिलिंग दो बोरहोल्स में की गई — DPS-BH1 (34 मीटर) और DPS-BH2 (30 मीटर)। इससे 53 नमूनों का प्रमुख ऑक्साइड्स, और 36 नमूनों मामूली तत्वों, ट्रेस तत्वों और दुर्लभ पृथ्वी तत्वों (REEs) के लिए विश्लेषण किया गया। भू-रासायनिक परिणामों से पता चलता है कि K₂O, पोटैश संवर्धन का एक प्रमुख संकेतक, 0.70% से 4.79% तक है, जबकि Li सामग्री 3.0 ppm से 47.4 ppm तक भिन्न है। अन्य प्रमुख ऑक्साइड्स में SiO₂ (25.09-96.46%), Al₂O₃ (1.37-9.67%), Fe₂O₃ (0.72-6.35%), MgO (0.08-11.70%), CaO (<0.05-19.06%), Na₂O (<0.08-0.25%), TiO₂ (0.07-0.70%), MnO (<0.05-0.29%), P₂O₅ (<0.05-0.10%), SO₃ (<0.05-1.30%), और LOI (0.25-29.83%) शामिल हैं। मामूली और ट्रेस तत्वों में Ni (5-19 ppm), Cu (5-21 ppm), Zn (<5-144 ppm), Pb (5-55 ppm), Sr (9-57 ppm), और Zr (21-300 ppm) उल्लेखनीय हैं। REEs में La (7.2-32.9 ppm), Ce (14.6-68.6 ppm), Nd (6.0-28.6 ppm), Sm (0.9-5.5 ppm), Gd (0.7-5.4 ppm), और Yb (<0.5-4.7 ppm) उल्लेखनीय हैं।
1. 14. भूवैज्ञानिक रिपोर्ट MMPL कार्यालय में G-4 प्रारंभिक सर्वेक्षण के दौरान प्राप्त भूवैज्ञानिक, संरचनात्मक और विश्लेषणात्मक डेटा को एकीकृत करके तैयार की गई थी। क्षेत्रीय अवलोकनों को डिजिटाइज किया गया, GIS का उपयोग करके मैप किया गया, और चार्ट्स और विश्लेषणात्मक तालिकाओं के साथ संकलित करके ब्लॉक की एक व्यापक भूवैज्ञानिक रिपोर्ट तैयार की गई।
1. 15. प्रारंभिक सर्वेक्षण ने K₂O-समृद्ध क्षेत्रों (~2%) को 15 किमी² और सतह पर लिथियम विसंगतियों (>100 ppm) को 9.207 किमी² में चित्रित किया, जिसमें दोनों के बीच स्थानिक ओवरलैप था। बोरहोल्स DPS-BH01 और DPS-BH02 ने क्रमशः 9 मीटर और 7 मीटर की ग्लॉकोनाइटिक बलुआ पत्थर जोन को काटा, जिसमें औसत K₂O ~2% था। हालांकि बोरहोल नमूनों में लिथियम संवर्धन की पुष्टि नहीं हुई, सतह की विसंगतियाँ और स्ट्रेटिग्राफिक निरंतरता बहु-तत्व अन्वेषण के लिए आशाजनक परिस्थितियों का सुझाव देती हैं।
1. 16. G-4 चरण ने ग्लॉकोनाइट-युक्त जोनों की सफलतापूर्वक पहचान की, जिसमें 44% नमूनों में K₂O ≥1%, 18% में ≥2%, और 1.5% में ≥3% दर्ज किया गया। K₂O और लिथियम सतह विसंगतियों का ओवरलैप स्वदेशी पोटेसियम-युक्त संसाधनों के लिए ब्लॉक की रणनीतिक अन्वेषण क्षमता को उजागर करता है।

1. 17. संसाधन का आकलन द्वैतिज रूप से स्थित ग्लॉकोनाइटिक बलुआ पत्थर पर आधारित है, जिसमें शैल और फेरुजिनस अंतःस्तरों के साथ खनिजीकृत जोन ($\geq 2.0\%$ K_2O कट-ऑफ) पाए गए हैं। संसाधन का अनुमान रूढ़िवादी स्केयर ब्लॉक एरिया ऑफ़ इन्फ्लुएंस (ZOI) पॉलिगोनल विधि से किया गया, जिसमें प्रत्येक बोरहोल के लिए 400×400 मी (0.16 किमी²) का अलग, ओवरलैप-रहित ब्लॉक लिया गया और प्रयोगशाला-आधारित औसत थोक घनत्व 2.545 t/m^3 का उपयोग किया गया। टनन की गणना के लिए सूत्र $\text{Area (160,000 m}^2\text{)} \times \text{Thickness (m)} \times \text{Bulk Density (t/m}^3\text{)}$ अपनाया गया, जिसके अनुसार DPS-BH01 से कुल 8.75 मिलियन टन (BH1/A: 5.09 Mt, 2.43% K_2O , मोटाई 12.5 m; BH1/B: 3.66 Mt, 3.07% K_2O , मोटाई 9 m) तथा DPS-BH02 से 6.52 मिलियन टन (BH2/A: 5.29 Mt, 2.39% K_2O , मोटाई 13 m; BH2/B: 1.22 Mt, 3.85% K_2O , मोटाई 3 m) प्राप्त हुए। दोनों बोरहोल ब्लॉकों को मिलाकर कुल अनुमानित संसाधन 15.27 मिलियन टन ग्लॉकोनाइट-धारक शैल का है, जिसे सीमित डेटा और प्रारंभिक भूवैज्ञानिक जानकारी के कारण UNFC कोड 334 के अंतर्गत अनुमानित (Inferred) संसाधन के रूप में वर्गीकृत किया गया है।
1. 18. इन परिणामों के आधार पर, धमनी-पिपरवासी-सिमलिया ब्लॉक को G-3 चरण अन्वेषण में अपग्रेड करने की सिफारिश की जाती है, विशेष रूप से 15 किमी² के लक्षित क्षेत्र में, जहाँ K_2O और Li के उन्नत स्तर हैं। यह ब्लॉक निरंतर अन्वेषण और संभावित वाणिज्यिक विकास के लिए काफी संभावना रखता है।

Chapter 1. Executive Summary

1. 1. A reconnaissance (G4-Stage) survey was carried out for glauconite and associated mineralization in Dhamni-Piparwasi-Simliya Area, Sheopur District, Madhya Pradesh, **under NMEDT, File No. 23/492/2024-NMET/ 283, dated, 21st Aug, 2024.** This area is covered in Survey of India Toposheet No. 54G/05. Block is geographically defined by latitude 25°52'17.700" N to 25°59'26.590" N and longitude 77°18'48.981" E to 77°24'59.923" E (bounding box approximately 136 sq km), located in Vijaypur Tehsil, Sheopur District, Madhya Pradesh. The project area includes parts of Dhamni, Piparwasi, Similiya, Khari, and Chandapura villages under Bijaipur tehsil. The proposal was recommended by the 66th Technical Committee of NMET and approved by the 36th Executive Committee (EC) of NMET on 21 August 2024.
1. 2. The recommendation was based on earlier geological work by the Geological Survey of India (GSI) in parts of Morena, Shivpuri, and Sheopur districts, where glauconitic sandstones were identified within the Upper Rewa Sandstone Formation of the Vindhyan Supergroup. During the 1989–90 field season, GSI teams (Jadia & Srivastava; Srivastava & Mehrotra; Ramteke & Patel) conducted detailed geological mapping over a combined area of more than 2,100 sq. km. These investigations revealed glauconite contents of 5–10% in various locations and reported significant Upper Rewa Sandstone thickness (~200 m) with marine depositional indicators. Minimal tectonic disturbance and preserved sedimentary features supported glauconite accumulation in a shallow marine setting. More recently, NGCM carried out in 2020–21 by GSI officers Arun Dev and Mohammad Danish further confirmed glauconitic potential with K₂O values ranging from 1.45% to 3.30%. These findings were substantiated through sampling by Maheshwari Mining Pvt. Ltd., which reported K₂O values ranging from 1.15% to 2.81%, forming the basis for the G-4 proposal.
1. 3. Potash, an essential component of fertilizers (K in N-P-K), is widely used to enhance crop yield, plant nutrition, and overall soil health. While globally potash is extracted from deep-seated evaporite deposits, India remains dependent on imports to meet its agricultural demand. However, glauconitic sandstones (greensands) offer a promising indigenous alternative.
1. 4. Glauconitic sandstones/greensands deposits can be used as an alternative indigenous resource for potash. Glauconite is essentially a complex hydrous silicate of iron and

potassium chiefly with ferric oxide and partly with ferrous oxide. It contains about 4-7% K₂O. Major part of these resources (91%) are located in Nagaur district of Rajasthan, followed by Panna district, Madhya Pradesh (5%) and the balance in Sonbhadra & Chitrakut districts, Uttar Pradesh (4%), (Indian Bureau of Mines, 2021).

1. 5. Large-scale geological mapping of 116 sq. km at a 1:12,500 scale in the Dhamni–Piparwasi–Simliya Block, Sheopur district, Madhya Pradesh, targeted the Govindgarh Sandstone Formation (Upper Rewa Sandstone) of the Vindhyan Supergroup's Rewa Group. Well-exposed in eastern (Simliya, Benipura) and western (Khari, Piparwasi) areas, the formation features glauconitic sandstone and sandstone-shale intercalations, notably along the Jamka Kho tributary. The sandstone is white to greyish-white or greenish-grey, fine to medium-grained, thinly to thickly bedded, hard, compact, and moderately to well sorted. The region is structurally stable with nearly horizontal beds and orthogonal to sub-orthogonal vertical joints, indicating brittle deformation without major folding or faulting. Field data, collected using GPS, Brunton compass, and geological tools, were digitized in QGIS to create a geological map integrating field observations, satellite imagery, and toposheets.
1. 6. Petrographic analysis of five selected bedrock samples revealed significant glauconite content (70–80%) in only two, while others showed sparse or no presence. This indicates glauconite occurs in isolated stratigraphic pockets rather than being uniformly distributed, likely forming under localized depositional and geochemical conditions favorable to glauconitization.
1. 7. A total of 253 samples—including 150 bedrock, 50 pit, and 53 borehole core samples—were collected. XRF analysis was conducted on all 253 samples to determine major oxides such as K₂O, Fe₂O₃, Al₂O₃, and SiO₂. Additionally, 111 samples were analyzed by ICP-MS, comprising 75 bedrock samples and 36 out of 53 borehole core samples.
1. 8. Major oxide analysis (XRF) of 50 pit and 150 bedrock samples reveal compositionally varied sedimentary rocks. Silica (SiO₂) content spans 49–97%, indicating quartz-rich lithologies. Alumina (Al₂O₃) ranges from 0.5–7%, and Fe₂O₃ from 0.5–6.9%, suggesting the presence of iron-bearing minerals. High CaO (0.06–36%) and MgO (<0.05–15%) values indicate carbonate-rich components. K₂O varies from 0.1–3.65%, likely linked to glauconite, while low Na₂O (0.08–0.44%) implies minimal feldspar. Minor oxides include MnO (0.05–0.8%), TiO₂ (<0.05–0.34%), and P₂O₅/V₂O₅ (<0.05–0.54%). SO₃ reaches up to 1.8%, SrO and BaO are below 0.4%, and LOI is wide-

ranging (0.2–40%), reflecting variable carbonate or hydrous content. The overall profile supports quartzose, calcareous, and glauconitic sedimentary rocks.

1. 9. K₂O values show that over 75% of bedrock samples exceed 0.5%, about 20% exceed 1.5%, and only 3 samples are above 3%..
1. 10. ICP-MS analysis shows lithium (Li) ranging from 2.2–383.9 ppm, with most samples in the 10–60 ppm range. However, a few samples (e.g., DPS-1 to DPS-5, DPS-63, DPS-S-114) exhibit high Li (>220 ppm) and correspondingly high K₂O (>2%, some >3.4%), indicating a strong K₂O–Li correlation. This suggests Li may be hosted in potassium-bearing phases, such as glauconite, clays, or detrital micas, though no consistent lithological support for significant Li mineralization is present.
1. 11. Other trace elements vary moderately: Co (0.7–22.9 ppm), Ga (1.0–26.6 ppm), Rb (10.6–125 ppm), Cu (10–232 ppm), Ni (<5–69 ppm), Pb (<5–453 ppm). High field strength elements such as Y (1.5–20.9 ppm), Zr (8–482 ppm), Th (<0.5–18 ppm), and U (<0.5–46 ppm) reflect variable source rocks.
1. 12. REEs show light REE (LREE) enrichment and heavy REE (HREE) depletion: La (~24.8 ppm), Ce (~60 ppm), Nd (~46 ppm), Sm (~11.9 ppm), Eu (~2.8 ppm) dominate, while HREEs (Tb, Tm, Lu) are mostly <0.5 ppm. Intermediate REEs (Gd ~9 ppm, Dy ~3.7 ppm, Er ~1.7 ppm, Yb ~1.6 ppm) are moderately present. This REE pattern supports sedimentary origin influenced by provenance and diagenesis.
1. 13. A total of 64 meters were drilled across two boreholes — DPS-BH1 (34 m) and DPS-BH2 (30 m). From this, 53 representative samples were selected and analyzed for major oxides, and 36 for minor elements, trace elements, and rare earth elements (REEs). The geochemical results reveal that K₂O, a key indicator of potash enrichment, ranges from 0.70% to 4.79%, while Li content varies between 3.0 ppm and 47.4 ppm. Other major oxides include SiO₂ (25.09–96.46%), Al₂O₃ (1.37–9.67%), Fe₂O₃ (0.72–6.35%), MgO (0.08–11.70%), CaO (<0.05–19.06%), Na₂O (<0.08–0.25%), TiO₂ (0.07–0.70%), MnO (<0.05–0.29%), P₂O₅ (<0.05–0.10%), SO₃ (<0.05–1.30%), and LOI (0.25–29.83%). Minor and trace elements show Ni (5–19 ppm), Cu (5–21 ppm), Zn (<5–144 ppm), Pb (5–55 ppm), Sr (9–57 ppm), and Zr (21–300 ppm). Among the REEs, La (7.2–32.9 ppm), Ce (14.6–68.6 ppm), Nd (6.0–28.6 ppm), Sm (0.9–5.5 ppm), Gd (0.7–5.4 ppm), and Yb (<0.5–4.7 ppm) are notable.
1. 14. The geological report was prepared at the MMPL office by integrating geological, structural, and analytical data obtained during the G-4 reconnaissance survey. Field

observations were digitized, mapped using GIS, and compiled with charts and analytical tables to produce a comprehensive geological report of the block.

1. 15. The reconnaissance survey delineated K₂O-enriched zones (~2%) over 15. km² and surface lithium anomalies (>100 ppm) across 9.207 km², with spatial overlap between the two. Boreholes DPS-BH01 and DPS-BH02 intersected glauconitic sandstone zones of 9 m and 7 m, respectively, with average K₂O ~2%. While lithium enrichment was not confirmed in borehole samples, surface anomalies and stratigraphic continuity suggest promising conditions for further multi-element exploration.
1. 16. The G-4 stage successfully identified glauconite-bearing zones, with 44% of samples recording K₂O ≥1%, 18% ≥2%, and 1.5% ≥3%. The overlap of K₂O and lithium surface anomalies highlights the strategic exploration potential of the block for indigenous potassium-bearing resources.
1. 17. Resource Estimated assuming Horizontal-bedded glauconitic sandstone with shale and ferruginous intercalations hosts mineralized zones (≥2.0% K₂O cutoff). Resources were estimated using the conservative Square Block Area of Influence (ZOI) polygonal method, assigning each borehole a non-overlapping 400×400 m (0.16 km²) zone. Bulk density averaged 2.545 t/m³ from lab data. Tonnage formula: Area (160,000 m²) × Thickness (m) × Bulk Density (t/m³). DPS-BH01 yielded 8.75 Mt (BH1/A: 5.09 Mt at 2.43% K₂O, 12.5 m thick; BH1/B: 3.66 Mt at 3.07% K₂O, 9 m thick). DPS-BH02 added 6.52 Mt (BH2/A: 5.29 Mt at 2.39% K₂O, 13 m thick; BH2/B: 1.22 Mt at 3.85% K₂O, 3 m thick). Total Inferred Resource (UNFC 334): 15.27 Mt.
1. 18. Based on these outcomes, it is recommended to upgrade the Dhamni–Piparwasi–Simliya Block to G-3 stage exploration, particularly within the 15 km² target zone of elevated K₂O and Li. The block holds considerable promise for continued exploration and potential commercial development.

Chapter 2. Details of the Qualified Person(s) / Exploration Agency

2.1 Details of the Exploration Agency

Table 1 Details of the Exploration Agency

| TITLE | DETAILS |
|-------------------------------|--|
| (a) Name: | M/s. MMPL Private Limited (formerly Maheshwari Mining Pvt. Ltd.), |
| (b) Communication Address: | The MMPL Pvt. Ltd. Corporate Office FR 07 Shilpangan, Plot No. LB 1 Sector-3, Salt Lake, Kolkata- 700098 West Bengal India |
| (c) Contact Mobile No: | +91 9399694242 |
| (d) E-Mail id: | geology@maheshwaree.com |

2.2 Details of the Qualified Persons

Table 2 Details of the Qualified Persons

| Responsibility Assigned | Personal of MMPL Involved | Designation | Experience in year |
|--------------------------------|----------------------------------|-----------------------|---------------------------|
| Supervision | Mr. Nagendra Pratap Arya | Asso. General manager | 18 |
| Overall Co-ordination | Mr. Sourabh Sarkar, | DGM | |
| Geological Report Preparation | Dr. Sunil Kumar Panday | Senior Geologist | 4 |
| | Mr Akhand Pratap Singh | Geologist | 1 |
| | Ms. Shravya Mehta | Geologist | 2 |
| Field Geology | Mr Akhand Pratap Singh | Geologist | 1 |
| | Mr Sourav Panda | Junior Geologist | 1 |
| Petrographic Studies | Mr. Medha Sarkar | Geologist | 2 |
| Field Co-ordinator | Ms. Shravya Mehta | Geologist | 2 |
| GIS Work | Dr. Sunil Kumar Panday | Senior Geologist | 4 |
| Survey | Mr. Harihar Maity | Surveyor | |
| Drilling | Mr. Awdhesh Gour | Drilling In charge | |

Chapter 3. Title and ownership

3.1 Title and ownership

This item, under **File No. 23/492/2024-NMET/ 283, dated, 21st Aug, 2024**, has been approved by NMET.

Table 3 Showing Ownership of Reconnaissance Survey (G4) for Glauconite and associated mineralization in Dhamni-Piparwasi Simliya area, Sheopur district, Madhya Pradesh

| | |
|---|--|
| Name of the explorer/Mining or prospecting rights holder. | Maheshwari Mining Private limited, NMET and The Office of Directorate of Geology & Mining, Madhya Pradesh |
| Address: | Directorate of Geology & Mining, Madhya Pradesh , 29-A, Khanij Bhawan, Area Hills, Bhopal Madhya Pradesh-462002 |
| Telephone No. | 0755- 2551795 |
| E-Mail id: | dirgeomn@nic.in |
| (ii) Details of period of prospecting/mineral right if any: | 05 November 2024 to 15/ 3/ 2026 |

Table 4 Timeline of Reconnaissance Survey (G-4) for Glauconitic Sandstone in Dhamni, Piparwasi, Simliya, Vijaypur, District- Sheopur, Madhya Pradesh Project

| Name of the Project | Date of Approval | Date of Commence | Reason for delay in commencement /time over run (if any) | Date of Completion |
|---|-------------------------|-------------------------|--|---------------------------|
| <i>Reconnaissance Survey (G4) for Glauconite and associated mineralization in Dhamni- Piparwasi Simliya area, Sheopur district, Madhya Pradesh</i> | 21/08/2024 | 05/11/2024 | <ol style="list-style-type: none"> 1. Due to harsh weather condition, rainy season up till mid- October, field work was hampered. 2. By elections in Sheopur District on 13th November 2024, created vehicle unavailability. 3. Forest permission for mapping and bed rock sampling from PCCF and DFO. 4. 10th meeting of Technical-cum-Cost Committee - II (TCC - II) held on 23rd, 24th & 25th June 2025, approved time extension of 3 months up to 20th November 2025 for submission of final geological report. 5. 88th TCC-1 extended timeline up to 28th February 2026 6. In 92nd TCC-1 meeting extended timeline up to 15th March 2026 | 15/03/2026 |

Chapter- 4. Details of the Area Under Study

4.1 Village, District, State:

The study area comprises parts of the villages Dhamni, Piparwasi, Similiya, Khari, and Chandapura, located within Vijaypur Tehsil of Sheopur District, Madhya Pradesh.

4.2 Survey of India Toposheet No. & Coordinates:

The region lies in the northwestern part of the district and falls within Survey of India Toposheet No. 54G/05(Plate No 2). The total mapped area covers approximately 116 square kilometers and forms a part of the northern fringe of the Vindhyan Basin, displaying characteristic sedimentary sequences of the Vindhyan Supergroup.

Table 5 Coordinates of the corner points block area

| Points | X | Y |
|--------|-------------------|-------------------|
| A | 77° 18' 48.981" E | 25° 59' 16.852" N |
| B | 77° 24' 59.923" E | 25° 59' 26.590" N |
| C | 77° 24' 59.898" E | 25° 53' 39.706" N |
| D | 77° 19' 29.231" E | 25° 52' 17.700" N |

Table 6 Coordinates of Borehole Points

| Agency | Maheshwari Mining Pvt Ltd | |
|---------------------|---------------------------|----------------|
| BH NO | DPS/BH-01 | DPS/BH-02 |
| Easting | 734452.9 | 733524.788 |
| Northing | 2864576 | 2866738.401 |
| Collor RL | 297.7743 | 282.1039 |
| Latitude | 25:52:50.94191 | 25:54:01.72442 |
| Longitude | 77:20:23.81120 | 77:19:51.86654 |
| Total Drilling in m | 34 | 30 |
| EOH | 263.77 | 252.103 |

4.3 Cadastral details of the area:

1. The block area predominantly falls under protected forest land, interspersed with agricultural fields and rural settlements.
2. No National Park or Wildlife Sanctuary exists within the block boundary. However, Kuno National Park is located approximately 10 km from the block, indicating proximity to an ecologically sensitive zone.
3. There is no officially notified Eco-Sensitive Zone (ESZ) within the proposed block.
4. The majority of the block is covered by dense to moderately dense forest vegetation, as observed from satellite imagery and field verification.
5. No major or minor mineral concessions (leases) have been granted within the block area to date.
6. The block does not contain any monuments, archaeological sites, or heritage structures as per available records.
7. There are no power substations located within the block boundary.
8. A few primary schools are present in the peripheral villages, catering to the local rural population.

Source: MP Geoportal (<https://mpgeoportal.gov.in>), accessed for forest cover, infrastructure, and land use details.

4.4 Mineral(s) under investigation or granted under licence or lease:

Glauconite and associated mineralization

PLATE I Location map of the block

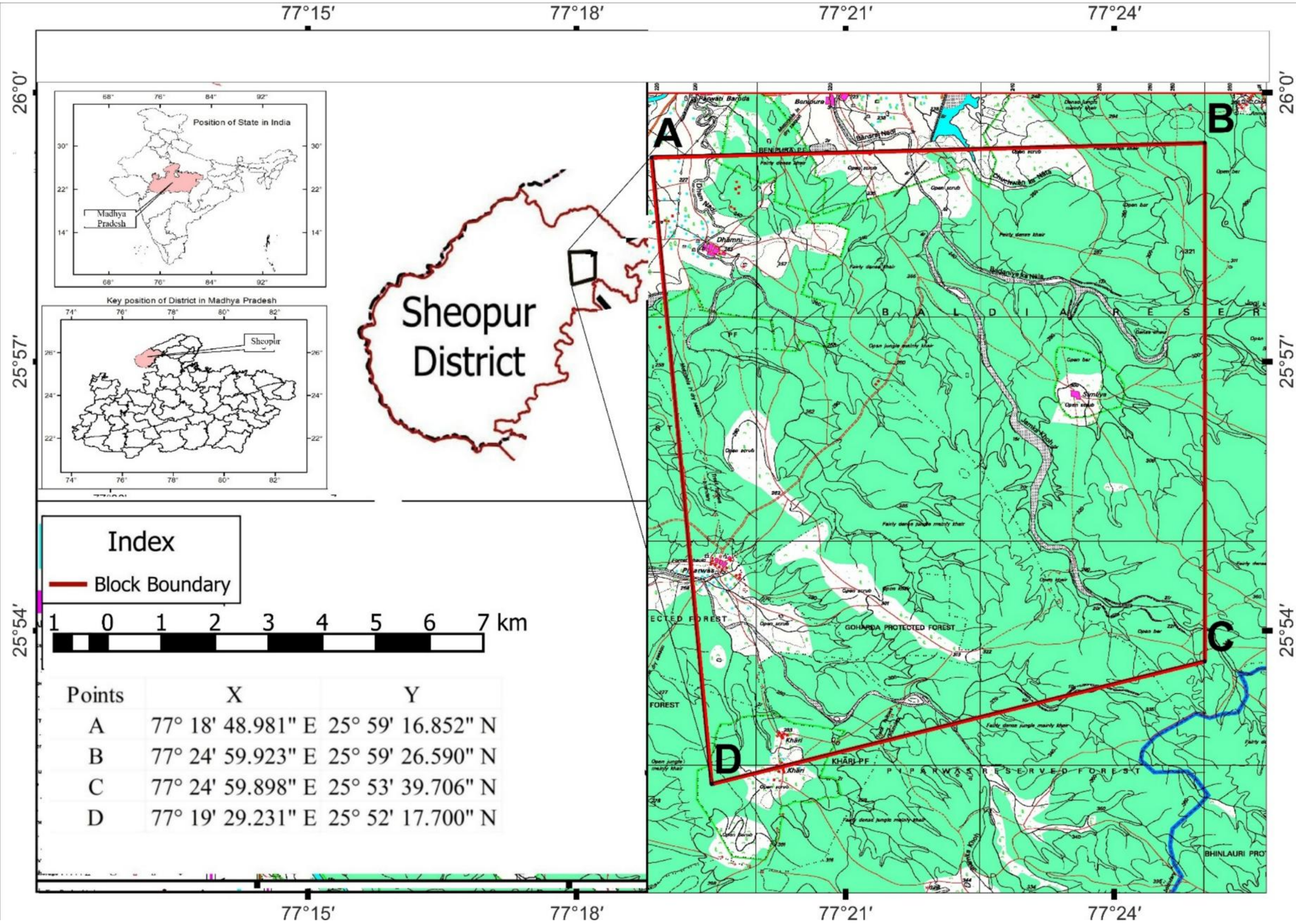
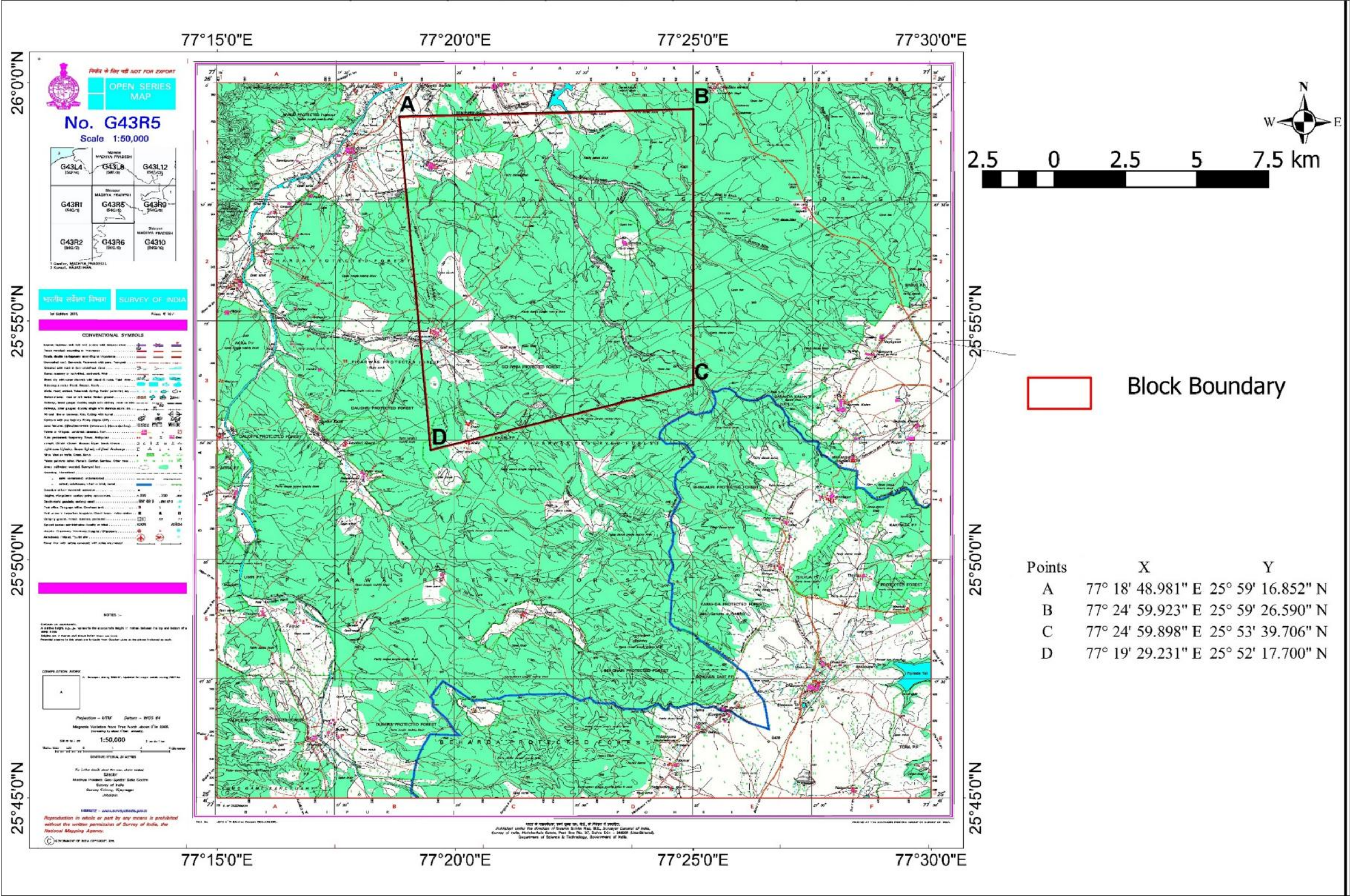


PLATE II Location of the block on toposheet no 54G/05



Chapter 5. Physiography and environment

5.1 Relief and Drainage- The **physiographic character** of the study area is largely governed by its **lithological composition**, dominated by sandstones and shales of the **Rewa Group** within the **Vindhyan Supergroup**. The terrain features a mix of **plateau-like surfaces** and **scarp slopes**, resulting from **differential erosion** between harder sandstone units and softer shale layer. The elevation within the block ranges from approximately **230 to 320 metres above mean sea level (MSL)**, reflecting a relatively subdued relief.

Area drained by Badaniya Nala/Bansrai Nadi, Jhumka Khoh and Dham Nadi all flows towards northwest and merge in Kunwari river a tributary of Sindh River of Gangetic system.

The general **slope of the terrain** (Plate no .3) is directed **north westward**, aligning with the regional drainage flow. The **drainage system** is primarily defined by **tributaries such as Jamka Kho, Badaniya ka Nala, Dham Nadi, and Jhalmal Nadi**, which ultimately discharge into the **Kuno River**. The overall **drainage pattern** is **dendritic to sub-dendritic**; a form typically associated with **horizontal, homogeneous sedimentary formations** like those of the Vindhyan basin (Valdiya, 2010, Central Ground Water Board [CGWB], 2013). This geomorphological expression reflects the structural uniformity of the region, largely undisturbed by intense tectonic activity.

5.2 Accessibility and infrastructure- The nearest urban centre to the proposed block is Vijaypur, a tehsil town located in the northern part of the mapped area. Vijaypur is well-connected via road to Shivpuri (approximately 110 km) and Gwalior (approximately 130 km). The closest railway facility is at Sabalgarh Railway Station, situated around 31 km from Vijaypur. Additional major railway stations include Gwalior (125 km) and Morena (95 km). The nearest airport is Gwalior Airport, located at a distance of approximately 130 km. Access to the proposed block is available through several approach points: Western side: Entry via Dhamni and Piparwasi villages, Eastern side: Entry via Similiya and Boroda Kalan village, Northern side: Access through Benipura village. These villages are interlinked by a network of cart tracks, gravel roads, and forest footpaths, making the block moderately accessible, especially during the dry season.

5.3 Local Demography- The demographic profile of the exploration block consists of three villages in the Vijaypur Tehsil of Sheopur, Madhya Pradesh, showing a total combined population of 2,785. **Dhamini** is the largest settlement with 1,458 residents, followed

by **Piparwas**, a medium-sized village of 1,227 people living in 308 families. **Similiya** is the smallest with only 100 residents and 17 families. While overall gender distribution across the block leans male, Similiya stands out with a **Child Sex Ratio of 1143**, which is notably higher than the state average. The area is dominated by tribal population of Sahariya tribe.

5.4 Forest and other land- More than 80 % of the block area falls under Goharda Protected Forest land, remaining area belongs to private and some part to govt. land. The **proximity to Kuno National Park**, located approximately **10 km from the block boundary**, significantly enhances the faunal diversity of the area.

5.5 Flora and Fauna within and nearby:

The Beharda PF, Piparwas PF, Goharda PF, Araud PF, Dubera PF, Baldia RF and Palpur reserve forest support mixed forest and the main species are Kher, Salaiya, Kardhai, Mahua, Tendu and Jamun. Apart from these, grass upto 3 m. high is found in abundance in the plateau areas formed by Lower Bhander Sandstone. The presence of this formed by Lower Bhander Sandstone. The presence of this grass causes a lot of problems during field work. The Kuno-Game-Sanctuary area occurs within the covered area and a variety of wild animals are found here. Apart from a few panthers and leopards; chital, nilgai, chinkara, sambhar, bear, wild bear, fox, wolf, monkey, rabbit and peacock are also found. The species of trees commonly found in the district are Khair, Kardhai, Dhow, Salaj, Tendu, Palas, Mahua, Karch, Karey, Saja, Koha, Jamun, Saj, Dhaman Kaim, Semal, Tinachand, Amaltas. The normal height of a tree is about 15 m to 20 m and the thickness is 40 cm to 50 cm. Wild life has been steadily declining in district due to indiscriminate shooting and hunting of animals and cutting of forests. In ancient times forests were thick and a good number of animals could be seen. The district has a national park where a good number of animals can be seen and admired including Nahar Tiger (Felistigris), Tendua (Panther) (Pelispardus), Ldaya (jackal) (Cummins aurens), LakkadBaggha (Hyena) (Hyena striata), Bhalu, (Sloth bear) (Melxerusursinus), Sambhar (Carvasunicolar), Suar, (Wild bear) (Sus crislatus), Lomdi (fox) (Vulpesbengaleneis), Chinkara (Gasellsbenetti), Kala Hiran (Black buck) (Antelope Cervicapra) and Langur (Black faced monkeys) (Semlipetheous entellus). Among main common birds, following are found Myna, Shikra (hawk), Crow, Gray house Crow and all Black Crows, Harival Green Pigeon, grey Jungle fowl, Mor (Peacock), Jungle Bush Quail and Bustard Quail

The **proximity to Kuno National Park**, located approximately **10 km from the block**

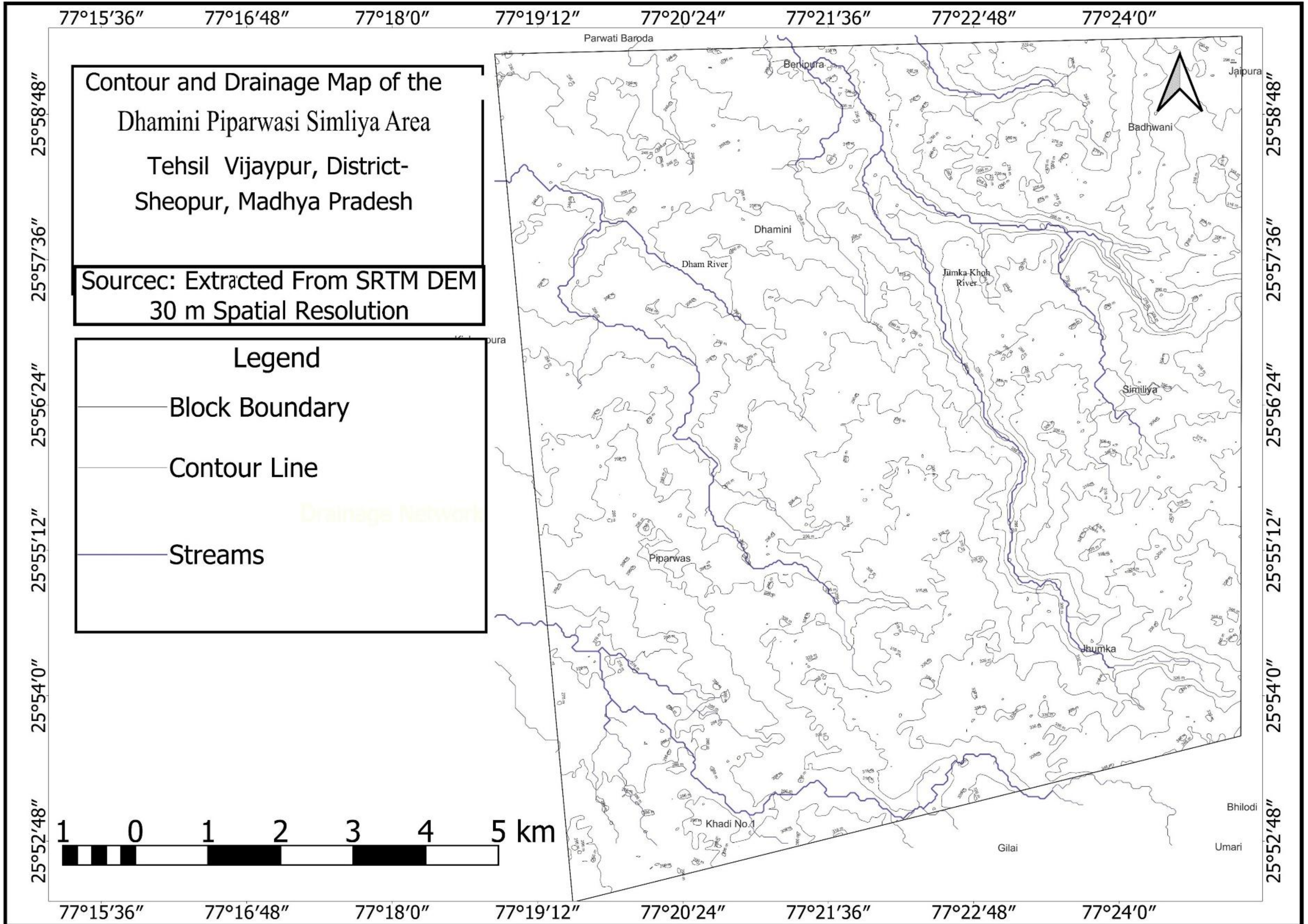
boundary, significantly enhances the faunal diversity of the area. The park and its surrounding forest landscape support major carnivores such as the **tiger (*Panthera tigris*)**, **leopard (*Panthera pardus*)**, and **reintroduced cheetah (*Acinonyx jubatus*)**. Other carnivores like the **striped hyena (*Hyaena hyaena*)**, **Indian grey wolf (*Canis lupus pallipes*)**, and **dhole (*Cuon alpinus*)** are also present (Wildlife Institute of India [WII], 2022). Herbivorous mammals include **chinkara**, **nilgai**, **chital**, **sambar**, **wild pig**, and **Indian hare**, while **monkeys** and other **primates** are frequently observed near human settlements and forest fringes. Additionally, the region hosts a diverse **avian population**, comprising both **resident and migratory species**, contributing to its ecological richness.

5.6 Climatic conditions: The study area exhibits semi-arid to dry climatic conditions with very hot summers from April to June and severe dry winters from December to February. In summer, the temperature rises up to 45°C to 48°C in summer. However, it is very cold in winter and the temperature drops to 7°-10°C. Dust storms and small wind vortices are quite common in summer. The average annual temperature in the study area is 26.2 °C. With an average of 33.0 °C, May is the warmest month. January has the lowest average temperature of 19.5 °C. Rains normally commence from July and continue till September. The area also receives occasional winter rains. The driest month is February. With an average rainfall of 249 mm, the most precipitation falls in July. There is 0 mm of precipitation in February. The rainfall here averages 795 mm. The climate is pleasant during the autumn and spring seasons in the months of October-November and February- March respectively

The area experiences a subtropical climate. The winter season starts from November and continues up to end of February. During this season, the temperature falls upto 5° C. May and June are the hottest months during which the temperature shoots upto 45°C. Monsoon continues from June end to September and the area receives on an average about 110 cm annual rainfall. October to March is the best period for field work.

Though the block does not fall within any formally declared **protected area** or **eco-sensitive zone**, its **proximity to a high-biodiversity conservation landscape** demands environmentally responsible planning.

PLATE III Drainage and contour map of the area



Chapter 6. Infrastructure

6.1 Infrastructure and industrial environment in and around the block area

Table 7 Block Infrastructure details

| Infrastructure | Distance & Location Details |
|-----------------|---|
| Roads | The block is accessed via NH46 at Mohana via SH 50 . Internal village connectivity to Piparwas is through PMGSY roads, approximately 12–15 km from the main town of Vijaypur. |
| Railways | Gwalior Junction (147 km) is the major rail hub for broad-gauge cargo. Sawai Madhopur (~70 km) in Rajasthan is the nearest station for north-south regional connectivity. |
| Port Facilities | No sea ports are nearby. The nearest Inland Container Depot (ICD) for export is at Birla Nagar, Gwalior (approx. 150 km) . |
| Electricity | The area is under the MP Middle Zone grid. While local lines serve Piparwasi, industrial-grade power is available near Vijaypur (15 km). |
| Water | The Kuwari River (~10 km away) flows through the tehsil and is a primary source. The Bansirai river dam is within block and seasonal nalas provide secondary water resources. |

The Piparwas area is strategically positioned near major fertilizer hubs, most notably the **National Fertilizers Limited (NFL)** plant in Vijaipur (~150 km), which is a prime potential consumer for glauconite-based potash integration. The **Malanpur Industrial Area** near Gwalior also hosts specialized organic fertilizer and chemical units that can process and distribute the mineral as a soil conditioner for the region's dominant **mustard and wheat** crops. Additionally, large-scale distributors like **Indian Potash Limited (IPL)** operate extensively in the Gwalior-Morena belt, providing a ready market for indigenous potassic resources to replace expensive imports.

Chapter 7. Geology

7.1 Regional geology of the area:

Geologically, the area is underlain by a thick sequence of sedimentary rocks belonging to the Vindhyan Supergroup, ranging in age from Mesoproterozoic to Late Neoproterozoic (Table no 8). The sequence is predominantly composed of sandstone, shale, and limestone, with laterite of Cenozoic age and alluvium of Quaternary age covering parts of the region. Group of Vindhyan Supergroup exposed and the region are Kaimur Group Rewa group and Bhandar Group.

Systematic geological mapping by Jadia and Shrivastava (1989–90) on Toposheet Nos. 54G/1 and 54G/5 identified the presence of the Upper Rewa Sandstone (Rewa Group) and Ganurgarh Shale, Bhandar Limestone, and Lower Bhandar Sandstone (Bhandar Group). Subsequent mapping by Shrivastava and Mehrotra (1989–90) on Toposheet Nos. 54G/5 and 54G/9

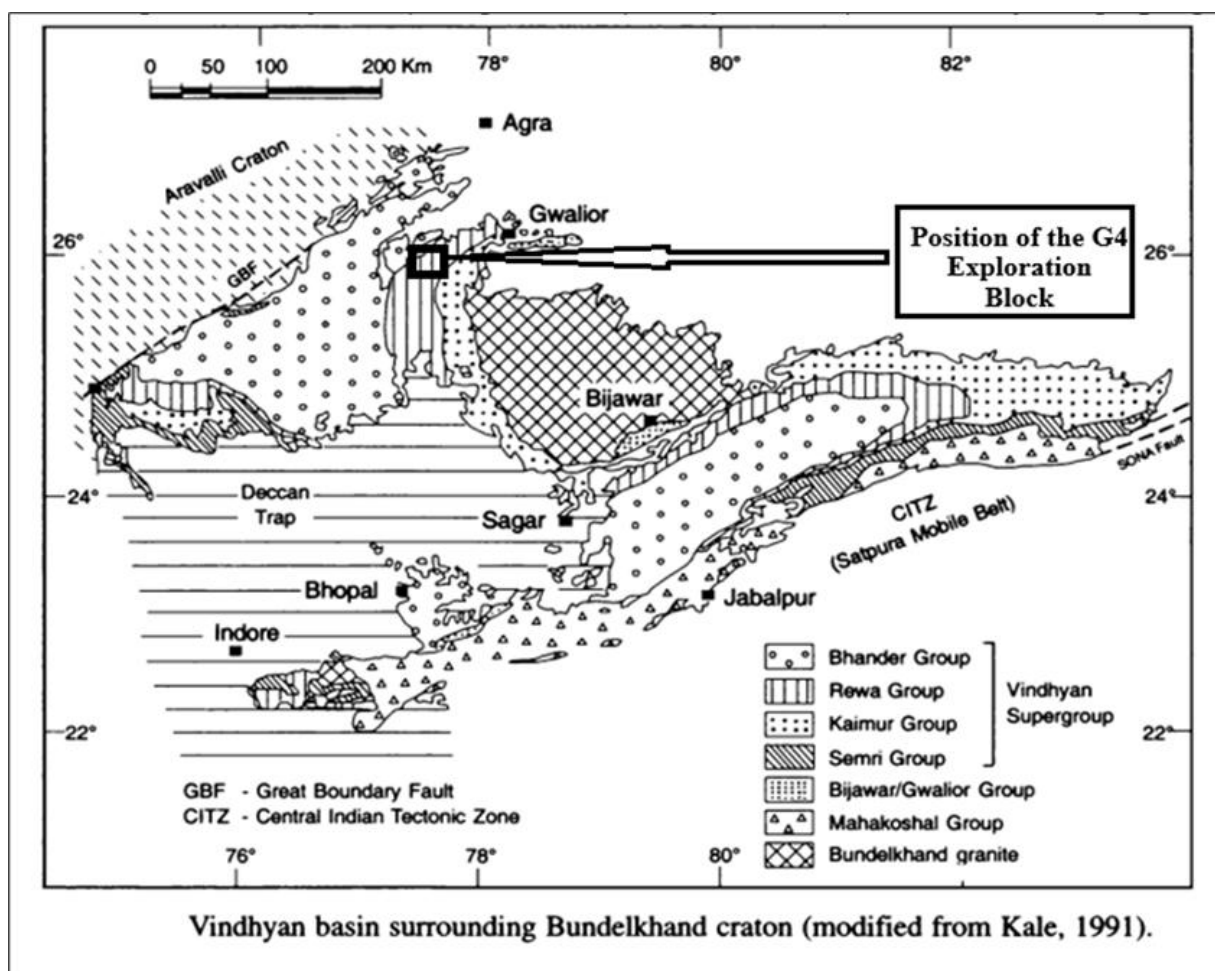


Figure 1 Location of the block in the Vindhyan Supergroup of rocks

identified the Dudauni Member of the Bila Formation (Kaimur Group) as the oldest lithological unit exposed in the area. This unit is conformably overlain by the Jhiri Formation and then by the Upper Rewa Formation, both of which belong to the Rewa Group. More recently, Arun Dev and Mohammad Danish (2020–21) carried out geochemical mapping in parts of Shivpuri and Morena districts (Toposheet No. 54G/5), reaffirming the dominance of Rewa and Bhandar Group rocks. Based on these studies, the regional stratigraphy of the area, from oldest to youngest, comprises the Dudauni Member of the Bila Formation (Kaimur Group), Jhiri Formation and Upper Rewa Sandstone (Rewa Group), and Ganurgarh Shale, Bhandar Limestone, and Lower Bhandar Sandstone (Bhandar Group).

Table 8 Stratigraphy of the Vindhyan Supergroup of rocks

| Group | Thickness (m) | Formation (Top → Bottom) | Alternative Names / Remarks |
|----------------------|---------------|--------------------------|--|
| Bhandar Group | 1300–1500 | Maihar Sandstone | Upper Bhandar Sandstone; divided into Bhavpura Shale, Balwan Limestone, Shikaoda Sandstone |
| | | Sirbu Shale | — |
| | | Bundi Hill Sandstone | Lower Bhandar Sandstone |
| | | Lakheri Limestone | Bhandar Limestone; Nagod Limestone |
| | | Ganurgarh Shale | Simrawal Shale |
| | | Contact | <i>Disconformity / Gradational Contact</i> |
| Rewa Group | 100–300 | Govindgarh Sandstone | Upper Rewa Sandstone; Gahadra Sandstone |
| | | Drummondganj Sandstone | — |
| | | Jhiri Shale | Variiegated Shale |
| | | Asan Sandstone | Lower Rewa Sandstone; Itwa Sandstone; Kanar Sandstone |
| | | Panna Shale | — |
| | | Contact | <i>Normal Contact / Facies Change</i> |
| Kaimur Group | ~400 | Dhandraul Quartzite | Upper Kaimur Sandstone; Scarp Sandstone |
| | | Mangesar Formation | — |
| | | Bijaigarh Shale | — |
| | | Markundi Sandstone | Ghaghar Sandstone |
| | | Ghurma Shale | Susnai Breccia |
| | | Sasaram Sandstone | Lower Kaimur Sandstone |
| | | Contact | <i>Unconformity / Normal Contact</i> |
| Semri Group | 3000–4000 | Suket Shale | Baghwar Shale |
| | | Rohtas Limestone | Nimbahera Limestone; divided into Bari Shale, Jiran Sandstone & Khorl Malan Conglomerate |
| | | Chorhat Sandstone | Glauconite Bed; Rampur Sandstone; Basuhari Sandstone; Tirohan Breccia |
| | | Bargawan Limestone | Salkhan Limestone; Fawn Limestone; Chorhat Limestone; Tirohan Limestone |
| | | Kheinjua Shale | Olive Shale; Kodaha Shale; Binota Shale |
| | | Chopan Porcellanite | Deonar Porcellanite |
| | | Kajrahat Limestone | Kuteshwar Limestone; Bhagwanpura Limestone; Tirohan Limestone; Lohar Dolomite |
| | | Arangi Shale | — |
| | | Deoland Sandstone | Khardeola Sandstone; Pandwafall Sandstone |
| | | Basement Contact | <i>Angular Unconformity / Non-conformity</i> |
| Basement | — | Granites & Supracrustals | — |

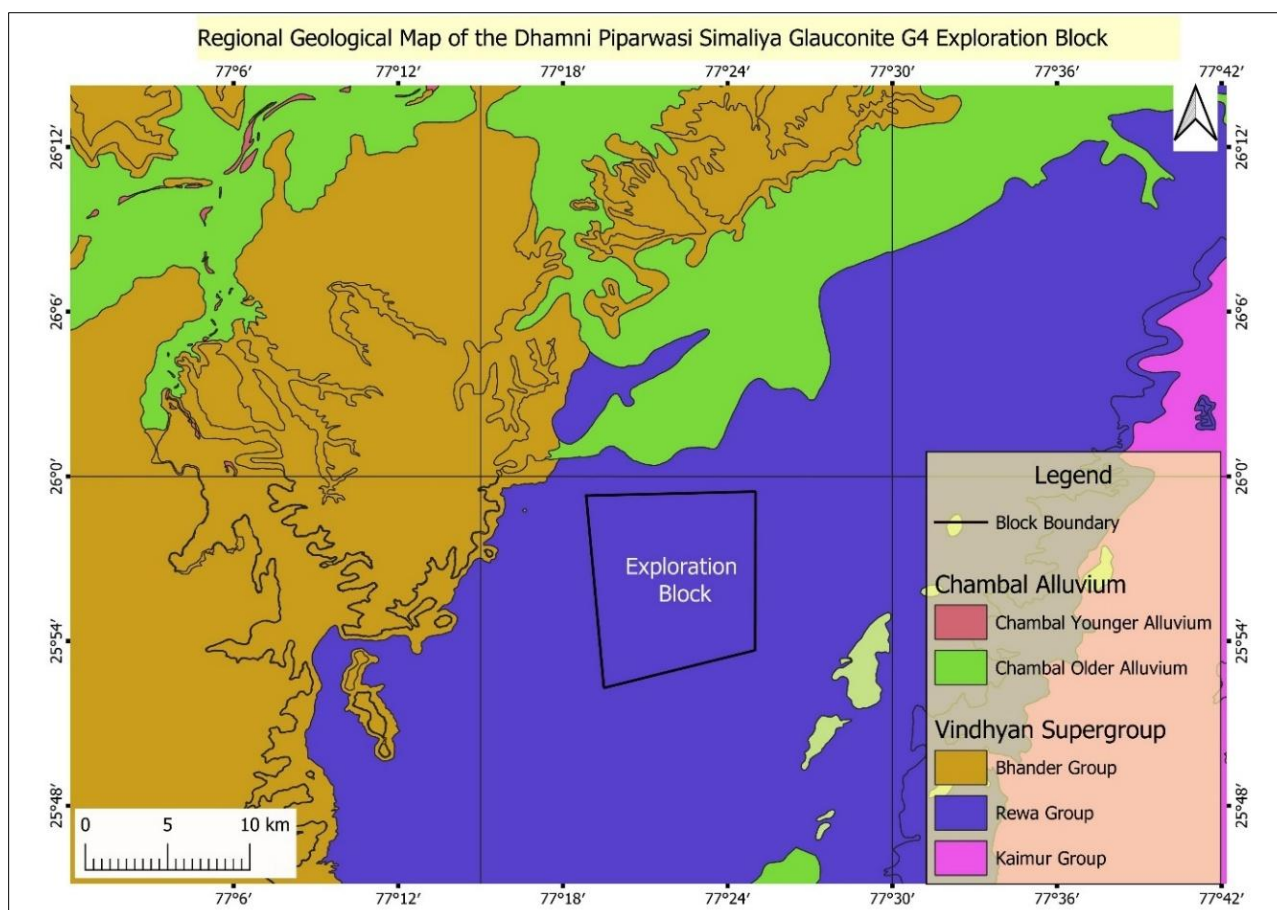


Figure 2 Overlay of block boundary on regional geological map (1:50000 Map from NGDR)

7.2 Local geology of the block area

This part of the report is based on Large Scale Mapping of the area carried out during this project, which covers parts of Sheopur district in Madhya Pradesh, belongs to the Upper Rewa Formation of the Rewa Group of the Vindhyan Supergroup of Upper Proterozoic age (Table 9). The litho-units exposed in the area are mainly sandstones, i.e. Govindgarh Sandstone. It is the oldest formation exposed in the area and is represented by sandstone with interbands of shales (Jadia & Shrivastava, 1989–90; Shrivastava & Mehrotra, 1989–90). The exposures of the Upper Rewa Sandstone Formation are found in the eastern part of the study area in the Simliya and Benipura region, and in the Khari and Piparwas area in the western part. A well-exposed succession is observed along the Jamka Kho tributary in the eastern region. The maximum thickness of the observed succession is about 20 m. Physically, the sandstone consists of white to dirty white, creamy white, greyish white, greenish grey colours, is fine to medium grained, thinly to thickly bedded, hard, massive and compact, and moderately to well sorted,

orthoquartzitic type. In some regions, the sandstone is flaggy in nature (Arun Dev & Danish, 2020–21).

Table 9 stratigraphy of the block area adopted from Jadia & Shrivastava, 1989–90; Shrivastava & Mehrotra, 1989–90

| Group | Formation | Member | Description |
|---|---|----------------|---|
| Recent/Quaternary | | | Alluvium / soil / laterite |
| Rewa Group | Upper Formation/ Govindgarh Formation | | Massive to thinly bedded sandstone, glauconite bearing at places, with interbands of siltstone, shale, and occasional lensoidal impure limestones |
| | Jhiri Formation | | Olive green to khaki green / reddish brown to chocolate brown splintery shale with interbands of ferruginous sandstone / siltstone |
| (Conformable sharp to gradational contact) | | | |
| Kaimur Group (part) | Bila Formation (part) | Duduani Member | White to dirty white, massive to thinly bedded sandstone with interbands of siltstone |
| BASE NOT SEEN | | | |

7. 3 Descriptions of lithologies mapped in the area

7.3.1. Sandstone

The dominant lithology across the study block is sandstone, forming thick sequences with wide areal distribution (Photograph 1). It is primarily fine- to medium-grained, with colour variations including white, creamy-white, greyish-white, and occasionally greenish-grey. The sandstone is typically hard, compact, and showing moderate to good sorting. In certain localities, flaggy characteristics are observed due to thin bedding, indicating variations in sedimentation rates. These physical features, combined with field exposures, suggest deposition in a shallow marine to nearshore environment.

Prominent sandstone outcrops are visible throughout the block, particularly in Simliya, Benipura, and along the Jamka Kho tributary, where the stratigraphic thickness reaches up to 20 meters. In Khari and Piparwasi areas, exposures are moderate and interbedded with shale. **Modal Analysis** (Annexure 21) shows it has **quartz-dominated composition (73.4%)**, with significant lithic fragments (19.4%), minor glauconite (6.2%), and a very low concentration of matrix (0.8%) and feldspar (0.2%).

Petrographic report (Annexure 22) shows sandstone is composed predominantly of fine-grained, anhedral quartz grains showing tight packing, interlocking textures, and well-developed triple junctions that indicate advanced diagenetic recrystallization and burial compaction under elevated pressure. Primary porosity has largely been lost due to these processes.



Photograph 1 *Showing Outcrop of bedded sandstone near Jhumka,*

7.3.2. Glauconitic Sandstone

The greenish-grey sandstone horizons observed at different locations within the block correspond to glauconitic sandstone (Photograph 2). Glauconite occurs as disseminations within the sandstone matrix as well as in discrete intercalated layers, indicating a stratiform mode of occurrence rather than localized or concentrated enrichment. The presence of glauconite was initially recognized during field observations and subsequently corroborated by geochemical analyses, which show elevated K_2O contents. The glauconitic horizons are limited in extent and could not be traced laterally beyond their observed occurrences

Although not economically significant in the current exploration phase, these glauconitic units highlight the favourable depositional environment under low oxygen marine shelf conditions, indicative of slow sedimentation with intermittent siliciclastic input. This makes the block worthy of low-scale localized interest for glauconite.

Thin sections (Annexure 22) collectively reveal a glauconite-rich lithology with variable modal abundances, ranging from 10% to nearly 80%. In two samples, glauconite dominates (70–80%), occurring as rounded to sub-rounded green grains under plane-polarized light, often dispersed within a fine siliceous matrix along with subordinate quartz, feldspar, and occasional

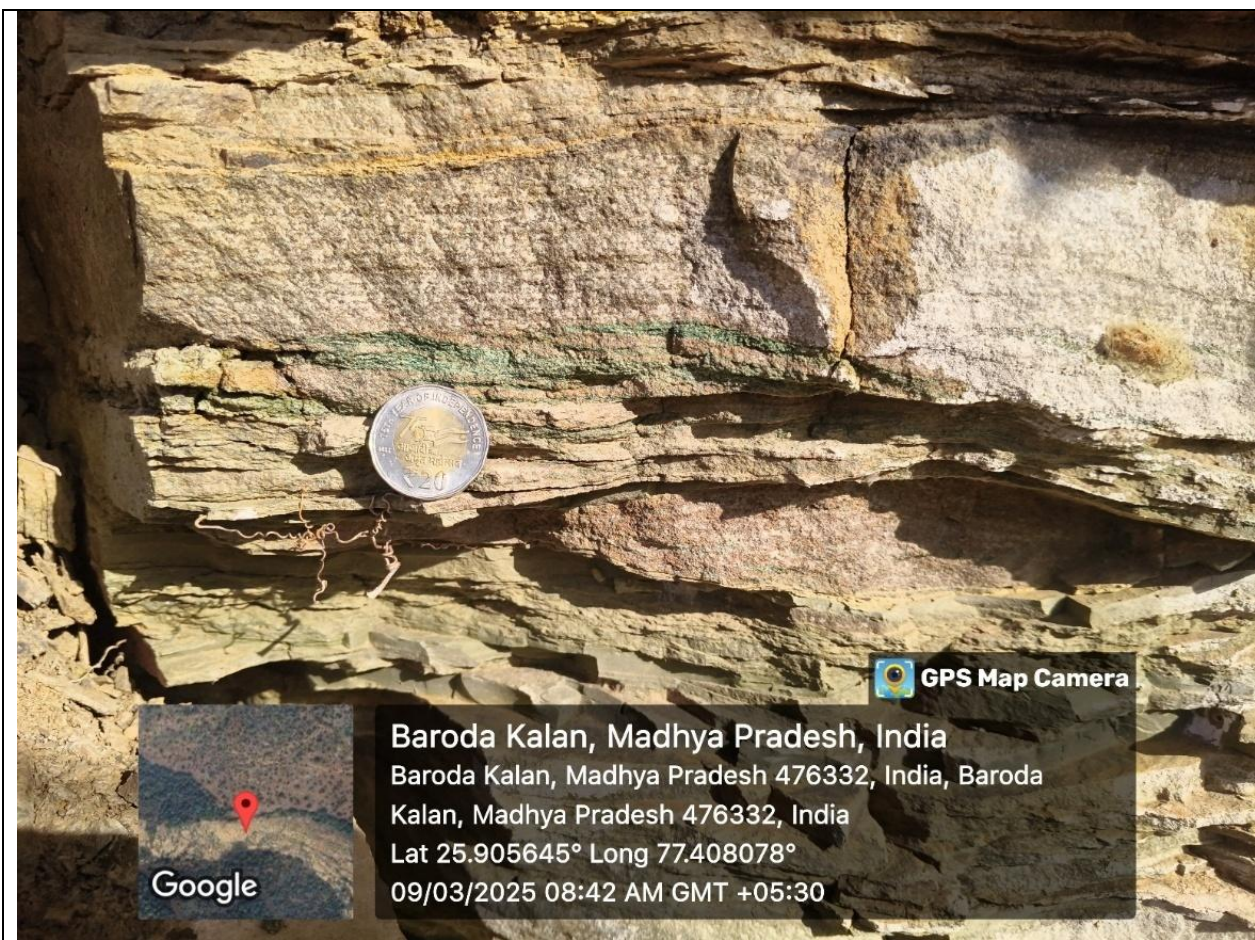
lithic fragments. These glauconite-rich facies show matrix-supported fabrics, moderate to poor sorting, and evidence of reworking, consistent with deposition under relatively low-energy conditions with mixed sediment input and subsequent sediment recycling. In contrast, the third sample is quartz-dominated, with medium-grained, moderately sorted, sub-rounded quartz grains and only about 10% glauconite, which occurs as rounded grains locally aligned along weak planes, suggesting limited glauconitic enrichment within an otherwise quartz arenite framework. Together, these petrographic features indicate a single lithology characterized by heterogeneity in glauconite content, reflecting fluctuating depositional energy and sediment supply in a shallow marine to marginal setting, with episodes of glauconite concentration through reworking and localized enrichment, followed by continued burial diagenesis.

Modal analysis (Annexure 21) of the selected glauconitic sandstone samples (DPS01 and DPS04) highlights the overwhelming dominance of glauconite, comprising 80.6% and 72.2% of the respective modal compositions. In both cases, quartz occurs as a fine-grained matrix (11.6% in DPS01 and 18.4% in DPS04), with lithic fragments making up 7.7% and 9.4% respectively. Notably, the quartz grains are consistently finer than typical sand size, reinforcing the presence of a very fine-grained matrix. The exceptionally high glauconite content in both samples confirms the development of a glauconite-rich lithounits of considerable significance, consistent with petrographic observations of glauconite-rich sandstone within the sequence. Phase analysis for identification of K₂O hosting mineral by XRD (Annexure 24) suggest that glauconite phase is responsible for localized K₂O enrichment.

7.3.3. Intercalated Sandstone Shale

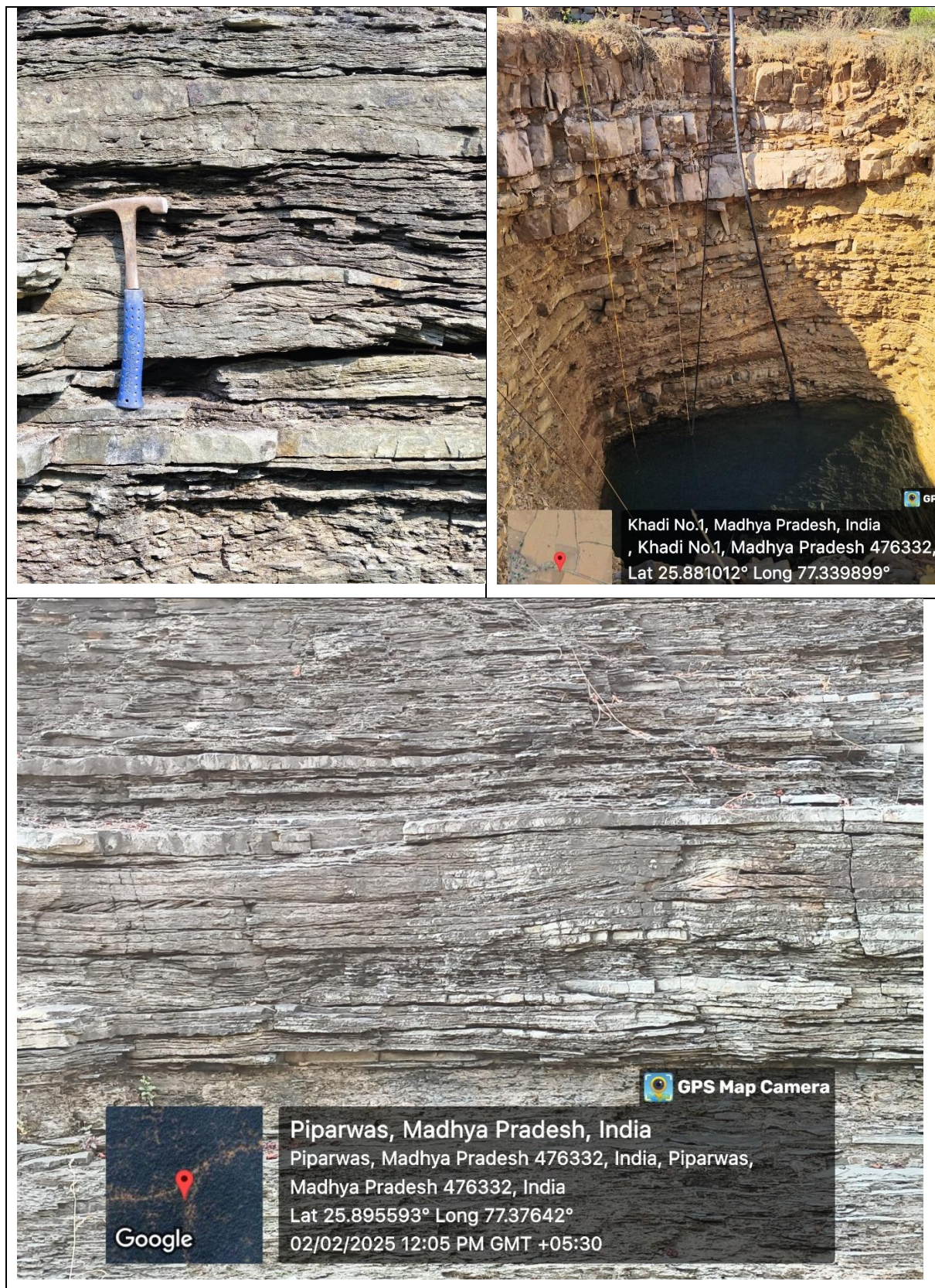
In several parts of the formation, especially in southern sectors, shaly sandstone has been identified (Photograph 3). These zones consist of sandstone interbedded with shale and siltstone bands. The interbedding creates a layered lithology with varying resistance to weathering, causing scattered exposures on the surface. This rock type represents episodic sediment influx, likely tied to fluctuating depositional regimes in a nearshore transitional environment.

The thin soil cover (1–2 feet) throughout much of the block enables good visibility and access to these interbedded zones, supporting effective field mapping and sampling



Photograph 2 Showing Exposer of Glauconitic Bearing Sandstone Bed, near Barodakalan,

Within the sandstone–shale intercalated lithology, the shale thin section reveals a very fine-grained, laminated fabric dominated by a clay-rich matrix. Distinct calcite-rich laminae, composed of coarse micritic to microsparry calcite, interrupt the shale layers and correspond with field observations of strong effervescence. Occasional silt-sized detrital quartz grains are dispersed within the matrix, while opaque minerals are locally concentrated in the carbonate-rich zones. Under PPL, calcite shows low relief and under XPL it displays clear third-order interference colours, indicating secondary recrystallization during early diagenesis. These petrographic features confirm the calcareous nature of the shale component interbedded with glauconitic sandstone, reflecting alternating siliciclastic input and episodic carbonate enrichment within the depositional setting.



Photograph 3 Showing Intercalated Sandstone shale sections near Khari Piparwas area,

7.4 Structural Details

The structural characteristics of the Govindgarh Sandstone Formation within the study block can be broadly classified into **primary (sedimentary)** and **secondary (deformational)** structures. These features provide important insights into the depositional environment and post-depositional tectonic evolution of the region.

7.4 1 Primary Sedimentary Structures

Bedding & Laminations

Bedding is well-preserved throughout the block and is clearly visible in sections and exposures. The sandstone beds of the **Govindgarh Formation** exhibit variable bedding thicknesses from thin to thick, and are prominently exposed due to limited soil cover. Bedding is nearly horizontal with 2 to 3 degree rolling dip towards south west. Laminations are observed in shale and shale intercalations in sandstone (Photograph 4.)



Photograph 4. Left one Showing Laminations while right one Bedding in Dhamni-Piparwasi Simliya area, Sheopur district, Madhya Pradesh block

Ripple marks

Ripple marks are well-developed in the Govindgarh Sandstone Formation within the Dhamni–Piparwasi–Simliya Block. Both symmetrical and asymmetrical ripple marks (Photograph 5) were observed on exposed bedding planes, indicating deposition under alternating wave and current conditions, suggestive of a shallow marine to deltaic environment. The ripple wavelength ranges from 3 cm to 20 cm, with amplitudes between 2 mm and 2 cm, and a ripple index generally between 5 and 10. Preliminary field observations of ripple crest orientations indicate a probable paleocurrent direction trending from northwest to west-northwest.



Photograph 5. Showing Asymmetrical Ripple marks in a outcrop in Dhamni-Piparwasi Simliya area, Sheopur district, Madhya Pradesh block, Hammer Head Oriented towards north.

7.4.2 Secondary (Deformational) Structures

Joints: Joint sets are well-developed in the Govindgarh Sandstone across the study area. The joints are typically **vertical**, two dominant vertical joint sets are consistently observed (Figure

4): **Joint Set 1:** Mostly strikes around **130°**, ranging from **110° to 150°**, **Joint Set 2:** Usually between **40° and 80°**.

Joints are typically **vertical** and **orthogonal or sub-orthogonal**, reflecting brittle deformation without significant tectonic folding or faulting. These joints, particularly in sandstone, influence **rock breakage, permeability, and weathering**, which are important for both geological interpretation and resource assessment.

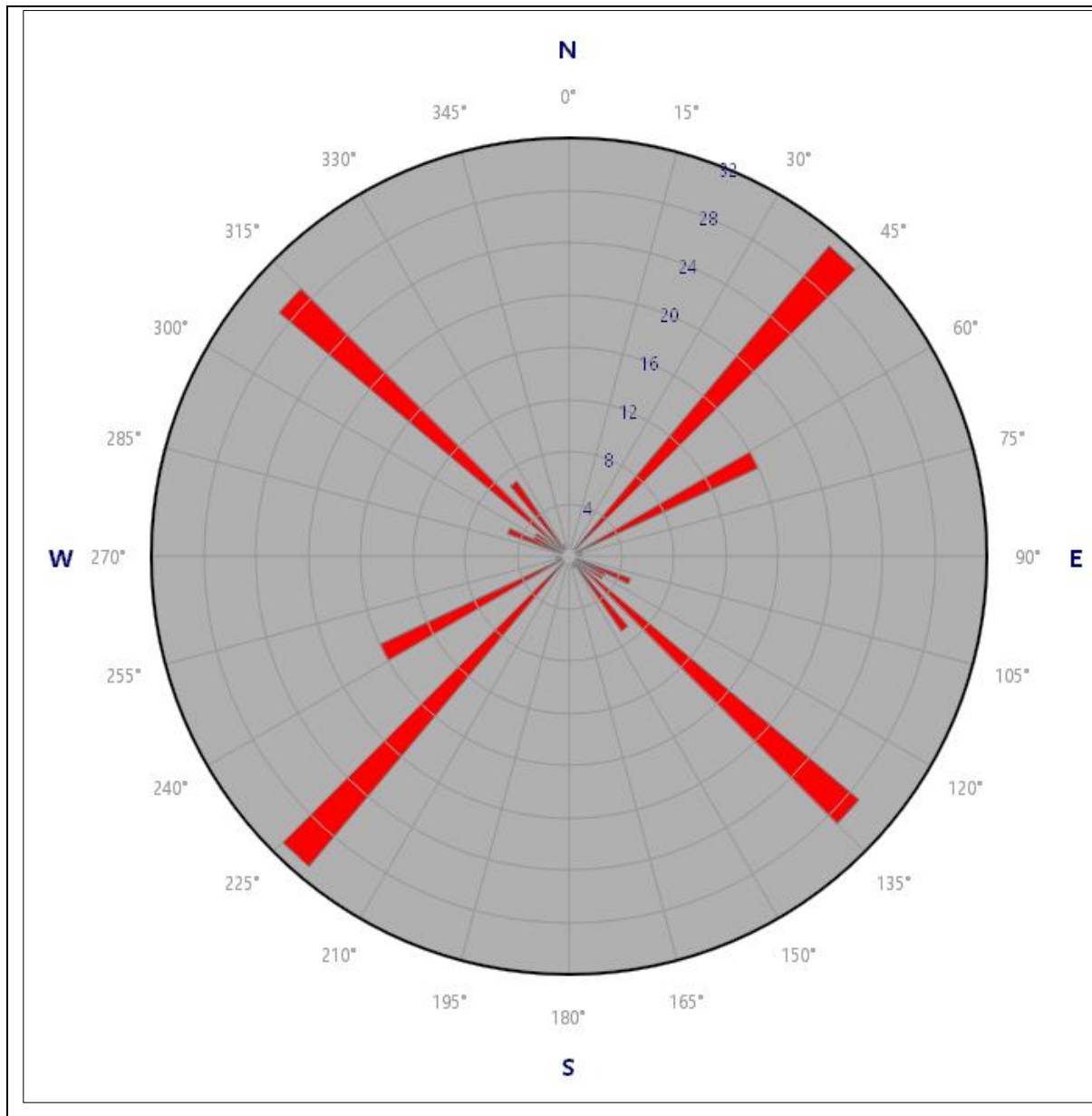


Figure 3 Rose Diagram of Joints, in Dhamni-Piparwasi Simliya area, Sheopur district, Madhya Pradesh



Photograph 6 Showing Joint Patterns in rock exposers in in Dhamni-Piparwasi Simliya area, Sheopur district, Madhya Pradesh ,

7.5 Sedimentation and Provenance

Petrographic analyses and field observations from the present study suggest that the deposition of clastic sediments of the Upper Rewa Formation occurred in a shallow marine shelf environment characterized by fluctuating energy conditions and episodic sediment supply. The moderate to good sorting, sub-rounded to well-rounded quartz grains, and overall textural maturity observed in the sandstones indicate prolonged sediment transport and reworking. The frequent occurrence of glauconite, especially in samples such as DPS01 and DPS04, points toward low sedimentation rates, a typical condition favoring glauconite formation. In contrast, samples like DPS25, which are dominated by tightly packed quartz grains showing diagenetic overprinting, reflect either higher-energy depositional settings or deeper burial conditions.

The earlier findings of Mehrotra and Shrivastava (1989–90), who reported that the deposition of Upper Rewa Formation sediments occurred under shallow water conditions, evidenced by the presence of cross-bedding, ripple marks, and glauconite—the latter indicative of a **shelf to tidal marine environment**. They also noted poor sorting, feldspar presence, and interbeds of siltstone/shale, reflecting low to moderate energy conditions and minor basin fluctuations. Their identification of impure and cherty limestone with oolitic structures in the upper parts of the formation suggests deposition under turbulent shallow water conditions, supporting the interpretations derived from the present investigation.

XRD phase identification shows presence of glauconite as the principal K₂O-hosting mineral supports formation under, Low-sedimentation, marine shelf conditions, slightly reducing to sub-oxic environments, Slow burial and prolonged residence time at the sediment–water interface Subsequent carbonate cementation, diagenesis, and surface/near-surface weathering resulted in partial amorphization of K-bearing phases without complete loss of structural potassium.

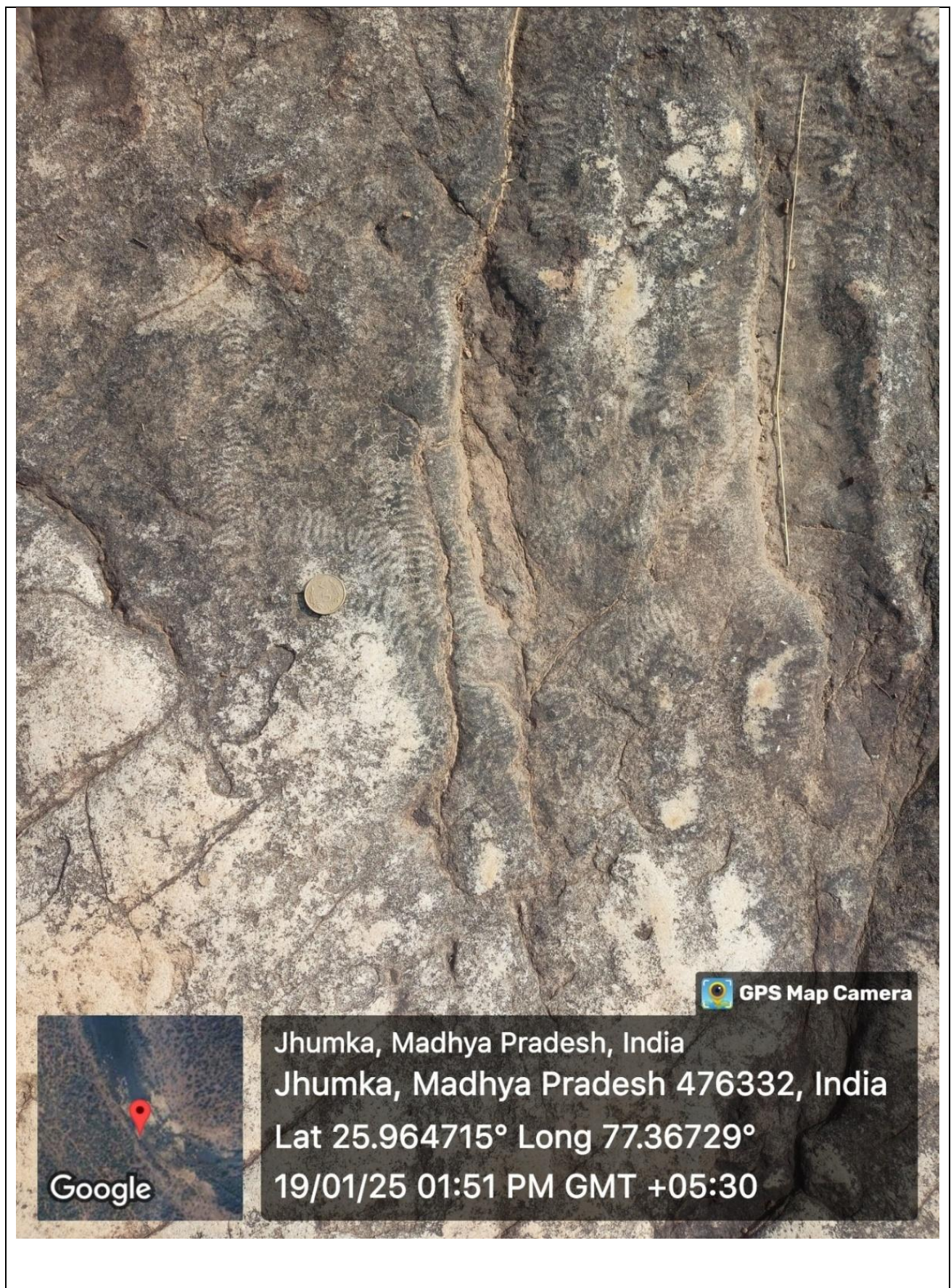
Field observations reveal the presence of interbedded sandstone, siltstone, and shale, representing minor fluctuations in energy and depth within the depositional basin. The presence of ripple marks, cross-bedding, and load casts supports the interpretation of shallow water depositional conditions. The glauconitic horizons further indicate deposition in a shelf to **tidal marine environment**. The observed alternations of fine- and coarse-grained sediments, as well as sedimentary structures, are consistent with a transgressive depositional system, characterized by shifting shoreline positions and dynamic hydrodynamic regimes.

The paleocurrent indicators, such as the orientation of cross-bedding and ripple marks, suggest a paleocurrent direction from east to southeast to west-northwest, implying that the **provenance lay toward the east and southeast of the mapped area**. The presence of feldspar grains indicates mineralogical immaturity, further supporting a **proximal granitic source**. These features collectively suggest a mixed sediment source, predominantly granitic, with limited sediment recycling and short transport distance.

Together, both the current study and earlier works converge on a model of shallow marine sedimentation influenced by variable hydrodynamics, proximity to a granitic hinterland, and intermittent sediment supply, leading to the development of glauconitic sandstone with significant provenance implications.

7.6 Trace Fossils?

Well-preserved trace fossils were observed (Photographs 8.7, 8.8) on bedding planes of fine- to medium-grained sandstone at Jhumka (Lat 25.964715°N; Long 77.36729°E) and Piparwas (Lat 25.895593°N; Long 77.37642°E), Sheopur District, Madhya Pradesh. The traces occur as bilaterally symmetrical, elongated to oval impressions ranging from 8 to 20 cm in length and 3 to 8 cm in width. The margins of the traces exhibit a series of fine, transverse to crescentic scratch-like markings arranged in a repetitive pattern, interpreted as locomotory or feeding traces of arthropods. Similar trace fossils have previously been documented from the Rewa Group of the Vindhyan Supergroup (Kumar & Pandey, 2008).



Photograph 7 Fossils Impressions are observed near Jhumkha,



Photograph 8 Fossil Impressions are observed near Piparwasi,

7.7 Mineral Prospect

The prospect for glauconite mineralization in the study area is supported by both surface observations and detailed subsurface investigations, including petrographic and geochemical analyses. The evidence collectively indicates that glauconite occurs in varying concentrations across multiple lithological units, predominantly within glauconitic sandstones and interbedded shale-sandstone sequences, which are typical of a shallow marine depositional environment.

7.7.1 Surface indication of mineralization

Surface manifestations of glauconite mineralization are clearly visible in several parts of the study area, especially near Kharee and Piparwasi villages. Greenish-grey glauconitic sandstone outcrops with disseminated pellets and thin glauconitic bands have been identified another lithology is shale and sometimes sandstone shale intercalations, based on the modal analysis of selected minerals. glauconite in glauconitic sandstone and glauconitic lithic arenite ranges from 80 percent to 70 percent and up to 6 percent glauconite. These occur not only in prominent exposures along roadsides and river sections but also as part of sandstone–shale alternations in localities like Jhumka Khoh, Dhamini, and Piparwasi. In many places, glauconitic beds of about 5 inches in thickness are found interlayered within sandstone and shale successions. The weathered surfaces often display a distinct greenish tint due to glauconite enrichment, aiding field identification. Supporting this, geochemical analyses using portable XRF revealed elevated K_2O values in these units, ranging from 0.70% to 3.65%. A significant proportion of samples (around 44%) recorded K_2O values equal to or greater than 1.0%, and approximately 5.5% exceeded 2.0%, strongly reinforcing surface indications of glauconite presence.

7.7.2 Mode of occurrence

Glauconite in this region occurs primarily in disseminated and banded forms. The most common mode of occurrence is as dispersed pellets within medium- to fine-grained sandstones, particularly in the Kharee–Piparwasi region, where glauconite comprises a major portion of the rock fabric. In some cases, glauconite-rich layers or lenses are observed within shale–sandstone alternations and calcareous shale units. Petrographic studies further confirm the presence of matrix-supported glauconitic sandstone, with glauconite grains forming up to 80% of the modal composition in some sections. The grains are typically rounded to sub-rounded, indicating

some degree of sediment transport and reworking before final deposition. Additionally, certain samples exhibit localized glauconite-rich pockets within otherwise glauconite-poor matrices, indicating selective settling under varying energy conditions. Glauconite is thus mainly authigenic but displays signs of reworking and multi-stage sediment input.

7.7.3 Details of Mineralization

Thin sections show variations from immature, lithic-rich glauconitic sandstones to mature quartz arenites with sparse glauconite presence. In the more enriched units, glauconite constitutes up to 80% of the rock's modal composition, with grains ranging from sub-rounded to well-rounded and exhibiting green hues in plane-polarized light. Geochemically, K₂O values from surface samples range between 0.70% and 3.65%, with around 44% of the samples showing K₂O \geq 1.0%, and 5.5% surpassing 2.0%. Additionally, ICP-MS analysis indicates lithium (Li) content varying from 2.2 ppm to as high as 383.9 ppm. Several samples such as DPS-1 to DPS-5, DPS-63, and DPS-S-114 exhibit both high K₂O and high Li concentrations, suggesting a strong K₂O–Li correlation. This points toward lithium substitution within the glauconite structure or association with other fine-grained clay minerals. An approximately 15 km² area around Khari and Piparwasi villages hosts clustered anomalies of elevated K₂O and Li, defining a potentially favourable glauconite-bearing zone with possible economic interest.

7.9.4 Genesis of glauconite formation

The glauconite mineralization observed in the area, specifically within the Govindgarh Formation sandstone of the Rewa Group, is interpreted as primarily syngenetic to early diagenetic in origin, with later reworking evident in some sandstone units. This interpretation is supported by field mapping and petrographic analyses, which confirmed the presence of greenish-grey glauconitic sandstones, especially in the Kharee and Piparwasi regions. The genesis of this glauconite is attributed to a specific interplay of physical and chemical conditions within an ancient shallow epeiric sea characterized by exceptionally low rates of sedimentation, which provided the necessary time for the mineral to mature in place (an authigenic process). The process involved the in-situ replacement of porous precursor materials, such as detrital K-feldspar grains and clay pellets, facilitated by a source of potassium from altering K-feldspars and iron from the surrounding environment. This transformation took place under mildly reducing or suboxic conditions within the sediment pore waters. Glauconite (KMg(Fe, Al) (SiO₃)₆ • 3H₂O) occurs as disseminated green pellets and flakes primarily hosted within ferruginous sandstone and shale interbeds. Authigenic

glauconite formed under marine conditions is preserved in matrix-supported sandstones with fine siliceous material. Thin sections reveal various degrees of glauconite enrichment, from trace levels in mature quartz arenite to glauconite-dominant compositions in glauconitic lithic arenite. The glauconite grains exhibit a characteristic green color under plane-polarized light and are mostly rounded, suggesting low to moderate energy deposition. The mineralization is strata-bound and lithologically controlled, mostly confined to glauconitic sandstone and shale–sandstone intercalations. The presence of quartz, feldspar, lithic fragments, and occasional micas in association with glauconite indicates a mixed provenance with moderate sediment maturity. The mineralization is typically found within sedimentary sequences of marine origin, deposited under conditions favorable for glauconite formation and subsequent preservation. The host sandstones are moderately sorted, suggesting a low-energy marine shelf depositional setting, where glauconite occurs as disseminated pellets and occasional thin bands, rather than massive accumulations.

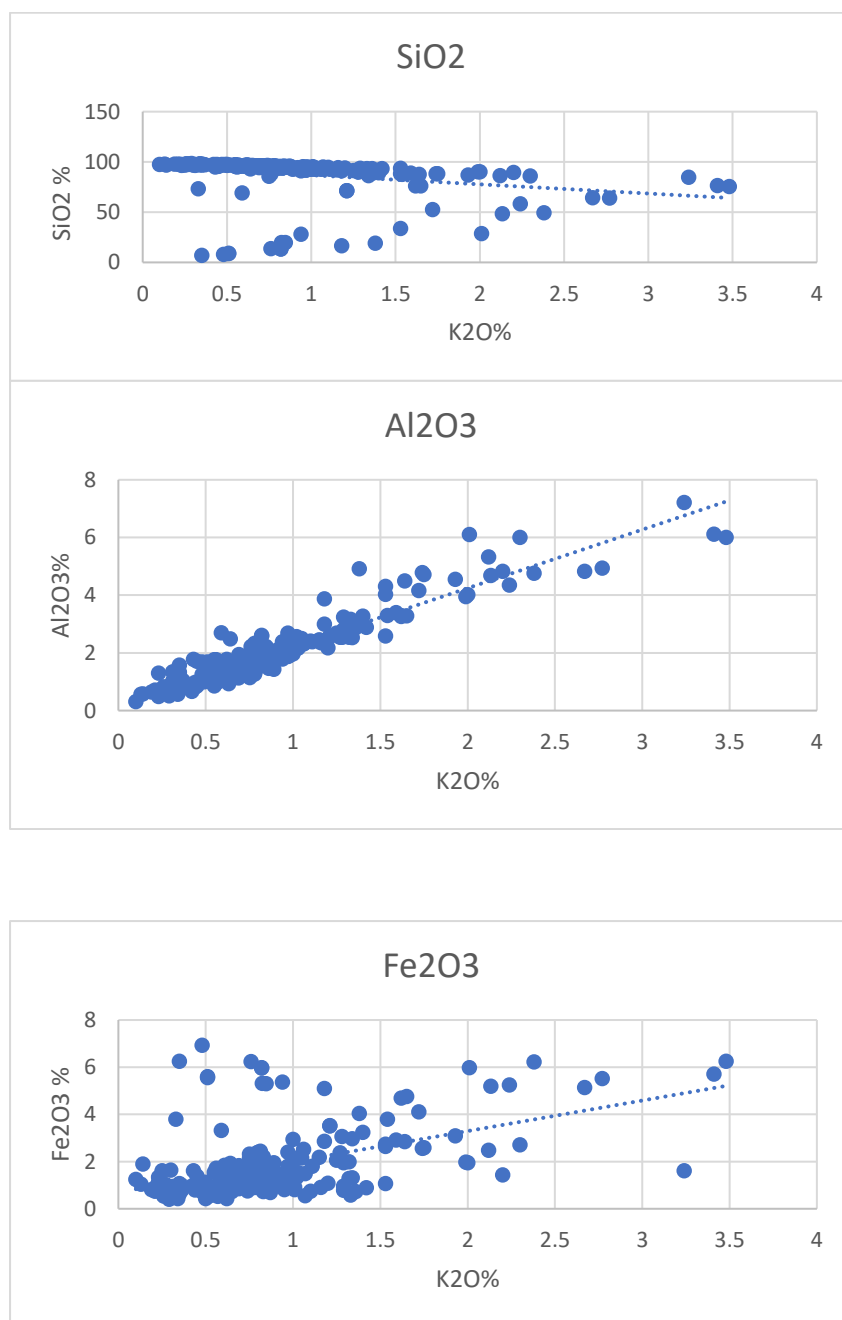
7.9.5 Statistical correlation analysis:

Statistical analysis confirms the predicted mineralogical relationships. The extremely strong correlation ($r=0.94$) between K_2O and Al_2O_3 reflects structural potassium binding within glauconite-illite phyllosilicates (formula: $(K,Na)(Fe^{3+}, Al^{3+}, Mg^{2+})_2(Si,Al)_4O_{10}(OH)_2$), as verified by XRD (Section 7.6, Shiva Labs). Moderate Fe_2O_3 correlation ($r=0.51$) indicates Fe-substitution in octahedral sites, while weak inverse SiO_2 relation ($r=-0.25$) reflects quartz dilution of glauconitic matrix. These relationships statistically validate the glauconite-illite control on geochemistry predicted by mineralogy.

Pearson correlation analysis was performed on major oxide data from 200 surface samples (150 bedrock + 50 pit samples) analysed by XRF. The Pearson correlation coefficient (r) measures linear relationship strength between variables, ranging from -1.0 (perfect inverse) to +1.0 (perfect positive), with $r=0$ indicating no linear relationship. Microsoft Excel 365 (CORREL function) performed on Raw XRF major oxides (no normalization required; analytical totals 76-99%) with Sample size: $n=200$ (surface samples) and Two-tailed t-test ($p<0.001$ for all pairs)

Table 10 Correlation Matrix Calculation of selected oxides of surface samples

| Oxide Pair | r-value | p-value | Geological Interpretation |
|--|---------|---------|---------------------------|
| K ₂ O vs Fe ₂ O ₃ | 0.51 | <0.001 | Moderate-strong positive |
| K ₂ O vs Al ₂ O ₃ | 0.94 | <0.001 | Extremely strong positive |
| K ₂ O vs SiO ₂ | -0.25 | <0.001 | Weak-moderate inverse |

Figure 4 Scatter Plot showing K₂O relationship with Al₂O₃, SiO₂, and Fe₂O₃ in surface samples

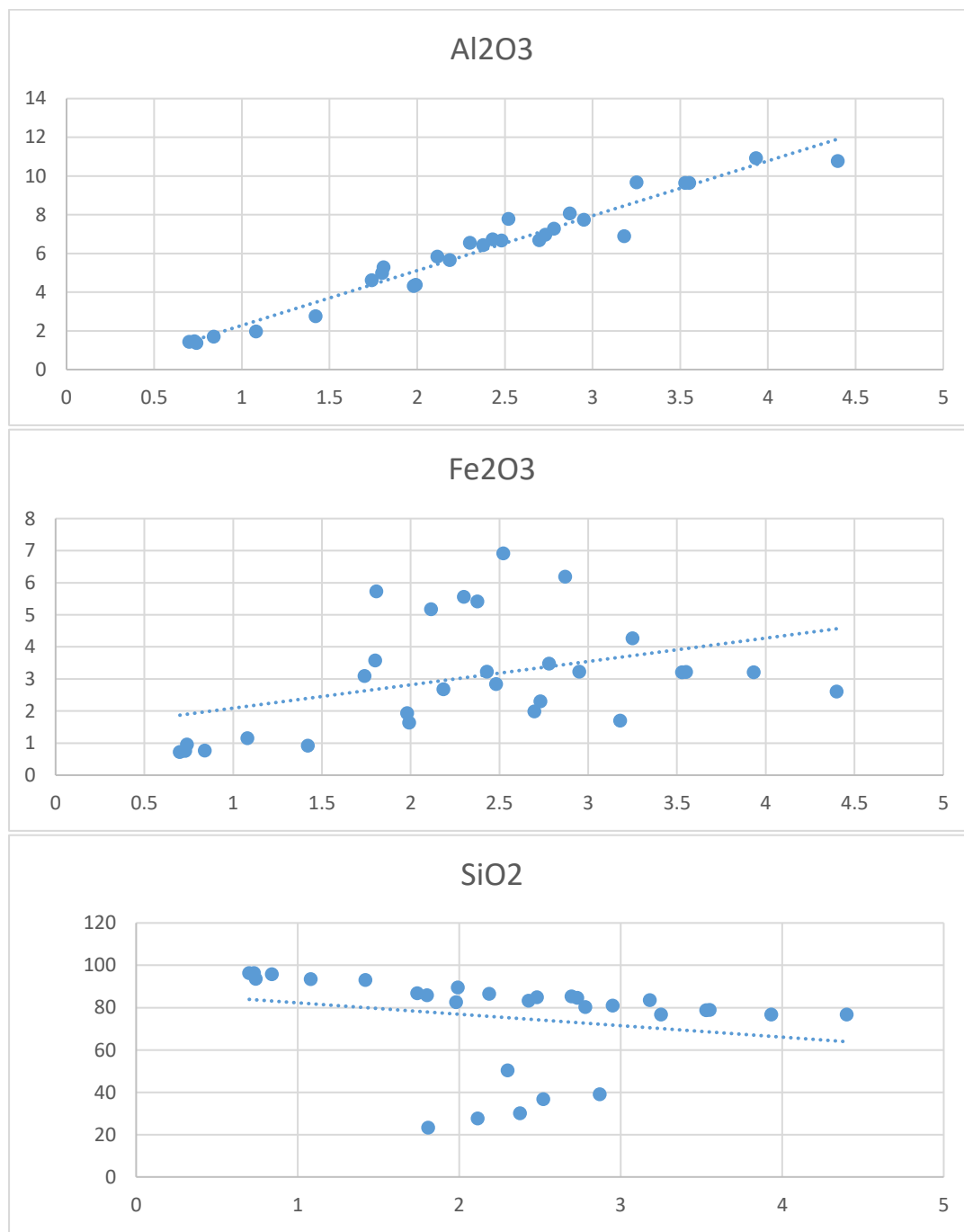
Scatter Plot of $K_2O\%$ against Al_2O_3 , Fe_2O_3 , SiO_2 in Borehole samples**a. DPS BH1**

Figure 5 Scatter Plot showing K_2O relationship with Al_2O_3 , SiO_2 , and Fe_2O_3 in Borehole DPS BH-1

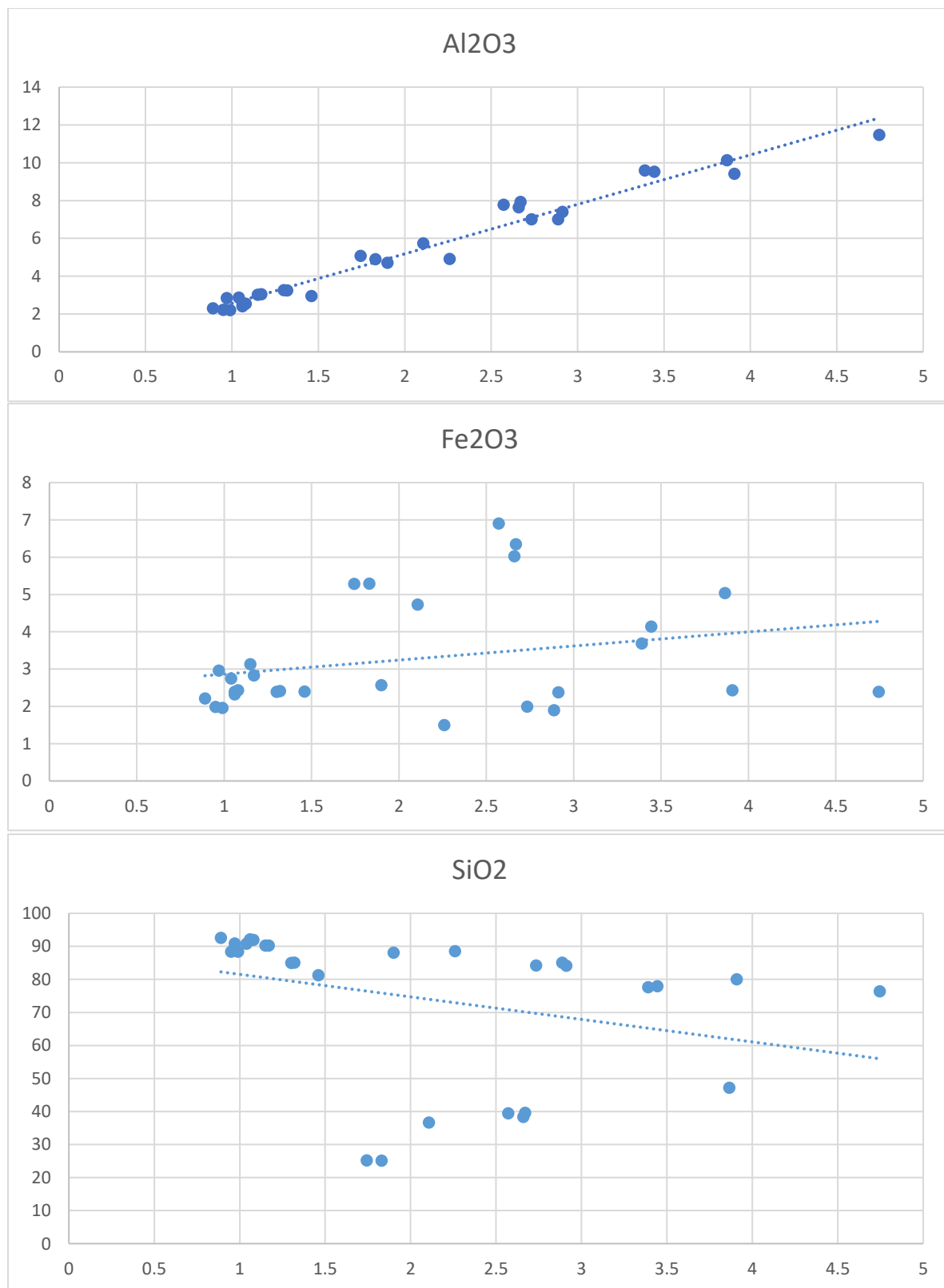
b. DPS BH2

Figure 6 Scatter Plot showing K_2O relationship with Al_2O_3 , SiO_2 , and Fe_2O_3 in Borehole DPS BH-2

77°21'0"

77°24'0"

77°27'0"

25°57'0"

25°57'0"

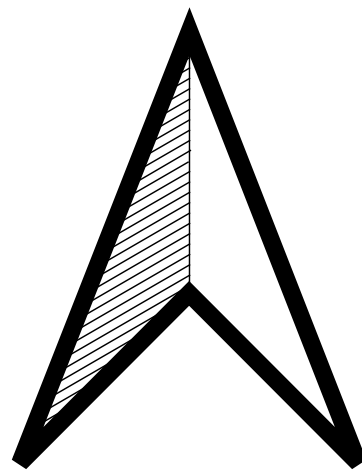
25°54'0"

25°54'0"

77°21'0"

77°24'0"

77°27'0"



OUTCROP GEOLOGICAL MAP OF DHAMINI-PIPARWASI SIMLIYA
AREA, DISTRICT SHEOPUR (M.P.)
MAPPING SCALE : 1: 12500

PROJECT: RECONNAISSANCE SURVEY (G4) FOR GLAUCONITE
AND ASSOCIATED MINERALIZATION IN DHAMINI - PIPARWASI
SIMLIYA AREA, SHEOPUR DISTRICT, MADHYA PRADESH

FUNDED BY NMET
EXECUTED BY MMPL PRIVATE LIMITED

Legend

- Block Boundary
- River
- Waterbody
- Dip and Strike
- Joint

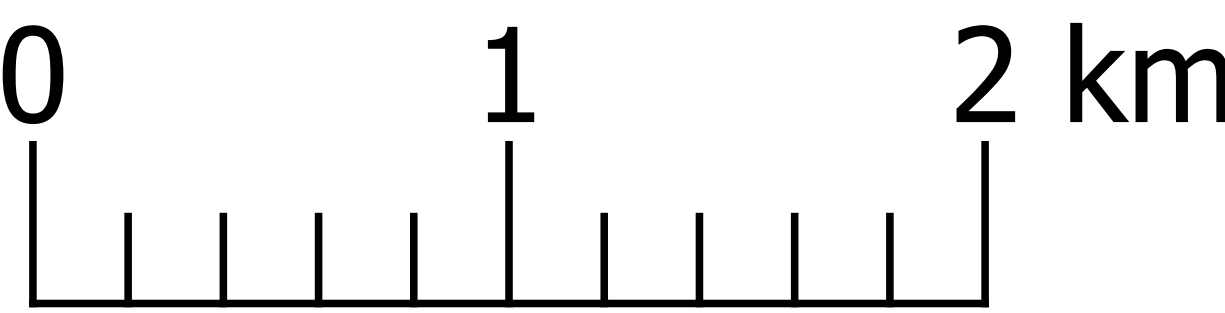
Lithological units

- Soil Cover
- Glauconitic Sandstone
- Sandstone
- Intercalated Sandstone Shale

Stratigraphic units

- Quaternary
- Vindhyan Supergroup
- Rewa Group
- Govindgarh Formation

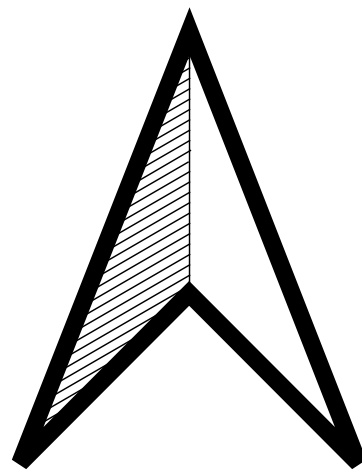
1:12,500



77°21'0"

77°24'0"

77°27'0"



LARGE SCALE GEOLOGICAL MAP OF DHAMINI-PIPARWASI
SIMLIYA AREA, DISTRICT SHEOPUR (M.P.)
MAPPING SCALE : 1: 12500

PROJECT: RECONNAISSANCE SURVEY (G4) FOR GLAUCONITE
AND ASSOCIATED MINERALIZATION IN DHAMINI - PIPARWASI
SIMLIYA AREA, SHEOPUR DISTRICT, MADHYA PRADESH

FUNDED BY NMET
EXECUTED BY MMPL PRIVATE LIMITED

Legend

- Block Boundary
- River
- Waterbody
- Dip and Strike
- JOINT.

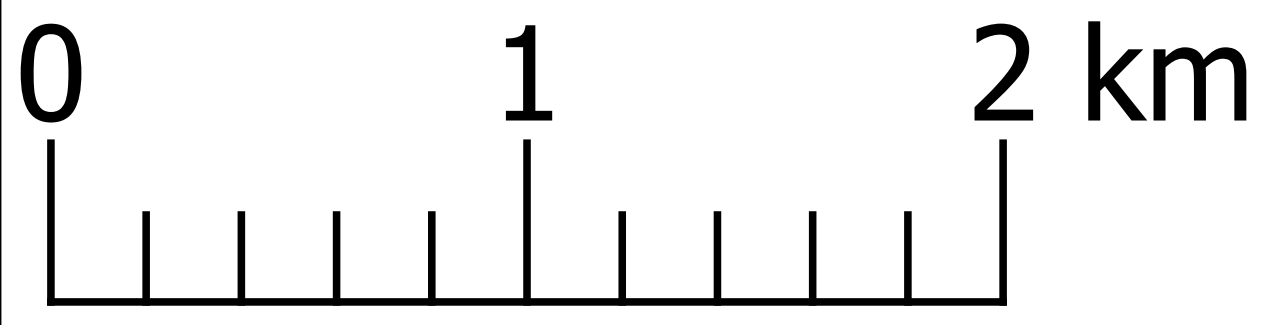
Lithological units

- Glauconitic Sandstone
- Sandstone
- Intercalated Sandstone - Shale

Stratigraphic units

- Vindhyan Supergroup
- Rewa Group
- Govindgarh Formation

1:12,500



77°21'0"

77°24'0"

77°27'0"

25°57'0"

25°54'0"

25°57'0"

25°54'0"

Chapter-8: Previous Exploration

Previous geological exploration in the region encompassing the present study area—which now falls in Sheopur district but was part of Morena district during earlier surveys—has provided significant insight into the stratigraphy and mineralogical characteristics of the Vindhyan Supergroup.

A geological mapping of a 700 sq. km area in Morena district, MP was carried out by Jadia and Shrivastava (FS 1989-90) on a scale of 1:50,000 encompassing portions of toposheet Nos. 54G/1 & 5 revealing rocks from Vindhyan Supergroup which comprises of Upper Rewa Sandstone of Rewa Group and Ganurgarh Shale, Bhandar Limestone and Lower Bhandar Sandstone of Bhandar Group. In the Upper Rewa Sandstone thin bands of glauconitic sandstone have been observed in the Kapeli Nadi region south of Kapeli Hor, in the Nala regions west of Basantpura and southeast of Dhamni along the Dham River. With roughly 5-10% glauconite (visual estimate), this sandstone is fine grained, light green, thinly bedded and moderately sorted suggesting that the Rewa Group (in the present area) was deposited under marine conditions. Presence of primary features such as ripple marks and current bedding in sandstone indicate shallow water marine depositional environment.

Srivastava and Mehrotra (FS1989-90, GSI) carried out a systematic geological mapping of Vindhyan Supergroup on a scale of 1:50,000 in parts of the district of Shivpuri and Morena, Madhya Pradesh. A total of about 702 sq. km were covered, including parts of Survey of India toposheets No. 54G/5 and 54G/9 stating Dadauni Member of Bila Formation of Kaimur Group is the oldest lithological unit exposed in the area which is conformably overlain by Jhiri Formation and Upper Rewa Formation belonging to Rewa Group. From their study, Upper Rewa Formation is mostly exposed from Dhodha-Burera in east (toposheet No – 54G/9) to Bagwani-Piparwas-Surae-Magarda-Dubera in the west (Toposheet No. 54G/5) giving a total thickness of about 200m. This unit consist of two distinct sandstones i.e. massive to thickly bedded grayish white to pinkish white, coarse to medium grained sandstone containing a few feldspars and glauconite grains as well as flaggy to thinly bedded, medium to fine grained, greenish white to dirty white glauconitic sandstone with siltstone intercalation. The formations in the Rewa Group exhibit minor folding and non-plunging folds within the thinly bedded sandstone and siltstone indicating the sediments in the area have suffered minimal deformation. In general, the lithounits show NNW-SSE to NNE-

SSW trend with occasional EW trend. They show good joint development. All lithological units commonly show primary sedimentary features such as cross bedding, ripple marks etc indicating shallow water deposition while oolitic structures in the western part of Upper Rewa Formation suggests turbulent shallow water environment.

An adjacent area was also studied by Ramteke and Patel (FS 1989–90), who mapped about 710 sq. km within toposheets 54G/1 and 54G/2 in Morena district. Though outside the current block, this area shares similar lithological characteristics, with the Upper Rewa Sandstone representing the oldest exposed formation, containing intercalated sandstone and shale. The presence of glauconite here further reinforces the shallow marine depositional setting. Their work also recorded minor tectonic features, such as broad warping and variations in formation altitudes, without significant structural disturbances.

More recently, the Geological Survey of India (GSI) undertook **National Geochemical Mapping (NGCM)(Figure 1)** in parts of Shivpuri and former Morena districts (Toposheet 54G/05) during the 2020–21 field season (FSP ID: M1AGCS-GCM/NC/CR/SU-MP-BHO/2020/29746), covering an area of approximately 700 sq. km on 1:50,000 scale, bounded by 25°45'N–26°00'N and 77°25'E–77°50'E. The mapped region comprises predominantly the Rewa and Bhandar Group rocks of the Vindhyan Supergroup. Glauconitic sandstone occurrences were recorded near Dubera, Kopli Nadi, Kopli Hor, and Dham. Importantly, the **current study area**, including **Dhamni, Piparwasi, Simliya, Khari, and Badoda Kalan villages**, lies within this NGCM-mapped territory, offering direct geochemical correlation with the ongoing exploration effort. The NGCM survey placed special emphasis on Potassium (K_2O) as an element of interest. Analytical results showed K_2O values ranging from **1.45% to 3.30%**, with a mean of **2.26%**, and higher concentrations found near Khari (NW), south of Galai, and in areas near Magarda, Bheelpura, and Bagwani. These values are linked to glauconite-bearing facies within the **Govindgarh Sandstone Formation**—a member of the Rewa Group—and strengthen the case for glauconitic sandstone as a potential K-bearing resource in the region.

A K_2O contour map (figure.) generated using NGCM data and supplemented by field results clearly highlights zones of elevated potassium, particularly in and around **Dhamni, Piparwasi, Simliya, and Khari**, supporting their significance for future exploration and resource estimation.

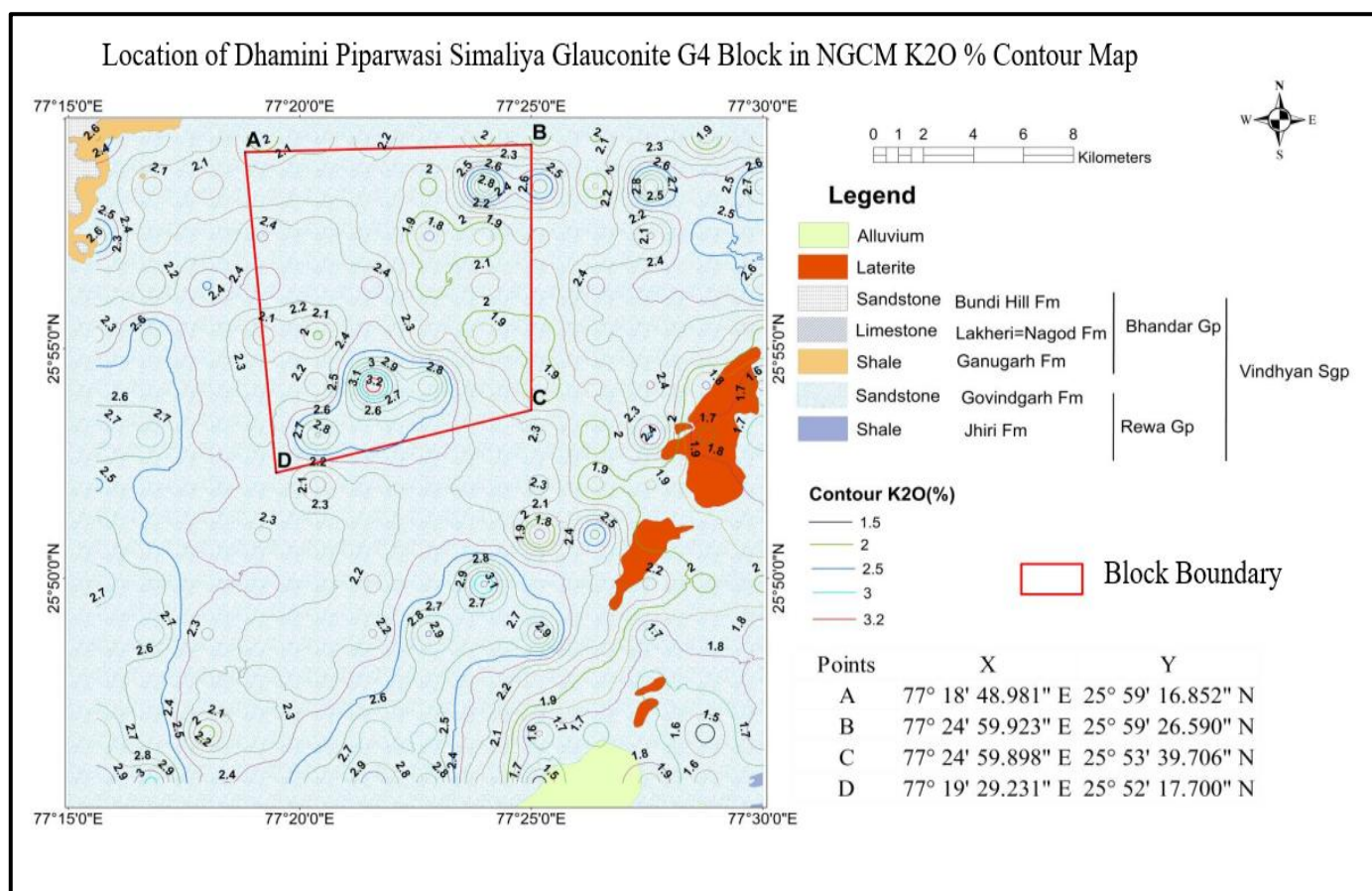


Figure 7 K2O% Values of NGCM Survey

Chapter-9: Geochemical Data

9.1 Geochemical data

A total of **253 samples** were analyzed during the reconnaissance (G-4) stage exploration in the Dhamni–Piparwasi–Simliya Block, using an integrated approach of surface and subsurface sampling. This included **150 bedrock samples**, **50 pit samples** (collected from **25 pits**, each approximately 2 m³ in volume, with two samples per pit) (**Plate VI**), and **53 drill core samples** obtained from boreholes DPS-BH1 and DPS-BH2. All **253 samples** were analyzed for **major oxides using X-Ray Fluorescence (XRF)** to determine potassium oxide (K₂O) concentration, a key proxy for glauconite enrichment. In addition, **ICP-MS analysis** was conducted on a total of **111 selected samples**, comprising **75 bedrock samples** and **36 drill core samples**, to determine trace elements and rare earth elements (REEs). Sampling was carried out systematically: bedrock samples were taken from outcrop and float zones; pit samples from vertical profiles of manually excavated pits; and drill core samples were collected from lithologically logged intervals. The resulting geochemical dataset significantly contributed to delineating glauconitic zones and characterizing the elemental signatures of the potential host lithologies.

9.1.1 Surface geochemical analysis results and interpretations

A total of **200 surface samples** (150 BRS and 50 pit samples) were collected using standard procedures, labelled, and dispatched in tamper-evident packaging to the laboratory for multi-element analysis (Annexure **2, 3, and 4**).

Major oxide analysis (XRF) of 50 pit and 150 bedrock samples reveal compositionally varied sedimentary rocks. Silica (SiO₂) content spans 49–97%, few samples are low to 13%, indicating quartz-rich lithologies. Alumina (Al₂O₃) ranges from 0.5–7%, and Fe₂O₃ from 0.5–6.9%, suggesting the presence of iron-bearing minerals. High CaO (0.06–36%) and MgO (<0.05–15%) values indicate carbonate-rich components. K₂O varies from 0.1–3.65%, likely linked to glauconite (**Plate No VII & VIII**), while low Na₂O (0.08–0.44%) implies minimal feldspar. Minor oxides include MnO (0.05–0.8%), TiO₂ (<0.05–0.34%), and P₂O₅/V₂O₅ (<0.05–0.54%). SO₃ reaches up to 1.8%, SrO and BaO are below 0.4%, and LOI is wide-ranging (0.2–40%), reflecting variable carbonate or hydrous content. The overall profile supports quartzose, calcareous, and glauconitic sedimentary rocks.

Table 11 Potassium Oxide (K₂O) Distribution in surface samples

| K ₂ O Threshold | No. of Samples | Percentage |
|----------------------------|----------------|------------|
| ≥ 3.0% | 3 | 1.5% |
| ≥ 2.0% | 11 | 5.5% |
| ≥ 1.0% | 88 | 44% |

These findings suggest localized K₂O enrichment without any observable lateral continuity or stratigraphic control, thereby reducing the potential for defining consistent surface mineralization zones.

ICP-MS analysis of 75 bedrock samples shows lithium (Li) ranging from 2.2–383.9 ppm (**Plate No IX & X**), with most samples in the 10–60 ppm range. However, a few samples (e.g., DPS-1 to DPS-5, DPS-63, DPS-S-114) exhibit high Li (>220 ppm) and correspondingly high K₂O (>2%, some >3.4%), indicating a strong K₂O–Li correlation. This suggests Li may be hosted in potassium-bearing phases, such as glauconite, clays, or detrital micas, though no consistent lithological support for significant Li mineralization is present.

Other trace elements vary moderately: Co (0.7–22.9 ppm), Ga (1.0–26.6 ppm), Rb (10.6–125 ppm), Cu (10–232 ppm), Ni (<5–69 ppm), Pb (<5–453 ppm). High field strength elements such as Y (1.5–20.9 ppm), Zr (8–482 ppm), Th (<0.5–18 ppm), and U (<0.5–46 ppm) reflect variable source rocks.

REEs show light REE (LREE) enrichment and heavy REE (HREE) depletion: La (~24.8 ppm), Ce (~60 ppm), Nd (~46 ppm), Sm (~11.9 ppm), Eu (~2.8 ppm) dominate, while HREEs (Tb, Tm, Lu) are mostly <0.5 ppm. Intermediate REEs (Gd ~9 ppm, Dy ~3.7 ppm, Er ~1.7 ppm, Yb ~1.6 ppm) are moderately present. This REE pattern supports sedimentary origin influenced by provenance and diagenesis.

Lithium (Li) Distribution

From the 75 samples analysed for Li: Most values ranged between 10 ppm and 60 ppm. A few isolated anomalies reached up to 383.9 ppm (**Plate No IX & X**).

Table 12 Li Distribution in surface samples

| Li Threshold | No. of Samples | Percentage |
|--------------|----------------|------------|
| ≥ 300 ppm | 5 | 6.67% |
| ≥ 200 ppm | 7 | 9.33% |
| ≥ 100 ppm | 7 | 9.33% |

9.1.2 Borehole geochemical analysis and results

To assess vertical distribution and continuity of glauconitic mineralization, two scout boreholes, **DPSBH01** and **DPSBH02**, were drilled. A total of **53 borehole core samples** have been analysed for major oxide by XRF and 36 for Trace and REE by ICPMS.

Two boreholes—DPS-BH1 and DPS-BH2—were drilled to evaluate the subsurface continuity of glauconite-bearing strata. DPS-BH1 was drilled to a depth of 34 meters, from which 27 samples were analyzed for major oxides (XRF), and 17 were analysed for trace and REE content using ICP-MS. In DPS-BH2, 30-meter drilling was conducted from which, 26 core samples were analyzed by XRF and 19 by ICP-MS. These analyses provided essential depth-wise geochemical information and helped in establishing vertical zonation of glauconitic enrichment. All core samples were systematically logged and submitted to the Core Repository of the Geological Survey of India (GSI), Nagpur, for archival and future research use.

The geochemical analysis of boreholes DPSBH01 and DPSBH02, based on K₂O% (potassium oxide) values, reveals distinct mineralization zonation where zones are defined by an average K₂O% exceeding 2% over specific depth intervals. Lithium concentrations, being below 40 ppm, were not considered for interpretation (**Annexure 15 &16**).

In **DPSBH01**, two zones also meet the criterion of average K₂O% exceeding 2%. The **first mineralized zone extends from 5–17.5 m**, with a cumulative thickness of **12.5 m**. Within this zone, K₂O values range from **1.74% to 3.25%**, peaking at **3.25% (5–6 m)**. A consistently enriched interval is observed between **7–12 m (2.3–2.95%)**, while moderate values are sustained between **13.5–15.5 m (2.87–2.38%)**, before gradually tapering to **1.98% (16.5–17.5 m)**. This horizon represents a moderately mineralized potash-bearing zone. A barren stretch follows between **18–25 m**, with K₂O mostly below 1.5%, indicating poor enrichment.

The **second mineralized zone occurs between 25–34 m**, with a cumulative thickness of **9 m**. This deeper interval is comparatively higher grade, highlighted by the **maximum K₂O value of 4.399% (25–26 m)**. Other significant peaks include **3.93% (29–30 m)**, **3.55% and 3.53% (31–32 m)**, and **3.18% (27–28 m)**. The lower portion, **32–34 m**, records slightly reduced but still mineralized values (2.18–2.48%).

For **DPSBH02**, two zones also meet the criterion of average K₂O% exceeding 2%. The first zone, from 2–14 m (13 m thickness), has an average K₂O% of 2.39%, with values ranging

from 0.888% (3 m) to 3.444% (11 m). Notable peaks occur at 10 m (3.393%) and 11 m (3.444%), suggesting localized potassium enrichment, potentially indicative of mineralized or altered horizons. The second zone, from 28–30 m (3 m thickness), has a higher average K₂O% of 3.85%, driven by a peak of 4.746% at 28 m, alongside 3.908% (29 m) and 2.888% (30 m). This shorter but more potassic zone points to intense mineralization. The total mineralized thickness in DPSBH02 is 16 m, with lower K₂O% values (e.g., 0.888% at 3 m, 0.974% at 8 m) outside these zones suggesting different lithological units.

Overall, the mineralization zonation in both boreholes highlights areas of significant potassic enrichment, with DPSBH01 showing a broader depth range (21 m total thickness) and DPSBH02 exhibiting higher peak K₂O% values (up to 4.746%) over a slightly thinner total interval (16 m). Thus total 35-meter zone of > 2% K₂O

The borehole geochemistry demonstrates that vertical zones of K₂O enrichment do exist within greenish glauconitic sandstone units and Sandstone Shale intercalations. These bands are present at shallow to moderate depths and exhibit moderate continuity across both boreholes.

The map displays the study area with various lithological units and well locations. The legend indicates three types of lithology: Sandstone shale intercalation (light blue), Glauconite Bearing Sandstone (green), and Sandstone (light grey). The map also includes a scale bar (0 to 2 km) and a north arrow. Well locations are marked with black dots and labeled with numbers. The map shows a network of roads and a river system.

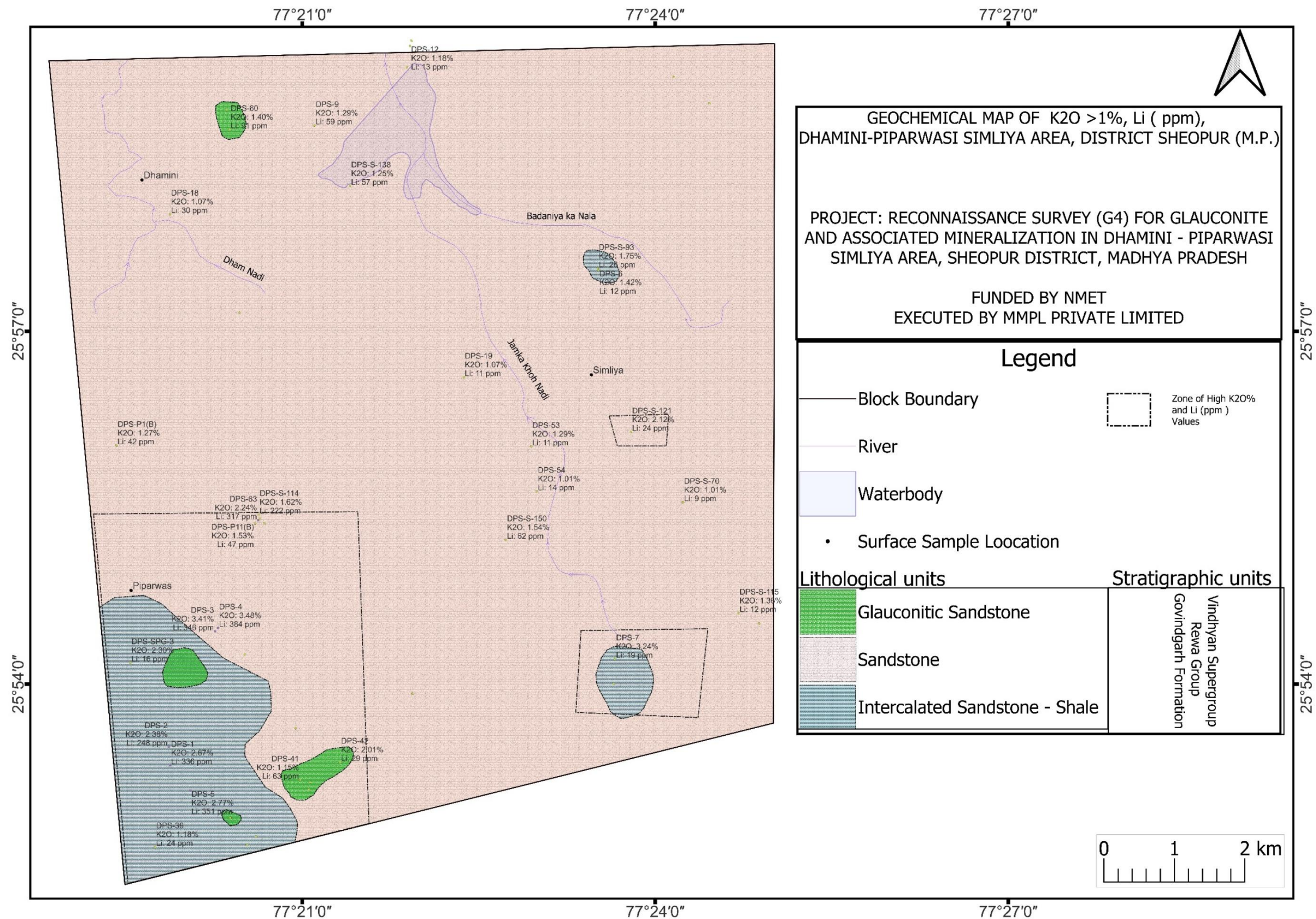
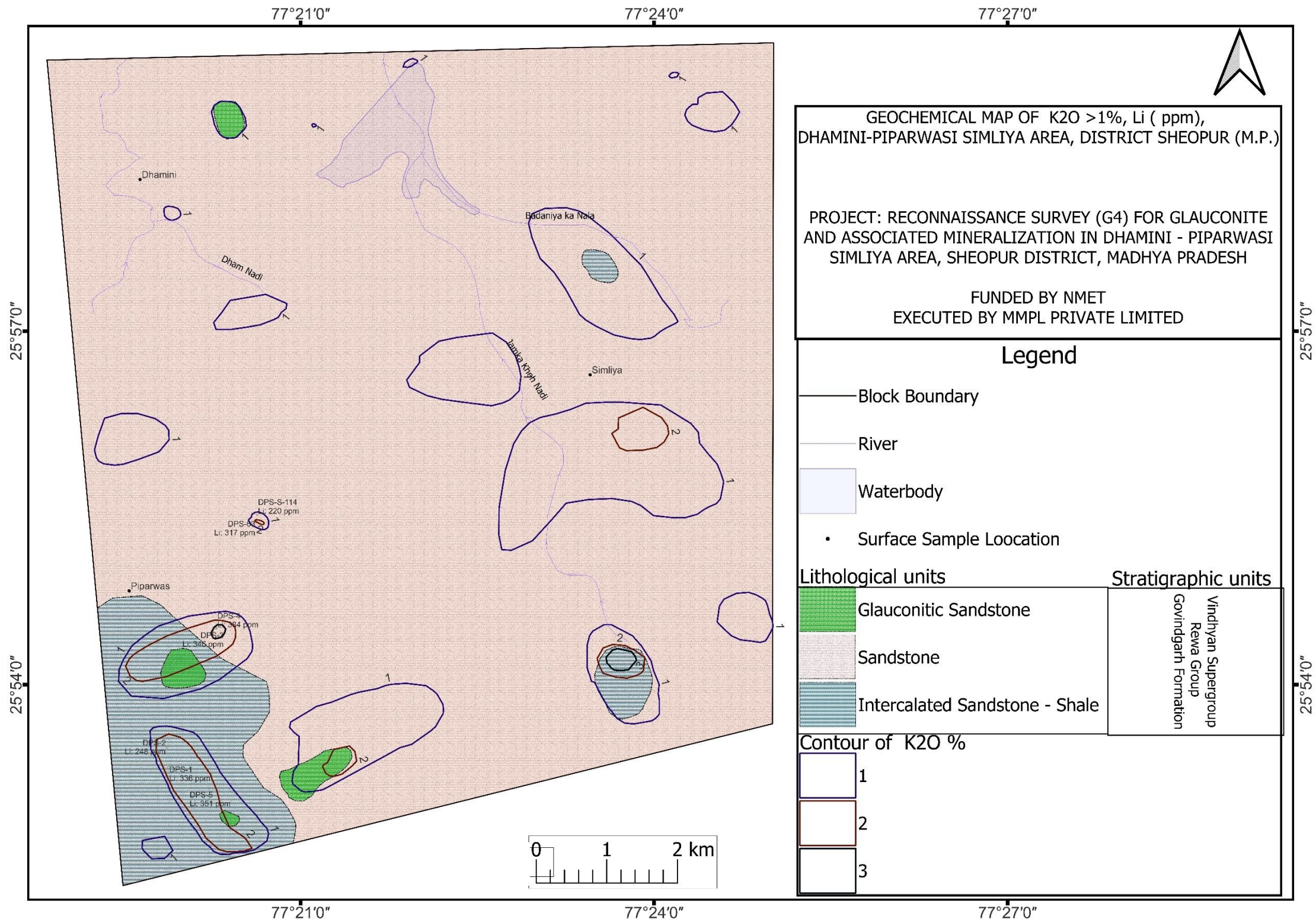
PLATE VII Geochemical Map of K₂O and Li Enrichment Zone Based on Surface Sample Values

PLATE VIII Geochemical Contour map of K2O% and Elevated Lithium Values of Dhamini Piparwasi Simliya Glauconite G4 Block



10. Exploration undertaken during current investigation

10.1 Introduction

Glaucanite is a potassium- and iron-bearing phyllosilicate mineral belonging to the mica group, commonly found in sedimentary rocks, particularly in marine shelf environments where sedimentation rates are slow. It occurs as greenish grains within fine- to medium-grained sandstones, often interbedded with siltstone and shale layers. These depositional conditions are typically associated with quiet, low-energy marine settings that favour the authigenic growth of glauconite over geologic time.

Globally, the majority of potassium (potash) production comes from traditional marine evaporite deposits such as sylvite (KCl), carnallite ($\text{KMgCl}_3 \cdot 6\text{H}_2\text{O}$), kainite ($\text{KMg}(\text{SO}_4)\text{Cl} \cdot 3\text{H}_2\text{O}$), and polyhalite ($\text{K}_2\text{SO}_4 \cdot \text{MgSO}_4 \cdot 2\text{CaSO}_4 \cdot 2\text{H}_2\text{O}$), along with potash-rich brine sources. These resources are dominantly located in a handful of countries—Canada, Russia, Belarus, China, Germany, Chile, Brazil, and the United States—which together supply more than 90% of the global potash fertilizer demand (USGS, 2024).

India lacks commercially viable evaporite-type potash deposits, resulting in near-total dependence on imported potash to meet domestic agricultural requirements. This dependency makes the national supply chain vulnerable to international market volatility, geopolitical instability, and trade-related uncertainties. Consequently, the search for alternative, indigenous sources of potash has become a strategic priority for ensuring long-term food security and agricultural self-reliance (Indian Bureau of Mines, 2021).

As per NMI database, based on UNFC system, the total resources of potash as on 1.4.2015 have been estimated at 22,508 million tonnes, all of which are placed under Remaining Resource category. Rajasthan alone contributes 91% to the total resources, followed by Madhya Pradesh (5%) and Uttar Pradesh (4%).

In this context, **glauconitic sandstones and potash-bearing shales** offer promising potential as non-traditional sources of potassium. These have been exploited in other countries facing similar constraints. For example, Australia has commercially mined alunite, which contains 5–10% K_2O , while the former USSR utilized glauconite as a direct potassium fertilizer. These global case studies confirm the technical and economic

feasibility of extracting potassium from silicate and non-silicate minerals, particularly where conventional potash deposits are absent (Harley, 2013).

India is geologically endowed with significant occurrences of glauconitic sandstone, with an estimated 3,000 million tonnes containing 4–8% K₂O, predominantly located in Madhya Pradesh, Uttar Pradesh, Rajasthan, and Gujarat (Indian Bureau of Mines, 2021).

The mineral can be used directly as a slow-release potash fertilizer, making it a sustainable and locally available substitute for conventional potash fertilizers. As potassium is a major macronutrient essential for plant growth—alongside nitrogen and phosphorus—a consistent domestic supply is vital for maintaining agricultural productivity.

Earlier studies by the Geological Survey of India (GSI) have indicated the presence of glauconitic sandstone within the Upper Rewa Sandstone Formation of the Vindhyan Supergroup in parts of Morena, Shivpuri, and adjoining districts of Madhya Pradesh. Geological mapping by Jadia and Srivastava (FS 1989–90) in Toposheets 54G/1 and 54G/5, and later by Srivastava and Mehrotra in adjoining areas (Toposheets 54G/5 and 54G/9), documented glauconite-bearing sandstone units in multiple nala sections, especially around Basantpura, Kapeli Nadi, and Dham Nadi. These sandstones were described as greenish, fine- to medium-grained, and interbedded with shales and siltstones, consistent with glauconite deposition under fluctuating marine conditions. Visual estimates suggested glauconite content in the range of 5–10%.

Further validation was provided by the National Geochemical Mapping (NGCM) programme, which recorded glauconitic occurrences and K₂O values ranging from 1.45% to 3.30% near Dubera, Kopli Nadi, and Agra (Dev and Danish, 2023). To supplement and validate these findings, MMPL Pvt. Ltd., collected additional samples from the area, reporting K₂O values between 1.15% and 2.81%, which confirmed earlier geochemical anomalies.

Given the favourable geological and geochemical indicators, the 66th Technical Committee of the National Mineral Exploration Trust (NMET) recommended a Reconnaissance Stage (G-4) exploration programme for **glauconitic sandstone and associated mineralization** in the Dhamni–Piparwasi–Simliya Block, located in Vijaypur Tehsil, Sheopur District, Madhya Pradesh. The proposal received formal approval from the 36th Executive Committee of NMET on 21 August 2024, and exploration activities were initiated by the notified agency in accordance with NMET guidelines. The exploration programme commenced on 05 November

2024 and is being implemented by the Notified Private Exploration Agency (NPEA) The MMPL Pvt. Ltd. Kolkata, West Bengal.

This initiative is expected to contribute significantly to India's long-term potash resource base, reduce import dependency, and support the national objective of fertilizer self-sufficiency through indigenous mineral development.

10.2 Objectives of exploration

1. To carry out Geological Mapping on 1:12,500 scale of the block (116 Sq. Km) to assess various litho-units using field equipment and mapping of glauconite bearing outcrops along with other lithounits.
2. To study different geological sections to build up local stratigraphy.
3. Classification of glauconite bearing sandstone of Govindgarh formation.
4. To carry out systematic grab/channel sampling of bed rocks.
5. Petrological studies of possible host rock and their chemical analysis.
6. Pitting-trenching of selected area and sampling.
7. Based on the outcome of surface geochemical sample results, and trenching/ pitting work total 5 numbers of scout boreholes shall be drilled to assess the thickness of the glauconite bearing sandstone,
8. Attempt to delineate a glauconitic block or more than one block to upgrade the investigation in G3 stage.

10.3 Basis of taking investigation

- 1 Jadia and Srivastava (FS 1989-90, GSI), carried out Systematic Geological Mapping in parts of Morena district of Madhya Pradesh on 1: 50,000 scale in Survey of India toposheet No. 54 G/1 & 5. They observed thin bands of **glauconitic sandstone** within the Upper Rewa Sandstone in the nala sections west of Basantpura, in Kapeli nadi south of Kapel Hor and along Dham nadi southeast of Dhamni. This sandstone is fine-grained, light green coloured thinly bedded and moderately sorted with about **5-10% of glauconite** (Visual Estimate).
- 2 **Srivastava and Mehrotra (FS 1989–90, GSI)** conducted 1:50,000 scale geological mapping of the Vindhyan Supergroup in parts of Shivpuri and the then Morena district (now including present-day Sheopur), covering parts of SOI toposheets 54G/5 and 54G/9. Asper their study Upper Rewa Formation sandstone exposed from Dhodha Burera in the east (toposheet No. 54 G/9) to Bagwani Piparwas – Surad – Magarda - Dubera in the west (toposheet No. 54 G/5). This unit is constituted by massive to thickly bedded greyish white to pinkish white, coarse to

medium grained sandstone containing few feldspars and **glaucanite grains**; flaggy to thinly bedded, medium to fine grained, greenish white to dirty white **glaucanitic sandstone** with intercalation of siltstone and thinly bedded olive green coloured splintery shales.

- 3 **National Geochemical Mapping (NGCM)** was carried out on 1:50,000 scale in parts of **Shivpuri, Morena, and Sheopur districts** of Madhya Pradesh, falling within Survey of India toposheet no. **54G/5**. The NGCM results indicated **K₂O values ranging from 1.45% to 3.30%**, suggesting potential for potassium-bearing lithologies in the area (**Dev & Danish, 2023**)
- 4 The geologists of MMPL Pvt. Ltd. visited the area twice and collected samples from glauconitic sandstone. In the first phase the analyses received for five samples. Out of five two samples analysed as 1.31 and 2.81% K₂O. In the second phase seven samples were collected. Out of seven samples four samples analysed as 1.15, 1.59, 1.30 and 1.33% K₂O.
- 5 Subsequently, based on the recommendation of the 66th TCC of NMET, the proposal for undertaking a Reconnaissance Survey (G4) for Glaucanite and associated mineralisation in the Dhamni-Piparwasi-Simliya area, Sheopur district, Madhya Pradesh was approved by the 36th Executive Committee (EC) of NMET on 21 August 2024, and the work was initiated accordingly.

2.4 Details of work approved vs achieved by MMPL

All approved exploration components (Table no 3) under the project were successfully executed by Maheshwari Mining Pvt. Ltd. (MMPL) within the stipulated timeline (Table no 2.). The originally approved drilling target comprised 150 meters across 5 boreholes, with 100 core samples for major oxide analysis using XRF, and 75 core samples for trace and rare earth element (REE) analysis using ICP-MS.

However, based on the preliminary surface geochemical data, which did not indicate significantly promising K₂O concentrations, the Technical Committee of NMET (TCC) recommended limiting the drilling activity to only 2 boreholes.

Accordingly, a total of 2 boreholes were drilled, achieving 64 meters of cumulative drilling. From these, 53 core samples were analysed for major oxides (XRF) and 36 core samples for trace elements and REEs (ICP-MS).

Table 13 Timeline of Reconnaissance Survey (G-4) for Glauconitic Sandstone in Dhamni, Piparwasi, Simliya, Vijaypur, District- Sheopur, Madhya Pradesh Project

| Name of the Project | Date of Approval | Date of Commence | Reason for delay in commencement /time over run (if any) | Date of Completion |
|---|------------------|------------------|--|--------------------|
| <i>Reconnaissance Survey (G4) for Glauconite and associated mineralisation in Dhamni- Piparwasi Simliya area, Sheopur district, Madhya Pradesh</i> | 21/08/2024 | 05/11/2024 | <p>7. Due to harsh weather condition, rainy season up till mid- October, field work was hampered.</p> <p>8. By elections in Sheopur District on 13th November 2024, created vehicle unavailability.</p> <p>9. Forest permission for mapping and bed rock sampling from PCCF and DFO.</p> <p>10. 10th meeting of Technical-cum- Cost Committee - II (TCC - II) held on 23rd, 24th & 25th June 2025, approved time extension of 3 months up to 20th November 2025 for submission of final geological report.</p> | 15/03/2026 |

Table 14 Quantum of work Proposed & Achieved by MMPL in Reconnaissance Survey (G-4) for Glauconitic Sandstone in Dhamni, Piparwasi, Simliya, Vijaypur, District- Sheopur, Madhya Pradesh

| S. No. | Item of Work * | Target Assigned | Target Achieved |
|----------|---|-----------------|-----------------|
| A | Geological Mapping | | |
| | Geological mapping, (1:12,500 scale) | | |
| B | Survey work | | |
| | DGPS Survey for BH fixation & RL determination | 5 | 2 |
| C | Trenching/Pitting | | |
| | a) Pitting (up to 2 m) | 50 | 50 |
| D | DRILLING | | |
| 1 | Drilling up to 150 m (Hard rock) | 150 | 64 |
| E | LABORATORY STUDIES | | |
| 1 | Chemical Analysis | | |
| i) | Geochemical Sampling-Surface samples (Bedrock/Channel /Soil/Stream sediment) | | |
| | a. Analysis of major oxides by XRF | 150 | 150 |
| | b. Trace elements -ICPMS | 75 | 75 |
| ii) | Surface Check samples (10% External) | | |
| | a. Analysis of major oxides samples by XRF | 15 | 15 |
| | b. Trace elements -ICPMS | 7 | 7 |
| iii) | Trench & Check Samples from Trench | | |
| | a. Analysis of major oxides samples by XRF | 50 | 50 |
| | Trench samples | | |
| iv) | Trench Check samples (10% External) | | |
| | a. Analysis of major oxides samples by XRF | 5 | 5 |
| v) | BH Core samples | | |
| | a. Analysis of major oxides samples by XRF | 100 | 53 |
| | b. Trace elements -ICPMS | 75 | 36 |
| vi) | BH Core samples (10%External) | | |
| | a. Analysis of major oxides samples by XRF | 10 | 7 |
| | b. Trace elements -ICPMS | 7 | 3 |
| 2 | <u>Physical & Petrological Studies</u> | | |
| i | Preparation of thin section | 10 | 10 |
| ii | Study of thin section | 10 | 10 |
| iii | Preparation of polish section | | |
| iv | study of polished section | | |
| v | Digital Photographs | 10 | 10 |

| | | | |
|----------|--------------------------------------|----|----|
| vi | Modal Analysis for Potash Phase | 03 | 03 |
| vii | XRD | 03 | 03 |
| vii | Bulk density analysis | 3 | 3 |
| F | Geological Report Preparation | | |

10.5 Mode of operation of work components & associated agency

Work components as mentioned in the above Table are completed with departmental resources of Maheswari Mining Private Limited, except Chemical Analysis was done in Shiva Analytics Bangalore and XRD analysis at GSI and Shiva Labs.

10.6 Scheme of exploration

This scheme outlined a Reconnaissance Survey (G4 stage) for glauconite and associated mineralisation in the Dhamni–Piparwasi–Simliya block, located in Sheopur district, Madhya Pradesh. The primary objective was to identify glauconite-bearing formations, delineate their surface and subsurface extents, and evaluate their mineralogical and geochemical characteristics. The program was aimed at assessing the block's potential for advancement to G3 or higher stages of exploration. The scheme was prepared in accordance with the provisions of the **Mineral (Evidence of Mineral Contents) Rules, 2015 (MEMC Rules)** and the technical guidelines issued by the **National Mineral Exploration Trust (NMET)**.

The total area of 116 km² was systematically covered through **large-scale geological mapping (LSM)** at a scale of 1:12,500. Mapping was carried out to delineate lithological contacts, structural features, and surface manifestations of glauconite-bearing horizons.

Although geophysical surveys were not included in the scheme, shallow subsurface investigation was executed through systematic **pitting**, which was not originally sanctioned but was carried out as part of field modifications. A total of **50 cubic meters of pitting** was conducted at selected locations. From these, **50 pit samples** were collected and analyzed for major oxides using **X-ray Fluorescence (XRF)**.

Bedrock sampling formed a core part of the geochemical investigation. In total, **150 bedrock samples** were collected and analyzed for major oxides by XRF, of which **75 samples** were further analyzed by **Inductively Coupled Plasma Mass Spectrometry (ICP-MS)** for trace and rare earth elements (REE). In addition, **7 bedrock check samples** were analyzed using ICP-MS and **15 by XRF** to ensure analytical precision and reproducibility.

Subsurface exploration was initially proposed through the drilling of five boreholes totalling 150 meters. However, as per the recommendations of the **TCC**, this was revised to **two boreholes** totalling

64 meters. These boreholes were drilled to validate the vertical continuity of glauconite-bearing lithounits and to recover fresh core samples for laboratory analysis. From the drill cores, **53 samples** were analyzed for major oxides by XRF and **36 samples** for trace and REE by ICP-MS. The scheme had made provision for up to **100 core samples** for XRF and **75 for ICP-MS**, aligning with approved norms. **Differential GPS (DGPS)** was employed to fix the collar coordinates and RLs of the boreholes.

For mineralogical characterization, **10 petrographic thin sections** were prepared from glauconite-bearing samples and examined under a polarizing microscope. Additionally, **digital photographs** of drill core segments were captured to document textures, structural features, and sampling intervals.

Bulk density testing was completed successfully of three samples, and the results is utilised in resource estimation exercises.

All chemical analysis reports were received, and based on the results of geological mapping, drilling, and geochemical analyses, **zones of elevated K₂O concentrations** were identified and demarcated both on the surface and in the borehole profiles. These zones indicated significant glauconite potential and were deemed worthy of further exploration.

Pursuant to the recommendations made during the 10th meeting of the Technical-cum-Cost Committee-II (TCC-II) held from 23rd to 25th June 2025(**Annexure 19**), the scheme of exploration was revised to incorporate the suggested technical components, all of which have been successfully completed. Modal analysis of potash-bearing minerals was carried out to determine the dominant mineral phases contributing to potash content. The maturity of glauconite was evaluated through petrographic studies, and its stratigraphic horizon was clearly identified and documented. Additionally, in response to the reported lithium concentrations ranging from 10 to 60 ppm, with isolated values up to 383.9 ppm, targeted investigations were conducted to identify the specific lithium-bearing mineral phase and K₂O bearing phase by XRD.

A comprehensive **geological report** was compiled, integrating field observations, sampling records, laboratory results, and geological interpretations. The findings of the reconnaissance survey justified the classification of the area under the **Inferred Mineral Resource (G4)** category.

The entire exploration program was executed in strict compliance with the **MEMC Rules, 2015** and the **technical standards of NMET**, ensuring conformity with national protocols for mineral exploration in India.

10.7 Large Scale Geological Mapping

An extensive Large-Scale Geological Mapping (LSM) exercise was carried out over an area of 116 sq. km at a 1:12,500 scale in the Dhamni–Piparwasi–Simliya Block, situated in Sheopur district, Madhya Pradesh. This block lies within the Vindhyan Supergroup terrain and is entirely occupied by the Govindgarh Sandstone Formation of the Rewa Group. The key objective of the survey was to systematically map the lithological units and structural elements through detailed field observations.

Mapping was conducted using standard geological tools such as GPS units, Brunton compasses, and geological hammers. During field traverses, important observations such as lithological boundaries, sedimentary structures, and bed attitudes were recorded in field notebooks and later digitized. The field area displayed good rock exposures, as the soil cover was generally shallow—about 1 to 2 feet—allowing direct observation of underlying bedrock in most places.

Field data, including lithological and structural observations along with GPS waypoints, were compiled and imported into QGIS software. The geological map was prepared by integrating this data with satellite imagery and topographic sheets. Geological boundaries were digitized, and structural features were accurately annotated to reflect field conditions. The final geological map presents a comprehensive understanding of the surface geology, structural configuration, and stratigraphic disposition within the block, forming the foundation for further geochemical evaluation and exploration planning.

Outcrops are widely distributed throughout the area, facilitated by a thin soil cover of only about 1 to 2 feet in most parts of the block. This relatively shallow overburden allows for clear exposure of bedrock, aiding field mapping and sampling activities. Prominent outcrop zones are observed in the eastern parts near Simliya and along the Jamka Kho tributary, where the stratigraphic sequence is well exposed and reaches a cumulative thickness of up to 20 meters. Western sectors such as Khari and Piparwasi also exhibit moderate exposure, with alternating bands of sandstone and shale visible in scattered patches.

The lithology is dominated by thick sequences of sandstone interbedded with occasional bands of shale. The sandstone is primarily fine- to medium-grained, with colours ranging from white, creamy-white, greyish-white to greenish-grey. It is mostly hard, compact, moderately to well sorted, and orthoquartzitic in nature. In some localities, a flaggy character is noted due to thin bedding. These physical characteristics point towards a shallow marine to nearshore

depositional environment with intermittent siliciclastic input. The occurrence of greenish-grey coloration in some sandstone beds indicates the presence of glauconitic material, which is further supported by geochemical analyses conducted during the study.

Structurally, the block is relatively undisturbed, with the sandstone beds showing predominantly horizontal disposition. In some parts, particularly towards the southwestern margin of the block, a gentle rolling dip of 2° – 3° towards the southwest is observed. No major tectonic structures such as faults or folds have been identified within the mapped area, indicating a stable sedimentary regime with minimal post-depositional deformation.

Glauconite was observed visually in greenish sandstone layers and shales, and confirmed through geochemical results indicating elevated K_2O values. These glauconitic beds occur as disseminated grains within the matrix and in certain intercalated beds, indicating stratiform distribution rather than massive or lenticular enrichment.

Overall, the geological mapping has successfully established that the block is largely constituted by sandstone of **Govindgarh Formation**, showing favourable conditions for glauconite occurrence, although not in economically significant concentrations at this stage.

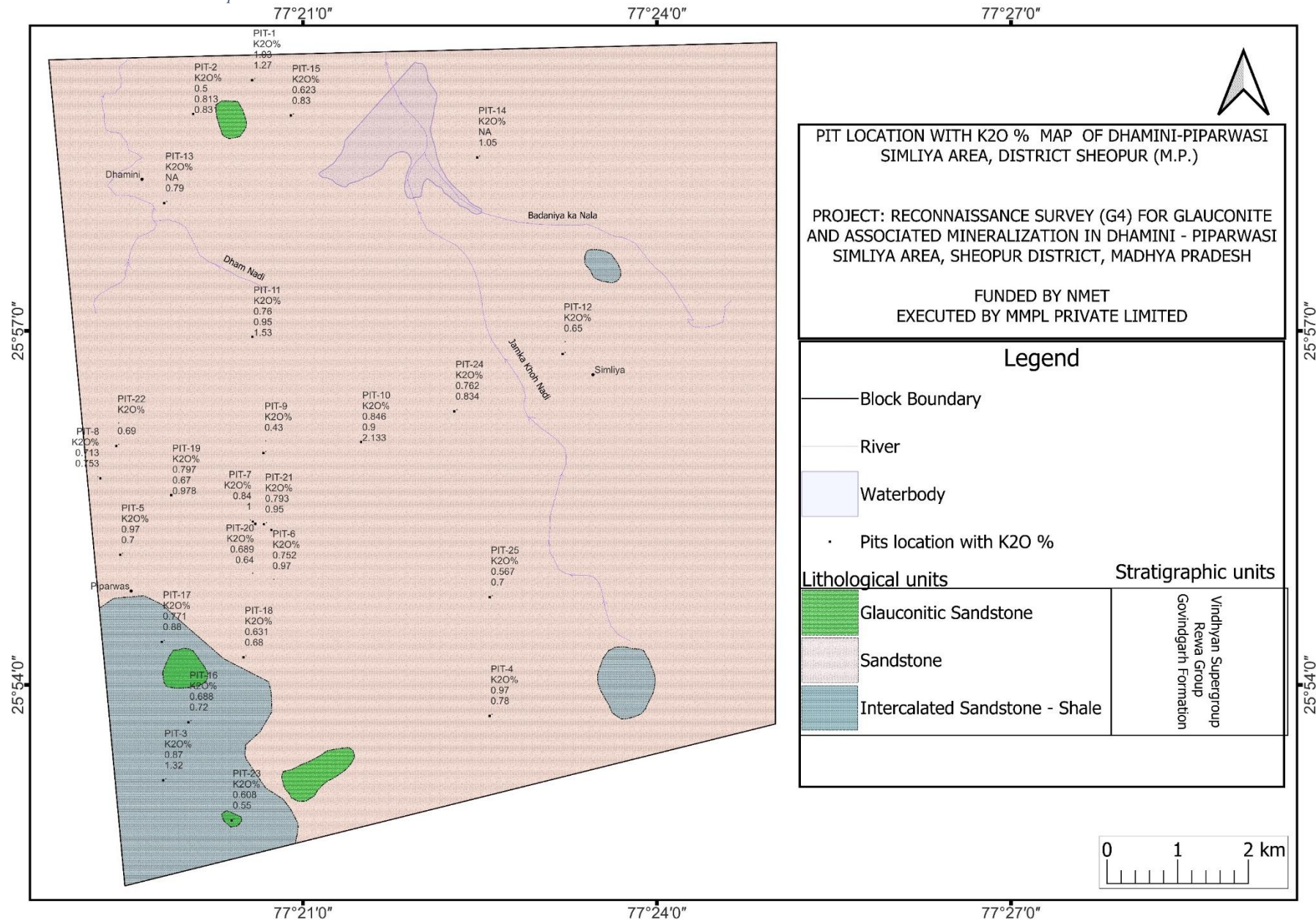
10.8 Pitting

A total of **25 pits**, each measuring **2 m deep and 1 m × 1 m in plan**, were excavated in locations where the rock exposure was poor. The total volume of excavation carried out was **approximately 50 m³**. Total 50 samples were collected and one sample per meter cube and analysed for measure oxide by XRF. Location and K_2O % value of each pit is given in Plate - IV.

10.9 Bedrock sampling

Bedrock sampling formed a core part of the geochemical investigation. In total, **150 bedrock samples** were collected and analysed for major oxides by XRF, of which **75 samples** were further analysed by **Inductively Coupled Plasma Mass Spectrometry (ICP-MS)** for trace and rare earth elements (REE). In addition, **7 bedrock check samples** were analysed using ICP-MS and **15 by XRF** to ensure analytical precision and reproducibility. Details of geochemical sampling and analysis given in 9th chapter.

PLATE IX Pit Location Map with K2O%



10.10 Petrographic and Modal Analysis

10.10.1 Petrography of surface samples

Five representative samples were collected from different locations across the Dhamini–Piparwasi–Simliya Glauconite Block for petrographic analysis, with the primary objective of verifying glauconite presence, estimating its modal abundance, and understanding associated mineralogical and textural characteristics. These samples were initially selected based on visual field indications of greenish hue, friable texture, and stratigraphic association with glauconite-bearing horizons. However, subsequent microscopic examination revealed significant variability in mineral composition, glauconite content, and textural maturity, indicating complex depositional and post-depositional conditions within the block.

Based on initial petrographic study, three representative samples (two surface samples and one drill core sample) were identified as glauconite-bearing and were recommended for modal analysis. The objective of this exercise was to quantify mineral proportions in the thin section and validate petrographic observations and evaluate the significance of glauconite mineralization in both surface and subsurface lithologies.

The modal analysis was conducted using the **point counting method**, with **1,000 counts per thin section under 20 × magnification**. This method provides statistically reliable estimates of modal mineralogy, ensuring accurate representation of the mineral assemblage.

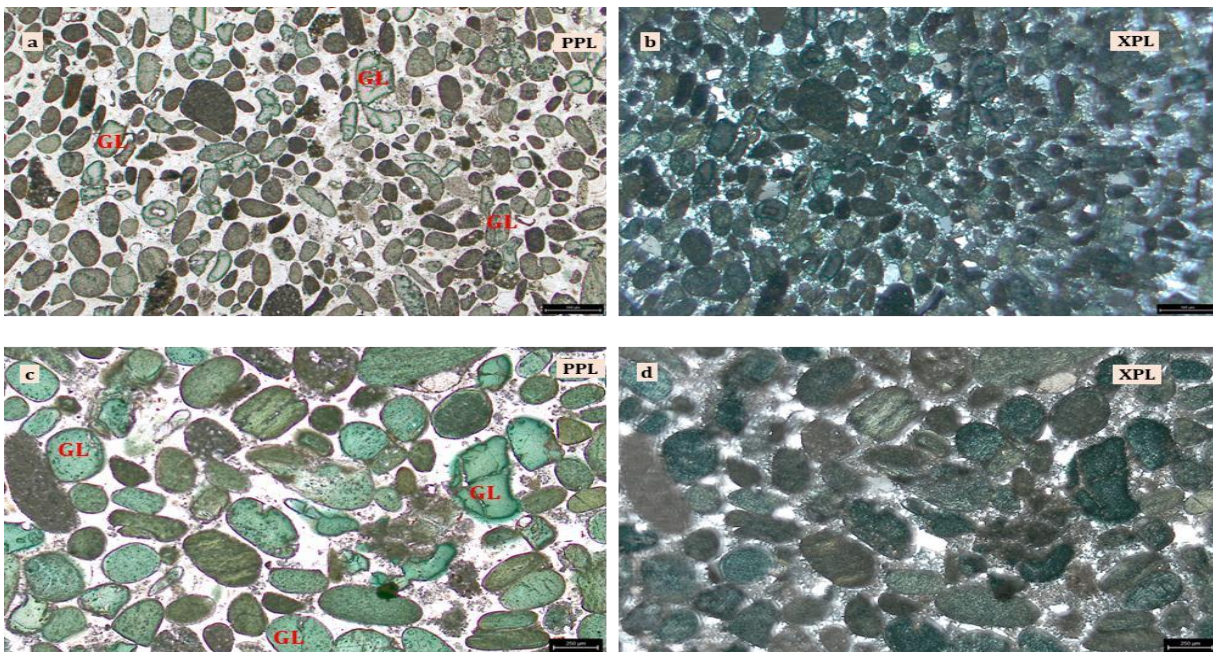
Sample: DPS01: Glauconitic Sandstone

Petrographic Analysis:

The thin section reveals a matrix-supported sandstone composed primarily of rounded grains. The rock exhibits a high glauconite concentration, forming approximately 80% of the modal composition. Glauconite grains are rounded and exhibit a distinct green colour under plane-polarized light (PPL). Quartz and feldspar are present in subordinate amounts, with the matrix comprising fine siliceous material. The abundance and rounding of glauconite grains suggest considerable sediment reworking prior to final deposition.

Modal Analysis:

The modal study of DPS01 reveals **glauconite as the dominant constituent (80.6%)**, accompanied by a subordinate quartz-rich matrix (11.6%) and lithic fragments (7.7%). The exceptionally high glauconite proportion establishes this sample as a glauconite-rich lithounit of considerable significance. The results confirm earlier petrographic. The quartz present in the thin section occurs as grains finer than typical sand size, forming part of a very fine-grained matrix.



Photomicrograph 1 of thin section DPS01

Show (a, c) rounded glauconite grains forming a significant portion of the rock under PPL, with green coloration and fine siliceous matrix, (b, d) quartz and glauconite under XPL exhibiting moderate sorting

Sample: DPS04: Glauconitic Lithic Sandstone

| Minerals | Modal% |
|--|--------|
| Glauconite | 80.6 |
| Matrix (with very fine-grained Quartz) | 11.6 |
| Lithic Fragments | 7.7 |

Petrographic Analysis

This sample is texturally similar to DPS01 but exhibits a higher abundance of lithic fragments. Glauconite remains a prominent component, constituting approximately 70% of the modal composition, and appears sub-rounded with a greenish hue in PPL. The lithic fragments are angular to sub-angular and suggest a multi-source sediment provenance. Quartz and feldspar grains are present in minor quantities within a fine matrix. The overall fabric indicates moderate sorting and deposition under relatively low-energy conditions with mixed input, consistent with field observations of interbedded sandstone and mudstone.

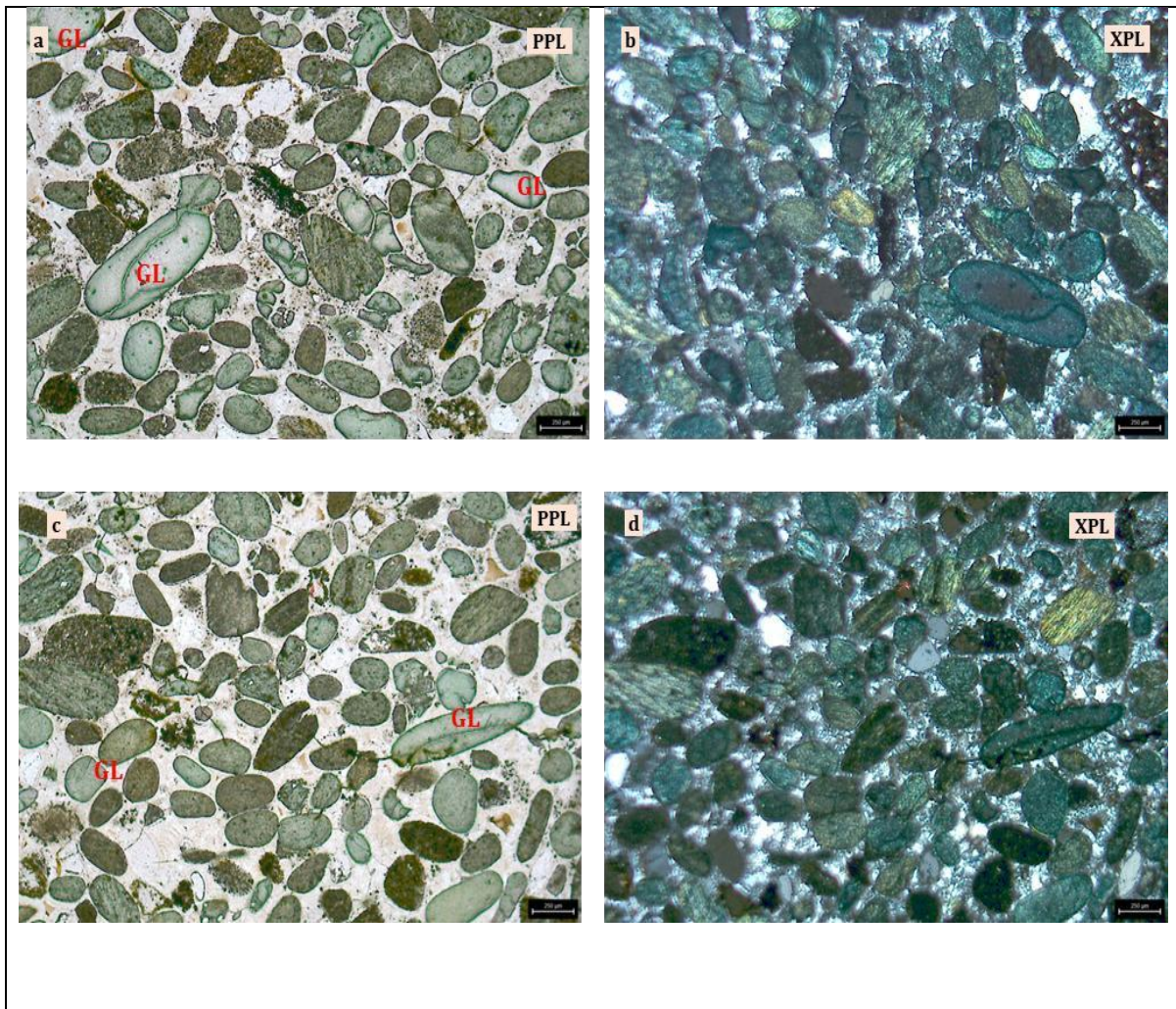
Modal Analysis

In DPS04, modal analysis indicates **glauconite (72.2%)** as the principal constituent, with quartz in the fine-grained matrix (18.4%) and lithic fragments (9.4%) forming secondary components. However, the quartz grains observed in the thin section are predominantly finer than sand size, indicated by a very fine-grained matrix.

*Table 15*MODAL ANALYSIS OF SAMPLE ID: DPS04

| Minerals | Modal% |
|--|--------|
| Glauconite | 72.2 |
| Matrix (with very fine-grained Quartz) | 18.4 |
| Lithic Fragments | 9.4 |

The photomicrographs are as follows:

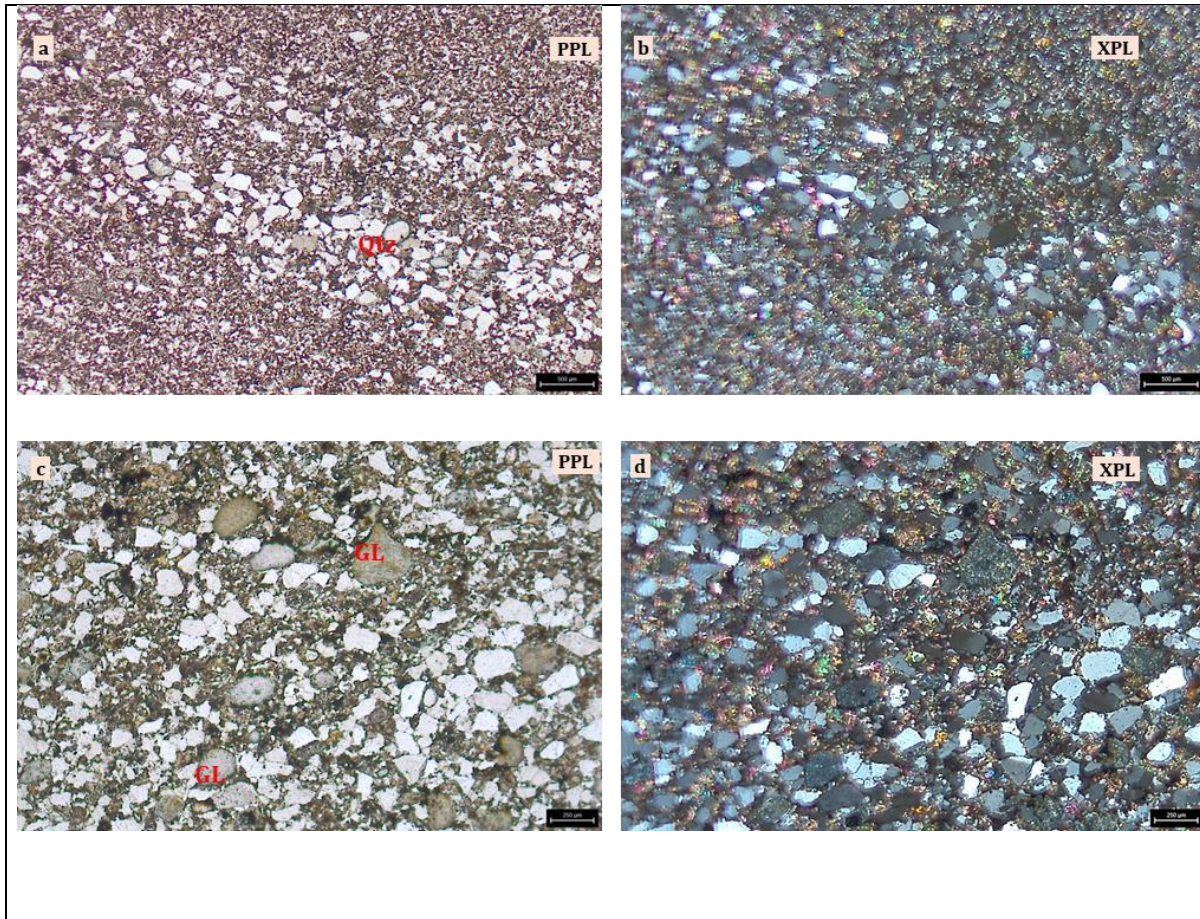


Photomicrograph 2 Showing thin section DPS04

Show (a, c) abundant glauconite and lithic fragments under PPL; glauconite appears sub-rounded and green, while lithic fragments are sub- angular, (b, d) under XPL, reflecting moderate sorting.

Sample: DPS11: Fine-Grained Sandstone with Localized Glauconitic Zones

This thin section is dominated by fine-grained anhedral quartz grains. Glauconite is sporadically present, concentrated mainly in small, localized zones associated with coarser quartz grains. The finer-grained portions of the rock are nearly devoid of glauconite, highlighting heterogeneous distribution. The glauconitic pockets show pale green grains under PPL, whereas the rest of the section is composed of tightly packed fine quartz grains. This textural variation suggests fluctuating depositional energy and selective glauconite settling.

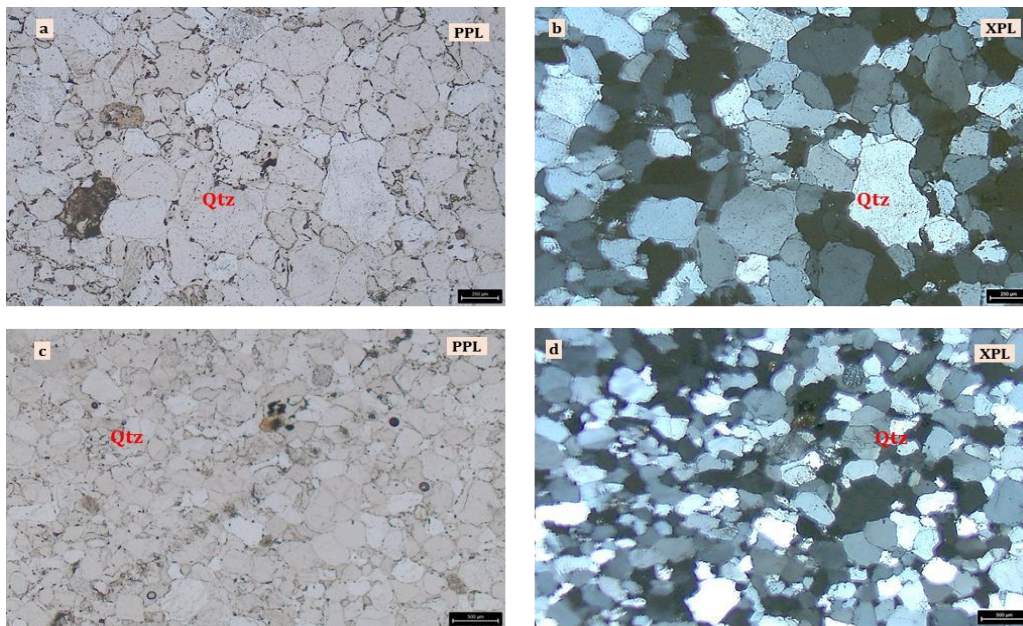


Photomicrograph 3 Showing thin section DPS11

show (a, c) fine-grained anhedral quartz grains with localized glauconite zones under PPL; glauconite appears pale green and concentrated near coarser quartz grains, (b, d) interlocking textures of quartz under XPL, illustrating heterogeneous glauconite distribution.

Sample: DPS25: Quartz-Rich Sandstone

The sample is composed entirely of anhedral quartz grains, exhibiting no evidence of glauconite. The grains are tightly packed, showing interlocking textures and well-developed triple junctions—clear indicators of advanced diagenetic recrystallization and compaction under elevated pressure. The absence of glauconite, coupled with the high degree of grain contact and lack of rounding, suggests that the rock has undergone significant burial diagenesis. These petrographic features align with field observations of fine-grained quartz arenite, likely representing high-energy fluvial or reworked sediments subjected to deep burial conditions, resulting in the loss of primary porosity.

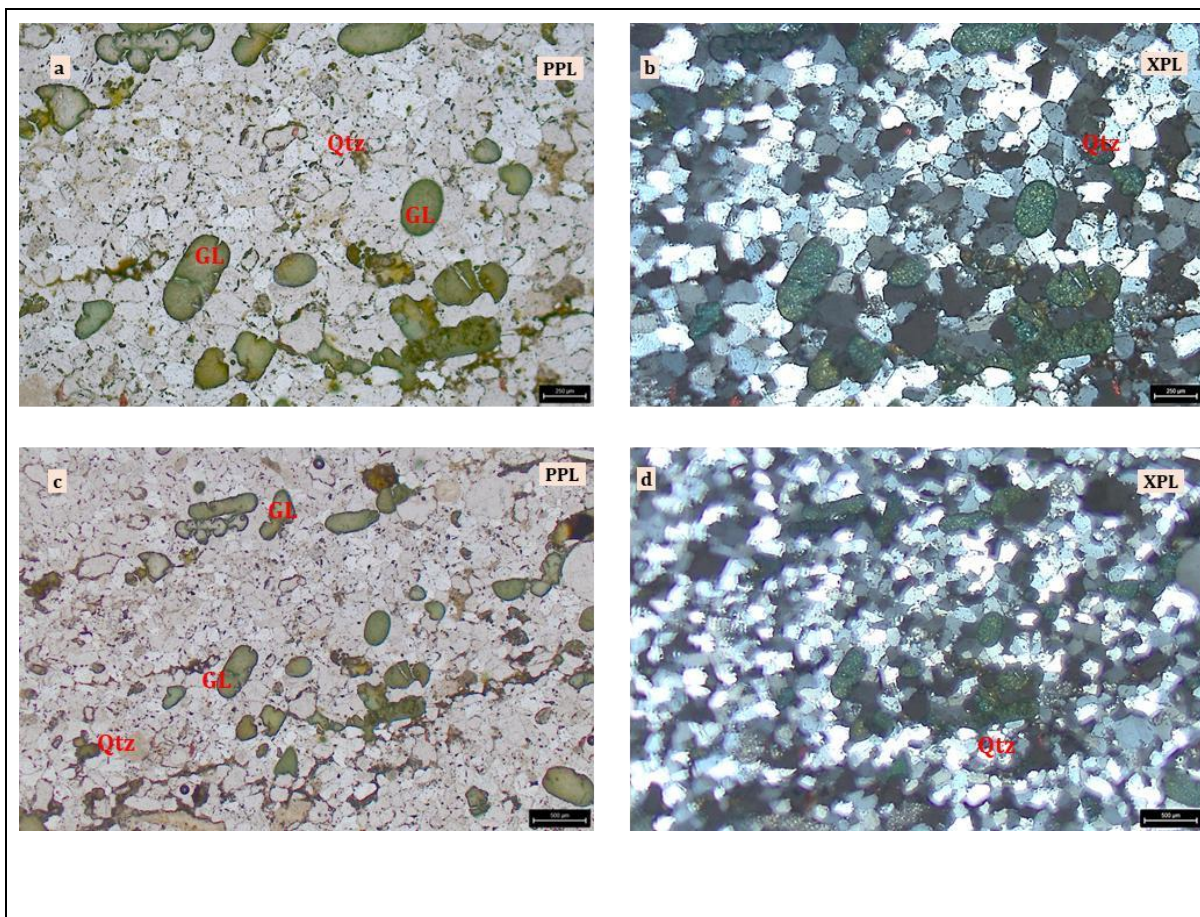


Photomicrograph 4 Showing thin section DPS25

show (a, c) tightly packed anhedral quartz grains lacking glauconite under PPL, with evidence of triple junctions, (b, d) strong interlocking textures under XPL, indicative of diagenetic recrystallization.

Sample: DPS41: Glauconitic bearing Sandstone

This section displays medium-grained quartz with sub-rounded morphology, interspersed with rounded glauconite grains comprising about 10% of the modal composition. Glauconite grains appear distinctly green under PPL. These glauconite grains seem to be oriented along a preferred direction, maybe along a weak plane within the host sandstone. The quartz framework is moderately sorted, and the overall fabric suggests deposition in a shallow marine setting with limited glauconitic enrichment. The presence of both quartz and glauconite, with moderate maturity, points toward mixed sedimentary dynamics.



Photomicrograph 5 Showing thin section DPS41

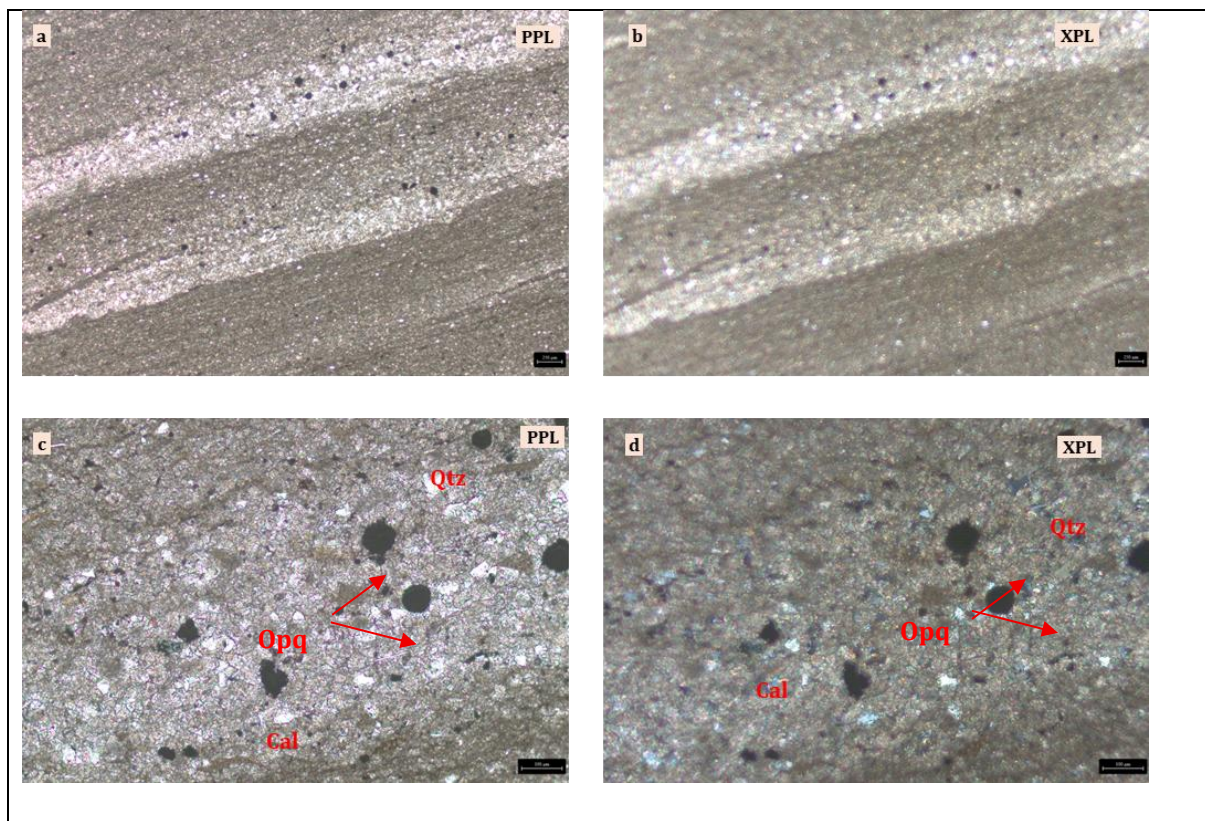
show (a, c) medium-grained quartz with sub- rounded grains and oriented glauconite grains under PPL; glauconite appears distinct green and rounded, (b, d) quartz framework under XPL showing moderate sorting.

7.5.2 core samples petrographic study

Table 16 Details of Petrographic Sampling of Cores

| Sample id | Depth From(m) | Depth To(m) | Borehole no. | Lithology |
|-------------|---------------|-------------|--------------|-----------------------------------|
| DPS-BH1-PG1 | 12.5m | 12.70m | BH1 | Calcareous shale |
| DPS-BH1-PG2 | 16.5m | 16.7m | BH1 | Glaucanite bearing lithic arenite |
| DPS-BH1-PG3 | 21m | 21.7m | BH1 | Glaucanite bearing quartz arenite |
| DPS-BH2-PG4 | 7.2m | 7.35m | BH2 | Glaucanite bearing quartz arenite |
| DPS-BH2-PG5 | 23.40m | 23.50m | BH2 | Glaucanite bearing quartz arenite |

Sample: DPS-BH1-PG1 **Rock Type:** Calcareous shale



Photomicrograph 6 Showing of thin section DPS-BH1-PG1

show (a, c) fine laminations and alternating calcite-rich bands under PPL, with micritic to microsparry calcite grains concentrated in discrete zones, and (b, d) under XPL, supporting field evidence of carbonate enrichment

The thin section reveals a very fine-grained, laminated shale. Distinct calcite-rich bands are present, where coarse micritic to microsparry calcite grains are concentrated. These carbonate-rich layers

interrupt the dominant clay-rich matrix, consistent with field observations of effervescence. The fabric is compact with occasional silt-sized detrital quartz grains. Under PPL, the calcite appears with low relief and distinct 3rd order colours under XPL, suggesting secondary carbonate enrichment during early diagenesis. Some Opaque minerals are seen within these layers.

Sample: DPS-BH1-PG2 Rock Type: Glauconite bearing lithic arenite

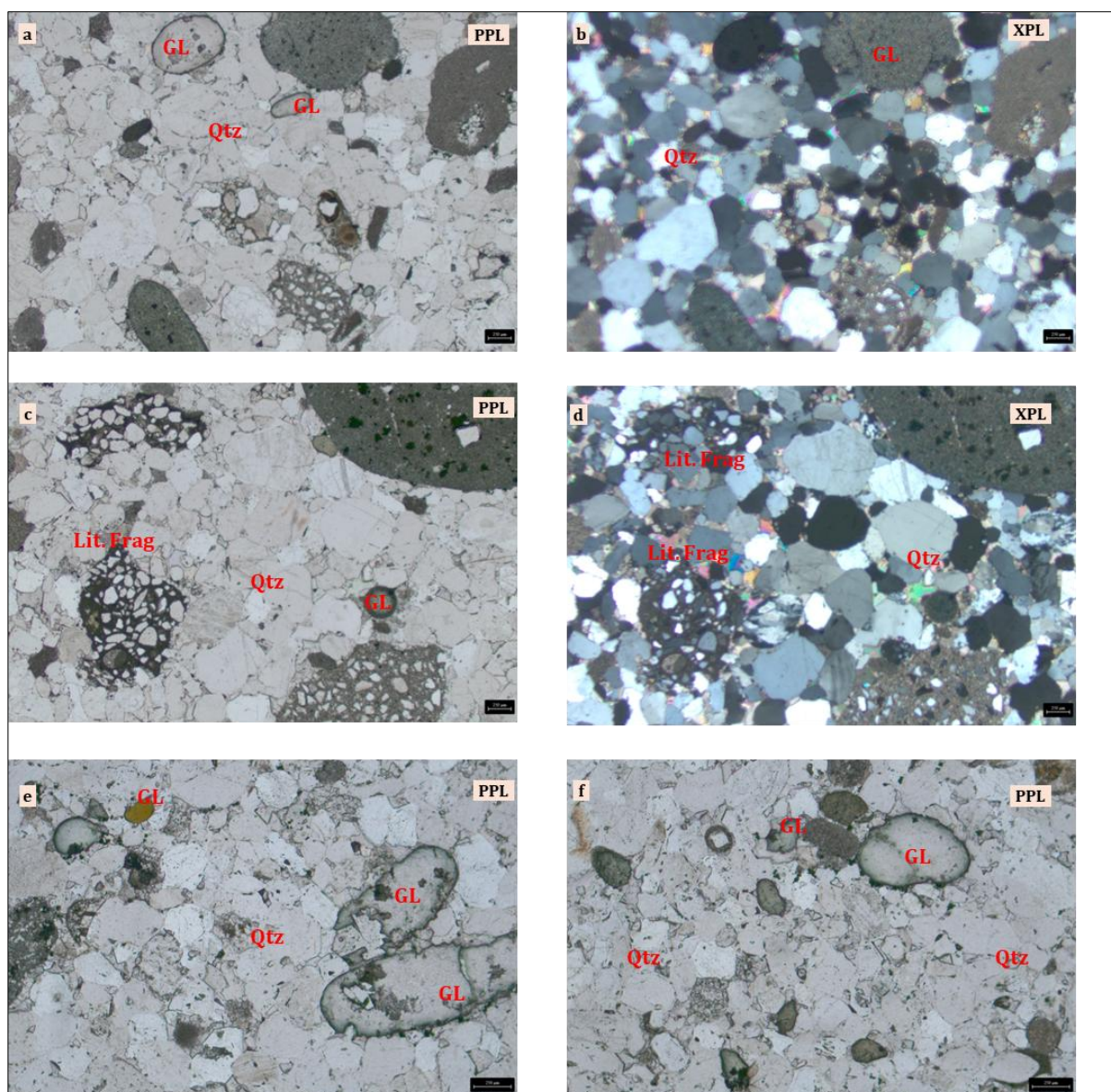
Petrographic Analysis

The thin section displays a sandstone composed of medium-grained, sub-rounded quartz grains with scattered, well-rounded glauconite pellets showing characteristic green coloration under PPL. Numerous lithic fragments are present, varying in composition and texture, contributing to the immature character of the rock. The matrix is sparse, and the grains are in close contact, indicating a grain-supported framework. The texture suggests moderate sorting with low matrix support and limited post-depositional compaction.

Modal Analysis The drill core sample DPS-BH1-PG2 presents a **quartz-dominated composition (73.4%)**, with significant lithic fragments (19.4%), minor glauconite (6.2%), and a very low concentration of matrix (0.8%) and feldspar (0.2%).

*Table 17*Modal analysis of Sample ID: DPS-BH1-PG2

| Minerals | Modal% |
|------------------|--------|
| Quartz | 73.4 |
| Lithic Fragments | 19.4 |
| Glauconite | 6.2 |
| Matrix | 0.8 |
| Felspar | 0.2 |

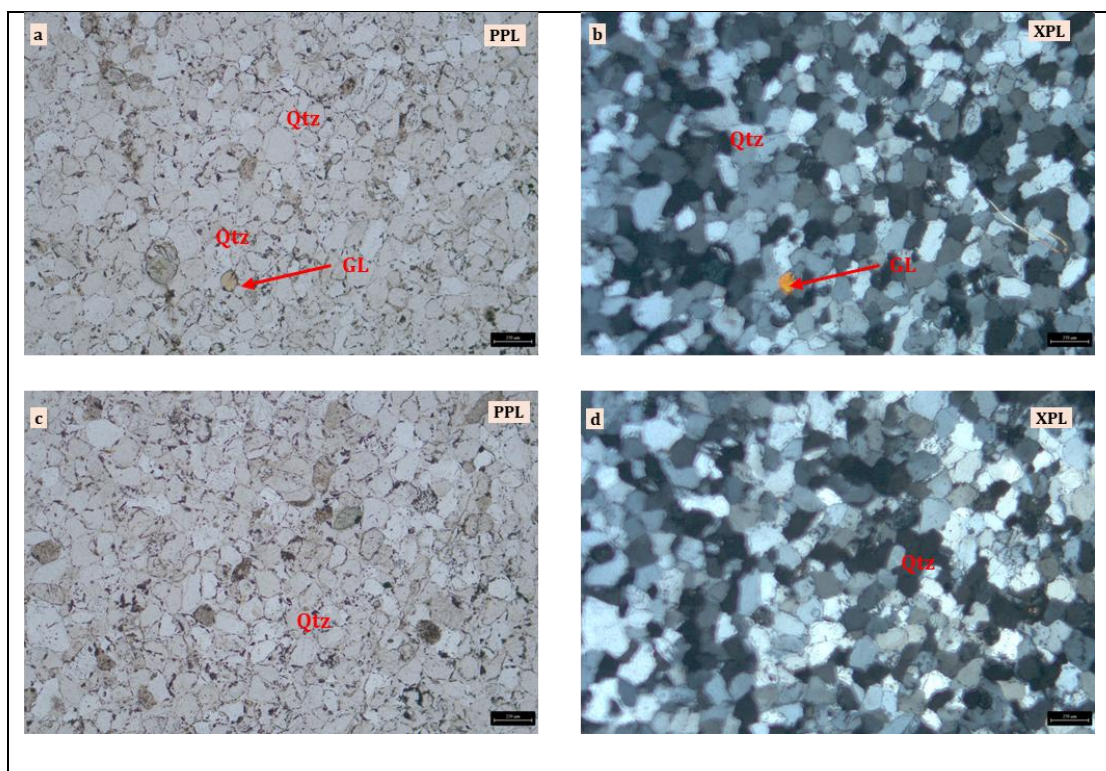


Photomicrograph 7 Showing thin section DPS-BH1-PG2

show (a, c) medium-grained quartz with well-rounded glauconite pellets and numerous lithic fragments under PPL, (b, d) quartz and lithics in a grain-supported framework with minimal matrix under XPL, reflecting moderate sorting and immature texture. Photomicrographs in (e,f) shows glauconite grains in PPL within sandstone

Sample: DPS-BH1-PG3 Rock Type: Glauconite bearing quartz arenite

The thin section shows a quartz arenite composed almost entirely of medium- to fine-grained, sub-rounded quartz grains with well-developed point and long grain contacts. Quartz grains exhibit weak roundness and minimal alteration. One to two glauconite grains are present, appearing as rounded greenish grains under PPL. Minor feldspar grains and small lithic fragments are scattered throughout the section. The rock is cemented by overgrowth silica, with little to no matrix, indicating a mature, well-washed sandstone.

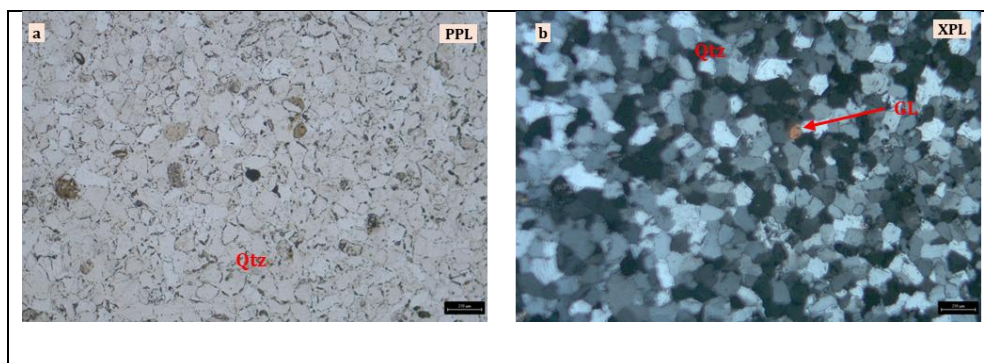


Photomicrograph 8 Showing thin section DPS-BH1-PG3

show (a, c) sub-rounded medium- to fine-grained quartz grains with isolated glauconite pellets and occasional feldspar and lithic fragments under PPL, (b, d) well-developed quartz grain contacts and overgrowths under XPL

Sample: DPS-BH2-PG4 Rock Type: Glauconite bearing quartz arenite

The thin section comprises a quartz arenite with tightly packed medium- to fine-grained quartz grains. Quartz shows sub-rounded boundaries and displays uniform extinction under XPL. One to two glauconite grains are visible, appearing as isolated rounded green grains under PPL. The framework is grain-supported with silica cement, and no significant feldspar or lithic grains are present. The texture indicates high compositional and textural maturity, consistent with reworking and prolonged transport.

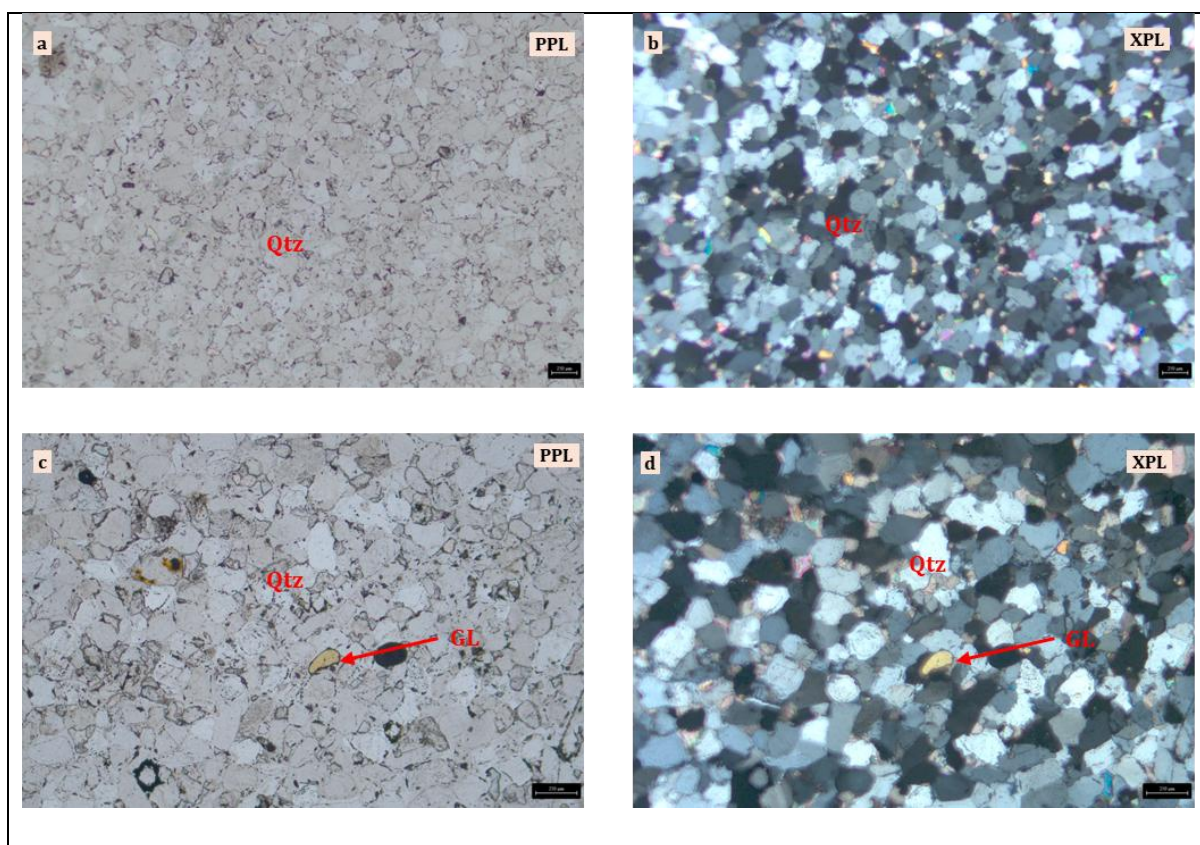


Photomicrograph 9 Showing thin section DPS-BH2-PG4

show medium- to fine-grained quartz grains with sub-rounded grain boundaries and isolated glauconite grains under PPL in (a) and XPL in (b).

Sample: DPS-BH2-PG5 Rock Type: Glauconite bearing Quartz arenite

This thin section is a quartz arenite composed of medium- to fine-grained quartz grains exhibiting sub-rounded boundaries and point contacts. One to two glauconite grains are present and show characteristic green color and rounded shape under PPL. Muscovite or other micaceous minerals are occasionally observed intergrown with the quartz framework. Minor feldspar grains and small lithic fragments are also present, reflecting a slightly less mature composition than PG4. The rock is silica-cemented with minimal matrix.



Photomicrograph 10 Showing thin section DPS-BH2-PG5

show (a, c) quartz grains with minor glauconite, feldspar, and micaceous minerals under PPL, (b, d) quartz with sub-rounded contacts and occasional lithic fragments under XPL, indicating a mature framework with slightly more compositional variation

8.5.3 MINERALOGY

The thin section analysis of sandstone and shale samples from borehole cores reveals a clastic sedimentary suite dominated by **quartz**, with **glauconite** as the principal accessory mineral. Minor constituents include **feldspar**, **lithic fragments**, **calcite**, **opaque minerals**, and occasional **muscovite**. The sandstones range from lithic to quartz arenites and show moderate to good sorting with grains mostly sub-rounded to well-rounded. The overall textures and

mineralogical maturity suggest multiple depositional and diagenetic processes, including prolonged sediment transport, reworking, cementation, and localized weathering

Glaucconite

Glaucconite is the dominant accessory mineral across most arenite samples and occurs as sub-rounded to elliptical green grains under PPL. It exhibits pale to dark green hues, with some altered zones showing brownish-yellow to reddish-brown coloration due to oxidation. Under XPL, glauconite shows very dark grey interference colours and mottled extinction. Grains appear in various forms—ellipsoidal, circular, elongated, and fragmented. It is particularly abundant in samples like **DPS01 (Khari)** and **DPS04 (Piparwasi)**, constituting up to **70–80%** of the rock. In **DPS41**, it occurs in limited quantities with weak preferred orientation, while in **DPS11**, it is restricted to isolated patches, and in **DPS25**, glauconite is absent. Its rounded form and abundance in some arenites indicate reworking and marine shelf deposition, while oxidation rims suggest post-depositional sub-oxic alteration.

In borehole thin sections glauconite appears in small but diagnostic quantities in all arenite samples (PG2 to PG5). It occurs as well-rounded, green-colored pellets under PPL, commonly interspersed among quartz grains. In the lithic arenite (PG2), glauconite is more abundant and contributes to the immature texture, while in the quartz arenites (PG3–PG5), it appears as isolated grains, reflecting a mature, reworked sedimentary origin.

The modal analysis of three representative samples—DPS01, DPS04, and DPS-BH1-PG2 were done, and results confirms the observations during petrography. The surface samples selected for thin section shows significant occurrence of glauconite, with concentrations reaching over 70% in surface samples and a measurable presence in drill core. The detailed logs of modal analysis are attached as annexures for reference.

Quartz

Quartz is the principal framework mineral in all arenite samples. Grains are generally medium- to fine-grained, sub-rounded to well-rounded, and monocrystalline, with occasional undulatory extinction, suggesting mild deformation either pre- or post-deposition. In mature quartz arenites (PG3, PG4, PG5), quartz grains show well-developed point and long grain contacts with silica overgrowth cement, reflecting high compositional and textural maturity. In glauconite-rich arenites like PG2, quartz appears moderately sorted and more rounded, indicating sedimentary reworking. In DPS25, quartz shows interlocking textures and triple junctions, indicative of deeper burial-related compaction and pressure dissolution.

Feldspar

Feldspar is a minor component, occurring primarily in **PG3**, **PG5**, and **DPS25**. The grains are sub-angular to sub-rounded and appear relatively fresh, lacking significant alteration. Their presence—especially in **DPS25**—suggests a **proximal source terrain**, likely granitic or gneissic in origin. Feldspar contributes to slight compositional immaturity in otherwise quartz-dominated samples.

Lithic Fragments

Lithic fragments are scattered in low abundance and appear sub-angular to angular. Their presence is most prominent in **PG2** and **DPS01**, where they contribute to the rock's immature texture. These fragments vary in composition and point toward **multi-source sediment provenance**, possibly involving volcanic, metamorphic, or sedimentary terrains. Their angularity suggests relatively short transport from source areas.

Calcite

Calcite is significant in the **calcareous shale sample (PG1)**, where it forms micritic to microsparry layers within a compact clay-rich matrix. Under XPL, calcite displays 3rd order interference colours and low relief under PPL. Its presence in banded form suggests **secondary carbonate enrichment during early diagenesis**, aligning with observed field effervescence. This early cementation likely occurred under marine reducing conditions.

Opaque Minerals

Opaque minerals, likely iron oxides or sulphides, are observed in **PG1**, particularly within calcite-rich bands. These may represent **diagenetic byproducts** formed under anoxic conditions. Their spatial association with carbonate suggests they were precipitated during early chemical changes in pore fluids.

Muscovite

Muscovite appears occasionally, especially in **PG5**, where it is intergrown within the quartz framework. These platy minerals exhibit characteristic high birefringence and indicate derivation from **low-grade metamorphic rocks** such as phyllites or schists. Their limited presence reinforces the idea of **mixed sediment sources**, including metamorphic terrains.

Petrographic Interpretation

Petrographic analysis of samples from the Dhamni Piparwasi Shimliya Glauconite Block reveals that glauconite bearing sandstones are not encountered everywhere and does not show

much lateral or vertical continuity. Significant glauconite content was observed only in two surface samples, DPS01 and DPS04 where glauconite comprises ~80% and ~70% of the modal composition respectively. These samples show well-rounded glauconite grains within a fine siliceous matrix, consistent with a low-energy marine depositional environment.

Other surface samples, DPS11, DPS41, and DPS25 show minimal to no glauconite. DPS11 has patchy glauconite, DPS41 contains only about 10%, and DPS25 is entirely barren of glauconite, composed mainly of tightly interlocked quartz grains, indicating mature quartz arenite.

Subsurface borehole samples reflect a similar trend. Only DPS-BH1-PG2 showed notable presence of glauconite, still limited. The rest thin sections are dominated by quartz with at the most 1–2 glauconite grains per field, suggesting glauconite is not sustained in these samples.

These findings indicate that glauconite enrichment is confined to specific beds or lenses formed under favourable conditions at limited locations, and it does not persist across the block or at depth. Targeted exploration guided by stratigraphy and detailed petrography is essential, as glauconite occurrence is unpredictable and restricted.

7.6. Mineral Phase analysis by XRD

Three samples were approved by TCC for XRD-based mineral phase identification and determination of the K₂O-hosting phases. Accordingly, samples showing elevated K₂O and Lithium values based on geochemical analysis selected and these three samples were submitted to the GSI–CR Laboratory for XRD analysis, and the results were received.

The XRD results from GSI identified major mineral phases such as quartz, muscovite, microcline, dolomite, and calcite. However, modal analysis carried out through petrographic studies on one of these three samples revealed the presence of glauconite, quartz, and lithic fragments. The occurrence of glauconite is consistent with and adequately explains the elevated K₂O values observed in the geochemical analysis.

In contrast, the mineral assemblage reported in the GSI XRD analysis—dominated by quartz, calcite, dolomite, and microcline—does not satisfactorily justify the elevated K₂O and associated Li values.

To resolve this discrepancy and for independent validation, the same sample that was subjected to modal petrographic analysis was re-analysed externally for XRD phase analysis at Shiva Laboratory.

The XRD results obtained from Shiva Laboratory clearly identified glauconite/illite as a significant mineral phase, along with quartz, dolomite, , and calcite. This mineralogical assemblage strongly supports the elevated K₂O values observed in the geochemical analysis, confirming that glauconite/illite is the principal K₂O-hosting phase in the sample.

Therefore, in this report XRD analysis by Shiva labs is being used for interpretation in this report.

7.6.1 Results of three XRD analysis by GSI

(Annexure 23)

Table 18 XRD Results of GSI lab with Geochemical Values

| Sample ID | Quartz (%) | Dolomite (%) | Calcite (%) | Microcline (%) | Muscovite (%) | K₂O (%) (XRF Geochemical) | Li (ppm) (ICPMS Geochemical) |
|------------------|-------------------|---------------------|--------------------|-----------------------|----------------------|---|---|
| DPS-XRD-01 | ~65 | ~30 | — | — | ~5 | 2.67 | 335.9 |
| DPS-XRD-02 | ~60 | ~20 | ~15 | — | ~5 | 2.38 | 248.1 |
| DPS-XRD-03 | ~65 | ~20 | — | ~10 | ~5 | 3.41 | 346.3 |

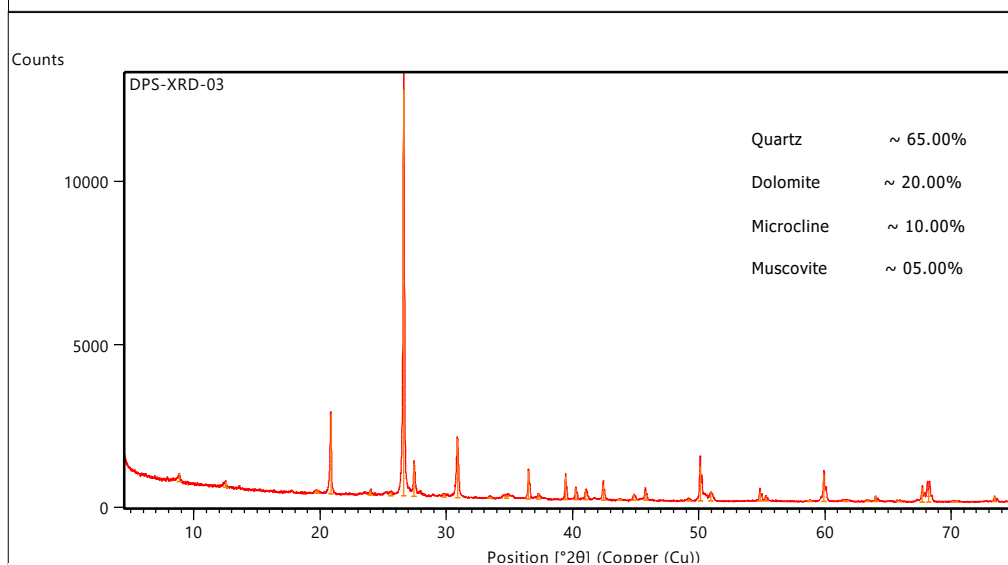
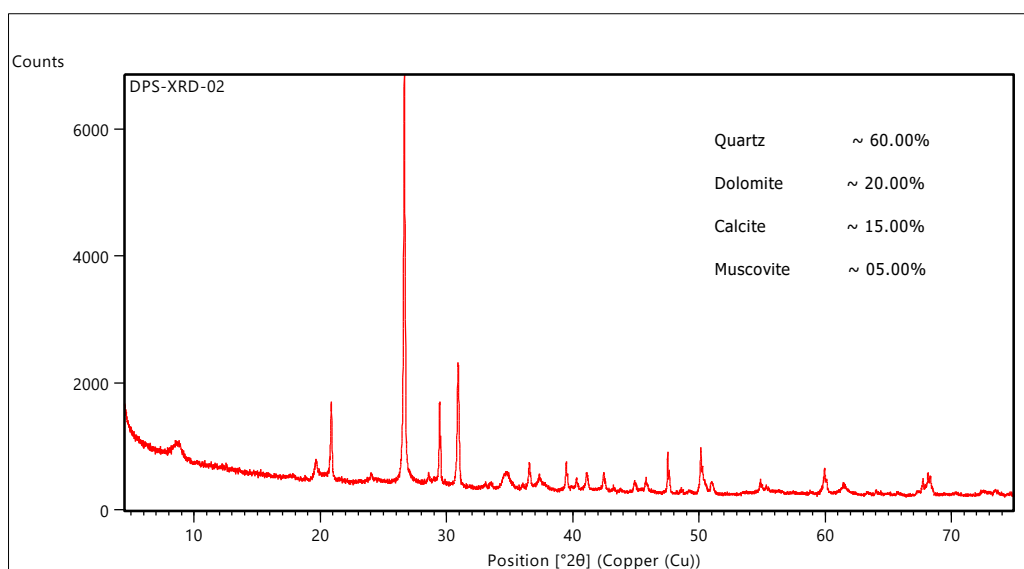
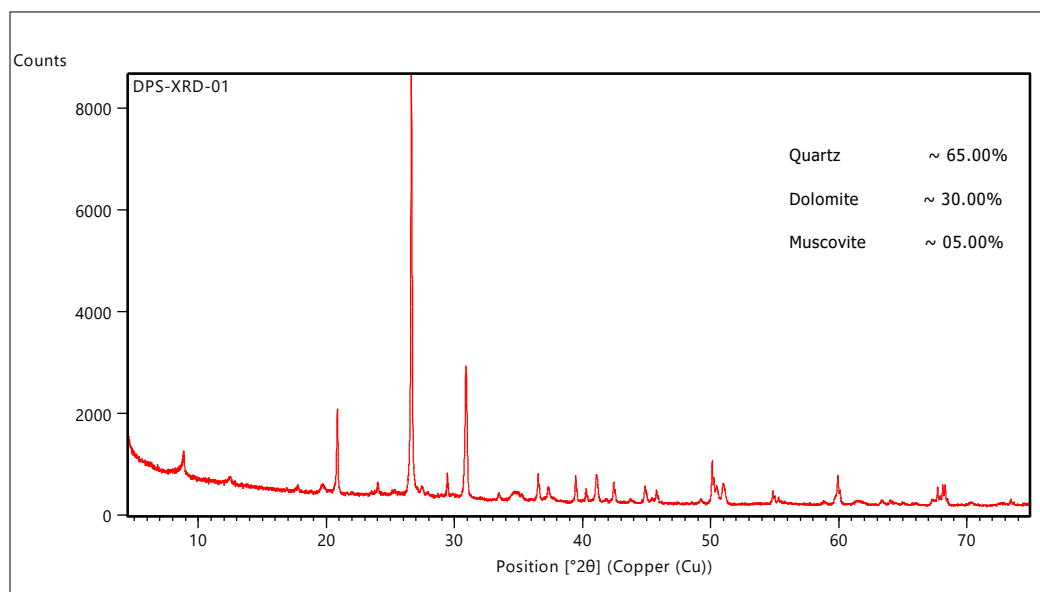


Figure 8 XRD Plots of Phase identification by GSI labs

7.6.2 XRD analysis by Shiva Analyticals of one Sample

DPS XRD-1 sample analysed for cross check and validation, in which quartz dominates the mineralogy with **53.26 wt% of silica is crystalline**. Additionally, **10.95 wt% corresponds to amorphous**, indicating the presence of opaline silica, microcrystalline quartz, or silica cement not detected by XRD.

Carbonates are significant, with crystalline calcite/dolomite (**CaO 4.00 wt%, CO₂ 4.61 wt%**) plus an additional **2.04 wt% amorphous Ca-bearing phases**, showing mixed crystalline and poorly crystalline carbonate components.

Clay-mica minerals (**illite-glaucanite-biotite**) account for most of the **Al₂O₃, K₂O, MgO, and structural H₂O**, confirming a silicate-rich, moderately altered sediment source.

Iron (Fe²⁺ and Fe³⁺) traces responsible for the green colour of the sample that is split among the crystalline and amorphous phases. The amorphous phase contains **~5.09 wt% as Fe-oxyhydroxides**, indicating weathering or diagenetic alteration.

High LOI (**10.62 wt%**) reveals substantial volatile-bearing components—structural water, hydroxyls, organics, and amorphous carbonates—together contributing to the overall **22.60 wt% amorphous fraction**, which strongly influences the material reactivity and physical behaviour.

Secondary/Amorphous Phases: Silica from non-crystalline Si-rich material. Carbonates from poorly crystalline Ca-Mg phases. Fe–Mg–Al silicates from altered clay/mica and Fe-oxyhydroxides.

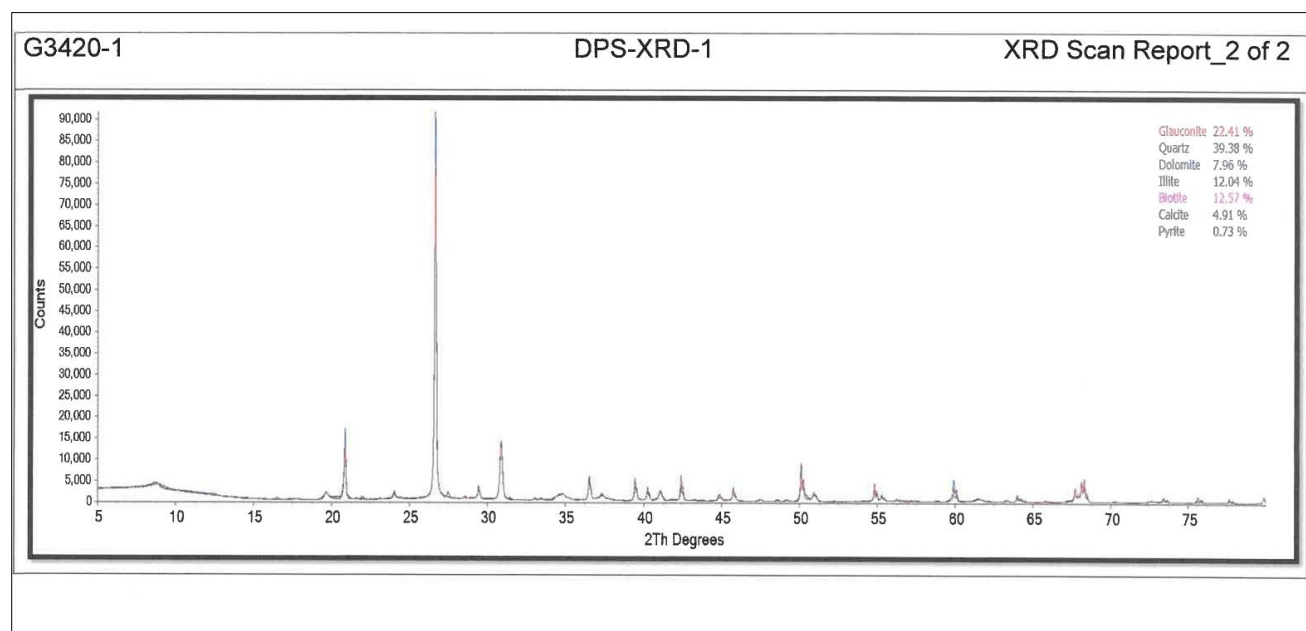


Figure 9 XRD Plots of Phase identification by Shiva Labs

Results;

Crystallinity: **77.40%** and Amorphous: **22.60%**, primarily dominated by silica (**64.21 wt%**).

The sample is a **glauconitic quartzite dominated by crystalline quartz (53.26% crystalline SiO₂)**, with a significant amorphous silica component (**10.95 wt%**), indicating partial alteration and silica gel formation.

Clay-mica minerals (glauconite/illite/biotite) contain the main **Al₂O₃, K₂O, MgO, and structural H₂O**, confirming mixed detrital and authigenic silicate phases.

Carbonate minerals (calcite + dolomite) account for **9.96 wt% crystalline CaO**, further with additional amorphous Ca-bearing phases (**2.63 wt%**), showing both crystalline and poorly crystalline carbonate contributions.

Total amorphous content is **22.60 wt%**, consisting of amorphous silica, Fe–Mg–Al silicate gels, amorphous carbonates, and volatile-bearing phases reflected in the high LOI (**10.62%**).

Interpretation of K₂O-Hosting Mineral Phases

The phase analysis clearly demonstrates that K₂O is predominantly hosted within clay–mica group minerals, primarily glauconite and illite, with minor contribution from K-bearing biotite. No significant contribution from K-feldspar is observed, indicating that potassium is mainly structurally bound within phyllosilicate lattices rather than framework silicates.

Glauconite–illite phases account for the major share of K₂O, where potassium is present as interlayer cations, confirming its structural incorporation rather than adsorbed or exchangeable form. The presence of both crystalline and partially amorphous clay-mica phases suggests

diagenetic evolution of glauconite, possibly through alteration, oxidation, or partial breakdown. Amorphous Fe–Mg–Al silicate gels contribute indirectly to the K₂O budget, representing altered remnants of primary glauconitic material.

The coexistence of authigenic glauconite and detrital illite/biotite indicates mixed provenance, with potassium derived from both marine authigenic processes and continental hinterland sources.

Genetic implication for K₂O enrichment

The dominance of glauconite as the principal K₂O-hosting mineral supports formation under, Low-sedimentation, marine shelf conditions, slightly reducing to sub-oxic environments, Slow burial and prolonged residence time at the sediment–water interface Subsequent carbonate cementation, diagenesis, and surface/near-surface weathering resulted in partial amorphization of K-bearing phases without complete loss of structural potassium.

Since K₂O is structurally bound within glauconite–illite, its distribution is expected to show lithological control rather than simple geochemical dispersion. The confirmation of glauconite as the dominant K₂O carrier validates the use of mineralogical constraints during resource estimation, beneficiation planning, and grade interpretation. The absence of feldspathic K phases implies limited rapid leaching, enhancing the geological reliability of K₂O grades. XRD-based phase analysis confirms glauconite–illite as the principal K₂O-hosting mineral phases, with potassium structurally bound within clay–mica lattices, supporting a marine glauconitic depositional environment and providing a robust mineralogical basis for K₂O resource evaluation.

Table 19 XRD Results of XRD DPS-1 by Shiva Labs

Bulk Oxides by WDXRF:

| Oxides | Wt% |
|--------------------------------|-------|
| Al ₂ O ₃ | 4.71 |
| BaO | <0.05 |
| CaO | 6.04 |
| Cr ₂ O ₃ | <0.05 |
| Fe ₂ O ₃ | 5.22 |
| K ₂ O | 2.72 |
| MgO | 4.44 |
| MnO | 0.06 |
| Na ₂ O | 0.07 |
| P ₂ O ₅ | <0.05 |
| SiO ₂ | 64.21 |
| SO ₃ | 1.43 |
| SrO | <0.05 |
| TiO ₂ | 0.20 |
| V ₂ O ₅ | <0.05 |
| ZrO ₂ | <0.05 |
| HfO ₂ | <0.05 |
| CuO | <0.05 |
| NiO | <0.05 |
| PbO | <0.05 |
| ZnO | 0.19 |
| LOI | 10.62 |

Mineral Phases by XRD:

| Sl. No. | Mineral Name | Chemical Formula | XRD Wt. % | XRD Crystallinity (Wt%*0.774) | Molecular Weight (g/mol) |
|---------|-------------------|---|------------|-------------------------------|--------------------------|
| 1 | Glauconite/illite | KAl ₂ (AlSi ₃ O ₁₀)(OH) ₂ | 34.45 | 26.66 | 375-422 |
| 2 | Quartz | SiO ₂ | 39.38 | 30.48 | 60.08 |
| 3 | Dolomite | CaMg(CO ₃) ₂ | 7.96 | 6.16 | 184.4 |
| 4 | Biotite | K(Mg,Fe) ₃ AlSi ₃ O ₁₀ (OH) ₂ | 12.57 | 9.73 | 425 |
| 5 | Calcite | CaCO ₃ | 4.91 | 3.80 | 100.09 |
| 6 | Pyrite | FeS ₂ | 0.73 | 0.57 | 119.98 |
| | Total | | 100 | 77.40 | |

Table 20 Stoichiometric Comparison Table of XRD DPS-1 by shiva Labs

Stoichiometric Comparison Table:

| Oxides | XRF (wt%) | XRD crystallinity (wt%) | Amorphous (wt%) |
|--------------------------------|-----------|-------------------------|-----------------|
| Al ₂ O ₃ | 4.71 | 4.24 | 0.47 |
| CaO | 6.04 | 4.00 | 2.04 |
| Fe ₂ O ₃ | 5.22 | 2.63 | 2.59 |
| K ₂ O | 2.72 | 2.11 | 0.61 |
| MgO | 4.44 | 2.58 | 1.86 |
| SiO ₂ | 64.21 | 53.26 | 10.95 |
| SO ₃ | 1.43 | 0.38 | 1.05 |
| TiO ₂ | 0.20 | 0.00 | 0.20 |
| LOI | 10.62 | 0.00 | 10.62 |
| CO ₂ | 0.00 | 4.61 | - |
| H ₂ O | 0.00 | 3.58 | - |
| Trace | 0.41 | 0.00 | 0.41 |

Table 21 Stoichiometric Oxide Table of XRD-DPS-1 By Shiva labs

Stoichiometric Oxide Table:

| Sl.No | Mineral (wt %) | Chemical Formula | Mineral wt% | SiO ₂ | Al ₂ O ₃ | K ₂ O | MgO | CaO | Fe ₂ O ₃ | CO ₂ | H ₂ O | SO ₂ |
|--------------|-------------------|---|--------------|------------------|--------------------------------|------------------|-------------|-------------|--------------------------------|-----------------|------------------|-----------------|
| 1 | Glauconite/Illite | KAl ₂ (AlSi ₃ O ₁₀)(OH) ₂ | 26.66 | 19.10 | 3.20 | 1.15 | 0.00 | 0.00 | 0.00 | 0.00 | 3.21 | 0.00 |
| 2 | Quartz | SiO ₂ | 30.48 | 30.48 | 0.00 | 0.00 | 0.00 | 0.00 | 0.00 | 0.00 | 0.00 | 0.00 |
| 3 | Dolomite | CaMg(CO ₃) ₂ | 6.16 | 0.00 | 0.00 | 0.00 | 1.35 | 1.87 | 0.00 | 2.94 | 0.00 | 0.00 |
| 4 | Biotite | K(Mg,Fe) ₃ AlSi ₃ O ₁₀ (OH) ₂ | 9.73 | 3.68 | 1.04 | 0.96 | 1.23 | 0.00 | 2.44 | 0.00 | 0.37 | 0.00 |
| 5 | Calcite | CaCO ₃ | 3.80 | 0.00 | 0.00 | 0.00 | 0.00 | 2.13 | 0.00 | 1.67 | 0.00 | 0.00 |
| 6 | Pyrite | FeS ₂ | 0.57 | 0.00 | 0.00 | 0.00 | 0.00 | 0.00 | 0.19 | 0.00 | 0.00 | 0.38 |
| Total | | | 77.40 | 53.26 | 4.24 | 2.11 | 2.58 | 4.00 | 2.63 | 4.61 | 3.58 | 0.38 |

11. Location of data point

11.1 Location of data points:

Borehole fixation of was done by DGPS presented in table below.

Table 22 Location of Borehole Points

| | | |
|---------------------|---------------------------|----------------|
| Agency | Maheshwari Mining Pvt Ltd | |
| BH NO | DPS/BH-01 | DPS/BH-02 |
| Date of Commence | 04-05-2025 | 09-05-2025 |
| Date of Closing | 08-05-2025 | 13-05-2025 |
| Easting | 734452.9 | 733524.788 |
| Northing | 2864576 | 2866738.401 |
| RL | 297.7743 | 282.1039 |
| Latitude | 25:52:50.94191 | 25:54:01.72442 |
| Longitude | 77:20:23.81120 | 77:19:51.86654 |
| Azimuth | NA | NA |
| Inclination | 90 | 90 |
| Total Drilling in m | 34 | 30 |
| EOH | 263.77 | 252.103 |

DGPS Location of Pits presented in table below

| id | northing | mrl | | latitude | longitude |
|--------|-------------|---------|--|-----------|-----------|
| PIT-1 | 2876171.692 | 246.564 | | 25.985427 | 77.342833 |
| PIT-2 | 2875626.219 | 243.909 | | 25.980639 | 77.3345 |
| PIT-3 | 2865188.121 | 288.639 | | 25.8865 | 77.330278 |
| PIT-4 | 2866279.855 | 332.723 | | 25.895605 | 77.376361 |
| PIT-5 | 2868707.48 | 293.639 | | 25.918361 | 77.324194 |
| PIT-6 | 2869136.802 | 288.979 | | 25.921892 | 77.345556 |
| PIT-7 | 2869262.885 | 287.258 | | 25.923072 | 77.342917 |
| PIT-8 | 2869899.766 | 276.779 | | 25.929167 | 77.321403 |
| PIT-9 | 2870336.167 | 277.368 | | 25.932735 | 77.344417 |
| PIT-10 | 2870533.397 | 294.897 | | 25.93429 | 77.358222 |
| PIT-11 | 2872152.738 | 274.546 | | 25.949155 | 77.342861 |
| PIT-12 | 2871965.631 | 286.639 | | 25.94675 | 77.386694 |

| | | | | | |
|--------|-------------|----------|--|-----------|-----------|
| PIT-13 | 2874224.687 | 256.259 | | 25.968056 | 77.330417 |
| PIT-14 | 2875018.372 | 256.869 | | 25.9745 | 77.374611 |
| PIT-15 | 2875628.256 | 253.287 | | 25.980434 | 77.348306 |
| PIT-16 | 2866105.293 | 284.7195 | | 25.894721 | 77.333837 |
| PIT-17 | 2867356.349 | 277.88 | | 25.906072 | 77.330069 |
| PIT-18 | 2867133.618 | 291.3482 | | 25.903876 | 77.341622 |
| PIT-19 | 2869654.412 | 293.3297 | | 25.926792 | 77.33141 |
| PIT-20 | 2869225.644 | 286.965 | | 25.92273 | 77.343275 |
| PIT-21 | 2869224.028 | 283.126 | | 25.922696 | 77.344497 |
| PIT-22 | 2870412.47 | 278.5607 | | 25.933758 | 77.32365 |
| PIT-23 | 2864579.107 | 297.7774 | | 25.880848 | 77.339927 |
| PIT-24 | 2870550 | 284 | | 25.93864 | 77.37139 |
| PIT-25 | 2867700 | 281 | | 25.91239 | 77.37639 |

11. 2 Quality of Topographic Data:

SRTM 30m spatial resolution data was used to generate topographic map.

Chapter-12. Sampling technique

12.1 Bedrock Sampling:

Bedrock sampling was carried out in the study area to assess the lithochemical characteristics of the glauconite-bearing formations. A total of **one hundred and fifty (150) bedrock samples** were collected from surface exposures using the **chip sampling method** from glauconitic sandstone, shale and calcareous shale horizons. The samples were collected from fresh exposures in a systematic manner so as to obtain representative material from the lithological units occurring within the study area. **Approximately 1 kg of sample material was collected at each sampling location.** The collected samples were properly labeled and dispatched to the laboratory for preparation and analysis.

At the laboratory, the samples were **dried, crushed and pulverized to about 200 mesh size.** The powdered samples were then **homogenized and reduced using the cone and quartering method** to obtain representative aliquots for chemical analysis. The prepared samples were subjected to chemical analysis with emphasis on **K₂O content**, along with other major oxides such as **Al₂O₃, Fe₂O₃ and SiO₂**, in order to evaluate the presence and distribution of glauconite mineralization.

All **150 bedrock samples were analyzed for major oxides using X-ray Fluorescence (XRF).** In addition, **seventy-five (75) representative samples were further analyzed for trace elements using Inductively Coupled Plasma Mass Spectrometry (ICP-MS)** to determine the geochemical characteristics of the glauconite-bearing formations. For analytical quality assurance and reproducibility, **fifteen (15) external check samples were analyzed for major oxides by XRF and seven (7) samples were analyzed for trace elements using ICP-MS.** The analytical results indicate variable **K₂O concentrations within the sampled horizons**, reflecting heterogeneous distribution of glauconite within the sedimentary sequence. The mineralization is mainly associated with **calcareous shale, shale and shale-sandstone intercalation units** observed in the study area.

12.2 Pit Sampling:

As part of shallow subsurface investigation and to examine the continuity of the glauconite-bearing horizons, **fifty (50) pits** were excavated at selected locations across the study area.

Representative samples were collected from the exposed lithological horizons in the pits using the **chip sampling method**, and **approximately 1 kg of sample material was collected from each pit horizon**. The collected samples were properly labeled and sent to the laboratory for preparation.

In the laboratory, the samples were **crushed and pulverized to about 200 mesh size**, after which **cone and quartering was carried out to obtain representative portions for analysis**. These samples were analyzed for **major oxides using X-ray Fluorescence (XRF)** to evaluate the lithochemical characteristics of the shallow horizons and to correlate them with the results obtained from bedrock sampling. For quality control purposes, **five (5) check samples, representing approximately ten percent of the pit samples, were also analyzed through an external laboratory** to ensure analytical accuracy and reliability.

12.3 Petrological Samples

For petrographic studies, **ten (10) representative samples** covering different lithological units were collected from surface exposures as well as drill cores. Thin sections of these samples were prepared at **Narayani Rock Thin and Polish Section Unit, West Bengal**, and petrographic examination was carried out to determine the mineralogical composition, textural characteristics and occurrence of glauconite within the host rock.

12.4 Core Sampling:

Subsurface investigation was carried out through **core drilling of two boreholes (DPS/BH1 and DPS/BH2)** with a total drilled depth of **64 meters**. Core samples were collected from the identified glauconite-bearing intervals generally at **approximately 1 m spacing**, taking into account lithological boundaries and mineralized zones. **About 1 kg of sample material was collected from each designated sampling interval**, properly labeled and sent to the laboratory for preparation and analysis.

In the laboratory, the core samples were **crushed, pulverized to about 200 mesh size and homogenized**, after which **cone and quartering was performed to obtain representative aliquots for chemical analysis**. A total of **fifty-three (53) borehole core samples were analyzed for major oxides using X-ray Fluorescence (XRF)**, while **thirty-six (36) samples were analyzed for trace elements using ICP-MS**. For analytical quality assurance and quality

control, seven (7) external check samples were analyzed for major oxides by XRF and three (3) samples were analyzed for trace elements using ICP-MS. All chemical analyses were carried out at **Shiva Analytical (India) Private Limited**, and the results were used to evaluate the grade, thickness and vertical distribution of glauconite mineralization within the drilled sequence.

Chapter- 13. Exploratory Drilling

13.1 Introduction

As part of the reconnaissance (G-4) stage exploration for glauconitic sandstone in the Dhamni–Piparwasi–Simliya Block, a total of two scout boreholes were drilled to investigate the subsurface lithology and assess the occurrence and continuity of glauconite-bearing strata (Table 20, Plate XIII). The drilling was conducted using rotary/core methods under geological supervision.

- **Borehole DPS/BH/01** was drilled from 4th May 2025 to 8th May 2025, with a Base RL of 297meters and a total depth of 34 meters.
- **Borehole DPS/BH/02** was drilled from 9th May 2025 to 13th May 2025, with a Base RL of 282 meters and a total depth of 30 meters.

In total, 64 meters of scout drilling was completed during the campaign. The borehole locations were selected based on favourable surface geological indicators to validate the depth, thickness, and grade of glauconitic horizons for resource assessment.

13.2 Borehole Planning

Two scout boreholes DPSBH-1 & DPSBH2 were panned as per approved quantum of G4 project, and MEMC rules 2015 and amendment rules 2021, two vertical boreholes planned according to geochemical anomaly of elevated K₂O % and surface indication in south western part of the block near Piparwasi village and distance between two borehole is 2.39km.

13. 3 Methodology of Drilling

Drilling forms a vital component of mineral exploration, providing crucial subsurface data to assess the geological and economic potential of the target zone. In the Dhamini–Piparwasi–Simliya Glauconite Block, scout drilling was conducted to investigate the presence, thickness, and continuity of glauconite-bearing lithologies.

Hydrostatic diamond core drilling using the wireline method was employed for its efficiency and ability to retrieve continuous, high-quality core. All boreholes were drilled vertically using HQ size, with a borehole diameter of 96 mm and a core diameter of 63.5 mm. A triple-tube core barrel was used to enhance core recovery, especially in soft, weathered, or fractured formations.

A polymer-based drilling fluid was used throughout the operation. This fluid played a key role in cuttings removal, borehole wall stabilization, and cooling of the drill bit, thereby minimizing bit wear and reducing the risk of overheating or burning.

The overall core recovery exceeded 90%, indicating effective drilling practice and stable ground conditions. However, slightly lower recovery was encountered in clay-filled cavities, loose weathered zones, and highly fractured intervals, where formation cohesion was poor.

Table 23 General Information of Boreholes

| | | |
|---------------------|---------------------------|----------------|
| Agency | Maheshwari Mining Pvt Ltd | |
| BH NO | DPS/BH-01 | DPS/BH-02 |
| Date of Commence | 04-05-2025 | 09-05-2025 |
| Date of Closing | 08-05-2025 | 13-05-2025 |
| Easting | 734452.9 | 733524.788 |
| Northing | 2864576 | 2866738.401 |
| RL | 297.7743 | 282.1039 |
| Latitude | 25:52:50.94191 | 25:54:01.72442 |
| Longitude | 77:20:23.81120 | 77:19:51.86654 |
| Azimuth | NA | NA |
| Inclination | 90 | 90 |
| Total Drilling in m | 34 | 30 |
| EOH | 263.77 | 252.103 |

13.4 Drill Core Logging

The entire drill core recovered during exploration was subjected to **systematic and detailed geological logging**. Each lithological unit encountered in the boreholes was carefully described in terms of its **lithology, grain size, colour, texture, sedimentary structures, intercalations, and Rock Quality Designation (RQD)**. Where core recovery was poor—especially in weathered or fractured zones—**extrapolations were made proportionately**, using the physical characteristics of adjacent recovered core segments to maintain lithostratigraphic

continuity. There are two logs one is Run wise core log (Annexure 13) and other detailed Litholog (21 and 22).

Graphic Litholog with K₂O % and Intersection zone of > 2 % K₂O are prepared and attached in **annexure 14**.

All recovered cores were **properly preserved in GI core boxes** as per the specifications prescribed by the **National Mineral Exploration Trust (NMET)**, following the standard **“book pattern” arrangement**. A **duplicate half-core** has been preserved securely in the same boxes and is handed over to the RCL Nagpur, Geological **Survey of India** for future reference and verification.

13.5 Core Recovery and RQD

The Rock Quality Designation (RQD) values recorded in boreholes DPS/BH1 and DPS/BH2 were examined together with core recovery, lithology, assay values (K₂O %) and depth to understand the relationship between rock mass quality and the glauconite mineralized zones. The upper portion of both boreholes, consisting mainly of loose material up to about 8–9 m depth, shows very low RQD values despite moderate to high core recovery. This indicates highly weathered and unconsolidated material representing overburden, where K₂O values remain low and do not represent significant glauconite mineralization. Below this zone, shale–sandstone intercalations mark the transition into the glauconite bearing sequence, where K₂O values increase to around 2–3% while RQD remains generally low to poor, indicating a fractured and relatively weak rock mass. The calcareous shale units encountered between about 11–16.5 m in borehole DPS/BH1 and approximately 12–18 m in borehole DPS/BH2 represent the principal glauconite bearing horizon. In these intervals, K₂O values commonly range between about 1.7% and 3.8%, while RQD values fall mainly within the poor to fair category (approximately 30–68%). This suggests that the mineralized horizons occur within relatively softer and moderately fractured shale units. Sandstone units occurring below these horizons generally display comparatively higher RQD values, indicating stronger and more competent rock mass conditions; however, these intervals show lower K₂O values, reflecting dilution of glauconite mineralization. Localized enrichment of K₂O is observed again within deeper sandstone–shale intercalation zones, although these intervals also exhibit low RQD values due to increased fracturing along lithological contacts. Overall, the analysis indicates that glauconite mineralization is predominantly associated with shale and calcareous shale horizons characterized by moderate to low RQD values, whereas the more competent sandstone units

show higher RQD but comparatively lower K₂O values. The relationship between RQD, lithology, core recovery and assay values indicates that variations in rock mass quality are primarily lithologically controlled and that the mineralized zones occur within relatively softer and more fractured shale horizons, which may influence excavation characteristics and mining behaviour in future extraction activities.

Table 24 Core Recovery

| Borehole | Total Drilled Length (m) | Total Core Recovery (m) | Average Core Recovery (%) |
|----------|--------------------------|-------------------------|---------------------------|
| DPS/BH1 | 34 | 33.39 | 98.21 % |
| DPS/BH2 | 30 | 29.63 | 98.77 % |

Table 25 Core recovery and RQD

| Borehole | Depth Range (m) | Lithology | Core Recovery (%) | RQD Range (%) | Rock Quality | K ₂ O Range (%) | Mineralization Interpretation |
|----------|-----------------|-------------------------------|-------------------|---------------|----------------|----------------------------|-------------------------------------|
| DPS/BH 1 | 0–8 | Loose material | ~80–100 | 0–50 | Very Poor–Poor | 0–1.74 | Overburden, non-mineralized |
| DPS/BH 1 | 8–11 | Shale–sandstone intercalation | ~90–100 | 20–24 | Very Poor–Poor | ~2.3–2.95 | Entry into glauconite bearing zone |
| DPS/BH 1 | 11–16.5 | Calcareous shale | ~100 | 30–66.7 | Poor–Fair | ~1.8–2.9 | Main glauconite mineralized horizon |
| DPS/BH 1 | 16.5–21 | Shale | ~100 | 24–38 | Poor | ~1.9–2.1 | Continuation of mineralized zone |
| DPS/BH 1 | 21–27 | Sandstone | ~100 | 28–59 | Poor–Fair | ~0.7–1.08 | Weakly mineralized sandstone |
| DPS/BH 1 | 27–34 | Sandstone–shale intercalation | ~100 | 0–5.6 | Very Poor | up to ~4.39 | Localized glauconite enrichment |
| DPS/BH 2 | 0–9 | Loose material | ~90–100 | 0–16 | Very Poor | ~0.8–1.17 | Overburden / weak mineralization |
| DPS/BH 2 | 9–12 | Shale–sandstone intercalation | ~100 | 0–20 | Very Poor | ~1.9–3.4 | Beginning of mineralized zone |

| | | | | | | | |
|-------------|-------------|--|------|------------|-----------------------|--------------|---|
| DPS/BH 2 | 12–18 | Calcareous shale | ~100 | 13–68 | Poor– Fair | ~1.7– 3.8 | Main glauconite mineralized zone |
| DPS/BH 2 | 18– 22.5 | Sandstone / shale | ~100 | 0–37 | Very Poor– Poor | ~1.4– 2.9 | Transitional mineralized interval |
| DPS/BH 2 | 22.5– 27 | Sandstone | ~100 | 38– 100 | Fair– Excellent | ~1.0– 1.3 | Weak mineralization |
| DPS/BH 2 | 27–30 | Sandstone– shale intercalatio n | ~100 | ~20 | Poor | ~2.8– 4.7 | Localized high K ₂ O zone |

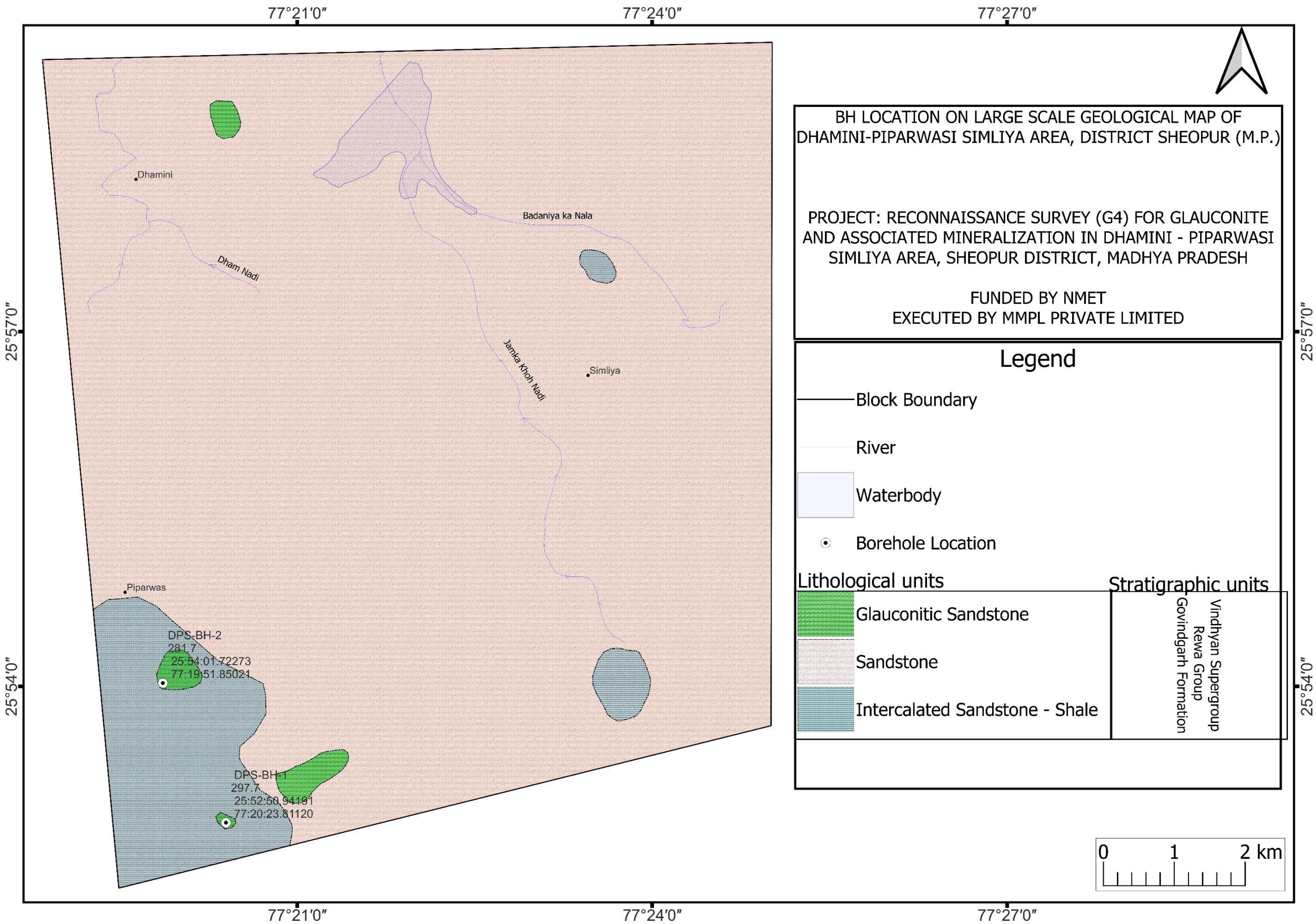
Table 26 Detailed Litholog of DPS/BH/01,

| Detailed Litholog of DPS/BH/01, in Reconnaissance Survey (G-4) for Glauconitic Sandstone in Dhamni, Piparwasi, Simliya, Vijaypur, District- Sheopur, Madhya Pradesh | | | | | | | |
|---|------------------------|-------------------------|--------------------------|-------------------------------------|--|-------------------------------------|---|
| Lithology From_Depth (m) | Lithology To_Depth (m) | Lithology contact angle | Lithology True Width (m) | Lithology Name | Lithology Description | Structures | Stratigraphic Unit |
| 0 | 4.5 | NA | 4.5 | Loose Material | Green to Brown color soil, mainly composed of clay and silt particles loose soil material also have broken pieces of sandstone of 1 to 2 inches and cores of boulders of up to inches. | | Govindgarh Formation Rewa Group Vindhyan Supergroup |
| 4.5 | 8.5 | 90° | 4 | Shale with sandstone intercalations | Greenish-grey weathered shale, fine-grained and thinly bedded, with sub-centimeter partings. Some core segments are completely weathered, resulting in poor or no recovery. The shale is composed primarily of clay minerals and quartz. Intercalated within the shale are medium-grained, light grey sandstone layers with sub rounded and moderately sorted grains. Glauconite mineral grains are visible within the sandstone bands, indicating marine depositional influence. | Laminations | |
| 8.5 | 10.5 | 90° | 2 | Sandstone with shale intercalation | Grey sandstone, fine- to medium-grained, occurring in core segments of 3 to 5 inches thickness. Grains are sub-rounded and moderately sorted. The sandstone is primarily composed of quartz, with subordinate feldspar and rare glauconite grains. Occasional lithic fragments are also observed. A distinct glauconitic band (~5 inches thick) is present at approximately 9 meters depth. Some portions of the core show signs of weathering and are discontinuous. Minor intercalations of shale occur between sandstone beds, indicating periodic shifts in depositional energy and environment. | Bedding of thin to medium thickness | |
| 10.5 | 16.50 | 90° | 6 | Calcareous Shale | Black color, evenly laminated, fresh shale with partings at less than one to eight inches, some discontinuous light green color lamination also presents with clay minerals, shale is calcareous, showing mild effervescences and 10 to 19 percent CaO present in geochemical analysis, secondary fillings are common in partings, mostly concordant but some are at angle with lamination plane, some secondary fillings are composed of sulfides while others are of Calcite. | Laminations | |
| 16.5 | 24.8 | 90° | 8.3 | Glauconite Bearing Lithic Arenite | Highly compact, fresh, fine grained, Dull white color, sorted, rounded and medium to thickly bedded, mainly composed of quartz but disseminated altered light green color grains are also present. Color changes from light grey to dark grey at the both ends of this unit adjacent to shale unit | Thin to Medium bedding | |
| 24.8 | 31 | 90° | 6.2 | Shale and sandstone intercalations | Dark grey shale with laminations is intercalated with grey color sandstone, sandstone is fine grained composed of quartz and some grains of glauconite and feldspar. | Thin bedding and laminations | |
| 31 | 34 | 90° | 3 | Shale | Black color, evenly laminated, fresh shale with partings at less than one to eight inches, secondary fillings are common in partings, mostly concordant but some are at angle with lamination plane. | | |

Table 27Detailed Litholog of DPS/BH/02

| Detailed Litholog of DPS/BH/02, in Reconnaissance Survey (G-4) for Glauconitic Sandstone in Dhamni, Piparwasi, Simliya, Vijaypur, District- Sheopur, Madhya Pradesh | | | | | | | |
|---|------------------------|-------------------------|--------------------------|-----------------------------------|--|-------------------------------|---|
| Lithology From_Depth (m) | Lithology To_Depth (m) | Lithology contact angle | Lithology True Width (m) | Lithology Name | Lithology Description | Structures | Stratigraphic Unit |
| 0 | 9.5 | NA | 9.5 | Loose Material | Green to Brown color soil, mainly composed of clay and silt particles loose soil material also have broken pieces of sandstone of 1 to 2 inches and cores of boulders of up to inches. | | Govindgarh Formation Rewa Group Vindhyan Supergroup |
| 9.5 | 12.5 | 90° | 3 | Sandstone with intercalated Shale | White sandstone interbedded with weathered shale. The sandstone is fine- to medium-grained, quartz-dominated, occurring in thick, massive beds exceeding 10 inches. Grains are sub-rounded to rounded and moderately sorted. The sandstone is very compact, with a Mohs hardness >7, indicating high induration. Intercalated shale units are greenish-grey, weathered, and range from 2 to 3 inches in thickness. Overall, the unit exhibits alternating hard, resistant sandstone beds with softer, weathered shale layers | Thick bedding and Laminations | |
| 12.5 | 18 | 90° | 5.5 | Calcareous Shale | Black, fresh, evenly laminated shale with partings ranging from <1 inch to 8 inches. Occasional discontinuous light green laminations are present, likely associated with clay minerals. The shale is calcareous, exhibiting mild effervescence with dilute HCl, corroborated by geochemical analysis indicating 10–19% CaO. Secondary mineral fillings are common within partings, predominantly concordant to lamination planes, though some occur at oblique angles. | Lamminations | |
| 18 | 20.5 | 90° | 2.5 | Sandstone | White sandstone, fine-grained, with sub-rounded grains that are poorly to moderately sorted. The unit is quartz-dominated. Sandstone exhibits a hardness >7 on the Mohs scale, indicating high induration. The rock mass shows frequent fractures, some of which are open or partially healed with secondary mineral infillings. The sandstone is compact, with minimal matrix and low porosity, suggesting a mature sedimentary provenance and diagenetic overprint. | bedding | |
| 20.5 | 22.5 | 90° | 2 | Shale | Black color, evenly laminated, fresh shale with partings at less than one to eight inches, secondary fillings are common in partings, mostly concordant but some are at angle with lamination plane. | laminations | |
| 22.5 | 27 | 90° | 4.5 | Sandstone | Light grey sandstone, fine-grained, compact, and well-indurated with a Mohs hardness >7. Grains are sub-rounded and poorly to moderately sorted. The rock mass exhibits numerous random fractures, many of which are filled with secondary minerals. Some fractures also contain visible sulfide mineralization, indicating late-stage hydrothermal activity or diagenetic processes. Overall, the sandstone shows low porosity and a tightly packed grain framework | Bedding | |
| 27 | 30 | 90° | 3 | Shale intercalated with sandstone | Dark grey shale with laminations is intercalated with grey color sandstone, sandstone is fine grained. | Laminations and bedding | |

PLATE X Borehole Location Plan on Geological Map



13.6 Sampling, Laboratory Procedure, and Quality of Assay

13.6 .1 Core Sampling

Drill core sampling was undertaken after detailed geological core logging, lithological examination, and interpretation of relevant field and subsurface data during the reconnaissance (G-4 level) exploration. The primary objective of core sampling was to obtain representative material for geochemical analysis in order to evaluate the grade, distribution, and continuity of glauconitic sandstone mineralization within the drilled sequence.

Core samples were collected from two boreholes with a **total drilled depth of 64 m**. The standard sample length of **1.00 m** was generally maintained; however, minor variations occurred depending on lithological changes and the extent of mineralization. Where the thickness of the mineralized zone was less than one meter, the entire interval was taken as a single sample. In zones where the mineralized horizon exceeded one meter, sampling was carried out with a maximum thickness of **1 m per sample** to maintain uniformity and ensure reliable grade representation. This sampling interval is considered suitable for sedimentary host rocks and conforms to practices followed under **Mineral (Evidence of Mineral Contents) Rules, 2015** and **UNFC guidelines**, ensuring adequate resolution of grade variability.

After drilling, the cores were carefully logged, photographed and examined for lithological characteristics. The cores were then split longitudinally into two equal halves using a **mechanical core splitter**. One half of the core was preserved in properly labelled core boxes for record and future reference and submitted to the core repository, while the other half was used for sampling and chemical analysis.

For sample preparation, the half-core samples were crushed into **3–5 mm chip samples**. Approximately **500–600 g** of representative material was obtained through **coning and quartering**, from which **200–300 g** was pulverized to about **100 mesh size** for analysis, while the remaining chip samples were preserved for future reference. The powdered sample was further homogenized through repeated coning and quartering and reduced to a **primary sample of about 150–200 g**, which was subsequently divided into two equal parts. One portion was submitted to **Shiva Analytical (India) Private Limited**, an NABL accredited laboratory, for chemical analysis and the other portion was preserved as a duplicate sample for quality control purposes. Prior to final powder preparation, about **1 kg of representative material** was

generally collected from each sampling interval and processed in the laboratory to approximately **200 mesh powder**, followed by coning and quartering before analysis.

Out of the total drilled interval, **53 core samples were analyzed for major oxides using X-ray Fluorescence (XRF)** and **36 samples were analyzed for trace elements using ICP-MS** to determine the geochemical characteristics of the glauconite-bearing horizons. In addition, **five representative samples were selected for petrographic study** to understand mineralogical composition and textural characteristics, and approximately **10% of the samples were subjected to external check analysis** to ensure analytical accuracy and reliability. The analyzed samples were tested for major oxides including **K₂O, SiO₂, Al₂O₃, Fe₂O₃, CaO, MgO, Na₂O, SO₃, P₂O₅ and Loss on Ignition (LOI)** using X-ray Fluorescence with appropriate standards and calibration procedures, while selected samples were further analyzed for trace elements through **ICP-MS**. These analytical results were subsequently used to assess the grade characteristics and vertical distribution of glauconite mineralization in the drilled sequence.

13.6 .2 Geochemical Analysis of Primary and External Check Samples

A total of 53 primary samples were analysed for major oxides (such as SiO₂, Al₂O₃, Fe₂O₃, K₂O, MgO, CaO, Na₂O, TiO₂, P₂O₅, etc.), using X-ray fluorescence (XRF) and wet chemical methods, as applicable (**Annexure 5**). 36 samples analysed for Trace and REE elements including Li (**Annexure 6**).

Additionally, 5 external check samples (approx. 10% of the total primary sample size) were submitted blindly to assess inter-laboratory consistency (**Annexure 10**).

For selected samples (n = 3), external checks were also carried out for trace and rare earth elements (REEs) using ICP-MS (Inductively Coupled Plasma – Mass Spectrometry) techniques (**Annexure 11**).

All chemical analyses were conducted at Shiva Analyticals (Shiva Laboratories), Bangalore, an NABL-accredited facility, with ISO/IEC 17025:2017 compliance, ensuring adherence to global best practices in analytical accuracy and precision.

The results were reviewed for repeatability, accuracy, and laboratory bias by comparing values from internal duplicates, and external check samples. These protocols are consistent with industry best-practice frameworks, as outlined under NMET guidelines and the JORC Code (2012 Edition), which requires critical evaluation of QA/QC results without prescribing universal numerical limits.

13.6.3 Evaluation of Potash Zone

Based on the 2% K₂O Cutoff two Mineralization Zones are identified in DPS/BH/01 Zone BH1/A from 5 to 17.5 m depth total 12.5 meter, and BH1/B from depth 25 to 34 m, total 9-meter-thick zone thus DPS/BH/01 has total 21.5 m thick mineralization zones (**Table 23**), while DPS/BH/02 has two mineralization zones of total 16-meter thickness. Zone BH2/A ranges from 9 to 22-meter total 13 meter thick and BH2/B 27 to 20 meter of 3-meter thickness making total 16-meter mineralization (**Table 24**) (**Annexure 15**).

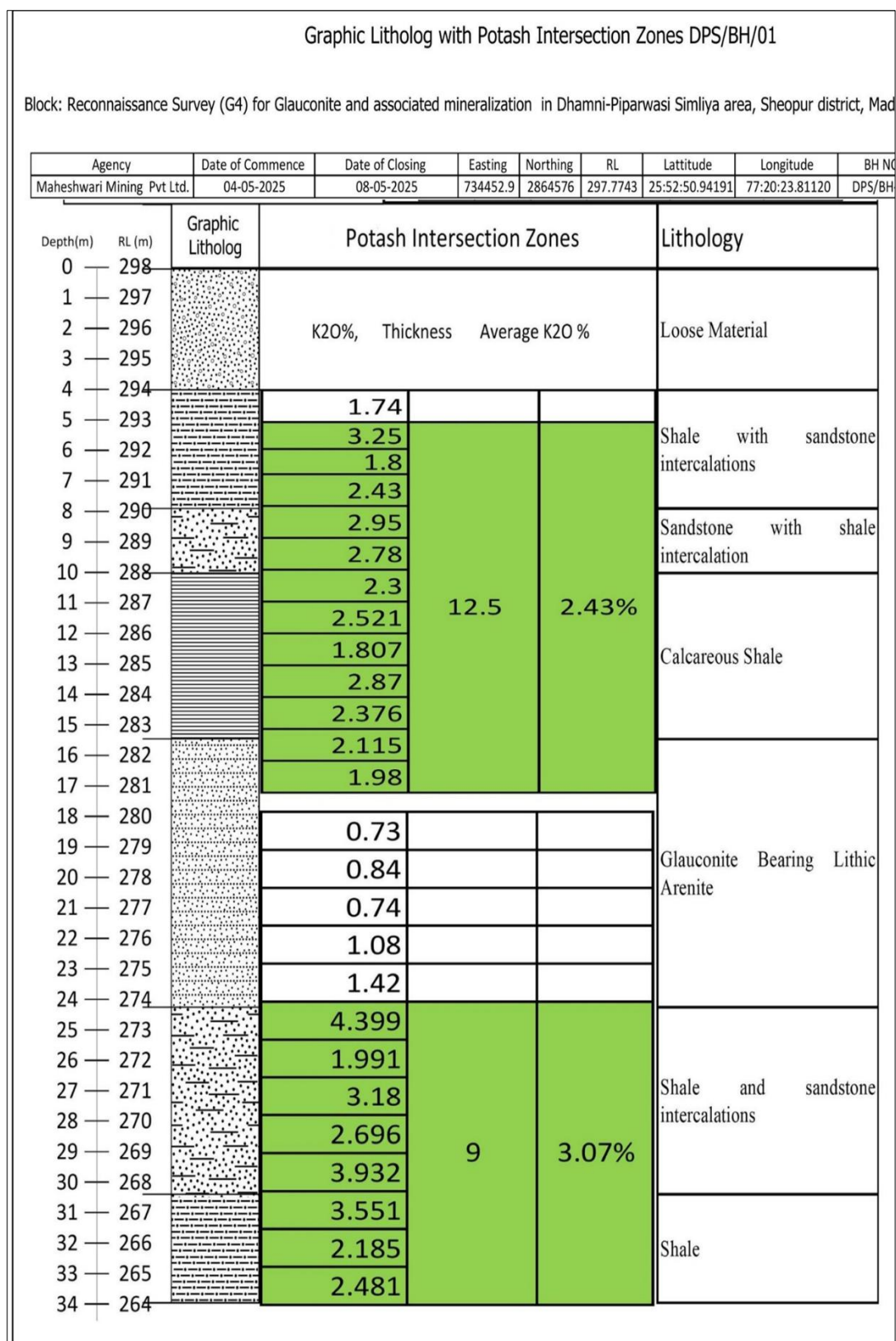


Figure 10 Litholog of DPSBH1

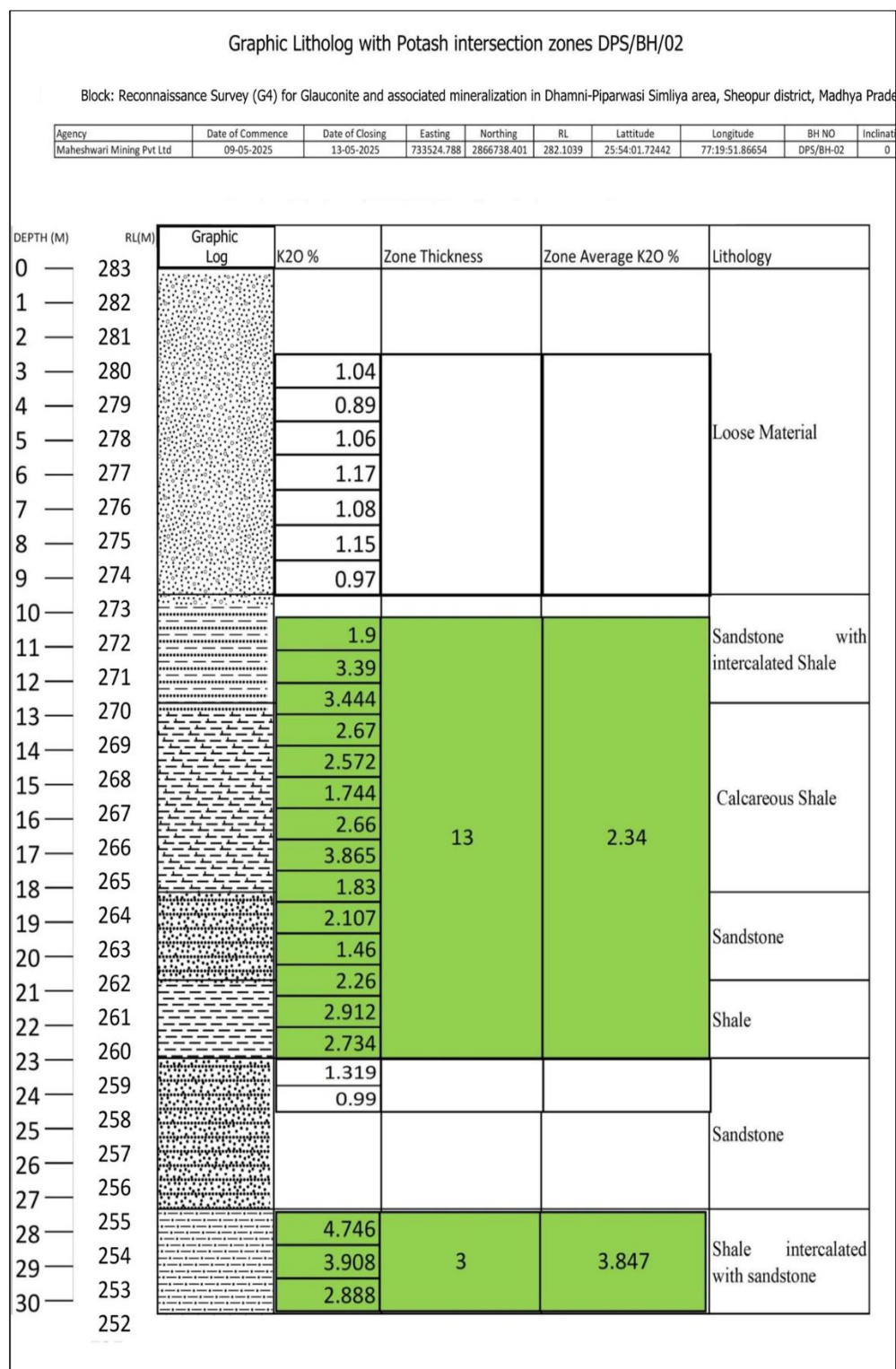


Figure 11 Litholog of DPS-BH2

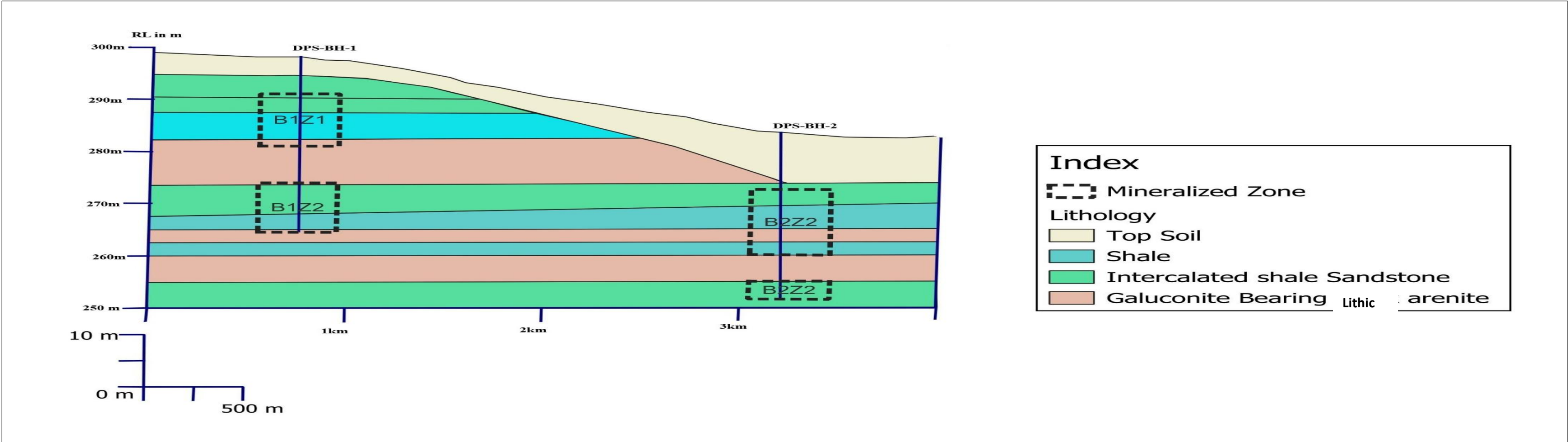
Table 28 Depth wise K₂O % and Mineralized Zone of >2% K₂O in DPS/BH/01

| Sample Id | Depth from | Depth to | K ₂ O | Mineralized Zone (m) | Zone K ₂ O % | Lithology |
|-----------------|------------|----------|------------------|----------------------|-------------------------|-------------------------------------|
| DPS-BH1-1 | 4m | 5m | 1.74 | 12.5 | 2.43% | Shale with sandstone intercalations |
| DPS-BH1-2 | 5m | 6m | 3.25 | | | |
| DPS-BH1-3 | 6m | 7m | 1.8 | | | |
| DPS-BH1-4 | 7m | 8m | 2.43 | | | |
| DPS-BH1-5 | 8m | 9m | 2.95 | | | |
| DPS-BH1-6 | 9m | 10m | 2.78 | | | Sandstone with shale intercalation |
| DPS-BH1-7 | 10m | 11m | 2.3 | | | Shale |
| DPS-BH1-16 | 11m | 12m | 2.521 | | | |
| DPS-BH1-17 | 12m | 13m | 1.807 | | | |
| DPS-BH1-8 | 13.5m | 14.5m | 2.87 | | | |
| DPS-BH1-18 | 14.5m | 15.5m | 2.376 | | | |
| DPS-BH1-19 | 15.5m | 16.5m | 2.115 | | | |
| DPS-BH1-9 | 16.5m | 17.5m | 1.98 | 9 | 3.07% | Shale and sandstone intercalations |
| DPS-BH1-10 | 18m | 19m | 0.73 | | | |
| DPS-BH1-10 | 18m | 19m | 0.7 | | | |
| DPS-BH1-11 | 19.5m | 20.5m | 0.84 | | | |
| DPS-BH1-12 | 21m | 22m | 0.74 | | | |
| DPS-BH1-13 | 22.50m | 23.5m | 1.08 | | | |
| DPS-BH1-14 | 24m | 25m | 1.42 | | | |
| DPS-BH1-20 | 25m | 26m | 4.399 | 9 | 3.07% | Shale and sandstone intercalations |
| DPS-BH1-21 | 26m | 27m | 1.991 | | | |
| DPS-BH1-15 | 27m | 28m | 3.18 | | | |
| DPS-BH1-22 | 28m | 29m | 2.696 | | | |
| DPS-BH1-23 | 29m | 30m | 3.932 | | | |
| DPS-BH1-24 | 30m | 31m | 2.731 | | | |
| DPS-BH1-25 | 31m | 32m | 3.551 | | | |
| DPS-BH1-25 | 31m | 32m | 3.529 | | | |
| DPS-BH1-26 | 32m | 33m | 2.185 | | | |
| DPS-BH1-27 | 33m | 34m | 2.481 | | | |
| Total Thickness | | | | 21.5 | | |

Table 29 Depth wise K2O % and Mineralized Zone of >2% K2O in DPS/BH/02

| Sample Id | Depth From | Depth To | K2O % | Zone Thickness | Zone Average K2O % | Lithology |
|-----------------|------------|----------|-------|----------------|--------------------|-----------------------------------|
| DPS-BH2-1 | 2m | 3m | 1.04 | | | Loose Material |
| DPS-BH2-2 | 3m | 4m | 0.89 | | | |
| DPS-BH2-3 | 4m | 5m | 1.06 | | | |
| DPS-BH2-4 | 5m | 6m | 1.17 | | | |
| DPS-BH2-5 | 6m | 7m | 1.08 | | | |
| DPS-BH2-6 | 7m | 8m | 1.15 | | | |
| DPS-BH2-7 | 8m | 9m | 0.97 | | | |
| DPS-BH2-8 | 9.5m | 10.5m | 1.9 | 13 | 2.34 | Sandstone-Shale |
| DPS-BH2-9 | 10.5m | 11.5m | 3.39 | | | Shale |
| DPS-BH2-16 | 11.5m | 12m | 3.444 | | | |
| DPS-BH2-10 | 12m | 13m | 2.67 | | | |
| DPS-BH2-17 | 13m | 14m | 2.572 | | | |
| DPS-BH2-18 | 14m | 15m | 1.744 | | | |
| DPS-BH2-11 | 15m | 16m | 2.66 | | | |
| DPS-BH2-19 | 16m | 16.5m | 3.865 | | | |
| DPS-BH2-12 | 16.5m | 17.50m | 1.83 | | | Sandstone-Shale |
| DPS-BH2-20 | 17.5m | 18.5m | 2.107 | | | |
| DPS-BH2-13 | 18.5m | 19.5m | 1.46 | | | shale |
| DPS-BH2-14 | 19.5m | 20.5m | 2.26 | | | |
| DPS-BH2-21 | 20.5m | 21.5m | 2.912 | | | Sandstone |
| DPS-BH2-22 | 21.5m | 22.5m | 2.734 | | | |
| DPS-BH2-23 | 22.5m | 23m | 1.319 | | | |
| DPS-BH2-15 | 23m | 24m | 0.99 | 3 | 3.847 | Shale intercalated with sandstone |
| DPS-BH2-24 | 27m | 28m | 4.746 | | | |
| DPS-BH2-25 | 28m | 29m | 3.908 | | | |
| DPS-BH2-26 | 29m | 30m | 2.888 | | | |
| Total Thickness | | | | 16 | | |

PLATE XI Cross Section across two boreholes



Chapter- 14. Sub-sampling techniques and sample preparation

14.1 Sample Preparation

Core samples were obtained from diamond drilling and were **split longitudinally into two equal halves using a mechanical core splitter** after detailed core logging and photography. **Half core was taken for sampling and chemical analysis**, while the **remaining half core was preserved in properly labelled core boxes** for record, reference, and future verification. **non-core samples were not collected** during the drilling stage of this investigation; therefore, methods such as riffle splitting, tube sampling, or rotary splitting were not applicable. All samples used for geochemical analysis were derived from drill cores.

The **sample preparation procedure followed standard laboratory protocols** to ensure reliable analytical results. The half-core samples were **crushed into 3–5 mm chips**, and a representative portion of about **500–600 g** was obtained through **coning and quartering**. Approximately **200–300 g** of the representative material was then **pulverized to about 100 mesh size**, and the powdered sample was further homogenized and reduced to a **primary sample of about 150–200 g**. This primary sample was split into two portions, one for **chemical analysis at an NABL-accredited laboratory (Shiva Analytical India Pvt. Ltd.)** and the other preserved as a **duplicate sample** for quality control and future reference. The procedures adopted are widely accepted and appropriate for geochemical analysis of sedimentary rock-hosted mineralization.

14.2 Quality control procedure

Quality control procedure was maintained at different stages of sampling and preparation to maximize sample representativeness. Approximately **10% of the samples were subjected to external check analysis** for verification of analytical accuracy. Duplicate samples were also preserved during sample preparation, and standard laboratory protocols such as proper homogenization, coning and quartering, and controlled pulverization were followed to minimize sampling bias and analytical error.

Several measures were adopted to ensure that the samples were **representative of the in-situ material**. Core sampling was carried out at **regular 1 m intervals**, with adjustments based on lithological boundaries and mineralized zones to accurately capture geological variability. Entire thicknesses were sampled where the mineralized interval was less than one meter, ensuring that no portion of the mineralized zone was excluded. Careful **core logging, photography, and lithological verification prior to sampling** further ensured that the collected samples accurately represented the geological characteristics of the drilled horizons.

The **sample size used during preparation was appropriate for the grain size of the glauconitic sandstone and associated lithologies**. The crushing of samples to **3–5 mm chips** followed by pulverization to **approximately 100 mesh** ensured adequate homogenization of the material. The selected sample quantities (**500–600 g chips and 150–200 g powdered samples**) are considered sufficient and suitable for obtaining representative analytical results for sedimentary rock-hosted glauconite mineralization.

Chapter- 15. Quality of assay data and laboratory tests

In this glauconite exploration project, accurate chemical analysis—particularly of K_2O —is essential, as it is the key indicator of potash potential. Assay work was carried out at Shiva Analyticals (India) Pvt. Ltd., Bangalore, using X-ray Fluorescence (XRF) under method SOP/OM/105, aligned with BIS IS 1473 (Part 2):2004.

To ensure analytical reliability, an internal quality check was performed on 15% of the samples by reanalysing them as duplicates. Four major oxides (K_2O , Fe_2O_3 , Al_2O_3 , SiO_2) were statistically evaluated for consistency between primary and duplicate results.

The following section presents a summary of the quality control data, statistical comparisons, and graphical analysis to demonstrate the precision and reliability of the assay process.

15.1 Analytical laboratory and method

Geochemical analysis of the primary and check samples was conducted at: **Shiva Analyticals (India) Private Limited** Bangalore.

All samples were analyzed using **X-ray Fluorescence Spectrometry (XRF)** under in-house Standard Operating Procedure **SOP/OM/105**, conforming to the Bureau of Indian Standards (BIS) specifications. The method aligns with **IS 1473:2004** for alumina-bearing materials and other oxide-specific BIS/ISO protocols applicable for Fe_2O_3 , K_2O , SiO_2 , etc. XRF is a widely used, non-destructive analytical method that provides rapid and accurate measurement of major and trace elements in geological samples.

A total of 16 oxides were analysed using XRF: Al_2O_3 , BaO , CaO , Cr_2O_3 , $Fe(T)$, Fe_2O_3 , K_2O , MgO , MnO , Na_2O , P_2O_5 , SO_3 , TiO_2 , SiO_2 , SrO , V_2O_5 , these oxides are critical for lithological classification, geochemical characterization, and resource assessment.

15.2 Internal quality check analysis

To assess analytical accuracy, an **internal quality control check** was implemented on **10% of the samples**, reanalysed under identical conditions by repeating every 10th sample and their analytical data included in primary analysis table itself.

15.3 External Check Analysis

10 percent of all samples analysed by each method XRF or ICPMS were reanalysed after receiving powdered samples of primary analysis from the same laboratory but with changed

names as it is acceptable norms. After receiving Check sample analysis, for XRF method four major oxides— Al_2O_3 , Fe_2O_3 , K_2O , and SiO_2 —were selected for detailed comparison between primary and check sample sets, based on their abundance and geological significance. For ICPMS method too results of four elements i.e. Li, Sc, Co, Ga selected for comparison analysis.

Below are the tables and scatter plots Showing comparisons and differences in results in Primary and Check samples of BRS-XRF, BRS-ICPMS, PIT-XRF, BOREHOLE-XRF, BOREHOLE- ICPMS.

10.3.1 Bed Rock Samples -XRF Primary Vs External Sample Result Comparison

Table 30 Statistical Evaluation of External Assay XRF Precision of bedrock samples

| Metric | $\Delta\text{Al}_2\text{O}_3$ | $\Delta\text{Fe}_2\text{O}_3$ | $\Delta\text{K}_2\text{O}$ | ΔSiO_2 |
|--------------------------------------|-------------------------------|-------------------------------|----------------------------|----------------------|
| No. of Sample Pairs | 15 | 15 | 15 | 15 |
| Arithmetic Mean of Differences (wt%) | -0.054 | 0.0233 | 0.0073 | 0.1047 |
| Standard Deviation | 0.1334 | 0.087 | 0.0243 | 0.1593 |
| Standard Error of Mean | 0.0344 | 0.0225 | 0.0063 | 0.0411 |
| Variance | 0.0178 | 0.0076 | 0.0006 | 0.0254 |
| Correlation Coefficient (r) | 0.9978 | 0.9988 | 0.9996 | 1.0000 |
| Mean Absolute Error (MAE) (wt%) | 0.118 | 0.0767 | 0.0193 | 0.1500 |
| Mean Relative Random Error (%) | 4.45% | 3.27% | 1.81% | 0.19% |
| Paired T-value | -1.568 | 1.039 | 1.167 | 2.545 |
| F-test value | 1.07 | 1.037 | 1.015 | 1.002 |

Table 31 Showing Comparison of Primary and External Check of Bedrock Samples

| Primary Samples | | | | | | | Check samples | | | | | Difference | | | |
|-----------------|--------------|---------------|-----------|-----------|-------------|-----------|---------------|-----------|-----------|-------------|-----------|------------|-----------|-----------|-----------|
| sampl e ID | latitu de | longi tude | Al2 O3 | Fe2 O3 | K 2 O | Si O2 | sampl e id | Al2 O3 | Fe2 O3 | K 2 O | Si O2 | Al2 O3 | Fe2 O3 | K2 O | Si O2 |
| DPS-5 | 25.8 8491 | 77.3 3413 | 4.9 4 | 5.5 2 | 2. 77 | 63. 93 | CH/D S-01 | 4.7 4 | 5.4 1 | 2. 78 | 63. 88 | 0.2 | 0.1 1 | -0. 01 | 0.0 5 |
| DPS-7 | 25.9 0357 | 77.3 9428 | 7.2 1 | 1.6 2 | 3. 24 | 84. 56 | CH/D S-02 | 7.2 2 | 1.5 7 | 3. 21 | 84. 46 | -0.0 1 | 0.0 5 | 0.0 3 | 0.1 |
| DPS-S-113 | 25.8 8106 | 77.3 3981 | 4.5 5 | 3.0 9 | 1. 93 | 87. 08 | CH/D S-03 | 4.5 5 | 3.0 2 | 1. 92 | 86. 67 | 0 | 0.0 7 | 0.0 1 | 0.4 1 |
| DPS-S-81 | 25.9 6925 | 77.3 2939 | 1.1 2 | 1.0 2 | 0. 62 | 96. 61 | CH/D S-04 | 1.2 4 | 0.9 1 | 0. 61 | 96. 61 | -0.1 2 | 0.1 1 | 0.0 1 | 0 |
| DPS-S-91 a | 25.9 5889 | 77.3 9183 | 4.4 9 | 2.8 5 | 1. 64 | 87. 68 | CH/D S-05 | 4.6 0 | 2.7 2 | 1. 58 | 87. 66 | -0.1 1 | 0.1 3 | 0.0 6 | 0.0 2 |
| DPS-S-94 | 25.9 04 | 77.3 4189 | 1.8 9 | 1.7 8 | 0. 73 | 94. 52 | CH/D S-06 | 1.8 3 | 1.7 1 | 0. 71 | 94. 38 | 0.06 | 0.0 7 | 0.0 2 | 0.1 4 |
| DPS-S-79 | 25.9 6542 | 77.3 9794 | 0.8 9 | 0.7 7 | 0. 36 | 97. 32 | CH/D S-07 | 0.9 7 | 0.8 0 | 0. 37 | 97. 03 | -0.0 8 | -0. 03 | -0. 01 | 0.2 9 |
| DPS-S-85 | 25.9 2344 | 77.3 4394 | 2.5 8 | 3.5 3 | 1. 21 | 71. 48 | CH/D S-08 | 2.5 1 | 3.4 6 | 1. 19 | 71. 72 | 0.07 | 0.0 7 | 0.0 2 | -0. 24 |
| DPS-S-91 b | 25.9 5889 | 77.3 9183 | 4.3 1 | 2.7 4 | 1. 53 | 88. 23 | CH/D S-09 | 4.1 6 | 2.7 5 | 1. 55 | 88. 07 | 0.15 | -0. 01 | -0. 02 | 0.1 6 |
| DPS-S-114 | 25.9 2403 | 77.3 4381 | 3.2 8 | 4.7 7 | 1. 65 | 76. 09 | CH/D S-10 | 3.5 0 | 4.6 3 | 1. 61 | 75. 85 | -0.2 2 | 0.1 4 | 0.0 4 | 0.2 4 |
| DPS-S-115 | 25.9 1006 | 77.4 1178 | 2.8 7 | 0.7 4 | 1. 36 | 93. 37 | CH/D S-11 | 2.9 2 | 0.7 8 | 1. 39 | 93. 46 | -0.0 5 | -0. 04 | -0. 03 | -0. 09 |
| DPS-S-127 | 25.9 2175 | 77.3 9956 | 0.8 1 | 3.8 | 0. 33 | 73. 17 | CH/D S-12 | 1.0 4 | 3.8 2 | 0. 33 | 73. 18 | -0.2 3 | -0. 02 | 0 | -0. 01 |
| DPS-S-133 | 25.9 595 | 77.3 7458 | 2.3 9 | 5.3 8 | 0. 94 | 27. 89 | CH/D S-13 | 2.6 0 | 5.4 4 | 0. 94 | 27. 72 | -0.2 1 | -0. 06 | 0 | 0.1 7 |
| DPS-S-147 | 25.9 0133 | 77.3 6169 | 1.3 3 | 1.3 3 | 0. 65 | 95. 61 | CH/D S-14 | 1.5 2 | 1.4 7 | 0. 67 | 95. 48 | -0.1 9 | -0. 14 | -0. 02 | 0.1 3 |
| DPS-S-54 | 25.9 8231 | 77.4 0767 | 2.1 3 | .82 | 1. 01 | 95. 22 | CH/D S-15 | 2.4 2 | 1.0 1 | 1. 15 | 94. 04 | 0.29 | 0.1 9 | 0.1 4 | 1.1 8 |

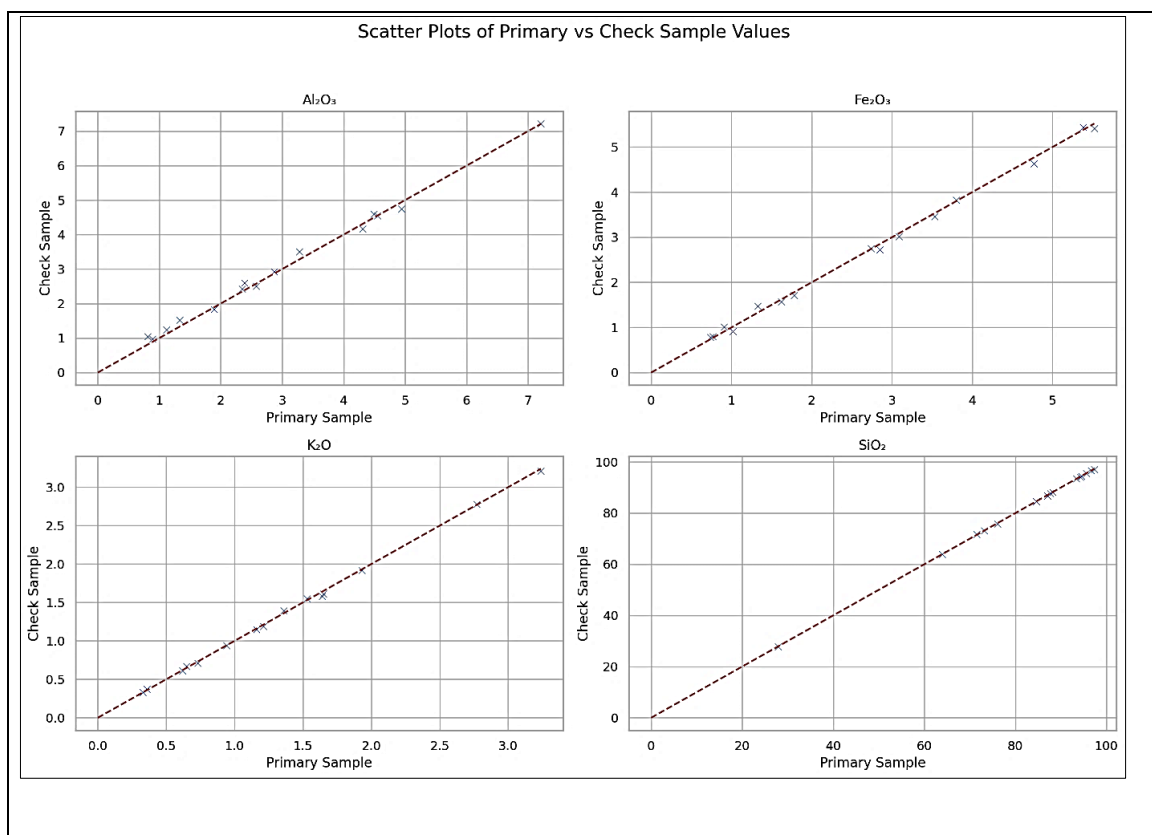


Figure 12 Scatter Plots of Primary vs External Check samples Chemical analysis results of Selected Major Oxides of BRS samples

Interpretations

The results indicate excellent precision, as evidenced by the very high correlation coefficients (≥ 0.9978) and low standard errors. K₂O, the most critical oxide for resource assessment in glauconite, showed minimal variation between primary and duplicate values (mean difference = 0.0073 wt.%, $r = 0.9996$).

Scatter plots were generated to visually assess the correlation between the primary and check analyses for each oxide:

- Each plot compares **primary assay values** (X-axis) against **check sample values** (Y-axis).
- A **1:1 reference line** was included in each plot to evaluate accuracy.
- A **combined scatter plot** was also generated, overlaying all four oxides to illustrate consistent agreement.

15.3.2 Bed rock samples ICPMS primary vs external sample result comparison

Table 32 Showing Comparison of Primary and External Check of Bedrock Samples

| Check Samples | | | | | Primary Sample | | | | | Difference | | | |
|---------------|-------|------|------|------|----------------|-------|------|-----|------|------------|-----|-------|-----|
| sample id | Li | Sc | Co | Ga | Sample Id | Li | Sc | Co | Ga | Li | Sc | Co | Ga |
| CH/DS-01 | 311.5 | 1.7 | 21.3 | 16.3 | DPS-5 | 350.8 | 3 | 21 | 16.8 | 39.3 | 1.3 | - 0.3 | 0.5 |
| CH/DS-04 | 7.6 | <0.5 | 1.0 | 1.9 | DPS-S-81 | 7.6 | <0.5 | 1.2 | 2.1 | 0 | — | 0.7 | 0.2 |
| CH/DS-06 | 30.7 | <0.5 | 1.4 | 3.6 | DPS-S-94 | 32.3 | 0.5 | 2.2 | 3.9 | 1.6 | 1 | 0.8 | 0.3 |
| CH/DS-09 | 19.6 | 1.4 | 3.4 | 4.6 | DPS-S-91 b | 23.7 | 2.2 | 4.6 | 5.1 | 4.1 | 0.8 | 0 | 0.5 |
| CH/DS-11 | 11.3 | <0.5 | 0.7 | 2.8 | DPS-S-115 | 12.1 | 1.8 | 1.3 | 3.0 | 0.8 | 1.3 | 0.6 | 0.2 |
| CH/DS-14 | 13.3 | <0.5 | 1.4 | 1.9 | DPS-S-147 | 15.4 | 0.7 | 2.1 | 2.1 | 2.1 | 1.2 | 0.7 | 0.2 |
| CH/DS-15 | 8.1 | <0.5 | 0.7 | 2.9 | DPS-54 | 13.7 | <0.5 | 2 | 1.9 | 0 | 5.6 | 1.3 | 1 |

Table 33 Statistical Evaluation of External Assay ICPMS Precision of bedrock samples

| Parameter | Li | Sc | Co | Ga |
|--------------------------------------|-----------|----------|----------|----------|
| No. of Sample Pairs | 7.0 | 7.0 | 7.0 | 7.0 |
| Arithmetic Mean of Differences (wt%) | 6.842857 | 0.514286 | 0.600000 | 0.142857 |
| Standard Deviation | 14.382496 | 0.606709 | 0.506623 | 0.479086 |
| Standard Error of Mean | 5.436073 | 0.229314 | 0.191485 | 0.181078 |
| Variance | 206.8562 | 0.368095 | 0.256667 | 0.229524 |
| Correlation Coefficient (r) | 0.999953 | 0.887764 | 0.998851 | 0.996488 |
| Mean Absolute Error (MAE) (wt%) | 6.842857 | 0.514286 | 0.685714 | 0.400000 |
| Mean Relative Random Error (%) | 25.03792 | 75.83857 | 11.86074 | 9.863544 |
| Paired T-value | 1.258787 | 2.242711 | 3.133398 | 0.788928 |
| F-test value | 1.271570 | 3.844797 | 0.906474 | 1.076787 |

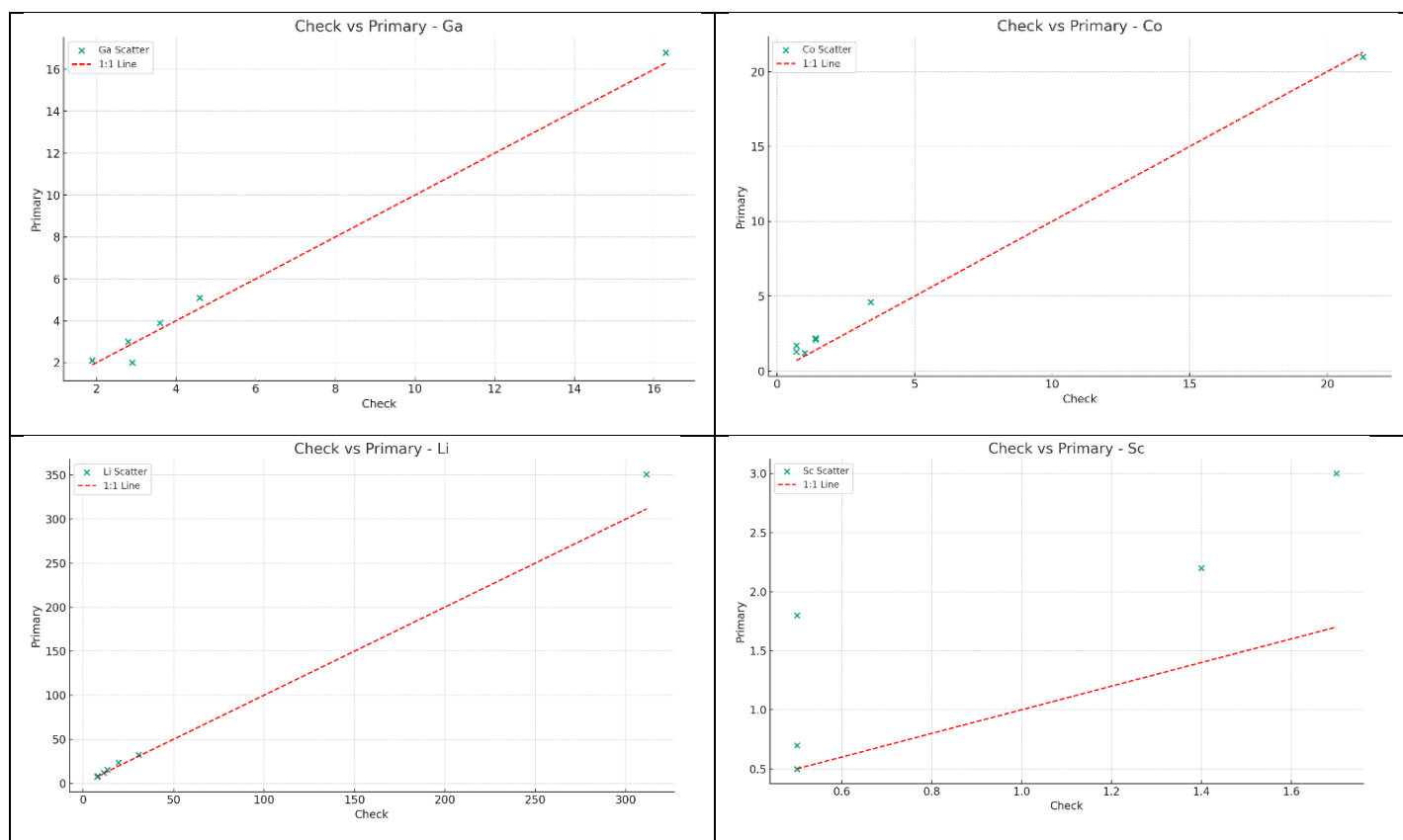


Figure 13 Scatter Plots of Primary vs External Check samples Chemical analysis results of Selected Trace Elements of BRS samples

Interpretations

All plots showed tight clustering near the 1:1 line, with minimal dispersion, confirming high reproducibility. The correlation coefficients ranged from **0.9978 to 1.000**, indicating **excellent analytical agreement**.

Low standard deviations and very high correlations confirm that the primary and check analyses are statistically equivalent.

Scatter plots visually affirm high concordance between datasets.

15.3.3 Pit samples-XRF primary vs external sample result comparison

Table 34 Showing Comparison of Primary and External Check of PIT Samples

| Primary Result | | | | | Check no | | | | | Difference | | | |
|--------------------|-----------|-----------|----------|-----------|---------------|-----------|-----------|----------|-----------|------------|----------------|----------------|----------------|
| samp le No | Al2 O3 | Fe2 O3 | K2 O | SiO 2 | sample Id | Al2 O3 | Fe2 O3 | K2 O | SiO 2 | Al2O 3 | Fe2 O3 | K2 O | SiO 2 |
| DPS- P1(B) | 2.54 | 2.38 | 1.2 7 | 91.7 9 | DPS/PC H-1 | 2.61 | 2.34 | 1.2 4 | 91.6 1 | 0.067 | - 0.03 9 | - 0.02 9 | - 0.17 6 |
| DPS- P3(A) | 2.65 | 2 | 1.3 2 | 92.4 1 | DPS/PC H-2 | 2.75 | 2.01 | 1.3 0 | 92.3 1 | 0.097 | 0.00 6 | - 0.01 8 | - 0.10 1 |
| DPS- P11(B) | 4.03 | 2.65 | 1.5 3 | 33.6 8 | DPS/PC H-3 | 3.90 | 2.65 | 1.5 2 | 33.7 3 | - 0.132 | 0.00 1 | - 0.00 7 | 0.04 5 |
| DPS- P-16 | 1.48 | 1.31 | 0.7 2 | 95.6 8 | DPS/PC H-4 | 1.43 | 1.35 | 0.7 2 | 95.5 8 | - 0.048 | 0.03 9 | 0.00 4 | - 0.09 6 |
| DPS- P-21 | 2.13 | 1.45 | 0.9 2 | 94.3 2 | DPS/PC H-5 | 2.06 | 1.42 | 0.9 7 | 94.3 7 | - 0.067 | - 0.02 7 | 0.04 5 | 0.05 2 |

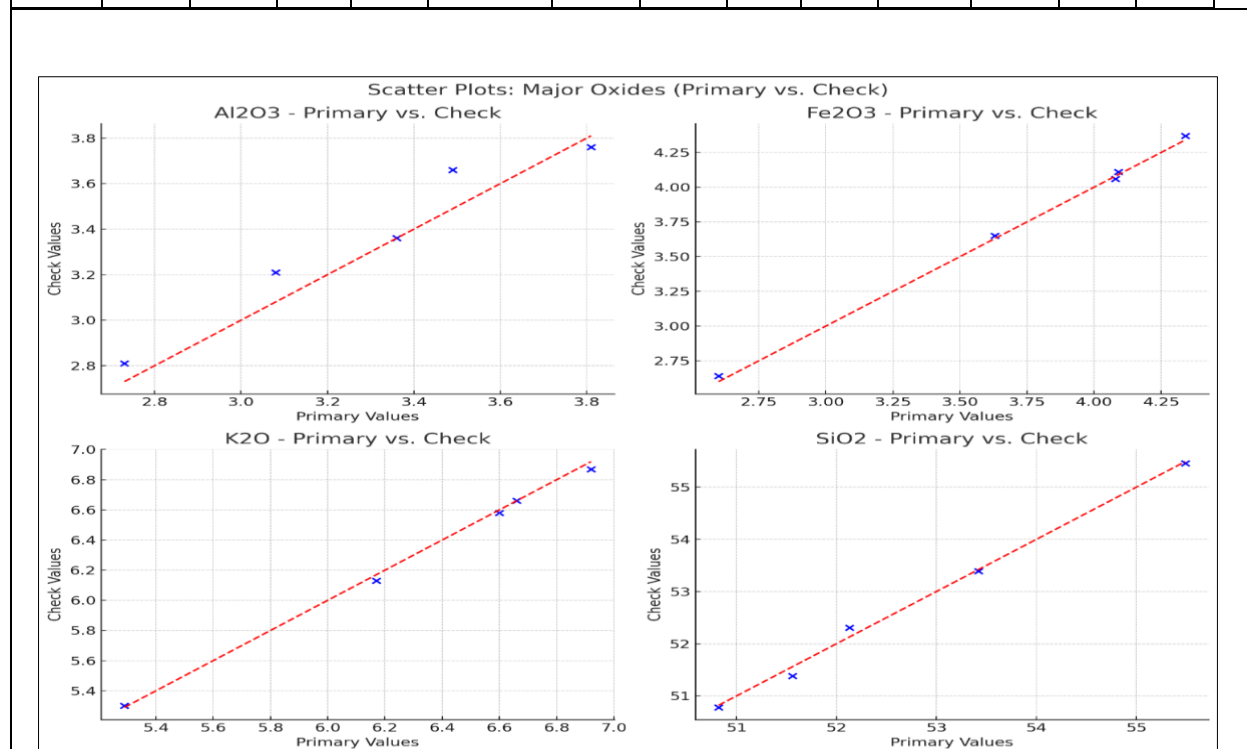


Figure 14 Scatter Plots of Primary vs External Check samples Chemical analysis results of Selected Major Oxides of PIT samples

15.3.4 BH Primary Vs External Check XRF Samples Comparision

Table 35 Statistical Evaluation of External Assay XRF & ICPMS Precision of Boreholes samples

| Assay | | Primary | | | | Check | | | | | Difference | | | |
|------------------------|------------|---------|-------|------|-------|-----------|-------|-------|------|-------|------------|---------|----------|---------|
| | Primary id | Al2O3 | Fe2O3 | K2O | Sio2 | Check Id | Al2O3 | Fe2O3 | K2O | Sio2 | Al2O3 | Fe2O3 | K2O | Sio2 |
| Major Oxides BY XRF | DPS-BH1-3 | 4.98 | 3.57 | 1.8 | 85.86 | DPS/BCH-1 | 5.13 | 3.59 | 1.80 | 85.89 | 0.152 | 0.015 | 0.001 | 0.028 |
| | DPS-BH1-15 | 6.89 | 1.7 | 3.18 | 83.65 | DPS/BCH-2 | 7.02 | 1.70 | 3.17 | 83.65 | 0.128 | 0.003 | -0.015 | -0.005 |
| | DPS-BH1-5 | 7.73 | 3.22 | 2.95 | 81.09 | DPS/BCH-3 | 7.49 | 3.23 | 2.96 | 81.27 | -0.245 | 0.012 | 0.009 | 0.177 |
| | DPS-BH2-8 | 4.71 | 2.57 | 1.9 | 88.06 | DPS/BCH-4 | 4.64 | 2.59 | 1.90 | 88.14 | -0.068 | 0.023 | 0 | 0.077 |
| | DPS-BH2-11 | 7.64 | 6.03 | 2.66 | 38.36 | DPS/BCH-5 | 7.49 | 6.10 | 2.68 | 37.85 | -0.154 | 0.068 | 0.024 | -0.512 |
| | Primary Id | Li | Sc | Co | Ga | Check Id | Li | Sc | Co | Ga | Li | Sc | Co | Ga |
| Trace and REE by ICPMS | DPS-BH1-3 | 28.2 | 5.4 | 13.7 | 6.7 | DPS/BCH-1 | 29.5 | 3.3 | 14.9 | 6.0 | 1.324696 | 2.12228 | 1.180389 | 0.73305 |
| | DPS-BH1-5 | 35.9 | 13.3 | 11.3 | 11.6 | DPS/BCH-3 | 35.2 | 5.9 | 11.5 | 9.9 | 0.72519 | 7.40881 | 0.216869 | 1.66968 |
| | DPS-BH2-11 | 42.1 | 10.4 | 8 | 9.1 | DPS/BCH-5 | 46.9 | 5.1 | 9.0 | 8.4 | 4.762908 | 5.32592 | 1.006092 | 0.7343 |

Table 36 Statistical Evaluation of External Assay XRF and ICPMS Precision of Borehole Samples

| Statistic | Li | Sc | Co | Ga |
|--------------------------------------|--------|--------|--------|---------|
| No. of Sample Pairs | 3 | 3 | 3 | 3 |
| Arithmetic Mean of Differences (wt%) | 1.8 | -4.933 | 0.8 | -0.3667 |
| Standard Deviation | 2.358 | 4.051 | 0.5745 | 0.6245 |
| Standard Error of Mean | 1.361 | 2.338 | 0.3317 | 0.36 |
| Variance | 5.56 | 16.41 | 0.33 | 0.39 |
| Correlation Coefficient (r) | 0.9999 | 0.9918 | 0.9998 | 0.9977 |
| Mean Absolute Error (MAE) (wt%) | 2.6 | 4.933 | 0.9333 | 0.5 |
| Mean Relative Random Error (%) | 6.66 | 47.3 | 8.22 | 5.41 |
| Paired T-value | 1.322 | -2.11 | 2.411 | -1.019 |
| F-test value | 1.05 | 4.03 | 1.23 | 1.46 |

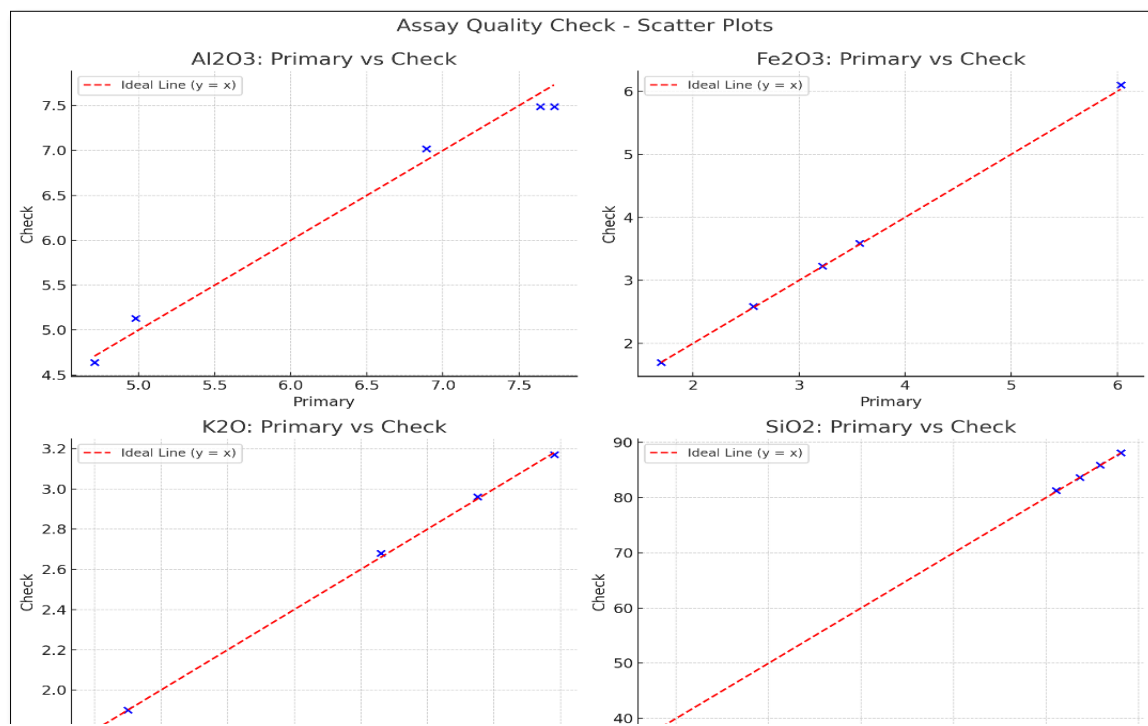


Figure 15 Scatter Plots of Primary vs External Check samples Chemical analysis results of Major oxides of Borehole samples

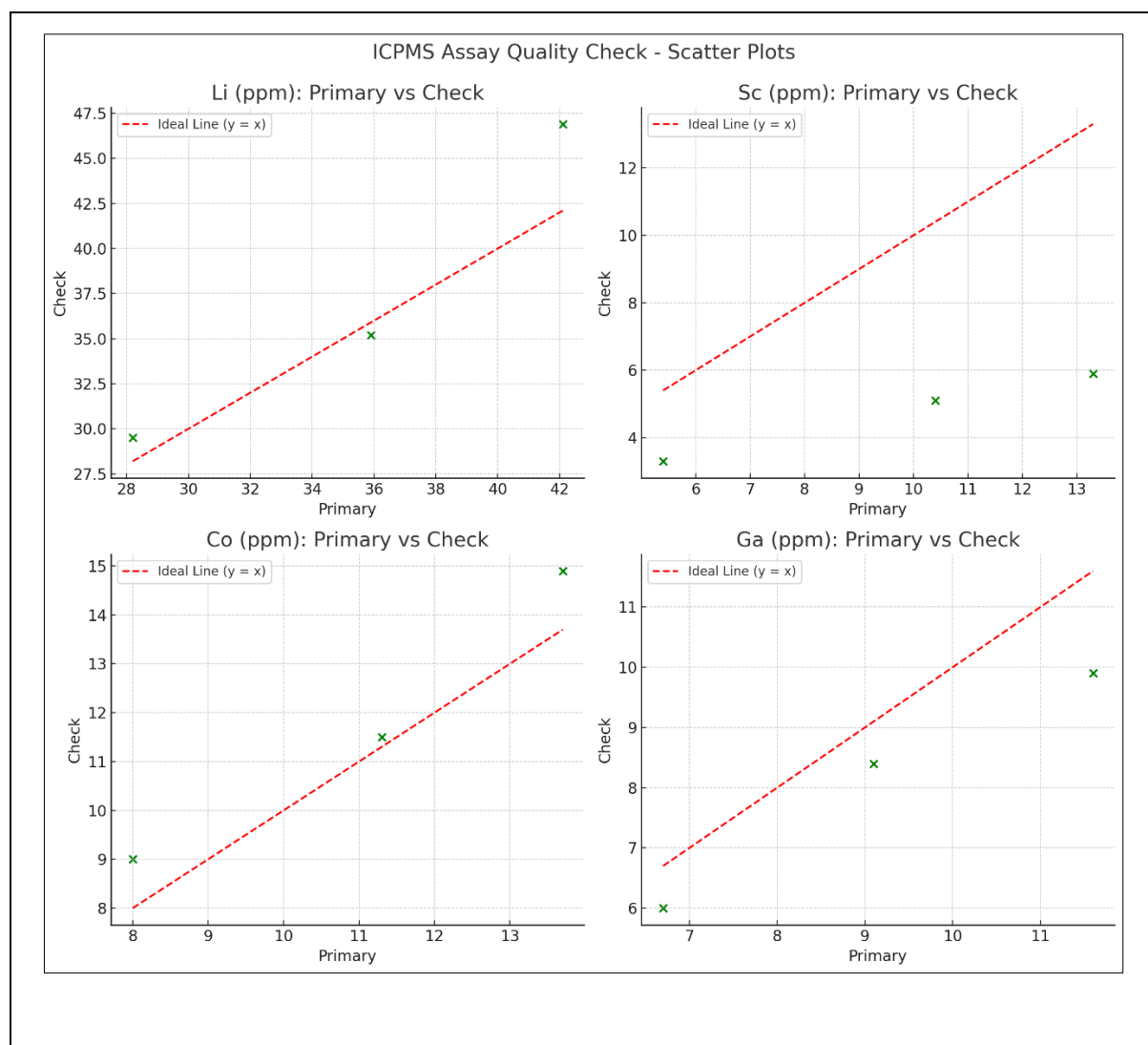


Figure 16 Scatter Plots of Primary vs External Check samples Chemical analysis results of Selected Trace Elements of Borehole samples

Interpretations

The quality analysis of four selected major oxides (SiO_2 , Al_2O_3 , Fe_2O_3 , and K_2O) indicates overall good consistency between duplicate sample pairs. The low arithmetic mean of differences for these oxides implies minimal systematic bias between the primary and duplicate sets.

The **correlation coefficients (r)** for all four oxides are high, approaching unity, which confirms strong linear association and analytical consistency. The **standard deviation** and **mean absolute error (MAE)** values are low, reflecting tight clustering of differences and limited dispersion. The **paired t-values** fall within acceptable statistical limits, suggesting that there is no significant difference at the 95% confidence level between the paired datasets. Similarly, the **F-test values** indicate comparable variance between the original and duplicate measurements. Overall, the oxide data confirms acceptable levels of **accuracy** and **precision**, validating the reliability of laboratory methods used in the geochemical analysis.

For the four trace elements studied (Ba, Sr, Ni, and Pb), the analytical precision shows moderate variability. While the **correlation coefficients (r)** remain high for elements like Ba and Sr, indicating good reproducibility, elements like Ni and Pb show slightly higher **standard deviation** and **MAE**, suggesting relatively larger deviations between paired samples.

The **mean relative random error (%)** is notably higher for some trace elements, which is expected due to their typically lower concentrations and more complex matrix interferences during analysis. The **t-values** and **F-test results** for these elements fall within acceptable ranges, suggesting that while minor discrepancies exist, they are statistically insignificant.

In summary, the trace element analysis maintains acceptable reproducibility.

Chapter 16. Bulk Density

16.1 Introduction

Bulk density and K₂O content are key parameters in glauconite exploration, as they help identify mineral-rich zones and support resource estimation. This chapter presents integrated results from three samples collected in the block, reflecting variations in lithology, density, and K₂O enrichment.

Table 37 Bulk Density Analysis of samples

| Sample ID | Lithology | Bulk Density (g/cm ³) | K ₂ O (%) |
|------------|-----------------|-----------------------------------|----------------------|
| DPS-BH1-10 | Sandstone | 2.60 | 0.70 |
| DPS-BH1-14 | Sandstone-Shale | 2.50 | 1.42 |
| DPS-BH2-9 | Sandstone-Shale | 2.59 | 3.39 |

16.2 Interpretation

- **DPS-BH1-10** shows the highest bulk density but lowest K₂O%, indicating clean sandstone with limited glauconite presence.
- **DPS-BH1-14**, with reduced density and moderate K₂O, suggests transitional facies where glauconite formation begins.
- **DPS-BH2-9** records the highest K₂O% (3.39%) in a sandstone-shale setting, implying favourable glauconite enrichment conditions.

16.3 Conclusion

Glauconite potential in the DPS G4 block is highest in **shale-intercalated sandstone zones**, as seen in DPS-BH2-9. These zones combine optimal bulk density with enriched K₂O content, making them prime targets for further exploration.

Chapter 17. Resource estimation

17.1 Introduction

A reconnaissance stage (G-4) exploration was conducted for glauconitic sandstone in the Dhamni–Piparwasi–Simliya Block, Vijaypur Tehsil, Sheopur District, Madhya Pradesh. The block spans an area of approximately 116 sq. km. Two boreholes—DPS-BH01 and DPS-BH02—were drilled approximately 2.3 km apart. The geology consists of horizontally bedded glauconitic sandstone with intercalated shale and ferruginous sandstone. Glauconite is present in the form of pelletal forms in the coarse-grained sandstone and limestone intercalated with green coloured shale/siltstone (glauconite bearing).

The objective of the resource estimation was to determine the inferred mineral potential in the immediate surroundings of the boreholes, based on K_2O assay results, thickness of mineralized zones of potash enriched sequence, and bulk density. Only zones with K_2O percentage equal to or greater than 2.0% were considered.

17.2 Methodology

Resource estimation was conducted using the Polygonal Method, more specifically the **Square Block Area of Influence (ZOI)** approach. This method is particularly appropriate in early-stage (G4) resource assessment when borehole data is limited and spatial continuity remains poorly constrained.

Each borehole has been assigned a square block of 400×400 m, centred on the drill collar, defining a zone of influence of 0.16 km^2 per hole based on patchy nature of the mineralization observed in the field. Only the grade and thickness recorded within the borehole are used to estimate the resource for that block—no lateral extrapolation or interpolation is performed. This ensures the estimates remain conservative, auditable, and reproducible.

Evans (2009) and Moon et al. (2006) confirm polygonal methods ideal for flat-lying, tabular sedimentary deposits like glauconitic sandstone under reconnaissance conditions (2 scout holes, partial correlation). Square Area Polygonal variant (400m influence) represents conservative adaptation for sparse data, validated via cross-section sensitivity.

The Square Block ZOI approach is particularly suited to scenarios with random or widely spaced boreholes, where geostatistical tools like kriging are not feasible due to insufficient sample density. The method relies solely on borehole-specific data, and assigns distinct, non-overlapping zones of

influence, avoiding artificial precision or grade smoothing, consistent with conventionally accepted early-stage resource estimation practices.

This methodology aligns with the **UNFC G4 classification**, suitable for **Inferred Resources** based on limited geological knowledge. The deterministic nature of block-based estimation, coupled with the absence of extrapolation beyond defined zones, meets the criteria for **geologically reasonable, transparent, and conservative resource declaration** at the reconnaissance stage.

The **Square Block Area of Influence polygonal method** provides a **geologically appropriate, conservative, and transparent framework** for resource estimation in settings with sparse, randomly distributed boreholes. Its simplicity and auditability, supported by authoritative geological literature, make it a sound choice for Inferred Resource reporting under international standards.

Table 38 Parameters Considered for Inferred Resource (UNFC code 334) estimation of Reconnaissance Survey (G-4) for Glauconitic Sandstone Block

| Parameter | Value | Justification |
|---------------------|--------------------------------------|---|
| Zone of Influence | 400 × 400 m = 160,000 m ² | Standard for fixed polygonal block per borehole |
| Bulk Density | 2.545 t/m ³ | Based on lab-determined average |
| Cut-off Grade | 2.0% K ₂ O | Conservative threshold for glauconite potential |
| Geological Setting | Horizontal stratification | Based on lithologs and field observation |
| Classification Code | UNFC 334 | Inferred Resource (Reconnaissance stage) |

Average Bulk Density

The mineralized horizons in the present study predominantly comprise sandstone-shale intercalations and shale-sandstone alternations, with measured bulk densities of 2.50 t/m³ and 2.59 t/m³, respectively. Given the limited number of boreholes (only two), and the consistently recurring lithological patterns, it is both statistically and geologically sound to apply the arithmetic mean of these values: Average Bulk Density=2.50+2.592=2.545 t/m³

17.3 Tonnage Estimation

Using the fixed area (400 × 400 m = 160,000 m²) for each borehole's influence zone and applying respective zone thickness, the tonnages were estimated based on:

$$\text{Tonnage (metric tonne)} = \text{Area (m}^2\text{)} \times \text{Thickness (m)} \times \text{Bulk Density (t/m}^3\text{)}$$

A bulk density of 2.545 t/m³, derived from representative samples, was applied uniformly.

In Borehole DPS/BH/01, two mineralized zones were delineated. The first zone (BH1/A) between 5.0 m and 17.5 m depth, with 12.5 m thickness, yielded a resource of about 5.09 million tonnes at an

average grade of 2.43% K₂O. The second zone (BH1/B), intersected between 25.0 m and 34.0 m with 9.0 m thickness, added another 3.66 million tonnes at 3.07% K₂O. Thus, the total resource around BH01 amounts to approximately 8.75 million tonnes.

Similarly, Borehole DPS/BH/02 also revealed two mineralized horizons. Zone BH2/A, between 9.0 m and 22.0 m depth, with a thickness of 13.0 m, accounted for about 5.29 million tonnes averaging 2.39% K₂O. Zone BH2/B, between 27.0 m and 30.0 m depth (3.0 m thickness), contributed about 1.22 million tonnes with 3.85% K₂O. The total for BH02 thus works out to 6.52 million tonnes.

By combining both borehole blocks, the total resource is estimated at 15.27 million tonnes of glauconite-bearing rock. Owing to the reconnaissance level of exploration (two boreholes only), the entire tonnage is placed under **Inferred Resource (UNFC code 334)**.

Total Resource (Inferred, UNFC 334): 15.27 million metric tonnes

Table 39 Inferred Resource (UNFC code 334), of Reconnaissance Survey (G-4) for Glauconitic Sandstone in Dhamni, Piparwasi, Simliya Block

| Inferred Resource (UNFC code 334), of Reconnaissance Survey (G-4) for Glauconitic Sandstone in Dhamni, Piparwasi, Simliya, Vijaypur, District- Sheopur, Madhya Pradesh | | | | | | | | |
|--|-------|----------------|--------------|---------------|-------------------------------|----------------------------------|------------------------------|-----------------------|
| Borehole ID | Zone | Depth From (m) | Depth To (m) | Thickness (m) | Bulk Density t/m ³ | Zone of influence m ² | Average K ₂ O (%) | Resource metric tonne |
| DPS/BH/01 | BH1/A | 5 | 17.5 | 12.5 | 2.545 | 1,60,000 | 2.43 | 5090000 |
| DPS/BH/01 | BH1/B | 25 | 34 | 9 | 2.545 | 1,60,000 | 3.07% | 3664800 |
| Total BH01 | | | | 21.5 | | | | |
| DPS/BH/02 | BH2/A | 9 | 22 | 13 | 2.545 | 1,60,000 | 2.39 | 5293600 |
| DPS/BH/02 | BH2/B | 27 | 30 | 3 | 2.545 | 1,60,000 | 3.85 | 1221600 |
| Total Resource | | | | 16 | | | | 1,52,70,000 |

17.4 Interpretation and Classification

- The glauconitic mineralization is narrow but enriched, concentrated in distinct bands.
- The estimate is conservative, as no lateral or vertical extrapolation was applied beyond logged and assayed intervals.
- As per the UNFC classification, this qualifies as a 334 – Inferred Resource, suitable for early-stage planning and follow-up exploration.

17.5 Stripping Ratio

The stripping ratio for the glauconitic sandstone resource was estimated by applying the **same zone of influence of 400 × 400 m (160,000 m²)** assigned to each borehole block. In **Borehole DPS-BH01**, the total mineralized thickness ($K_2O \geq 2\%$) is **21.5 m**, while the non-mineralized thickness encountered within the borehole is **12.5 m**, a **stripping ratio of approximately 0.58 : 1**. Similarly, in **Borehole DPS-BH02**, the mineralized thickness is **16 m**, whereas the non-mineralized thickness recorded within the borehole is **14 m**, **stripping ratio of approximately 0.87 : 1**.

It is pertinent to note that **both boreholes terminate within mineralized horizons**, indicating the possible continuation of the glauconitic sandstone sequence beyond the drilled depth. However, for the purpose of stripping ratio estimation, **only the observed non-mineralized intervals within the drilled sections have been considered**, without assuming any continuation of mineralization below the borehole termination. Accordingly, the **combined stripping ratio for the explored block is approximately 0.70 : 1**.

Table 40 Table presenting stripping ratio

| Parameter | DPS-BH01 | DPS-BH02 | Combined | Remarks |
|---|-----------------|-----------------|------------------|---|
| Area of Influence (m ²) | 160,000 | 160,000 | — | Square block of 400 × 400 m assigned to each borehole |
| Mineralized Thickness (m) | 21.5 | 16.0 | 37.5 | Thickness of zones with $K_2O \geq 2\%$ |
| Resource Volume (m ³) | 3440000 | 2560000 | 6000000 | |
| Non-Mineralized Thickness (m) | 12.5 | 14.0 | 26.5 | Intervals having $K_2O < 2\%$ within boreholes |
| Waste Volume (m ³) | 2,000,000 | 2,240,000 | 4,240,000 | Area × non-mineralized thickness |
| Stripping Ratio (Waste : resource) | 0.58 : 1 | 0.87 : 1 | 0.70 : 1 | Waste to resource ratio |

PLATE XII Zone of Influence Polygon

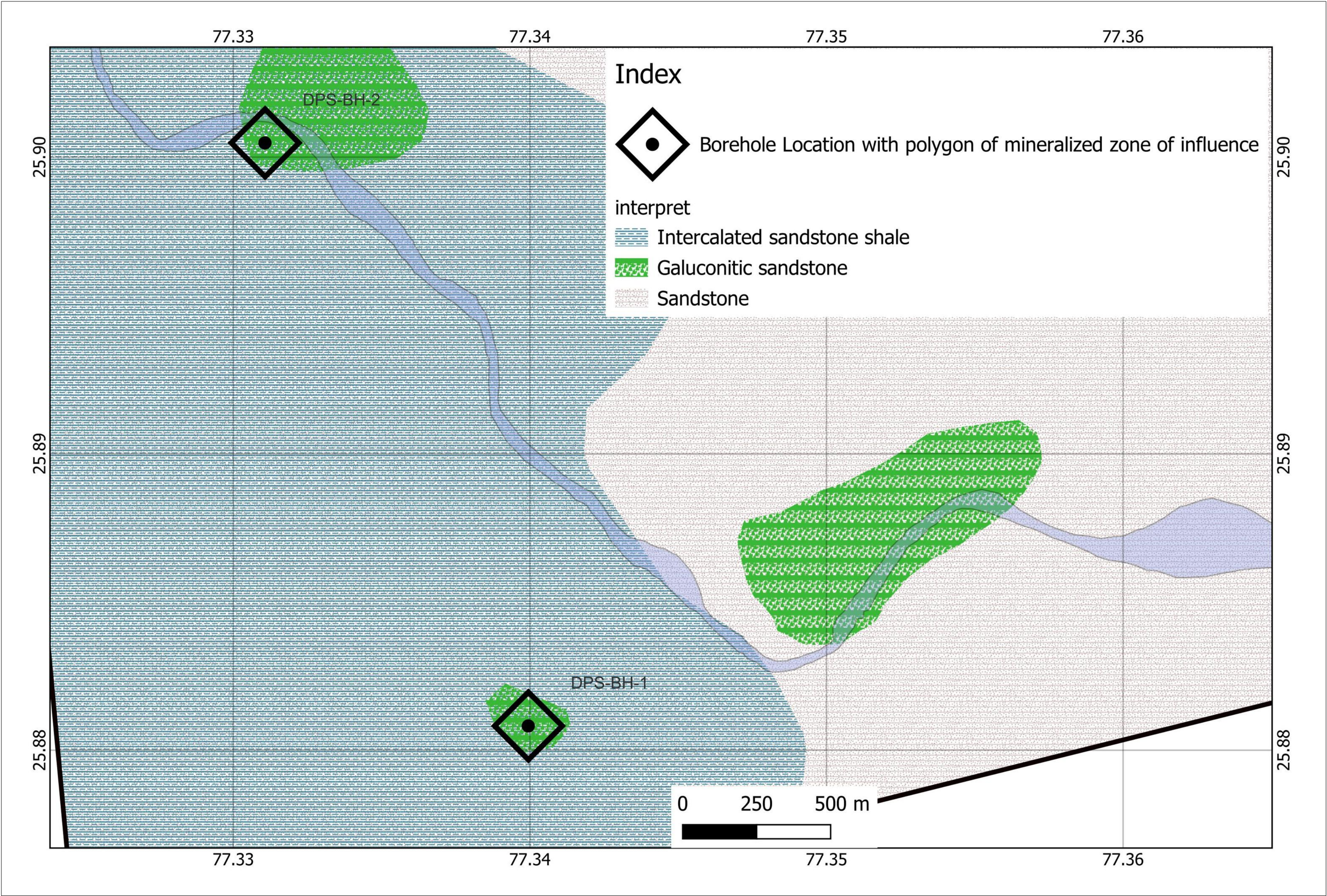
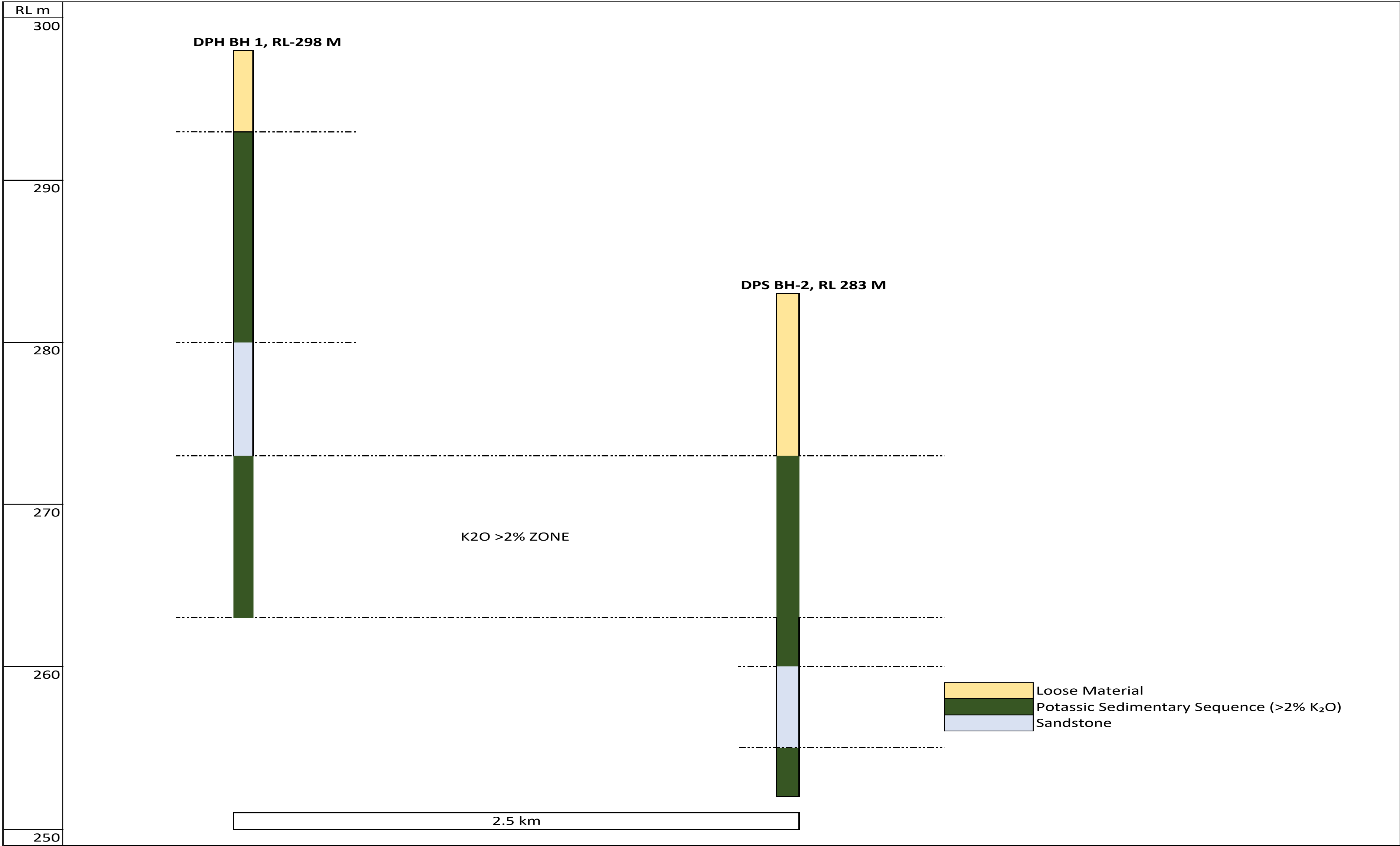


PLATE XIII Mineralized Zone Corelation



Chapter-18 Summary and recommendations

18.1 Conclusion

The reconnaissance (G-4) stage exploration conducted in the Dhamni–Piparwasi–Simliya Block of Sheopur district, Madhya Pradesh, under NMET project **File No. 23/492/2024-NMET/ 283, dated, 21st Aug, 2024**, has successfully delineated zones of glauconitic sandstone bearing significant potash (K_2O) and associated lithium anomalies. The investigation, grounded in prior findings by the Geological Survey of India (GSI) and validated by sampling from Maheshwari Mining Pvt. Ltd., targeted the Upper Rewa Sandstone (Govindgarh Formation) of the Vindhyan Supergroup, a unit already known for glauconite occurrences.

Extensive field mapping (1:25,000 Scale) across 116 km² and a comprehensive geochemical analysis of 253 samples—including bedrock, pit, and borehole core samples—revealed K_2O concentrations ranging from 0.1% to 3.65%. Notably, over 75% of bedrock samples exceeded 0.5% K_2O , 20% exceeded 1.5%, and selected borehole intervals recorded average K_2O of ~2%. Two boreholes (DPS-BH1 and DPS-BH2), drilled to 34 m and 30 m respectively, confirmed glauconitic horizons of 21.5 m and 16 m thickness. Concurrently, ICP-MS analysis highlighted spatially overlapping lithium anomalies, with surface values exceeding 100 ppm and isolated high values >220 ppm, though borehole samples did not confirm subsurface Li enrichment.

Exploration through boreholes **DPS/BH/01** and **DPS/BH/02** successfully delineated two distinct mineralized horizons in each location. Utilizing a uniform bulk density of **2.545 t/m³**, the total resource is estimated at **15.27 million metric tonnes** of glauconite-bearing rock.

Given the average grades of **K_2O** ranging from **2.39% to 3.85%**, the project demonstrates significant primary mineralization. However, due to the limited number of data points, this entire tonnage is currently categorized as an **Inferred Resource (UNFC Code 334)**.

Mineralogical and geochemical indicators suggest that glauconite is unevenly distributed in stratigraphic pockets, formed under specific localized depositional conditions. The presence of associated trace elements patterns supports a sedimentary-marine provenance with minimal structural disturbance. Integration of structural, petrographic, and geochemical datasets through GIS underscores the region's potential for indigenous potash resource development.

The outcome of this G-4 stage exploration justifies the recommendation for upgrading the block to further exploration. A focused exploration strategy within a 15 km² target zone—

encompassing ~10.27 km² of elevated K₂O and ~9.20 km² of Li surface anomalies—is proposed. Future work should include systematic borehole drilling, XRD studies, detailed petrography, and dedicated lithium resource evaluation. The block exhibits significant promise as an indigenous source of glauconitic potash and warrants continued, systematic exploration to assess its commercial viability.

18.2 Recommendations

1. Upgrade Exploration Stage: The Dhamni–Piparwasi–Simliya Block may be advanced to the G-3 stage of exploration, with focused investigation over the ~15 km² target zone identified on the basis of elevated K₂O and Li geochemical values.
2. Systematic Infill Drilling: A systematic infill drilling programme is recommended between Boreholes DPS-BH01 and DPS-BH02 to establish the lateral continuity and thickness variation of glauconitic sandstone horizons. This will help in improving geological confidence and enable the upgradation of the resource category from Inferred (UNFC 334) to Indicated (332) or Measured (331).
3. Mineability Assessment Based on Stripping Ratio: Preliminary stripping ratio calculations based on borehole data indicate an overall stripping ratio of approximately 0.71 : 1, with borehole-wise values of 0.58 : 1 for DPS-BH01 and 0.87: 1 for DPS-BH02. These values suggest relatively low overburden and potential mining conditions. However, detailed drilling and geotechnical investigations are recommended in subsequent exploration stages to refine the overburden characteristics, mine planning parameters, and economic feasibility of extraction.

REFERENCES

Reports

1. Central Ground Water Board. (2013). *District groundwater brochure: Sheopur District, Madhya Pradesh*. Ministry of Jal Shakti, Government of India.
2. Dev, A., & Danish, M. (2023). *Final report on geochemical mapping in toposheet 54G/05 in parts of Shivpuri and Morena districts of Madhya Pradesh*. Field Season 2020–21, Programme Item No. 29746/GCM/CR/MP/2020, FSP ID: M1AGCS-GCM/NC/CR/SEU-MP-BHO/2020/29746. Geological Survey of India, Mission-I, State Unit: Madhya Pradesh, Central Region, Bhopal. (Unpublished report).
3. Geological Survey of India. (2000). *Geology and mineral resources of Madhya Pradesh*. Miscellaneous Publication No. 30, Part XII.
4. Indian Bureau of Mines. (2021, August). *Indian minerals yearbook 2019 (Part-III: Mineral reviews) (58th ed., Potash, Final Release)*. Government of India, Ministry of Mines.
5. Jadia, S. K., & Shrivastava, S. K. (1990). *A report on systematic geological mapping in parts of Morena District, Madhya Pradesh*. Geological Survey of India. (Unpublished report, Field Season 1989–90).
6. Jain, V. K., & Dhar, N. (1988). *A report on the systematic geological mapping in parts of Shivpuri & Morena districts, Madhya Pradesh*. Geological Survey of India. (Unpublished progress report).
7. Ramteke, P. F., & Patel, N. P. (1990). *Progress report for the field season, 1989–90: Systematic geological mapping in parts of Morena District of Madhya Pradesh*. Geological Survey of India, Regional Geology Division, Bhopal, Ministry of Steel & Mines. (Unpublished report).
8. Shrivastava, M. P., & Mehrotra, R. D. (1990). *A progress report on the systematic geological mapping in parts of Shivpuri and Morena districts, Madhya Pradesh*. Geological Survey of India. (Unpublished report, Field Season 1989–90).
9. Wildlife Institute of India. (2022). *Kuno National Park wildlife management plan*. Dehradun: WII.

Books

10. Evans, A. M. (2009). *An introduction to economic geology and its environmental impact* (2nd ed.). Wiley-Blackwell.
11. Evans, A. M. (2009). *Introduction to economic geology* (2nd ed.). Oxford: Wiley-Blackwell.
12. Moon, C. J., Whateley, M. K. G., & Evans, A. M. (2006). *Introduction to mineral exploration* (2nd ed.). Blackwell Publishing.
13. Ramakrishnan, M., & Vaidyanadhan, R. (2010). *Geology of India* (Vol. 1). Bangalore: Geological Society of India.
14. Canadian Institute of Mining, Metallurgy and Petroleum (CIM). (2019). *Estimation of mineral resources and mineral reserves best practice guidelines*.
15. Mackenzie, F. T. (Ed.). (2004). *Sediments, diagenesis and sedimentary rocks* (Vol. 7). In H. D. Holland & K. K. Turekian (Eds.-in-Chief), *Treatise on geochemistry* (2nd ed.).

Websites

16. U.S. Geological Survey. (2024). *Mineral commodity summaries 2024: Potash*. U.S. Department of the Interior. <https://pubs.usgs.gov/periodicals/mcs2024/mcs2024-potash.pdf>

Research Articles

17. Kumar, S. (2016). Megafossils from the Vindhyan Basin, Central India: An overview. *Journal of the Palaeontological Society of India*, 61(2), 273–2

Annexure I Statement showing details of Block boundary co-ordinates of Reconnaissance Survey (G-4) for Glauconitic Sandstone Block Dhamni-Piparwasi-Simliya area Vijaypur District Madhya Pradesh

| Points | X | Y |
|--------|-------------------|-------------------|
| A | 77° 18' 48.981" E | 25° 59' 16.852" N |
| B | 77° 24' 59.923" E | 25° 59' 26.590" N |
| C | 77° 24' 59.898" E | 25° 53' 39.706" N |
| D | 77° 19' 29.231" E | 25° 52' 17.700" N |

Annexure 2 Showing co-ordinates & analyses results for major oxides (XRF analysis) of 150 bedrock samples

| sample ID | latitude | longitude | Al2O3 | BaO | CaO | Cr2O3 | Fe(T) | Fe2O3 | K2O | MgO | MnO | Na2O | P2O5 | SO3 | TiO2 | SiO2 | SrO | V2O5 | LOI |
|-----------|----------|-----------|-------|-------|-------|-------|-------|-------|------|-------|-------|-------|-------|-------|-------|-------|-------|-------|-------|
| DPS-1 | 25.88849 | 77.33124 | 4.83 | <0.05 | 6.01 | <0.05 | | 5.14 | 2.67 | 4.43 | <0.05 | <0.08 | <0.05 | 1.45 | 0.19 | 64.3 | <0.05 | <0.05 | 10.56 |
| DPS-2 | 25.89113 | 77.33109 | 4.76 | <0.05 | 10.54 | <0.05 | | 6.23 | 2.38 | 6.92 | 0.18 | <0.08 | <0.05 | 1.84 | 0.31 | 49.23 | <0.05 | <0.05 | 17.38 |
| DPS-3 | 25.90747 | 77.33765 | 6.11 | <0.05 | 0.16 | <0.05 | | 5.71 | 3.41 | 2.81 | 0.1 | <0.08 | <0.05 | <0.05 | 0.14 | 76.48 | <0.05 | <0.05 | 4.86 |
| DPS-4 | 25.90796 | 77.33805 | 6 | <0.05 | 0.08 | <0.05 | | 6.25 | 3.48 | 2.92 | 0.05 | <0.08 | <0.05 | <0.05 | 0.15 | 75.61 | <0.05 | <0.05 | 5.21 |
| DPS-5 | 25.88491 | 77.33413 | 4.94 | <0.05 | 6.11 | <0.05 | | 5.52 | 2.77 | 4.64 | 0.07 | <0.08 | <0.05 | 1.43 | 0.15 | 63.93 | <0.05 | <0.05 | 10.07 |
| DPS-6 | 25.95863 | 77.39192 | 2.88 | <0.05 | 0.08 | <0.05 | | 0.9 | 1.42 | 0.2 | <0.05 | 0.08 | <0.05 | 0.06 | 0.16 | 93.18 | <0.05 | <0.05 | 0.93 |
| DPS-7 | 25.90357 | 77.39428 | 7.21 | <0.05 | 0.13 | <0.05 | | 1.62 | 3.24 | 0.49 | <0.05 | 0.08 | <0.05 | <0.05 | 0.6 | 84.56 | <0.05 | <0.05 | 1.86 |
| DPS-8 | 25.97782 | 77.35094 | 1.64 | <0.05 | <0.05 | <0.05 | | 1.12 | 0.78 | 0.15 | <0.05 | 0.08 | <0.05 | <0.05 | 0.08 | 95.48 | <0.05 | <0.05 | 0.52 |
| DPS-9 | 25.97914 | 77.35173 | 2.56 | <0.05 | 0.1 | <0.05 | | 1.96 | 1.29 | 0.37 | <0.05 | 0.08 | <0.05 | <0.05 | 0.09 | 92.38 | <0.05 | <0.05 | 1.02 |
| DPS-10 | 25.98652 | 77.36434 | 2.59 | <0.05 | 26.66 | <0.05 | | 5.98 | 0.82 | 13.01 | 0.38 | <0.08 | <0.05 | 0.09 | 0.18 | 13.43 | <0.05 | <0.05 | 36.7 |
| DPS-10 | 25.98652 | 78.36434 | 2.61 | <0.05 | 26.57 | <0.05 | | 5.97 | 0.82 | 13.01 | 0.38 | <0.08 | <0.05 | 0.08 | 0.18 | 13.29 | <0.05 | <0.05 | 36.84 |
| DPS-11 | 25.99117 | 77.36545 | 4.16 | <0.05 | 19.13 | <0.05 | | 4.11 | 1.72 | 0.99 | 0.17 | <0.08 | <0.05 | <0.05 | 0.23 | 52.48 | <0.05 | <0.05 | 16.78 |
| DPS-12 | 25.9904 | 77.36525 | 3.87 | <0.05 | 33.98 | <0.05 | | 5.1 | 1.18 | 5.12 | 0.24 | <0.08 | <0.05 | 0.07 | 0.26 | 16.57 | <0.05 | <0.05 | 33.41 |
| DPS-13 | 25.98738 | 77.36479 | 4.92 | <0.05 | 36.76 | <0.05 | | 4.05 | 1.38 | 1.38 | 0.19 | <0.08 | <0.05 | <0.05 | 0.34 | 19.21 | <0.05 | <0.05 | 31.58 |
| DPS-14 | 25.98375 | 77.36066 | 2.7 | <0.05 | 12.26 | <0.05 | | 3.32 | 0.59 | 0.46 | 0.06 | <0.08 | <0.05 | <0.05 | 0.17 | 69.25 | <0.05 | <0.05 | 10.97 |
| DPS-15 | 25.98239 | 77.35538 | 0.99 | <0.05 | 0.35 | <0.05 | | 0.53 | 0.57 | 0.12 | <0.05 | 0.08 | <0.05 | <0.05 | <0.05 | 96.52 | <0.05 | <0.05 | 0.71 |
| DPS-16 | 25.97773 | 77.3552 | 1.58 | <0.05 | 29.4 | <0.05 | | 6.25 | 0.35 | 13.86 | 0.44 | <0.08 | <0.05 | 0.08 | 0.08 | 7.07 | <0.05 | <0.05 | 40.78 |
| DPS-17 | 25.97914 | 77.35173 | 2.38 | <0.05 | 0.06 | <0.05 | | 1.81 | 1.11 | 0.29 | <0.05 | 0.08 | <0.05 | <0.05 | 0.14 | 92.73 | <0.05 | <0.05 | 1.3 |
| DPS-18 | 25.96659 | 77.33124 | 2.36 | <0.05 | <0.05 | <0.05 | | 1.5 | 1.07 | 0.32 | <0.05 | 0.08 | <0.05 | <0.05 | 0.08 | 93.17 | <0.05 | <0.05 | 1.26 |
| DPS-19 | 25.94348 | 77.37286 | 2.35 | <0.05 | <0.05 | <0.05 | | 0.56 | 1.07 | 0.12 | <0.05 | 0.08 | <0.05 | <0.05 | 0.18 | 94.84 | <0.05 | <0.05 | 0.6 |
| DPS-20 | 25.90002 | 77.3941 | 2.53 | <0.05 | 0.47 | <0.05 | | 1.32 | 1.34 | 0.28 | <0.05 | 0.08 | <0.05 | <0.05 | 0.25 | 92.24 | <0.05 | <0.05 | 1.3 |
| DPS-20 | 25.90002 | 77.3941 | 2.54 | <0.05 | 0.46 | <0.05 | | 1.29 | 1.32 | 0.3 | <0.05 | 0.08 | <0.05 | <0.05 | 0.25 | 92.29 | <0.05 | <0.05 | 1.29 |
| DPS-21 | 25.96094 | 77.40644 | 1.01 | <0.05 | 0.11 | <0.05 | | 0.43 | 0.5 | <0.05 | <0.05 | 0.08 | <0.05 | <0.05 | <0.05 | 97.34 | <0.05 | <0.05 | 0.36 |
| DPS-22 | 25.94172 | 77.41483 | 1.76 | <0.05 | <0.05 | <0.05 | | 0.73 | 0.55 | 0.08 | <0.05 | 0.08 | <0.05 | <0.05 | 0.07 | 95.93 | <0.05 | <0.05 | 0.66 |
| DPS-23 | 25.94072 | 77.41378 | 0.61 | <0.05 | <0.05 | <0.05 | | 0.54 | 0.26 | <0.05 | <0.05 | 0.08 | <0.05 | <0.05 | <0.05 | 98.07 | <0.05 | <0.05 | 0.24 |
| DPS-24 | 25.94469 | 77.41544 | 0.93 | <0.05 | <0.05 | <0.05 | | 0.43 | 0.34 | <0.05 | <0.05 | 0.08 | <0.05 | <0.05 | <0.05 | 97.72 | <0.05 | <0.05 | 0.36 |
| DPS-25 | 25.941 | 77.41111 | 0.63 | <0.05 | 0.23 | 0.08 | | 0.76 | 0.32 | 0.07 | <0.05 | 0.08 | <0.05 | 0.12 | <0.05 | 97.21 | <0.05 | <0.05 | 0.39 |
| DPS-26 | 25.88456 | 77.35089 | 1.2 | <0.05 | <0.05 | <0.05 | | 0.44 | 0.62 | <0.05 | <0.05 | 0.08 | <0.05 | <0.05 | <0.05 | 96.96 | <0.05 | <0.05 | 0.5 |
| DPS-27 | 25.88508 | 77.35092 | 2.17 | <0.05 | 0.15 | <0.05 | | 1.09 | 1.2 | 0.17 | <0.05 | 0.08 | <0.05 | 0.39 | 0.15 | 93.85 | <0.05 | <0.05 | 0.64 |
| DPS-28 | 25.88606 | 77.35111 | 2.54 | <0.05 | 0.75 | 0.07 | | 3.07 | 1.28 | 0.44 | <0.05 | 0.08 | 0.33 | 0.08 | 0.12 | 89.69 | <0.05 | <0.05 | 1.49 |
| DPS-29 | 25.88039 | 77.35125 | 1.69 | <0.05 | <0.05 | <0.05 | | 1.43 | 0.69 | 0.1 | <0.05 | 0.08 | <0.05 | <0.05 | 0.07 | 95.1 | <0.05 | <0.05 | 0.75 |
| DPS-30 | 25.87722 | 77.34217 | 3.95 | <0.05 | 0.06 | 0.05 | | 1.98 | 1.99 | 0.37 | <0.05 | 0.08 | <0.05 | <0.05 | 0.21 | 90.26 | <0.05 | <0.05 | 0.94 |
| DPS-30 | 25.87722 | 77.34217 | 4.02 | <0.05 | 0.06 | 0.05 | | 1.96 | 2 | 0.37 | <0.05 | 0.08 | <0.05 | <0.05 | 0.21 | 90.26 | <0.05 | <0.05 | 0.85 |
| DPS-31 | 25.88242 | 77.35064 | 1.17 | <0.05 | <0.05 | <0.05 | | 0.83 | 0.62 | 0.08 | <0.05 | 0.08 | <0.05 | <0.05 | 0.09 | 96.7 | <0.05 | <0.05 | 0.32 |
| DPS-32 | 25.96153 | 77.29872 | 2.86 | <0.05 | 0.88 | 0.08 | | 2.97 | 1.34 | 0.81 | <0.05 | 0.08 | <0.05 | 2.15 | 0.12 | 86.39 | <0.05 | <0.05 | 2.21 |
| DPS-33 | 25.87842 | 77.34344 | 2.58 | <0.05 | 0.08 | <0.05 | | 1.07 | 1.53 | 0.12 | <0.05 | 0.08 | <0.05 | 0.06 | 0.17 | 93.64 | <0.05 | <0.05 | 0.55 |
| DPS-34 | 25.87925 | 77.34333 | 2.02 | <0.05 | <0.05 | 0.06 | | 1.8 | 0.97 | 0.22 | <0.05 | 0.08 | <0.05 | <0.05 | 0.11 | 93.93 | <0.05 | <0.05 | 0.69 |
| DPS-35 | 25.86981 | 77.33383 | 1.54 | <0.05 | <0.05 | <0.05 | | 1.31 | 0.78 | 0.12 | <0.05 | 0.08 | <0.05 | <0.05 | 0.07 | 95.41 | <0.05 | <0.05 | 0.56 |
| DPS-36 | 25.88994 | 77.34928 | 1.39 | <0.05 | 0.2 | <0.05 | | 1.48 | 0.57 | <0.05 | <0.05 | 0.08 | <0.05 | <0.05 | 0.07 | 95.5 | <0.05 | <0.05 | 0.55 |
| DPS-37 | 25.89264 | 77.34864 | 1.21 | <0.05 | <0.05 | <0.05 | | 0.62 | 0.55 | 0.11 | <0.05 | 0.08 | <0.05 | <0.05 | 0.08 | 96.8 | <0.05 | <0.05 | 0.45 |
| DPS-38 | 25.89375 | 77.34906 | 2.56 | <0.05 | <0.05 | <0.05 | | 2.15 | 1.02 | 0.21 | <0.05 | 0.08 | <0.05 | <0.05 | 0.15 | 92.72 | <0.05 | <0.05 | 0.99 |

| sample ID | latitude | longitude | Al2O3 | BaO | CaO | Cr2O3 | Fe(T) | Fe2O3 | K2O | MgO | MnO | Na2O | P2O5 | SO3 | TiO2 | SiO2 | SrO | V2O5 | LOI |
|-----------|----------|-----------|-------|-------|-------|-------|-------|-------|------|-------|-------|-------|-------|-------|-------|-------|-------|-------|-------|
| DPS-39 | 25.87694 | 77.32914 | 3 | <0.05 | 0.08 | <0.05 | | 2.86 | 1.18 | 0.48 | <0.05 | 0.08 | <0.05 | <0.05 | 0.11 | 90.96 | <0.05 | <0.05 | 1.12 |
| DPS-40 | 25.87642 | 77.33417 | 1.94 | <0.05 | <0.05 | <0.05 | | 1.66 | 0.82 | 0.16 | <0.05 | 0.08 | <0.05 | <0.05 | 0.09 | 94.36 | <0.05 | <0.05 | 0.8 |
| DPS-40 | 25.87642 | 77.33417 | 1.87 | <0.05 | <0.05 | <0.05 | | 1.7 | 0.83 | 0.14 | <0.05 | 0.08 | <0.05 | <0.05 | 0.09 | 94.44 | <0.05 | <0.05 | 0.75 |
| DPS-41 | 25.88642 | 77.34969 | 2.45 | <0.05 | 0.14 | 0.07 | | 2.18 | 1.15 | 0.36 | <0.05 | 0.08 | 0.09 | 0.09 | 0.1 | 92.02 | <0.05 | <0.05 | 1.19 |
| DPS-42 | 25.88894 | 77.35533 | 6.1 | <0.05 | 18.65 | <0.05 | | 5.98 | 2.01 | 10.19 | 0.15 | <0.08 | 0.07 | 0.06 | 0.41 | 28.7 | <0.05 | <0.05 | 27.54 |
| SGP-1 | 25.98769 | 77.40931 | 1 | <0.05 | <0.05 | <0.05 | 0.5 | 0.68 | 0.49 | <0.05 | <0.05 | 0.08 | <0.05 | <0.05 | <0.05 | 97.46 | <0.05 | <0.05 | 0.13 |
| SGP-2 | 25.90639 | 77.32569 | 1.06 | <0.05 | <0.05 | <0.05 | 0.6 | 0.91 | 0.47 | <0.05 | <0.05 | 0.08 | <0.05 | <0.05 | <0.05 | 97.31 | <0.05 | <0.05 | <0.1 |
| DPS-SPG-3 | 25.90303 | 77.33564 | 6 | <0.05 | 0.09 | <0.05 | 1.9 | 2.71 | 2.3 | 0.61 | <0.05 | 0.08 | <0.05 | <0.05 | 0.27 | 86.08 | <0.05 | <0.05 | 1.7 |
| DPS-48 | 25.90811 | 77.33542 | 1.77 | <0.05 | <0.05 | <0.05 | 0.8 | 1.09 | 0.79 | 0.09 | <0.05 | 0.08 | <0.05 | <0.05 | 0.15 | 95.28 | <0.05 | <0.05 | 0.58 |
| DPS-49 | 25.98253 | 77.35892 | 0.97 | <0.05 | <0.05 | <0.05 | 0.6 | 0.8 | 0.44 | <0.05 | <0.05 | 0.08 | <0.05 | <0.05 | <0.05 | 97.37 | <0.05 | <0.05 | 0.2 |
| DPS-50 | 25.93856 | 77.35053 | 1.89 | <0.05 | <0.05 | <0.05 | 1.5 | 2.16 | 0.75 | 0.21 | <0.05 | 0.08 | <0.05 | <0.05 | 0.08 | 93.95 | <0.05 | <0.05 | 0.76 |
| DPS-51 | 25.93321 | 77.37539 | 1.29 | <0.05 | <0.05 | <0.05 | 0.5 | 0.76 | 0.74 | 0.07 | <0.05 | 0.08 | <0.05 | <0.05 | 0.08 | 96.56 | <0.05 | <0.05 | 0.31 |
| DPS-52 | 25.93636 | 77.379 | 1.56 | <0.05 | <0.05 | <0.05 | 1 | 1.45 | 0.69 | 0.07 | <0.05 | 0.08 | <0.05 | <0.05 | 0.07 | 95.72 | <0.05 | <0.05 | 0.29 |
| DPS-53 | 25.93367 | 77.38242 | 3.24 | <0.05 | <0.05 | <0.05 | 0.7 | 0.97 | 1.29 | 0.19 | <0.05 | 0.08 | <0.05 | <0.05 | 0.14 | 92.83 | <0.05 | <0.05 | 1.08 |
| DPS-54 | 25.92731 | 77.38319 | 2.13 | <0.05 | <0.05 | <0.05 | 0.6 | 0.82 | 1.01 | 0.09 | <0.05 | 0.08 | <0.05 | <0.05 | 0.1 | 95.22 | <0.05 | <0.05 | 0.44 |
| DPS-55 | 25.89583 | 77.41478 | 0.73 | <0.05 | <0.05 | <0.05 | 0.5 | 0.64 | 0.35 | <0.05 | <0.05 | 0.08 | <0.05 | <0.05 | <0.05 | 97.86 | <0.05 | <0.05 | 0.25 |
| DPS-55 | 25.89583 | 77.41478 | 0.7 | <0.05 | <0.05 | <0.05 | 0.5 | 0.65 | 0.34 | <0.05 | <0.05 | 0.08 | <0.05 | <0.05 | <0.05 | 97.88 | <0.05 | <0.05 | 0.2 |
| DPS-56 | 25.89878 | 77.40281 | 0.57 | <0.05 | <0.05 | <0.05 | 0.4 | 0.59 | 0.34 | <0.05 | <0.05 | 0.08 | <0.05 | <0.05 | <0.05 | 98.18 | <0.05 | <0.05 | <0.1 |
| DPS-57 | 25.89822 | 77.39136 | 1.41 | <0.05 | <0.05 | <0.05 | 0.9 | 1.23 | 0.65 | 0.09 | <0.05 | 0.08 | <0.05 | <0.05 | 0.07 | 95.97 | <0.05 | <0.05 | 0.4 |
| DPS-58 | 25.90722 | 77.346 | 2.01 | <0.05 | <0.05 | <0.05 | 1.4 | 1.95 | 0.89 | 0.21 | <0.05 | 0.08 | <0.05 | <0.05 | 0.08 | 93.84 | <0.05 | <0.05 | 0.83 |
| DPS-59 | 25.98133 | 77.33928 | 3.4 | <0.05 | 0.081 | <0.05 | 2 | 2.92 | 1.59 | 0.8 | <0.05 | 0.08 | 0.05 | <0.05 | 0.11 | 88.83 | <0.05 | <0.05 | 2.01 |
| DPS-60 | 25.97858 | 77.33969 | 3.27 | <0.05 | 0.067 | <0.05 | 2.3 | 3.24 | 1.4 | 0.69 | <0.05 | 0.08 | 0.09 | <0.05 | 0.13 | 89.14 | <0.05 | <0.05 | 1.79 |
| DPS-61 | 25.98672 | 77.33789 | 1.47 | <0.05 | <0.05 | <0.05 | 1 | 1.45 | 0.62 | 0.13 | <0.05 | 0.08 | <0.05 | <0.05 | 0.1 | 95.32 | <0.05 | <0.05 | 0.7 |
| DPS-62 | 25.93075 | 77.32825 | 1.32 | <0.05 | <0.05 | <0.05 | 0.8 | 1.17 | 0.65 | 0.07 | <0.05 | 0.08 | <0.05 | <0.05 | 0.09 | 96.11 | <0.05 | <0.05 | 0.39 |
| DPS-63 | 25.92322 | 77.34375 | 4.35 | <0.05 | 13.61 | <0.05 | 3.7 | 5.25 | 2.24 | 1.92 | 0.17 | <0.08 | <0.05 | <0.05 | 0.17 | 58.37 | <0.05 | <0.05 | 13.66 |
| DPS-64 | 25.92322 | 77.34375 | 1.96 | <0.05 | 0.096 | <0.05 | 2.1 | 2.95 | 1 | 0.25 | <0.05 | 0.08 | 0.05 | <0.05 | 0.13 | 92.59 | <0.05 | <0.05 | 0.79 |
| DPS-65 | 25.92764 | 77.34128 | 1.26 | <0.05 | 0.612 | <0.05 | 0.9 | 1.28 | 0.71 | 0.11 | <0.05 | 0.08 | <0.05 | <0.05 | 0.08 | 94.75 | <0.05 | <0.05 | 0.96 |
| DPS-65 | 25.92764 | 77.34128 | 1.22 | <0.05 | 0.611 | <0.05 | 0.9 | 1.28 | 0.7 | 0.12 | <0.05 | 0.08 | <0.05 | <0.05 | 0.07 | 94.74 | <0.05 | <0.05 | 1.05 |
| DPS-S-66 | 25.95261 | 77.34111 | 2.31 | <0.05 | <0.05 | <0.05 | 1.8 | 2.53 | 1.06 | 0.11 | <0.05 | 0.08 | <0.05 | <0.05 | 0.12 | 92.71 | <0.05 | <0.05 | 0.92 |
| DPS-S-67 | 25.92381 | 77.36125 | 1.66 | <0.05 | <0.05 | 0.05 | 1.6 | 2.21 | 0.83 | 0.19 | <0.05 | 0.08 | <0.05 | <0.05 | 0.08 | 93.88 | <0.05 | <0.05 | 0.84 |
| DPS-S-68 | 25.90839 | 77.41447 | 0.64 | <0.05 | <0.05 | <0.05 | 0.6 | 0.82 | 0.19 | <0.05 | <0.05 | 0.08 | <0.05 | <0.05 | <0.05 | 97.86 | <0.05 | <0.05 | 0.26 |
| DPS-S-69 | 25.90861 | 77.41469 | 2.81 | <0.05 | <0.05 | <0.05 | 0.6 | 0.79 | 1.29 | 0.11 | <0.05 | 0.08 | <0.05 | <0.05 | 0.27 | 93.55 | <0.05 | <0.05 | 0.83 |
| DPS-S-70 | 25.92575 | 77.40392 | 2.28 | <0.05 | <0.05 | <0.05 | 0.7 | 0.92 | 1.01 | 0.1 | <0.05 | 0.08 | <0.05 | <0.05 | 0.13 | 94.53 | <0.05 | <0.05 | 0.75 |
| DPS-S-71 | 25.98786 | 77.40539 | 1.53 | <0.05 | <0.05 | <0.05 | 1.2 | 1.7 | 0.57 | <0.05 | <0.05 | 0.08 | <0.05 | <0.05 | 0.06 | 95.48 | <0.05 | <0.05 | 0.42 |
| DPS-S-72 | 25.98581 | 77.40267 | 0.81 | <0.05 | <0.05 | <0.05 | 0.5 | 0.74 | 0.26 | <0.05 | <0.05 | 0.08 | <0.05 | <0.05 | <0.05 | 97.63 | <0.05 | <0.05 | 0.3 |
| DPS-S-73 | 25.986 | 77.40256 | 2.41 | <0.05 | <0.05 | <0.05 | 0.5 | 0.75 | 1.1 | 0.07 | <0.05 | 0.08 | <0.05 | <0.05 | 0.22 | 94.47 | <0.05 | <0.05 | 0.61 |
| DPS-S-74 | 25.98231 | 77.40767 | 2.35 | <0.05 | <0.05 | <0.05 | 0.6 | 0.91 | 1.16 | 0.09 | <0.05 | 0.08 | <0.05 | <0.05 | 0.23 | 94.24 | <0.05 | <0.05 | 0.6 |
| DPS-S-75 | 25.98414 | 77.41572 | 1.69 | <0.05 | 27.07 | <0.05 | 3.9 | 5.57 | 0.51 | 15.06 | 0.42 | <0.08 | <0.05 | 0.07 | 0.1 | 8.9 | <0.05 | <0.05 | 40.58 |
| DPS-S-75 | 25.98414 | 77.41572 | 1.65 | <0.05 | 27.04 | <0.05 | 3.9 | 5.61 | 0.51 | 15 | 0.44 | <0.08 | <0.05 | 0.08 | 0.09 | 8.88 | <0.05 | <0.05 | 40.6 |
| DPS-S-76 | 25.97 | 77.41258 | 0.65 | <0.05 | <0.05 | <0.05 | 1.1 | 1.62 | 0.25 | <0.05 | <0.05 | 0.08 | <0.05 | <0.05 | <0.05 | 96.92 | <0.05 | <0.05 | 0.27 |
| DPS-S-77 | 25.973 | 77.40203 | 0.85 | <0.05 | 0.5 | 0.06 | 0.6 | 0.85 | 0.45 | 0.27 | <0.05 | 0.08 | <0.05 | <0.05 | 0.09 | 95.69 | <0.05 | <0.05 | 1.07 |
| DPS-S-78 | 25.96978 | 77.39397 | 1.05 | <0.05 | <0.05 | <0.05 | 0.7 | 0.97 | 0.61 | <0.05 | <0.05 | 0.08 | <0.05 | <0.05 | 0.07 | 96.92 | <0.05 | <0.05 | 0.17 |
| DPS-S-79 | 25.96542 | 77.39794 | 0.89 | <0.05 | <0.05 | 0.05 | 0.5 | 0.77 | 0.36 | <0.05 | <0.05 | 0.08 | <0.05 | <0.05 | <0.05 | 97.32 | <0.05 | <0.05 | 0.39 |

| sample ID | latitude | longitude | Al2O3 | BaO | CaO | Cr2O3 | Fe(T) | Fe2O3 | K2O | MgO | MnO | Na2O | P2O5 | SO3 | TiO2 | SiO2 | SrO | V2O5 | LOI |
|------------|----------|-----------|-------|-------|-------|-------|-------|-------|------|-------|-------|-------|-------|-------|-------|-------|-------|-------|-------|
| DPS-S-80 | 25.96381 | 77.39781 | 0.65 | <0.05 | <0.05 | <0.05 | 0.5 | 0.77 | 0.28 | <0.05 | <0.05 | 0.08 | <0.05 | <0.05 | <0.05 | 97.88 | <0.05 | <0.05 | 0.21 |
| DPS-S-81 | 25.96925 | 77.32939 | 1.12 | <0.05 | <0.05 | 0.07 | 0.7 | 1.02 | 0.62 | <0.05 | <0.05 | 0.08 | <0.05 | <0.05 | 0.07 | 96.61 | <0.05 | <0.05 | 0.3 |
| DPS-S-82 | 25.95792 | 77.34078 | 1.35 | <0.05 | 2.5 | <0.05 | 1.5 | 2.14 | 0.76 | 1.25 | <0.05 | <0.08 | <0.05 | 0.35 | 0.08 | 87.84 | <0.05 | <0.05 | 3.57 |
| DPS-S-83 | 25.94342 | 77.34808 | 1.2 | <0.05 | 0.13 | 0.06 | 0.8 | 1.18 | 0.68 | 0.12 | <0.05 | 0.08 | <0.05 | <0.05 | 0.07 | 95.76 | <0.05 | <0.05 | 0.59 |
| DPS-S-84 | 25.92414 | 77.37556 | 1.45 | <0.05 | <0.05 | <0.05 | 1 | 1.42 | 0.78 | 0.1 | <0.05 | 0.08 | <0.05 | <0.05 | 0.08 | 95.46 | <0.05 | <0.05 | 0.5 |
| DPS-S-85 | 25.92344 | 77.34394 | 2.58 | <0.05 | 10.12 | <0.05 | 2.5 | 3.53 | 1.21 | 1 | 0.11 | <0.08 | <0.05 | <0.05 | 0.09 | 71.48 | <0.05 | <0.05 | 9.63 |
| DPS-S-85 | 25.92344 | 77.34394 | 2.56 | <0.05 | 10.15 | <0.05 | 2.5 | 3.51 | 1.21 | 1.01 | 0.12 | <0.08 | <0.05 | <0.05 | 0.1 | 71.48 | <0.05 | <0.05 | 9.62 |
| DPS-S-86 | 25.94997 | 77.38558 | 1.65 | <0.05 | <0.05 | <0.05 | 0.6 | 0.91 | 0.84 | 0.06 | <0.05 | 0.08 | <0.05 | <0.05 | 0.07 | 95.9 | <0.05 | <0.05 | 0.39 |
| DPS-S-87 | 25.95461 | 77.38317 | 1.19 | <0.05 | 0.1 | 0.07 | 0.5 | 0.74 | 0.65 | <0.05 | <0.05 | 0.08 | <0.05 | <0.05 | 0.05 | 96.64 | <0.05 | <0.05 | 0.38 |
| DPS-S-88 | 25.956 | 77.38219 | 1.67 | <0.05 | <0.05 | <0.05 | 0.9 | 1.22 | 0.81 | <0.05 | <0.05 | 0.08 | <0.05 | <0.05 | 0.12 | 95.6 | <0.05 | <0.05 | 0.28 |
| DPS-S-89 | 25.9645 | 77.37197 | 1.14 | <0.05 | <0.05 | 0.06 | 0.5 | 0.69 | 0.55 | <0.05 | <0.05 | 0.08 | <0.05 | <0.05 | 0.07 | 96.97 | <0.05 | <0.05 | 0.36 |
| DPS-S-90 | 25.96531 | 77.36803 | 0.82 | <0.05 | 0.07 | <0.05 | 1.2 | 1.65 | 0.3 | <0.05 | <0.05 | 0.08 | 0.05 | <0.05 | <0.05 | 96.71 | <0.05 | <0.05 | 0.12 |
| DPS-S-91 a | 25.95889 | 77.39183 | 4.49 | <0.05 | 0.42 | <0.05 | 2 | 2.85 | 1.64 | 0.81 | <0.05 | 0.08 | 0.09 | <0.05 | 0.19 | 87.68 | <0.05 | <0.05 | 1.56 |
| DPS-S-91 b | 25.95889 | 77.39183 | 4.31 | <0.05 | 0.55 | <0.05 | 1.9 | 2.74 | 1.53 | 0.74 | <0.05 | 0.08 | 0.19 | <0.05 | 0.18 | 88.23 | <0.05 | <0.05 | 1.3 |
| DPS-S-91 c | 25.95889 | 77.39183 | 2.19 | <0.05 | 0.16 | 0.06 | 0.9 | 1.33 | 1.02 | 0.25 | <0.05 | 0.08 | <0.05 | 0.06 | 0.13 | 93.79 | <0.05 | <0.05 | 0.78 |
| DPS-S-92 | 25.95889 | 77.39183 | 4.83 | <0.05 | 0.06 | <0.05 | 1 | 1.44 | 2.2 | 0.41 | <0.05 | 0.08 | <0.05 | <0.05 | 0.24 | 89.6 | <0.05 | <0.05 | 0.93 |
| DPS-S-93 | 25.95889 | 77.39183 | 4.78 | <0.05 | 0.22 | <0.05 | 1.8 | 2.57 | 1.74 | 0.74 | <0.05 | 0.08 | <0.05 | <0.05 | 0.15 | 88.23 | <0.05 | <0.05 | 1.31 |
| DPS-S-93 | 25.95889 | 77.39183 | 4.72 | <0.05 | 0.23 | <0.05 | 1.8 | 2.59 | 1.75 | 0.72 | <0.05 | 0.08 | <0.05 | <0.05 | 0.15 | 88.28 | <0.05 | <0.05 | 1.3 |
| DPS-S-94 | 25.904 | 77.34189 | 1.89 | <0.05 | <0.05 | <0.05 | 1.3 | 1.78 | 0.73 | 0.3 | <0.05 | 0.08 | <0.05 | <0.05 | 0.07 | 94.52 | <0.05 | <0.05 | 0.51 |
| DPS-S-95 | 25.92339 | 77.34011 | 1.69 | <0.05 | 30.73 | <0.05 | 4.9 | 6.94 | 0.48 | 11.87 | 0.61 | <0.08 | <0.05 | 0.13 | 0.12 | 7.97 | <0.05 | <0.05 | 39.34 |
| DPS-S-96 | 25.98303 | 77.37242 | 0.71 | <0.05 | <0.05 | 0.07 | 0.5 | 0.75 | 0.21 | <0.05 | <0.05 | 0.08 | <0.05 | <0.05 | <0.05 | 97.76 | <0.05 | <0.05 | 0.27 |
| DPS-S-97 | 25.98158 | 77.37286 | 1.01 | <0.05 | 0.24 | <0.05 | 0.4 | 0.54 | 0.52 | 0.1 | <0.05 | 0.08 | <0.05 | <0.05 | 0.05 | 96.7 | <0.05 | <0.05 | 0.64 |
| DPS-S-98 | 25.98033 | 77.37878 | 0.66 | <0.05 | <0.05 | 0.11 | 0.7 | 1.03 | 0.27 | <0.05 | <0.05 | 0.08 | <0.05 | <0.05 | <0.05 | 97.59 | <0.05 | <0.05 | 0.16 |
| DPS-S-99 | 25.98022 | 77.37975 | 0.71 | <0.05 | 0.15 | 0.06 | 0.4 | 0.63 | 0.28 | <0.05 | <0.05 | 0.08 | 0.05 | <0.05 | <0.05 | 97.67 | <0.05 | <0.05 | 0.25 |
| DPS-S-100 | 25.97942 | 77.38078 | 0.89 | <0.05 | <0.05 | 0.07 | 0.7 | 0.92 | 0.34 | <0.05 | <0.05 | 0.08 | <0.05 | <0.05 | <0.05 | 97.24 | <0.05 | <0.05 | 0.31 |
| DPS-S-101 | 25.97878 | 77.38625 | 1.85 | <0.05 | <0.05 | 0.07 | 0.7 | 0.98 | 0.74 | 0.07 | <0.05 | 0.08 | <0.05 | <0.05 | 0.08 | 95.51 | <0.05 | <0.05 | 0.54 |
| DPS-S-102 | 25.97864 | 77.38825 | 1.62 | <0.05 | <0.05 | 0.08 | 0.7 | 0.96 | 0.57 | <0.05 | <0.05 | 0.08 | <0.05 | <0.05 | 0.06 | 96.07 | <0.05 | <0.05 | 0.45 |
| DPS-S-103 | 25.98039 | 77.39464 | 1.25 | <0.05 | <0.05 | 0.05 | 0.5 | 0.72 | 0.48 | <0.05 | <0.05 | 0.08 | <0.05 | <0.05 | 0.07 | 96.89 | <0.05 | <0.05 | 0.36 |
| DPS-S-104 | 25.97978 | 77.39619 | 1.72 | <0.05 | <0.05 | 0.06 | 0.8 | 1.21 | 0.61 | 0.09 | <0.05 | 0.08 | <0.05 | <0.05 | 0.08 | 95.41 | <0.05 | <0.05 | 0.56 |
| DPS-S-104 | 25.97978 | 77.39619 | 1.77 | <0.05 | <0.05 | 0.06 | 0.9 | 1.23 | 0.62 | 0.07 | <0.05 | 0.08 | <0.05 | <0.05 | 0.08 | 95.47 | <0.05 | <0.05 | 0.53 |
| DPS-S-105 | 25.97914 | 77.39761 | 1.76 | <0.05 | <0.05 | <0.05 | 1.2 | 1.72 | 0.56 | 0.19 | <0.05 | 0.08 | <0.05 | <0.05 | <0.05 | 94.92 | <0.05 | <0.05 | 0.61 |
| DPS-S-106 | 25.97731 | 77.39969 | 1.3 | <0.05 | <0.05 | 0.07 | 0.8 | 1.14 | 0.23 | <0.05 | <0.05 | 0.08 | <0.05 | <0.05 | <0.05 | 96.57 | <0.05 | <0.05 | 0.48 |
| DPS-S-107 | 25.97642 | 77.40047 | 1.02 | <0.05 | <0.05 | <0.05 | 0.3 | 0.49 | 0.31 | <0.05 | <0.05 | 0.08 | <0.05 | <0.05 | 0.05 | 97.54 | <0.05 | <0.05 | 0.4 |
| DPS-S-108 | 25.97514 | 77.40061 | 0.91 | <0.05 | <0.05 | 0.08 | 0.7 | 0.96 | 0.43 | <0.05 | <0.05 | 0.08 | <0.05 | <0.05 | <0.05 | 97.27 | <0.05 | <0.05 | 0.16 |
| DPS-S-109 | 25.97497 | 77.40261 | 1.71 | <0.05 | <0.05 | 0.05 | 1 | 1.39 | 0.45 | 0.07 | <0.05 | 0.08 | <0.05 | <0.05 | 0.06 | 95.79 | <0.05 | <0.05 | 0.32 |
| DPS-S-110 | 25.97617 | 77.40286 | 1.33 | <0.05 | <0.05 | 0.09 | 0.8 | 1.08 | 0.35 | <0.05 | <0.05 | 0.08 | <0.05 | <0.05 | 0.05 | 96.65 | <0.05 | <0.05 | 0.27 |
| DPS-S-111 | 25.97864 | 77.40094 | 1.34 | <0.05 | <0.05 | 0.05 | 0.7 | 0.95 | 0.31 | <0.05 | <0.05 | 0.08 | <0.05 | <0.05 | 0.06 | 96.59 | <0.05 | <0.05 | 0.52 |
| DPS-S-112 | 25.98378 | 77.40419 | 1.04 | <0.05 | <0.05 | 0.08 | 0.6 | 0.89 | 0.37 | 0.06 | <0.05 | 0.08 | <0.05 | <0.05 | 0.05 | 97 | <0.05 | <0.05 | 0.36 |
| DPS-S-113 | 25.88106 | 77.33981 | 4.55 | <0.05 | 0.26 | <0.05 | 2.2 | 3.09 | 1.93 | 0.83 | <0.05 | 0.08 | 0.15 | <0.05 | 0.17 | 87.08 | <0.05 | <0.05 | 1.75 |
| DPS-S-114 | 25.92403 | 77.34381 | 3.28 | <0.05 | 5.84 | 0.06 | 3.3 | 4.77 | 1.65 | 1.43 | <0.05 | <0.08 | <0.05 | <0.05 | 0.12 | 76.09 | <0.05 | <0.05 | 6.53 |
| DPS-S-114 | 25.92403 | 77.34381 | 3.26 | <0.05 | 5.86 | 0.06 | 3.3 | 4.7 | 1.62 | 1.47 | <0.05 | <0.08 | <0.05 | <0.05 | 0.12 | 76.07 | <0.05 | <0.05 | 6.62 |
| DPS-S-115 | 25.91006 | 77.41178 | 2.87 | <0.05 | <0.05 | 0.05 | 0.5 | 0.74 | 1.36 | 0.11 | <0.05 | 0.08 | <0.05 | <0.05 | 0.29 | 93.37 | <0.05 | <0.05 | 0.92 |
| DPS-S-116 | 25.91819 | 77.41167 | 0.58 | <0.05 | <0.05 | 0.14 | 1.3 | 1.9 | 0.14 | <0.05 | <0.05 | 0.08 | <0.05 | <0.05 | <0.05 | 96.7 | <0.05 | <0.05 | 0.33 |

| sample ID | latitude | longitude | Al2O3 | BaO | CaO | Cr2O3 | Fe(T) | Fe2O3 | K2O | MgO | MnO | Na2O | P2O5 | SO3 | TiO2 | SiO2 | SrO | V2O5 | LOI |
|-----------|----------|-----------|-------|-------|-------|-------|-------|-------|------|-------|-------|-------|-------|-------|-------|-------|-------|-------|-------|
| DPS-S-117 | 25.9225 | 77.41331 | 0.82 | <0.05 | <0.05 | 0.07 | 0.5 | 0.69 | 0.26 | <0.05 | <0.05 | 0.08 | <0.05 | <0.05 | <0.05 | 97.49 | <0.05 | <0.05 | 0.42 |
| DPS-S-118 | 25.91006 | 77.41178 | 0.49 | <0.05 | 0.18 | 0.13 | 0.9 | 1.35 | 0.23 | <0.05 | <0.05 | 0.08 | <0.05 | <0.05 | <0.05 | 96.99 | <0.05 | <0.05 | 0.43 |
| DPS-S-119 | 25.91819 | 77.41167 | 0.51 | <0.05 | <0.05 | <0.05 | 0.3 | 0.41 | 0.29 | <0.05 | <0.05 | 0.08 | <0.05 | <0.05 | <0.05 | 98.28 | <0.05 | <0.05 | 0.27 |
| DPS-S-120 | 25.9225 | 77.41331 | 0.67 | <0.05 | <0.05 | 0.08 | 0.7 | 0.97 | 0.42 | <0.05 | <0.05 | 0.08 | <0.05 | 0.09 | <0.05 | 97.4 | <0.05 | <0.05 | 0.19 |
| DPS-S-121 | 25.93572 | 77.39656 | 5.33 | <0.05 | 0.4 | 0.11 | 1.7 | 2.48 | 2.12 | 0.55 | <0.05 | 0.08 | <0.05 | 0.18 | 0.26 | 86.34 | <0.05 | <0.05 | 2.04 |
| DPS-S-122 | 25.90281 | 77.41522 | 0.81 | <0.05 | <0.05 | 0.11 | 0.7 | 1.03 | 0.44 | <0.05 | <0.05 | 0.08 | <0.05 | 0.19 | <0.05 | 96.83 | <0.05 | <0.05 | 0.33 |
| DPS-S-123 | 25.90356 | 77.41117 | 1.63 | <0.05 | <0.05 | 0.08 | 0.9 | 1.27 | 0.82 | 0.14 | <0.05 | 0.08 | <0.05 | 0.16 | 0.09 | 95.13 | <0.05 | <0.05 | 0.49 |
| DPS-S-124 | 25.90525 | 77.40725 | 0.61 | <0.05 | <0.05 | 0.11 | 0.7 | 0.96 | 0.22 | <0.05 | <0.05 | 0.08 | <0.05 | 0.08 | <0.05 | 97.37 | <0.05 | <0.05 | 0.39 |
| DPS-S-124 | 25.90497 | 77.39994 | 0.57 | <0.05 | <0.05 | 0.11 | 0.7 | 0.98 | 0.23 | <0.05 | <0.05 | 0.08 | <0.05 | 0.08 | <0.05 | 97.4 | <0.05 | <0.05 | 0.39 |
| DPS-S-125 | 25.91097 | 77.39808 | 0.31 | <0.05 | <0.05 | 0.06 | 0.9 | 1.25 | 0.1 | <0.05 | <0.05 | 0.08 | <0.05 | 0.11 | <0.05 | 97.59 | <0.05 | <0.05 | 0.41 |
| DPS-S-126 | 25.92175 | 77.39956 | 0.56 | <0.05 | <0.05 | 0.07 | 0.7 | 1.05 | 0.13 | <0.05 | <0.05 | 0.08 | <0.05 | 0.14 | <0.05 | 97.62 | <0.05 | <0.05 | 0.25 |
| DPS-S-127 | 25.92175 | 77.39956 | 0.81 | <0.05 | 7.07 | 0.08 | 2.7 | 3.8 | 0.33 | 3.46 | 0.24 | <0.08 | <0.05 | 0.24 | <0.05 | 73.17 | <0.05 | <0.05 | 10.66 |
| DPS-S-128 | 25.92428 | 77.39411 | 0.85 | <0.05 | 0.13 | 0.08 | 0.5 | 0.77 | 0.55 | <0.05 | <0.05 | 0.08 | <0.05 | 0.19 | 0.05 | 96.84 | <0.05 | <0.05 | 0.34 |
| DPS-S-129 | 25.91753 | 77.39211 | 1.4 | <0.05 | <0.05 | 0.08 | 0.6 | 0.86 | 0.69 | <0.05 | <0.05 | 0.08 | <0.05 | 0.17 | 0.08 | 96.17 | <0.05 | <0.05 | 0.35 |
| DPS-S-130 | 25.90069 | 77.41614 | 1.55 | <0.05 | <0.05 | 0.06 | 0.5 | 0.69 | 0.87 | <0.05 | <0.05 | 0.08 | <0.05 | 0.19 | 0.08 | 95.85 | <0.05 | <0.05 | 0.5 |
| DPS-S-131 | 25.973 | 77.37611 | 1.29 | <0.05 | 4.74 | <0.05 | 1.6 | 2.32 | 0.75 | 0.13 | 0.12 | <0.08 | <0.05 | 0.2 | 0.09 | 85.68 | <0.05 | <0.05 | 4.47 |
| DPS-S-132 | 25.96953 | 77.37747 | 1.79 | <0.05 | 2.03 | <0.05 | 0.7 | 0.98 | 0.94 | 0.39 | <0.05 | 0.08 | <0.05 | 0.05 | 0.12 | 91.13 | <0.05 | <0.05 | 2.34 |
| DPS-S-133 | 25.9595 | 77.37458 | 2.39 | <0.05 | 25.05 | <0.05 | 3.8 | 5.38 | 0.94 | 7.91 | 0.35 | <0.08 | <0.05 | 0.23 | 0.18 | 27.89 | <0.05 | <0.05 | 29.5 |
| DPS-S-134 | 25.95747 | 77.37072 | 1.48 | <0.05 | <0.05 | 0.07 | 0.6 | 0.91 | 0.78 | 0.11 | <0.05 | 0.08 | <0.05 | 0.22 | 0.07 | 95.64 | <0.05 | <0.05 | 0.55 |
| DPS-S-134 | 25.95597 | 77.36494 | 1.45 | <0.05 | <0.05 | 0.07 | 0.7 | 0.94 | 0.79 | 0.11 | <0.05 | 0.08 | <0.05 | 0.23 | 0.07 | 95.63 | <0.05 | <0.05 | 0.48 |
| DPS-S-135 | 25.96022 | 77.36028 | 1.43 | <0.05 | 1.39 | <0.05 | 1 | 1.43 | 0.89 | 0.14 | <0.05 | 0.08 | <0.05 | 0.17 | 0.08 | 92.7 | <0.05 | <0.05 | 1.54 |
| DPS-S-136 | 25.96636 | 77.35811 | 1.59 | <0.05 | <0.05 | 0.08 | 0.8 | 1.2 | 0.83 | 0.16 | <0.05 | 0.08 | <0.05 | 0.23 | 0.06 | 95.12 | <0.05 | <0.05 | 0.58 |
| DPS-S-137 | 25.96636 | 77.35811 | 0.71 | <0.05 | <0.05 | <0.05 | 0.6 | 0.85 | 0.25 | <0.05 | <0.05 | 0.08 | <0.05 | 0.2 | <0.05 | 97.59 | <0.05 | <0.05 | 0.2 |
| DPS-S-138 | 25.97058 | 77.35675 | 2.69 | <0.05 | 0.18 | 0.06 | 1.4 | 2.06 | 1.25 | 0.52 | <0.05 | 0.08 | 0.07 | 0.25 | 0.09 | 91.47 | <0.05 | <0.05 | 1.23 |
| DPS-S-139 | 25.96928 | 77.36211 | 1.3 | <0.05 | <0.05 | <0.05 | 0.6 | 0.91 | 0.78 | <0.05 | <0.05 | 0.08 | <0.05 | 0.31 | 0.06 | 96.18 | <0.05 | <0.05 | 0.24 |
| DPS-S-140 | 25.96794 | 77.36578 | 1.34 | <0.05 | <0.05 | <0.05 | 0.8 | 1.12 | 0.76 | 0.08 | <0.05 | 0.08 | <0.05 | 0.13 | 0.1 | 95.75 | <0.05 | <0.05 | 0.49 |
| DPS-S-141 | 25.98369 | 77.3345 | 1.26 | <0.05 | <0.05 | <0.05 | 1.1 | 1.55 | 0.55 | 0.05 | <0.05 | 0.08 | <0.05 | 0.24 | 0.11 | 95.53 | <0.05 | <0.05 | 0.51 |
| DPS-S-142 | 25.96981 | 77.32247 | 1.23 | <0.05 | <0.05 | <0.05 | 0.9 | 1.27 | 0.59 | 0.07 | <0.05 | 0.08 | <0.05 | 0.28 | 0.07 | 95.9 | <0.05 | <0.05 | 0.4 |
| DPS-S-143 | 25.92633 | 77.32211 | 1.62 | <0.05 | <0.05 | <0.05 | 1.2 | 1.73 | 0.86 | 0.14 | <0.05 | 0.08 | <0.05 | 0.16 | 0.08 | 94.53 | <0.05 | <0.05 | 0.67 |
| DPS-S-144 | 25.91503 | 77.32647 | 1.46 | <0.05 | <0.05 | <0.05 | 0.9 | 1.28 | 0.86 | 0.1 | <0.05 | 0.08 | <0.05 | 0.18 | 0.07 | 95.29 | <0.05 | <0.05 | 0.47 |
| DPS-S-144 | 25.90764 | 77.35194 | 1.49 | <0.05 | <0.05 | <0.05 | 0.9 | 1.3 | 0.87 | 0.1 | <0.05 | 0.08 | <0.05 | 0.22 | 0.07 | 95.26 | <0.05 | <0.05 | 0.49 |
| DPS-S-145 | 25.90433 | 77.35722 | 1.51 | <0.05 | <0.05 | <0.05 | 0.8 | 1.07 | 0.72 | 0.05 | <0.05 | 0.08 | <0.05 | 0.25 | 0.12 | 95.75 | <0.05 | <0.05 | 0.33 |
| DPS-S-146 | 25.90133 | 77.36169 | 1.48 | <0.05 | <0.05 | <0.05 | 0.9 | 1.26 | 0.72 | 0.1 | <0.05 | 0.08 | <0.05 | 0.21 | 0.08 | 95.43 | <0.05 | <0.05 | 0.54 |
| DPS-S-147 | 25.90133 | 77.36169 | 1.33 | <0.05 | <0.05 | <0.05 | 0.9 | 1.33 | 0.65 | 0.14 | <0.05 | 0.08 | <0.05 | 0.26 | 0.07 | 95.61 | <0.05 | <0.05 | 0.44 |
| DPS-S-148 | 25.89864 | 77.36558 | 3.16 | <0.05 | <0.05 | <0.05 | 0.4 | 0.59 | 1.33 | 0.12 | <0.05 | 0.08 | <0.05 | 0.09 | 0.29 | 93.28 | <0.05 | <0.05 | 0.9 |
| DPS-S-149 | 25.903 | 77.38164 | 1.77 | <0.05 | <0.05 | 0.05 | 0.7 | 0.94 | 0.74 | 0.08 | <0.05 | 0.08 | <0.05 | <0.05 | 0.09 | 95.73 | <0.05 | <0.05 | 0.42 |
| DPS-S-150 | 25.92044 | 77.37883 | 3.3 | <0.05 | 0.59 | 0.06 | 2.7 | 3.8 | 1.54 | 0.61 | 0.09 | 0.08 | 0.38 | <0.05 | 0.17 | 87.53 | <0.05 | <0.05 | 1.74 |

Annexure 3 Statement Showing co-ordinates & analyses results for REE and Trace Elements (ICPMS) of 75 bedrock samples

| sample ID | latitude | longitude | Li | Be | B | Sc | Co | Ga | Ge | Se | Rb | Y | Nb | Mo | Cd | In | Sn | Sb | Te | Cs | La | Ce | Pr | Nd | Sm | Eu | Gd | Tb | Dy | Ho | Er | Tm | Yb | Lu | Hf | Ta | W | Ti | Bi | Th | U | Cu | Ni | Pb | Sr | Zn | Zr | | |
|-----------|----------|-----------|------|------|----|------|------|------|------|------|-------|------|------|------|------|------|------|------|------|------|------|------|------|------|------|------|-----|------|------|------|------|------|------|------|------|------|------|------|------|------|------|------|------|-----|-----|------|-----|-----|----|
| DPS-1 | 25.88849 | 77.33124 | 336 | 3.2 | <5 | 4.2 | 22.9 | 17 | <0.5 | 1 | 100.5 | 11.2 | 1.8 | <0.5 | 1.4 | <0.5 | <0.5 | <0.5 | 1 | 4.6 | 7.4 | 18.1 | 2.5 | 11.3 | 3 | 0.9 | 3 | <0.5 | 2.1 | <0.5 | 1.1 | <0.5 | 0.9 | 0.6 | 2.4 | <0.5 | 1.9 | <0.5 | <0.5 | 3.9 | 0.7 | 112 | 26 | 75 | 24 | 1302 | 104 | | |
| DPS-2 | 25.89113 | 77.33109 | 248 | 3.4 | <5 | 4.3 | 10.6 | 14.8 | <0.5 | 1.4 | 89.4 | 13 | 1.6 | <0.5 | <0.5 | <0.5 | 3.3 | <0.5 | <0.5 | 4.6 | 8.7 | 20.3 | 2.6 | 12.3 | 3.2 | 0.8 | 3.1 | <0.5 | 2.6 | 0.5 | 1.4 | <0.5 | 1.2 | <0.5 | 2.2 | <0.5 | <0.5 | <0.5 | 1.9 | 3.9 | 0.8 | 56 | 14 | 180 | 29 | 482 | 77 | | |
| DPS-3 | 25.90747 | 77.33765 | 346 | 4.8 | <5 | 3.8 | 7 | 25 | <0.5 | <0.5 | 125 | 3.8 | <0.5 | <0.5 | <0.5 | <0.5 | <0.5 | <0.5 | <0.5 | 2.8 | 6.8 | 18.4 | 2 | 8 | 1.6 | <0.5 | 1.4 | <0.5 | 0.9 | <0.5 | 0.5 | <0.5 | <0.5 | <0.5 | <0.5 | <0.5 | <0.5 | <0.5 | <0.5 | 3.1 | 0.6 | 85 | 10 | 183 | 18 | 174 | 37 | | |
| DPS-4 | 25.90796 | 77.33805 | 384 | 5.1 | <5 | 2.9 | 7.9 | 26.6 | <0.5 | <0.5 | 124.1 | 4.3 | <0.5 | <0.5 | <0.5 | <0.5 | <0.5 | <0.5 | <0.5 | 2.7 | 5.5 | 13.5 | 1.7 | 6.8 | 1.4 | <0.5 | 1.3 | <0.5 | 1 | <0.5 | 0.5 | <0.5 | 0.5 | <0.5 | <0.5 | <0.5 | <0.5 | <0.5 | <0.5 | 2.5 | 0.7 | 188 | 12 | 453 | 15 | 365 | 43 | | |
| DPS-5 | 25.88491 | 77.33413 | 351 | 3.5 | <5 | 3 | 21 | 16.8 | <0.5 | <0.5 | 101.2 | 9.9 | 0.7 | 0.6 | 1.3 | <0.5 | <0.5 | <0.5 | <0.5 | 4.8 | 5.8 | 15.5 | 2.2 | 10.4 | 2.7 | 0.9 | 2.7 | <0.5 | 2 | <0.5 | 0.9 | <0.5 | 0.8 | <0.5 | 1.7 | <0.5 | <0.5 | <0.5 | 3.2 | 2.5 | 0.6 | 107 | 32 | 26 | 24 | 1332 | 46 | | |
| DPS-6 | 25.95863 | 77.39192 | 12 | 0.6 | <5 | 1.6 | 1.6 | 3.5 | <0.5 | <0.5 | 46 | 5.3 | <0.5 | <0.5 | <0.5 | <0.5 | 2.8 | <0.5 | <0.5 | 1.2 | 11.4 | 21.2 | 2.4 | 9.2 | 1.5 | <0.5 | 1.6 | <0.5 | 1.1 | <0.5 | 0.7 | <0.5 | 0.7 | <0.5 | 1.8 | <0.5 | <0.5 | <0.5 | <0.5 | 3.8 | 0.7 | 10 | <5 | 9 | 19 | 8 | 93 | | |
| DPS-7 | 25.90357 | 77.39428 | 18.5 | 1 | <5 | 4.8 | 7.4 | 7.2 | <0.5 | 1.6 | 97.7 | 15.8 | 4.2 | <0.5 | 0.6 | <0.5 | 60 | <0.5 | <0.5 | 3.6 | 24.8 | 47.8 | 5.5 | 21.5 | 4.1 | 0.8 | 4.1 | 0.6 | 3 | 0.7 | 1.8 | <0.5 | 2 | <0.5 | 6 | <0.5 | <0.5 | <0.5 | 1.8 | 13 | 2.1 | 6 | 13 | 17 | 30 | 8 | 246 | | |
| DPS-8 | 25.97782 | 77.35094 | 19.5 | <0.5 | <5 | 0.8 | 1.6 | 2.5 | <0.5 | <0.5 | 26.7 | 3.7 | <0.5 | <0.5 | <0.5 | <0.5 | <0.5 | <0.5 | <0.5 | 0.7 | 8.8 | 17.1 | 1.9 | 7.4 | 1.5 | <0.5 | 1.2 | <0.5 | 0.7 | <0.5 | <0.5 | <0.5 | 0.6 | <0.5 | <0.5 | <0.5 | <0.5 | <0.5 | <0.5 | 2.5 | <0.5 | 8 | <5 | 20 | 12 | 139 | 27 | | |
| DPS-9 | 25.97914 | 77.35173 | 58.7 | 1.6 | <5 | 2.6 | 5.6 | 5.8 | <0.5 | <0.5 | 43 | 6.6 | 0.8 | <0.5 | <0.5 | <0.5 | <0.5 | <0.5 | <0.5 | 1.3 | 12.6 | 20.2 | 3.4 | 15.3 | 3.6 | 0.8 | 3.2 | <0.5 | 1.7 | <0.5 | 0.8 | <0.5 | 0.6 | <0.5 | <0.5 | <0.5 | <0.5 | <0.5 | <0.5 | <0.5 | 3.1 | <0.5 | 24 | 7 | 51 | 17 | 15 | 26 | |
| DPS-12 | 25.9904 | 77.36525 | 13.3 | 0.8 | <5 | 4.4 | 8.2 | 5.3 | <0.5 | 1.2 | 49.7 | 13.7 | 3.4 | 2.1 | <0.5 | <0.5 | <0.5 | <0.5 | <0.5 | 2.3 | 11.6 | 27.2 | 3.3 | 13.6 | 3 | 0.8 | 3.1 | <0.5 | 2.6 | <0.5 | 1.3 | <0.5 | 1.2 | <0.5 | <0.5 | <0.5 | <0.5 | <0.5 | <0.5 | <0.5 | 4 | 1.4 | 7 | 37 | 21 | 63 | <5 | <5 | |
| DPS-14 | 25.98375 | 77.36066 | 9.5 | 0.6 | <5 | 4 | 10.2 | 3.8 | <0.5 | <0.5 | 23.3 | 7.9 | 2.9 | 0.8 | <0.5 | <0.5 | <0.5 | <0.5 | <0.5 | 0.9 | 12.6 | 23 | 3 | 11.5 | 2.2 | 0.5 | 2.2 | <0.5 | 1.5 | <0.5 | 0.8 | <0.5 | 0.7 | <0.5 | <0.5 | <0.5 | <0.5 | <0.5 | <0.5 | 1.4 | 4.6 | 0.8 | 11 | 27 | <5 | 94 | <5 | <5 | |
| DPS-17 | 25.97914 | 77.35173 | 50.1 | 1.4 | <5 | 2.5 | 6.3 | 5.4 | <0.5 | <0.5 | 39 | 6.2 | 1.1 | <0.5 | <0.5 | <0.5 | <0.5 | <0.5 | <0.5 | 1.2 | 17.7 | 29.9 | 4.3 | 18.4 | 3.9 | 0.7 | 3.3 | <0.5 | 1.6 | <0.5 | 0.7 | <0.5 | 0.6 | <0.5 | 1.1 | <0.5 | <0.5 | <0.5 | <0.5 | 5.3 | 1 | 43 | 6 | 58 | 19 | 15 | 47 | | |
| DPS-18 | 25.96659 | 77.33124 | 29.7 | 1 | <5 | 1.5 | 2.6 | 4.4 | <0.5 | 1 | 37.8 | 4.2 | <0.5 | <0.5 | <0.5 | <0.5 | <0.5 | <0.5 | <0.5 | 1 | 12.8 | 17.9 | 2.6 | 9.8 | 1.8 | <0.5 | 1.6 | <0.5 | 0.9 | <0.5 | 0.5 | <0.5 | <0.5 | <0.5 | <0.5 | <0.5 | <0.5 | 0.6 | 2.2 | <0.5 | 38 | <5 | 51 | 14 | 102 | 28 | | | |
| DPS-19 | 25.94348 | 77.37286 | 11.3 | <0.5 | <5 | 1.2 | 2 | 2.6 | <0.5 | <0.5 | 37.5 | 7.1 | 8.3 | <0.5 | <0.5 | <0.5 | <0.5 | <0.5 | <0.5 | 0.8 | 11.2 | 20.9 | 2.3 | 8.6 | 1.3 | <0.5 | 1.4 | <0.5 | 1.1 | <0.5 | 0.8 | <0.5 | 0.9 | <0.5 | 2.8 | <0.5 | <0.5 | <0.5 | <0.5 | 3.1 | 1 | 12 | <5 | 9 | 15 | 8 | 172 | | |
| DPS-21 | 25.96094 | 77.40644 | 3.3 | <0.5 | <5 | 1.2 | <0.5 | 1.2 | <0.5 | <0.5 | 17.6 | 2.3 | <0.5 | <0.5 | <0.5 | <0.5 | <0.5 | <0.5 | <0.5 | <0.5 | 7 | 14.1 | 1.6 | 5.8 | 1 | <0.5 | 0.7 | <0.5 | <0.5 | <0.5 | <0.5 | <0.5 | <0.5 | <0.5 | <0.5 | <0.5 | <0.5 | <0.5 | 1.1 | 2.2 | <0.5 | <5 | <5 | <5 | 8 | <5 | <5 | | |
| DPS-22 | 25.94172 | 77.41483 | 7.6 | <0.5 | <5 | 2.2 | 1.3 | 2.4 | <0.5 | <0.5 | 20.5 | 3.5 | 18 | 0.9 | <0.5 | <0.5 | <0.5 | <0.5 | <0.5 | 0.5 | 8.6 | 17.6 | 1.8 | 6.7 | 1 | <0.5 | 1 | <0.5 | 0.7 | <0.5 | <0.5 | <0.5 | <0.5 | <0.5 | <0.5 | <0.5 | <0.5 | <0.5 | 2.2 | 3.7 | <0.5 | <5 | 6 | <5 | 8 | <5 | <5 | | |
| DPS-24 | 25.94469 | 77.41544 | 2.8 | <0.5 | <5 | 1.2 | 0.7 | 1 | <0.5 | <0.5 | 10.6 | 2.3 | 3.1 | <0.5 | <0.5 | <0.5 | <0.5 | <0.5 | <0.5 | <0.5 | 7.1 | 13 | 1.7 | 6.9 | 1.6 | <0.5 | 1.5 | <0.5 | 0.6 | <0.5 | <0.5 | <0.5 | <0.5 | <0.5 | <0.5 | <0.5 | <0.5 | <0.5 | <0.5 | 1.4 | 2.4 | <0.5 | <5 | <5 | <5 | 8 | <5 | <5 | |
| DPS-25 | 25.941 | 77.41111 | 3.4 | <0.5 | <5 | 1.2 | 0.7 | 0.9 | <0.5 | <0.5 | 10.5 | 2 | <0.5 | 1.1 | <0.5 | <0.5 | <0.5 | <0.5 | <0.5 | <0.5 | 5.2 | 11.6 | 1.2 | 4.5 | 0.8 | <0.5 | 0.6 | <0.5 | <0.5 | <0.5 | <0.5 | <0.5 | <0.5 | <0.5 | <0.5 | <0.5 | <0.5 | <0.5 | <0.5 | <0.5 | 1.1 | 2.6 | <0.5 | <5 | 6 | <5 | 8 | <5 | <5 |
| DPS-35 | 25.86981 | 77.33383 | 26.7 | 0.6 | <5 | 1.3 | 1.4 | 2.7 | <0.5 | <0.5 | 25.4 | 3.2 | <0.5 | <0.5 | <0.5 | <0.5 | 1.8 | <0.5 | <0.5 | 0.8 | 9.4 | 17.5 | 2 | 7.6 | 1.3 | <0.5 | 1.2 | <0.5 | 0.7 | <0.5 | <0.5 | <0.5 | <0.5 | <0.5 | <0.5 | <0.5 | <0.5 | <0.5 | <0.5 | <0.5 | <0.5 | 2.4 | <0.5 | 18 | <5 | 32 | 15 | 232 | 26 |
| DPS-39 | 25.87694 | 77.32914 | 24.4 | 0.5 | <5 | 2.1 | 2.9 | 3.4 | <0.5 | <0.5 | 42.5 | 5 | <0.5 | <0.5 | <0.5 | <0.5 | 90.2 | <0.5 | <0.5 | 2.3 | 11.3 | 22.1 | 2.5 | 9.7 | 1.9 | <0.5 | 1.7 | <0.5 | 1.1 | <0.5 | 0.6 | <0.5 | 0.6 | <0.5 | 0.8 | <0.5 | <0.5 | <0.5 | <0.5 | <0.5 | <0.5 | 2.7 | <0.5 | 6 | 10 | 12 | 15 | 40 | 57 |
| DPS-41 | 25.88642 | 77.34969 | 62.9 | 1.8 | <5 | 2.3 | 8.1 | 5.7 | <0.5 | <0.5 | 39.4 | 13.4 | 1.5 | <0.5 | <0.5 | <0.5 | 0.8 | <0.5 | <0.5 | 1.4 | 10 | 24 | 3 | 15.3 | 5 | 1.2 | 5.3 | 0.7 | 3.4 | 0.6 | 1.3 | <0.5 | 0.9 | <0.5 | 0.8 | <0.5 | <0.5 | <0.5 | <0.5 | <0.5 | 2.8 | 0.7 | 26 | 10 | 46 | 84 | 99 | 41 | |
| DPS-42 | 25.88894 | 77.35533 | 29 | 0.9 | <5 | 6.4 | 11.6 | 7.7 | <0.5 | <0.5 | 77.9 | 16.2 | 4.1 | <0.5 | <0.5 | <0.5 | <0.5 | <0.5 | <0.5 | 4.4 | 17.1 | 34.9 | 4.1 | 16.7 | 3.6 | 0.8 | 3.6 | 0.5 | 3 | 0.6 | 1.7 | <0.5 | 1.6 | <0.5 | 1 | <0.5 | <0.5 | <0.5 | <0.5 | 7 | 1.6 | 33 | 15 | 28 | 65 | 15 | 80 | | |
| SGP-1 | 25.98769 | 77.40931 | 5.7 | <0.5 | <5 | <0.5 | 0.9 | 1.3 | <0.5 | <0.5 | 15.8 | 1.8 | <0.5 | <0.5 | <0.5 | <0.5 | 1 | <0.5 | <0.5 | <0.5 | 6.3 | 10.9 | 1.4 | 5 | 0.7 | <0.5 | 0.6 | <0.5 | <0.5 | <0.5 | <0.5 | <0.5 | <0.5 | <0.5 | <0.5 | <0.5 | <0.5 | 1 | <0.5 | <0.5 | <0.5 | <0.5 | <5 | <5 | <5 | 8 | 8 | 13 | |
| SGP-2 | 25.90639 | 77.32569 | 5.8 | <0.5 | <5 | <0.5 | 1.2 | 1.4 | <0.5 | <0.5 | 15.6 | 1.6 | 24.6 | <0.5 | <0.5 | <0.5 | <0.5 | <0.5 | <0.5 | <0.5 | 6 | 10.7 | 1.4 | 5 | 0.6 | <0.5 | 0.6 | <0.5 | <0.5 | <0.5 | <0.5 | <0.5 | <0.5 | <0.5 | <0.5 | <0.5 | <0.5 | <0.5 | <0.5 | <0.5 | <0.5 | <5 | <5 | <5 | 8 | <5 | 13 | | |
| DPS-SPG-3 | 25.90303 | 77.33564 | 15.6 | 0.7 | <5 | 3.2 | 5.8 | 6.4 | <0.5 | <0.5 | 79.2 | 12.7 | <0.5 | <0.5 | <0.5 | <0.5 | <0.5 | <0.5 | 3.5 | <0.5 | 2.5 | 23.2 | 54.7 | 5.1 | 19.1 | 4.5 | 0.9 | 4.3 | 0.5 | 2.4 | 0.6 | 1.7 | <0.5 | 1.9 | <0.5 | 5 | <0.5 | <0.5 | <0.5 | <0.5 | 8.3 | 1.5 | | | | | | | |
| DPS-49 | 25.98253 | 77.35892 | 2.7 | <0.5 | <5 | <0.5 | 0.7 | 0.7 | <0.5 | <0.5 | 14.5 | 4.2 | <0.5 | <0.5 | <0.5 | <0.5 | <0.5 | <0.5 | <0.5 | <0.5 | 6.1 | 12.2 | 1.3 | 4.6 | 0.6 | <0.5 | 0.6 | <0.5 | <0.5 | <0.5 | <0.5 | <0.5 | <0.5 | <0.5 | <0.5 | <0.5 | <0.5 | <0.5 | <0.5 | <0.5 | <0.5 | <0.5 | <5 | <5 | <5 | 7 | 20 | 17 | |
| DPS-50 | 25.93856 | 77.35053 | 29.7 | 0.6 | <5 | 1.2 | 5.4 | 3 | <0.5 | <0.5 | 27.9 | 3.5 | <0.5 | <0.5 | <0.5 | <0.5 | <0.5 | <0.5 | <0.5 | 0.9 | 12.5 | 21.1 | 2.7 | 9.6 | 1.7 | <0.5 | 1.5 | <0.5 | 0.8 | <0.5 | <0.5 | <0.5 | <0.5 | <0.5 | <0.5 | <0.5 | <0.5 | <0.5 | <0.5 | <0.5 | 1.7 | <0.5 | 19 | 9 | 62 | 11 | 60 | 25 | |
| DPS-51 | 25.93321 | 77.37539 | 14.6 | <0.5 | <5 | <0.5 | 0.7 | 1.6 | <0.5 | <0.5 | 25.4 | 2.8 | <0.5 | 2.3 | < | | | | | | | | | | | | | | | | | | | | | | | | | | | | | | | | | | |

| sample ID | latitude | longitude | Li | Be | B | Sc | Co | Ga | Ge | Se | Rb | Y | Nb | Mo | Cd | In | Sn | Sb | Te | Cs | La | Ce | Pr | Nd | Sm | Eu | Gd | Tb | Dy | Ho | Er | Tm | Yb | Lu | Hf | Ta | W | Tl | Bi | Th | U | Cu | Ni | Pb | Sr | Zn | Zr | |
|------------|----------|-----------|------|------|------|------|-----|------|------|------|------|------|------|------|------|------|------|------|------|------|------|------|------|-----|------|------|------|------|------|------|------|------|------|------|------|------|------|------|------|------|------|------|-----|----|-----|-----|----|-----|
| DPS-S-85 | 25.92344 | 77.34394 | 96.6 | 0.8 | <5 | 1.2 | 7.5 | 6.7 | <0.5 | <0.5 | 44.9 | 8.6 | <0.5 | <0.5 | <0.5 | <0.5 | 2.6 | <0.5 | <0.5 | 0.9 | 6 | 13.4 | 1.8 | 8 | 2.2 | 0.7 | 2.3 | <0.5 | 1.7 | <0.5 | 0.8 | <0.5 | 0.7 | <0.5 | <0.5 | <0.5 | <0.5 | <0.5 | 0.6 | <0.5 | 44 | 11 | 115 | 28 | 202 | 30 | | |
| DPS-S-85 | 25.92344 | 77.34394 | 96.7 | 0.9 | <5 | 1 | 7.3 | 6.9 | <0.5 | <0.5 | 44.3 | 8.6 | <0.5 | <0.5 | <0.5 | <0.5 | 2.3 | <0.5 | <0.5 | 0.8 | 6.1 | 13.2 | 1.9 | 8 | 2.2 | 0.6 | 2.4 | <0.5 | 1.7 | <0.5 | 0.8 | <0.5 | 0.7 | <0.5 | <0.5 | <0.5 | <0.5 | <0.5 | 0.5 | <0.5 | 43 | 12 | 116 | 29 | 200 | 30 | | |
| DPS-S-86 | 25.94997 | 77.38558 | 8.1 | <0.5 | <5 | <0.5 | 1.7 | 2 | <0.5 | <0.5 | 29.1 | 2.7 | 1.3 | 0.9 | <0.5 | <0.5 | <0.5 | <0.5 | <0.5 | <0.5 | 8.6 | 15.9 | 1.9 | 6.7 | 1 | <0.5 | 0.8 | <0.5 | <0.5 | <0.5 | <0.5 | <0.5 | <0.5 | <0.5 | <0.5 | <0.5 | <0.5 | <0.5 | <0.5 | <5 | <5 | 6 | 12 | <5 | 40 | | | |
| DPS-S-87 | 25.95461 | 77.38317 | 6.4 | <0.5 | <5 | <0.5 | 1.1 | 1.8 | <0.5 | <0.5 | 23.1 | 2.2 | <0.5 | <0.5 | <0.5 | <0.5 | <0.5 | <0.5 | <0.5 | <0.5 | 7.6 | 13.7 | 1.7 | 6.6 | 0.8 | <0.5 | 0.7 | <0.5 | <0.5 | <0.5 | <0.5 | <0.5 | <0.5 | <0.5 | <0.5 | <0.5 | <0.5 | <0.5 | <0.5 | <0.5 | <5 | <5 | 8 | 10 | <5 | 23 | | |
| DPS-S-88 | 25.956 | 77.38219 | 5.6 | <0.5 | <5 | <0.5 | 3.6 | 2.4 | <0.5 | <0.5 | 28.6 | 5.7 | <0.5 | <0.5 | <0.5 | <0.5 | <0.5 | <0.5 | <0.5 | <0.5 | 9.3 | 16.9 | 2.1 | 7.9 | 1.2 | <0.5 | 1.2 | <0.5 | 0.9 | <0.5 | 0.6 | <0.5 | 0.7 | <0.5 | <0.5 | <0.5 | <0.5 | <0.5 | <0.5 | <0.5 | 0.6 | <5 | <5 | 8 | 12 | <5 | 94 | |
| DPS-S-89 | 25.9645 | 77.37197 | 3.7 | <0.5 | <5 | <0.5 | 3.7 | 1.6 | <0.5 | <0.5 | 20 | 3.3 | <0.5 | <0.5 | <0.5 | <0.5 | <0.5 | <0.5 | <0.5 | <0.5 | 7.7 | 13.1 | 1.7 | 6 | 0.9 | <0.5 | 0.7 | <0.5 | 0.5 | <0.5 | <0.5 | <0.5 | <0.5 | <0.5 | <0.5 | <0.5 | <0.5 | <0.5 | <0.5 | <0.5 | <0.5 | <5 | <5 | 5 | 8 | <5 | 46 | |
| DPS-S-90 | 25.96531 | 77.36803 | 2.2 | <0.5 | <5 | <0.5 | 1.7 | 1.4 | <0.5 | <0.5 | 11.2 | 2.1 | <0.5 | <0.5 | <0.5 | <0.5 | <0.5 | <0.5 | <0.5 | <0.5 | 6.2 | 11 | 1.4 | 4.9 | 0.7 | <0.5 | 0.6 | <0.5 | <0.5 | <0.5 | <0.5 | <0.5 | <0.5 | <0.5 | <0.5 | <0.5 | <0.5 | <0.5 | <0.5 | <0.5 | <5 | 5 | 6 | 9 | 6 | 17 | | |
| DPS-S-91 a | 25.95889 | 77.39183 | 24.9 | 0.7 | <5 | 2.6 | 4.3 | 5.5 | <0.5 | <0.5 | 55 | 11.1 | 1 | <0.5 | <0.5 | <0.5 | <0.5 | <0.5 | <0.5 | <0.5 | 1.2 | 11.1 | 21.9 | 2.7 | 10.6 | 3 | 0.7 | 3.7 | <0.5 | 2.1 | <0.5 | 1.1 | <0.5 | 1.1 | <0.5 | <0.5 | <0.5 | <0.5 | 2.1 | 0.9 | 34 | 13 | 13 | 17 | 12 | 171 | | |
| DPS-S-91 b | 25.95889 | 77.39183 | 23.7 | <0.5 | <5 | 2.2 | 4.6 | 5.1 | <0.5 | <0.5 | 50.7 | 13.7 | <0.5 | <0.5 | <0.5 | <0.5 | <0.5 | <0.5 | <0.5 | <0.5 | 1 | 10.4 | 21.5 | 2.8 | 12.2 | 5.2 | 1.2 | 6.9 | 0.7 | 3.2 | 0.5 | 1.3 | <0.5 | 1.1 | <0.5 | <0.5 | <0.5 | <0.5 | <0.5 | <0.5 | 1.8 | 0.8 | 30 | 13 | 10 | 18 | 14 | 166 |
| DPS-S-91 c | 25.95889 | 77.39183 | 17.3 | <0.5 | <5 | 1 | 2.4 | 2.6 | <0.5 | <0.5 | 31.4 | 5.2 | <0.5 | <0.5 | <0.5 | <0.5 | <0.5 | <0.5 | <0.5 | <0.5 | 0.5 | 7.3 | 14.2 | 1.8 | 6.5 | 1.1 | 0.6 | 1.2 | <0.5 | 0.9 | <0.5 | 0.6 | <0.5 | 0.6 | <0.5 | <0.5 | <0.5 | <0.5 | <0.5 | 0.9 | 0.5 | 85 | 7 | 13 | 15 | <5 | 82 | |
| DPS-S-92 | 25.95889 | 77.39183 | 12 | 0.8 | <5 | 2.1 | 3.7 | 5.6 | <0.5 | <0.5 | 71.9 | 10 | 2.2 | <0.5 | <0.5 | <0.5 | <0.5 | <0.5 | <0.5 | <0.5 | 1.3 | 12.1 | 24.8 | 3 | 11.2 | 2 | 0.6 | 2 | <0.5 | 1.6 | <0.5 | 1 | <0.5 | 1.2 | <0.5 | 1 | 9.4 | 1.1 | <0.5 | <0.5 | 2.7 | 1.1 | 25 | 6 | 12 | 21 | 8 | 300 |
| DPS-S-93 | 25.95889 | 77.39183 | 25.9 | 0.9 | <5 | 2.3 | 4 | 5.9 | <0.5 | <0.5 | 57.5 | 6 | <0.5 | <0.5 | <0.5 | <0.5 | <0.5 | <0.5 | <0.5 | <0.5 | 1.6 | 10.2 | 20 | 2.4 | 8.8 | 1.6 | <0.5 | 1.4 | <0.5 | 1 | <0.5 | 0.6 | <0.5 | 0.6 | <0.5 | <0.5 | <0.5 | <0.5 | <0.5 | <0.5 | 1.1 | <0.5 | 44 | 11 | 7 | 17 | 9 | 95 |
| DPS-S-93 | 25.95889 | 77.39183 | 25.5 | 0.8 | <5 | 2.5 | 3.8 | 5.8 | <0.5 | <0.5 | 57.2 | 5.9 | <0.5 | <0.5 | <0.5 | <0.5 | <0.5 | <0.5 | <0.5 | <0.5 | 1.6 | 10.2 | 19.6 | 2.3 | 8.9 | 1.5 | <0.5 | 1.5 | <0.5 | 1 | <0.5 | 0.6 | <0.5 | 0.7 | <0.5 | <0.5 | <0.5 | <0.5 | <0.5 | <0.5 | 1.6 | <0.5 | 43 | 11 | 8 | 17 | 9 | 98 |
| DPS-S-94 | 25.904 | 77.34189 | 32.3 | 0.6 | <5 | 0.5 | 2.2 | 3.9 | <0.5 | <0.5 | 26.1 | 5.6 | 1.6 | <0.5 | <0.5 | <0.5 | <0.5 | <0.5 | <0.5 | <0.5 | 0.8 | 13 | 18.8 | 3.2 | 12.5 | 2.3 | <0.5 | 2.2 | <0.5 | 1.2 | <0.5 | <0.5 | <0.5 | <0.5 | <0.5 | <0.5 | <0.5 | <0.5 | <0.5 | <0.5 | <0.5 | <0.5 | 9 | 8 | 12 | 11 | 86 | 23 |
| DPS-S-95 | 25.92339 | 77.34011 | 6.7 | <0.5 | <5 | 1.7 | 5.8 | 2 | <0.5 | 1.5 | 19.8 | 10.9 | <0.5 | 3.3 | <0.5 | 0.6 | <0.5 | 1.7 | 5 | 1.2 | 6.8 | 16.3 | 2 | 10 | 3.5 | 0.9 | 3.5 | 0.5 | 2.3 | 0.5 | 1.4 | <0.5 | 1.1 | <0.5 | 1.5 | <0.5 | <0.5 | <0.5 | 9.9 | 3.1 | 0.9 | | | | | | | |
| DPS-S-97 | 25.98158 | 77.37286 | 4.3 | <0.5 | <5 | <0.5 | 1.3 | 1.1 | <0.5 | <0.5 | 19.7 | 2.4 | <0.5 | <0.5 | <0.5 | 0.9 | <0.5 | <0.5 | 3.2 | <0.5 | 10.4 | 20.4 | 1.8 | 7.4 | 1.4 | <0.5 | 1.1 | <0.5 | 0.5 | <0.5 | <0.5 | <0.5 | <0.5 | <0.5 | <0.5 | <0.5 | <0.5 | <0.5 | <0.5 | 1.5 | <0.5 | | | | | | | |
| DPS-S-101 | 25.97878 | 77.38625 | 7.5 | <0.5 | <5 | <0.5 | 3 | 2.3 | <0.5 | <0.5 | 31.4 | 3.6 | <0.5 | <0.5 | <0.5 | 0.8 | <0.5 | <0.5 | 1.7 | 0.7 | 13.5 | 26.3 | 2.3 | 8.6 | 1.5 | <0.5 | 1.4 | <0.5 | 0.7 | <0.5 | 0.6 | <0.5 | 0.6 | <0.5 | 0.6 | <0.5 | <0.5 | <0.5 | <0.5 | <0.5 | 2.1 | <0.5 | | | | | | |
| DPS-S-105 | 25.97914 | 77.39761 | 7.5 | <0.5 | <5 | <0.5 | 6.3 | 1.7 | <0.5 | <0.5 | 23.1 | 1.7 | <0.5 | <0.5 | <0.5 | 0.8 | <0.5 | <0.5 | <0.5 | 0.7 | 9 | 17.5 | 1.6 | 6.8 | 1.2 | <0.5 | 0.9 | <0.5 | <0.5 | <0.5 | <0.5 | <0.5 | <0.5 | <0.5 | <0.5 | 0.8 | <0.5 | <0.5 | <0.5 | <0.5 | 1.4 | <0.5 | | | | | | |
| DPS-S-111 | 25.97864 | 77.40094 | 5.4 | <0.5 | <5 | <0.5 | 1.3 | 1.3 | <0.5 | <0.5 | 14.5 | 1.9 | <0.5 | 2.2 | <0.5 | <0.5 | <0.5 | <0.5 | <0.5 | <0.5 | 9.5 | 17.2 | 1.7 | 6.7 | 1.2 | <0.5 | 0.8 | <0.5 | <0.5 | <0.5 | <0.5 | <0.5 | <0.5 | <0.5 | <0.5 | <0.5 | <0.5 | <0.5 | <0.5 | 5.5 | 1.7 | <0.5 | | | | | | |
| DPS-S-114 | 25.92403 | 77.34381 | 220 | 1.8 | <5 | 1.6 | 8.9 | 13.3 | <0.5 | <0.5 | 69.3 | 7 | <0.5 | <0.5 | <0.5 | 0.7 | <0.5 | <0.5 | <0.5 | 1.7 | 5.6 | 13 | 1.7 | 9.4 | 2.8 | 0.8 | 2.8 | <0.5 | 1.6 | <0.5 | 0.9 | <0.5 | 0.7 | <0.5 | 1.7 | <0.5 | <0.5 | <0.5 | <0.5 | <0.5 | 2.3 | 0.5 | | | | | | |
| DPS-S-114 | 25.92403 | 77.34381 | 222 | 1.8 | <5 | 1.1 | 8.7 | 13.4 | <0.5 | <0.5 | 69.5 | 7 | <0.5 | <0.5 | <0.5 | 0.8 | <0.5 | <0.5 | <0.5 | 1.7 | 5.7 | 13 | 1.8 | 9 | 3 | 0.8 | 2.8 | <0.5 | 1.6 | <0.5 | 0.9 | <0.5 | 0.7 | <0.5 | 1.1 | <0.5 | <0.5 | <0.5 | <0.5 | <0.5 | 2.2 | <0.5 | | | | | | |
| DPS-S-115 | 25.91006 | 77.41178 | 12.1 | <0.5 | <0.5 | 1.8 | 1.3 | 3 | <0.5 | <0.5 | 47.4 | 10.7 | 3.3 | <0.5 | <0.5 | <0.5 | <0.5 | <0.5 | <0.5 | <0.5 | 1 | 10.3 | 19.8 | 2.3 | 8.5 | 1.6 | 0.5 | 2.6 | <0.5 | 1.8 | <0.5 | 1.2 | <0.5 | 1.4 | <0.5 | 0.9 | <0.5 | 2.2 | <0.5 | <0.5 | 4.5 | 1.3 | <5 | <5 | 6 | 16 | <5 | 195 |
| DPS-S-121 | 25.93572 | 77.39656 | 24.4 | 1.7 | <0.5 | 4.7 | 4.1 | 8.1 | <0.5 | <0.5 | 82 | 9.1 | 3.9 | <0.5 | <0.5 | <0.5 | <0.5 | <0.5 | <0.5 | <0.5 | 3.9 | 16.4 | 34.7 | 3.8 | 14 | 2.7 | 0.7 | 4 | <0.5 | 1.9 | <0.5 | 1.1 | <0.5 | 1.1 | <0.5 | 2.6 | <0.5 | 0.9 | <0.5 | <0.5 | 8.1 | 1.1 | 21 | 11 | 67 | 23 | 25 | 109 |
| DPS-S-125 | 25.91097 | 77.39808 | 6 | <0.5 | <0.5 | 1 | 4.3 | 1.1 | <0.5 | <0.5 | 3.7 | 1.8 | <0.5 | <0.5 | <0.5 | <0.5 | <0.5 | <0.5 | <0.5 | <0.5 | 5 | 9.1 | 1.1 | 4 | 0.8 | <0.5 | 1 | <0.5 | <0.5 | <0.5 | <0.5 | <0.5 | <0.5 | <0.5 | <0.5 | <0.5 | <0.5 | <0.5 | <0.5 | 1.1 | <0.5 | <5 | 8 | 5 | <5 | 11 | 10 | |
| DPS-S-133 | 25.9595 | 77.37458 | 13 | <0.5 | <0.5 | 2.2 | 9.7 | 3.1 | <0.5 | <0.5 | 34.3 | 10.4 | 2.1 | 0.7 | <0.5 | <0.5 | 0.7 | <0.5 | <0.5 | 1.2 | 7 | 16.4 | 2 | 8.3 | 2.2 | 1 | 2.9 | <0.5 | 2 | <0.5 | 1 | <0.5 | 0.9 | <0.5 | 1.4 | <0.5 | 6.6 | <0.5 | <0.5 | 3.9 | 1.5 | 19 | 12 | 33 | 86 | 24 | 47 | |
| DPS-S-136 | 25.96636 | 77.35811 | 17.1 | 0.5 | <0.5 | <0.5 | 1.6 | 3.2 | <0.5 | <0.5 | 31 | 2.6 | 0.8 | 0.8 | 0.8 | <0.5 | <0.5 | <0.5 | <0.5 | 0.8 | 6.3 | 12.7 | 1.3 | 4.6 | 0.7 | <0.5 | 1.3 | <0.5 | <0.5 | <0.5 | <0.5 | <0.5 | <0.5 | <0.5 | <0.5 | <0.5 | <0.5 | <0.5 | <0.5 | 2.1 | <0.5 | <5 | <5 | 28 | 9 | 15 | 20 | |
| DPS-S-138 | 25.97058 | 77.35675 | 57.4 | 2 | <0.5 | 4.2 | 7.1 | 5.7 | <0.5 | <0.5 | 47.7 | 8.2 | 16.8 | 1.2 | 1.1 | <0.5 | <0.5 | <0.5 | <0.5 | <0.5 | 1.9 | 12 | 28.8 | 4.3 | 20.6 | 5.4 | 1.2 | 5.6 | 0.7 | 2.5 | <0.5 | 1 | <0.5 | 0.6 | <0.5 | 3.6 | <0.5 | <0.5 | <0.5 | <0.5 | 3.5 | <0.5 | 6 | 13 | 30 | 18 | 18 | 29 |
| DPS-S-143 | 25.92633 | 77.32211 | 25.4 | 0.5 | <0.5 | 2.1 | 6.4 | 3.1 | <0.5 | <0.5 | 32.8 | 4.3 | 0.8 | <0.5 | <0.5 | <0.5 | <0.5 | <0.5 | <0.5 | 0.9 | 10 | 19.4 | 2.2 | 7.9 | 1.6 | 0.5 | 2.2 | <0.5 | 1.1 | <0.5 | 0.6 | <0.5 | 0.5 | <0.5 | <0 | | | | | | | | | | | | | |

Annexure 4 Statement Showing co-ordinates & analyses results for major oxides (XRF analysis) of 50 Pit samples

| sample ID | latitude | longitude | Al ₂ O ₃ | BaO | CaO | Cr ₂ O ₃ | Fe(T) | Fe ₂ O ₃ | K ₂ O | MgO | MnO | Na ₂ O | P ₂ O ₅ | SO ₃ | TiO ₂ | SiO ₂ | SrO | V ₂ O ₅ | LOI |
|-----------|----------|-----------|--------------------------------|-------|-------|--------------------------------|-------|--------------------------------|------------------|-------|-------|-------------------|-------------------------------|-----------------|------------------|------------------|-------|-------------------------------|--------|
| DPS -P-14 | 25.92403 | 77.34381 | 2.5 | <0.05 | <0.05 | <0.05 | 1.5 | 2.16 | 1.05 | 0.22 | <0.05 | 0.08 | <0.05 | <0.05 | 0.13 | 92.92 | <0.05 | <0.05 | 0.78 |
| DPS-P-15 | 25.94675 | 77.38669 | 1.94 | <0.05 | <0.05 | <0.05 | 0.5 | 0.74 | 0.83 | 0.08 | <0.05 | 0.08 | <0.05 | <0.05 | 0.13 | 95.62 | <0.05 | <0.05 | 0.42 |
| DPS-P-16 | 25.92669 | 77.33158 | 1.48 | <0.05 | <0.05 | <0.05 | 0.9 | 1.31 | 0.72 | 0.1 | <0.05 | 0.08 | <0.05 | <0.05 | 0.08 | 95.68 | <0.05 | <0.05 | 0.42 |
| DPS-P-17 | 25.96806 | 77.33042 | 1.7 | <0.05 | <0.05 | <0.05 | 0.8 | 1.15 | 0.88 | 0.12 | <0.05 | 0.08 | <0.05 | <0.05 | 0.08 | 95.33 | <0.05 | <0.05 | 0.52 |
| DPS-P-18 | 25.98064 | 77.3345 | 1.44 | <0.05 | <0.05 | 0.06 | 0.9 | 1.35 | 0.68 | 0.1 | <0.05 | 0.08 | <0.05 | <0.05 | 0.07 | 95.68 | <0.05 | <0.05 | 0.46 |
| DPS-P-19 | 25.91836 | 77.32419 | 1.4 | <0.05 | <0.05 | 0.06 | 0.7 | 1.01 | 0.67 | 0.09 | <0.05 | 0.08 | <0.05 | <0.05 | 0.08 | 96.13 | <0.05 | <0.05 | 0.4 |
| DPS-P-20 | 25.90625 | 77.33011 | 2.49 | <0.05 | 0.18 | <0.05 | 1.4 | 1.93 | 0.64 | 0.09 | <0.05 | 0.08 | <0.05 | <0.05 | 0.16 | 93.08 | <0.05 | <0.05 | 1.22 |
| DPS-P-21 | 25.89469 | 77.33383 | 2.08 | <0.05 | <0.05 | 0.06 | 1 | 1.42 | 0.95 | 0.17 | <0.05 | 0.08 | <0.05 | <0.05 | 0.09 | 94.35 | <0.05 | <0.05 | 0.71 |
| DPS-P-21 | 25.89469 | 77.33383 | 2.13 | <0.05 | <0.05 | 0.06 | 1 | 1.45 | 0.92 | 0.19 | <0.05 | 0.08 | <0.05 | <0.05 | 0.08 | 94.32 | <0.05 | <0.05 | 0.68 |
| DPS-P-22 | 25.8865 | 77.33028 | 1.94 | <0.05 | <0.05 | 0.06 | 1.3 | 1.83 | 0.69 | 0.21 | <0.05 | 0.08 | <0.05 | <0.05 | 0.09 | 94.29 | <0.05 | <0.05 | 0.71 |
| DPS-P-23 | 25.9745 | 77.37453 | 1.17 | <0.05 | <0.05 | 0.06 | 0.5 | 0.65 | 0.55 | <0.05 | <0.05 | 0.08 | <0.05 | <0.05 | 0.05 | 97.12 | <0.05 | <0.05 | 0.24 |
| DPS-P-24A | 25.93864 | 77.37139 | 2.094 | <0.05 | <0.05 | 0.074 | 1.1 | 1.626 | 0.83 | 0.196 | <0.05 | 0.083 | <0.05 | <0.05 | 0.098 | 94.25 | <0.05 | <0.05 | 0.58 |
| DPS-P-24B | 25.93864 | 77.37139 | 1.783 | <0.05 | <0.05 | <0.05 | 1.4 | 2.02 | 0.76 | 0.096 | <0.05 | 0.081 | <0.05 | <0.05 | 0.161 | 94.13 | <0.05 | <0.05 | 0.78 |
| DPS-P-25A | 25.91239 | 77.37639 | 1.374 | <0.05 | <0.05 | 0.068 | 0.6 | 0.922 | 0.7 | <0.05 | <0.05 | 0.082 | <0.05 | <0.05 | 0.07 | 96.12 | <0.05 | <0.05 | 0.53 |
| DPS-P-25B | 25.91239 | 77.37639 | 1.317 | <0.05 | <0.05 | <0.05 | 0.5 | 0.781 | 0.57 | <0.05 | <0.05 | 0.083 | <0.05 | <0.05 | 0.098 | 96.75 | <0.05 | <0.05 | 0.25 |
| DPS-P-2A | 25.88105 | 77.33981 | 2.065 | <0.05 | <0.05 | 0.062 | 1.1 | 1.546 | 0.83 | 0.211 | <0.05 | 0.082 | <0.05 | <0.05 | 0.095 | 94.33 | <0.05 | <0.05 | 0.65 |
| DPS-P-2B | 25.88105 | 77.33981 | 1.736 | <0.05 | <0.05 | <0.05 | 1.7 | 2.446 | 0.81 | 0.092 | <0.05 | 0.083 | <0.05 | <0.05 | 0.158 | 93.84 | <0.05 | <0.05 | 0.65 |
| DPS-P-6A | 25.93273 | 77.34441 | 1.719 | <0.05 | <0.05 | <0.05 | 1 | 1.458 | 0.75 | 0.132 | <0.05 | 0.083 | <0.05 | <0.05 | 0.08 | 95.01 | <0.05 | <0.05 | 0.64 |
| DPS-P-8A | 25.92189 | 77.34556 | 1.215 | <0.05 | <0.05 | <0.05 | 0.8 | 1.11 | 0.71 | 0.102 | <0.05 | 0.082 | <0.05 | <0.05 | 0.073 | 96.08 | <0.05 | <0.05 | 0.5 |
| DPS-P-8B | 25.92189 | 77.34556 | 1.147 | <0.05 | 0.403 | 0.073 | 0.9 | 1.266 | 0.75 | <0.05 | <0.05 | 0.082 | <0.05 | <0.05 | 0.075 | 95.51 | <0.05 | <0.05 | 0.55 |
| DPS-P-10A | 25.92277 | 77.3446 | 2.217 | <0.05 | 26.17 | <0.05 | 3.7 | 5.301 | 0.85 | 10.82 | 0.39 | <0.08 | <0.05 | 0.076 | 0.175 | 19.63 | <0.05 | <0.05 | 33.91 |
| DPS-P-10A | 25.92277 | 77.3446 | 2.185 | <0.05 | 26.16 | <0.05 | 3.7 | 5.32 | 0.82 | 10.78 | 0.37 | <0.08 | <0.05 | 0.072 | 0.1662 | 19.66 | <0.05 | <0.05 | 33.954 |
| DPS-P-10B | 25.92277 | 77.3446 | 4.678 | <0.05 | 19.12 | <0.05 | 3.6 | 5.202 | 2.13 | 1.905 | 0.14 | <0.08 | <0.05 | <0.05 | 0.22 | 48.28 | <0.05 | <0.05 | 18.05 |
| DPS-P-11A | 25.92275 | 77.34331 | 2.214 | <0.05 | 27.92 | <0.05 | 4.4 | 6.247 | 0.76 | 11.74 | 0.43 | <0.08 | <0.05 | 0.095 | 0.161 | 13.69 | <0.05 | <0.05 | 36.59 |
| DPS-P-15A | 25.94675 | 77.38669 | 1.173 | <0.05 | 0.055 | 0.152 | 1 | 1.493 | 0.62 | 0.071 | <0.05 | 0.082 | <0.05 | <0.05 | 0.083 | 96.01 | <0.05 | <0.05 | 0.18 |
| DPS-P-16A | 25.92669 | 77.33158 | 1.127 | <0.05 | 0.311 | <0.05 | 1 | 1.482 | 0.69 | 0.206 | <0.05 | 0.081 | <0.05 | <0.05 | 0.088 | 94.94 | <0.05 | <0.05 | 0.97 |
| DPS-P-17A | 25.96806 | 77.33042 | 1.602 | <0.05 | <0.05 | 0.134 | 1.4 | 1.935 | 0.77 | 0.147 | <0.05 | 0.082 | <0.05 | <0.05 | 0.078 | 94.81 | <0.05 | <0.05 | 0.35 |
| DPS-P-18A | 25.98064 | 77.3345 | 0.927 | <0.05 | 0.13 | <0.05 | 0.7 | 1.027 | 0.63 | 0.054 | <0.05 | 0.082 | <0.05 | <0.05 | 0.074 | 96.6 | <0.05 | <0.05 | 0.35 |
| DPS-P-19A | 25.91836 | 77.32419 | 1.636 | <0.05 | 0.088 | <0.05 | 1.6 | 2.291 | 0.8 | 0.182 | <0.05 | 0.081 | <0.05 | <0.05 | 0.09 | 93.91 | <0.05 | <0.05 | 0.82 |
| DPS-P-19B | 25.90625 | 77.33011 | 2.043 | <0.05 | 0.09 | 0.062 | 1 | 1.495 | 0.98 | 0.145 | <0.05 | 0.083 | <0.05 | <0.05 | 0.148 | 94.09 | <0.05 | <0.05 | 0.75 |

| | | | | | | | | | | | | | | | | | | | |
|------------|----------|----------|-------|-------|-------|-------|-----|-------|------|-------|-------|-------|-------|-------|--------|-------|-------|-------|--------|
| DPS-P-20A | 25.90625 | 77.33011 | 1.271 | <0.05 | <0.05 | 0.117 | 1.2 | 1.776 | 0.69 | 0.098 | <0.05 | 0.082 | <0.05 | <0.05 | 0.086 | 95.38 | <0.05 | <0.05 | 0.41 |
| DPS-P-21A | 25.89469 | 77.33383 | 1.763 | <0.05 | <0.05 | <0.05 | 1.7 | 2.376 | 0.79 | 0.16 | <0.05 | 0.083 | <0.05 | <0.05 | 0.09 | 93.86 | <0.05 | <0.05 | 0.74 |
| DPS-P-21A | 25.89469 | 77.33383 | 1.735 | <0.05 | <0.05 | <0.05 | 1.7 | 2.404 | 0.8 | 0.166 | <0.05 | 0.086 | <0.05 | <0.05 | 0.0911 | 93.83 | <0.05 | <0.05 | 0.7597 |
| DPS-P-23A | 25.9745 | 77.37453 | 1.222 | <0.05 | <0.05 | 0.169 | 1.3 | 1.852 | 0.61 | 0.073 | <0.05 | 0.082 | <0.05 | <0.05 | 0.063 | 95.67 | <0.05 | <0.05 | 0.15 |
| DPS-P1(A) | 25.93381 | 77.32366 | 2.16 | <0.05 | 0.1 | <0.05 | 1.1 | 1.53 | 1.03 | 0.27 | <0.05 | 0.08 | 0.07 | <0.05 | 0.09 | 93.74 | <0.05 | <0.05 | 0.83 |
| DPS-P1(B) | 25.93381 | 77.32366 | 2.54 | <0.05 | 0.14 | 0.08 | 1.7 | 2.38 | 1.27 | 0.44 | <0.05 | 0.08 | 0.05 | <0.05 | 0.1 | 91.79 | <0.05 | <0.05 | 1.04 |
| DPS-P2 | 25.88105 | 77.33981 | 1.06 | <0.05 | <0.05 | <0.05 | 0.8 | 1.13 | 0.5 | <0.05 | <0.05 | 0.08 | <0.05 | <0.05 | 0.08 | 96.55 | <0.05 | <0.05 | 0.48 |
| DPS-P3(A) | 25.90419 | 77.34182 | 2.65 | <0.05 | <0.05 | <0.05 | 1.4 | 2 | 1.32 | 0.19 | <0.05 | 0.08 | <0.05 | <0.05 | 0.15 | 92.41 | <0.05 | <0.05 | 1.09 |
| DPS-P3(B) | 25.90419 | 77.34182 | 2.08 | <0.05 | <0.05 | <0.05 | 0.7 | 1.06 | 0.87 | 0.14 | <0.05 | 0.08 | <0.05 | <0.05 | 0.09 | 94.79 | <0.05 | <0.05 | 0.8 |
| DPS-P4(A) | 25.98042 | 77.34297 | 2.68 | <0.05 | <0.05 | <0.05 | 1.7 | 2.4 | 0.97 | 0.37 | <0.05 | 0.08 | <0.05 | <0.05 | 0.12 | 92.1 | <0.05 | <0.05 | 1.13 |
| DPS-P4(B) | 25.98042 | 77.34297 | 2.33 | <0.05 | <0.05 | <0.05 | 1.1 | 1.63 | 0.78 | 0.19 | <0.05 | 0.08 | <0.05 | <0.05 | 0.09 | 93.88 | <0.05 | <0.05 | 0.9 |
| DPS-P5(A) | 25.94915 | 77.34286 | 1.89 | <0.05 | <0.05 | <0.05 | 1 | 1.42 | 0.97 | 0.09 | <0.05 | <0.08 | <0.05 | <0.05 | 0.11 | 91.62 | <0.05 | <0.05 | 3.72 |
| DPS-P5(B) | 25.94915 | 77.34286 | 1.64 | <0.05 | <0.05 | <0.05 | 0.8 | 1.16 | 0.7 | 0.09 | <0.05 | 0.08 | <0.05 | <0.05 | 0.08 | 95.54 | <0.05 | <0.05 | 0.62 |
| DPS-P6 | 25.93273 | 77.34441 | 1.87 | <0.05 | 0.09 | <0.05 | 0.8 | 1.16 | 0.97 | 0.1 | <0.05 | 0.08 | <0.05 | <0.05 | 0.14 | 94.8 | <0.05 | <0.05 | 0.64 |
| DPS-P6 | 25.93273 | 77.34441 | 1.91 | <0.05 | 0.09 | <0.05 | 0.8 | 1.17 | 0.98 | 0.09 | <0.05 | 0.08 | <0.05 | <0.05 | 0.14 | 94.87 | <0.05 | <0.05 | 0.52 |
| DPS-P7(A) | 25.93429 | 77.35821 | 1.73 | <0.05 | <0.05 | <0.05 | 0.8 | 1.2 | 0.84 | 0.16 | <0.05 | 0.08 | <0.05 | <0.05 | 0.08 | 95.23 | <0.05 | <0.05 | 0.58 |
| DPS-P7(B) | 25.93429 | 77.35821 | 2.18 | <0.05 | <0.05 | <0.05 | 1.5 | 2.08 | 1 | 0.29 | <0.05 | 0.08 | <0.05 | <0.05 | 0.1 | 93.22 | <0.05 | <0.05 | 0.93 |
| DPS-P8 | 25.92189 | 77.34556 | 1.26 | <0.05 | 0.59 | <0.05 | 0.9 | 1.27 | 0.78 | 0.07 | <0.05 | 0.08 | <0.05 | <0.05 | 0.08 | 94.96 | <0.05 | <0.05 | 0.8 |
| DPS-P9 | 25.98543 | 77.37616 | 1.77 | <0.05 | <0.05 | <0.05 | 1.1 | 1.61 | 0.43 | <0.05 | <0.05 | 0.08 | <0.05 | <0.05 | 0.11 | 95 | <0.05 | <0.05 | 0.84 |
| DPS-P10 | 25.92277 | 77.3446 | 1.81 | <0.05 | 0.73 | <0.05 | 1 | 1.47 | 0.9 | 0.15 | <0.05 | 0.08 | 0.54 | <0.05 | 0.16 | 93.24 | <0.05 | <0.05 | 0.79 |
| DPS-P11(A) | 25.92275 | 77.34331 | 1.95 | <0.05 | <0.05 | <0.05 | 0.6 | 0.82 | 0.95 | 0.1 | <0.05 | 0.08 | <0.05 | <0.05 | 0.1 | 95.13 | <0.05 | <0.05 | 0.76 |
| DPS-P11(B) | 25.92275 | 77.34331 | 4.03 | <0.05 | 30.77 | <0.05 | 1.9 | 2.65 | 1.53 | 1.06 | 0.19 | <0.08 | <0.05 | <0.05 | 0.28 | 33.68 | <0.05 | <0.05 | 25.61 |
| DPS-P12 | 25.89561 | 77.37637 | 1.67 | <0.05 | 0.32 | <0.05 | 0.9 | 1.21 | 0.65 | 0.08 | <0.05 | 0.08 | <0.05 | <0.05 | 0.09 | 94.88 | <0.05 | <0.05 | 0.92 |
| PIT-13 | 25.96806 | 77.33042 | 1.44 | <0.05 | <0.05 | <0.05 | 0.7 | 1.06 | 0.79 | 0.08 | <0.05 | 0.08 | <0.05 | <0.05 | 0.11 | 95.76 | <0.05 | <0.05 | 0.49 |

Annexure 5 Statement Showing analyses results for major oxides (XRF analysis) of 53 Core samples

| Sample Id | Borehole ID | Depth from | Depth to | Al2O3 | BaO | CaO | Cr2O3 | Fe (T) | Fe2O3 | K2O | MgO | MnO | Na2O | P2O5 | SO3 | TiO2 | SiO2 | SrO | V2O5 | LOI |
|------------|-------------|------------|----------|--------|-------|-------|-------|--------|-------|------|--------|-------|-------|-------|-------|------|-------|-------|-------|-------|
| DPS-BH1-1 | DPS/BH/01 | 4m | 5m | 4.61 | <0.05 | 0.24 | <0.05 | 2.16 | 3.09 | 1.74 | 0.53 | <0.05 | 0.08 | <0.05 | <0.05 | 0.3 | 86.94 | <0.05 | <0.05 | 2.31 |
| DPS-BH1-2 | DPS/BH/01 | 5m | 6m | 9.67 | <0.05 | 0.2 | <0.05 | 2.98 | 4.26 | 3.25 | 0.92 | <0.05 | <0.08 | <0.05 | <0.05 | 0.65 | 76.84 | <0.05 | <0.05 | 3.94 |
| DPS-BH1-3 | DPS/BH/01 | 6m | 7m | 4.98 | <0.05 | 0.12 | <0.05 | 2.5 | 3.57 | 1.8 | 0.59 | <0.05 | 0.08 | <0.05 | <0.05 | 0.34 | 85.86 | <0.05 | <0.05 | 2.47 |
| DPS-BH1-4 | DPS/BH/01 | 7m | 8m | 6.72 | <0.05 | 0.1 | <0.05 | 2.25 | 3.22 | 2.43 | 0.76 | <0.05 | 0.08 | <0.05 | <0.05 | 0.42 | 83.36 | <0.05 | <0.05 | 2.72 |
| DPS-BH1-5 | DPS/BH/01 | 8m | 9m | 7.73 | <0.05 | 0.23 | <0.05 | 2.25 | 3.22 | 2.95 | 0.93 | <0.05 | <0.08 | 0.07 | <0.05 | 0.53 | 81.09 | <0.05 | <0.05 | 3.05 |
| DPS-BH1-6 | DPS/BH/01 | 9m | 10m | 7.27 | <0.05 | 0.88 | <0.05 | 2.43 | 3.47 | 2.78 | 0.94 | <0.05 | <0.08 | 0.07 | 0.1 | 0.46 | 80.41 | <0.05 | <0.05 | 3.43 |
| DPS-BH1-7 | DPS/BH/01 | 10m | 11m | 6.54 | <0.05 | 10.34 | <0.05 | 3.89 | 5.56 | 2.3 | 6.63 | 0.12 | <0.08 | 0.08 | 0.63 | 0.44 | 50.38 | <0.05 | <0.05 | 16.82 |
| DPS-BH1-16 | DPS/BH/01 | 11m | 12m | 7.787 | <0.05 | 12.71 | <0.05 | 4.835 | 6.912 | 2.52 | 9.185 | 0.092 | <0.08 | 0.093 | 1.445 | 0.55 | 36.84 | <0.05 | <0.05 | 21.72 |
| DPS-BH1-17 | DPS/BH/01 | 12m | 13m | 5.281 | <0.05 | 19.02 | <0.05 | 4.004 | 5.724 | 1.81 | 12.249 | 0.192 | <0.08 | 0.061 | 1.453 | 0.38 | 23.41 | <0.05 | <0.05 | 30.3 |
| DPS-BH1-8 | DPS/BH/01 | 13.5m | 14.5m | 8.07 | <0.05 | 12.23 | <0.05 | 4.32 | 6.18 | 2.87 | 8.74 | 0.1 | <0.08 | 0.1 | 1.1 | 0.57 | 39.17 | <0.05 | <0.05 | 20.72 |
| DPS-BH1-18 | DPS/BH/01 | 14.5m | 15.5m | 6.425 | <0.05 | 16.46 | <0.05 | 3.788 | 5.416 | 2.38 | 10.557 | 0.205 | <0.08 | 0.066 | 1.162 | 0.43 | 30.17 | <0.05 | <0.05 | 26.57 |
| DPS-BH1-19 | DPS/BH/01 | 15.5m | 16.5m | 5.837 | <0.05 | 17.56 | <0.05 | 3.615 | 5.169 | 2.12 | 11.125 | 0.208 | <0.08 | 0.058 | 1.429 | 0.35 | 27.66 | <0.05 | <0.05 | 28.35 |
| DPS-BH1-9 | DPS/BH/01 | 16.5m | 17.5m | 4.32 | <0.05 | 2.32 | <0.05 | 1.35 | 1.93 | 1.98 | 1.55 | <0.05 | <0.08 | <0.05 | 0.29 | 0.3 | 82.68 | <0.05 | <0.05 | 4.37 |
| DPS-BH1-10 | DPS/BH/01 | 18m | 19m | 1.46 | <0.05 | <0.05 | 0.05 | 0.52 | 0.75 | 0.73 | 0.08 | <0.05 | 0.08 | <0.05 | 0.05 | 0.08 | 96.38 | <0.05 | <0.05 | 0.26 |
| DPS-BH1-10 | DPS/BH/01 | 18m | 19m | 1.43 | <0.05 | <0.05 | 0.05 | 0.51 | 0.72 | 0.7 | 0.09 | <0.05 | 0.09 | <0.05 | 0.05 | 0.08 | 96.46 | <0.05 | <0.05 | 0.25 |
| DPS-BH1-11 | DPS/BH/01 | 19.5m | 20.5m | 1.7 | <0.05 | <0.05 | <0.05 | 0.53 | 0.76 | 0.84 | 0.09 | <0.05 | 0.08 | <0.05 | 0.1 | 0.08 | 95.83 | <0.05 | <0.05 | 0.39 |
| DPS-BH1-12 | DPS/BH/01 | 21m | 22m | 1.37 | <0.05 | 0.85 | 0.05 | 0.67 | 0.95 | 0.74 | 0.45 | <0.05 | 0.08 | <0.05 | 0.13 | 0.07 | 93.74 | <0.05 | <0.05 | 1.49 |
| DPS-BH1-13 | DPS/BH/01 | 22.50m | 23.5m | 1.97 | <0.05 | 0.47 | 0.06 | 0.8 | 1.15 | 1.08 | 0.32 | <0.05 | 0.08 | <0.05 | 0.22 | 0.12 | 93.53 | <0.05 | <0.05 | 0.93 |
| DPS-BH1-14 | DPS/BH/01 | 24m | 25m | 2.75 | <0.05 | 0.19 | <0.05 | 0.65 | 0.92 | 1.42 | 0.26 | <0.05 | 0.08 | <0.05 | 0.13 | 0.21 | 93.12 | <0.05 | <0.05 | 0.78 |
| DPS-BH1-20 | DPS/BH/01 | 25m | 26m | 10.775 | <0.05 | 0.302 | <0.05 | 1.821 | 2.604 | 4.4 | 1.034 | <0.05 | 0.198 | 0.071 | 0.334 | 0.9 | 76.75 | <0.05 | <0.05 | 2.45 |
| DPS-BH1-21 | DPS/BH/01 | 26m | 27m | 4.373 | <0.05 | 0.248 | 0.054 | 1.141 | 1.632 | 1.99 | 0.436 | <0.05 | 0.081 | <0.05 | 0.096 | 0.31 | 89.64 | <0.05 | <0.05 | 0.98 |
| DPS-BH1-15 | DPS/BH/01 | 27m | 28m | 6.89 | <0.05 | 0.52 | <0.05 | 1.19 | 1.7 | 3.18 | 0.75 | <0.05 | 0.22 | 0.05 | 0.07 | 0.7 | 83.65 | <0.05 | <0.05 | 2.07 |
| DPS-BH1-22 | DPS/BH/01 | 28m | 29m | 6.68 | <0.05 | 0.266 | 0.06 | 1.389 | 1.986 | 2.7 | 0.707 | <0.05 | 0.115 | <0.05 | <0.05 | 0.45 | 85.36 | <0.05 | <0.05 | 1.47 |
| DPS-BH1-23 | DPS/BH/01 | 29m | 30m | 10.921 | <0.05 | 0.174 | <0.05 | 2.239 | 3.201 | 3.93 | 1.128 | <0.05 | 0.18 | <0.05 | 0.333 | 0.71 | 76.83 | <0.05 | <0.05 | 2.36 |
| DPS-BH1-24 | DPS/BH/01 | 30m | 31m | 6.967 | <0.05 | 0.15 | 0.063 | 1.607 | 2.298 | 2.73 | 0.706 | <0.05 | 0.095 | <0.05 | 0.287 | 0.47 | 84.64 | <0.05 | <0.05 | 1.42 |
| DPS-BH1-25 | DPS/BH/01 | 31m | 32m | 9.647 | <0.05 | 0.109 | 0.072 | 2.249 | 3.215 | 3.55 | 0.971 | <0.05 | 0.153 | <0.05 | 0.561 | 0.66 | 78.92 | <0.05 | <0.05 | 1.98 |
| DPS-BH1-25 | DPS/BH/01 | 31m | 32m | 9.641 | <0.05 | 0.119 | 0.062 | 2.24 | 3.203 | 3.53 | 0.991 | <0.05 | 0.173 | <0.05 | 0.531 | 0.64 | 78.89 | <0.05 | <0.05 | 2.04 |
| DPS-BH1-26 | DPS/BH/01 | 32m | 33m | 5.658 | <0.05 | 0.19 | 0.068 | 1.872 | 2.676 | 2.19 | 0.7 | <0.05 | 0.081 | <0.05 | 0.118 | 0.37 | 86.6 | <0.05 | <0.05 | 1.17 |
| DPS-BH1-27 | DPS/BH/01 | 33m | 34m | 6.667 | <0.05 | 0.115 | 0.076 | 1.982 | 2.833 | 2.48 | 0.724 | <0.05 | 0.081 | <0.05 | 0.121 | 0.43 | 84.99 | <0.05 | <0.05 | 1.32 |
| DPS-BH2-1 | DPS/BH/02 | 2m | 3m | 2.87 | <0.05 | 0.17 | <0.05 | 1.92 | 2.75 | 1.04 | 0.32 | <0.05 | 0.08 | <0.05 | <0.05 | 0.19 | 90.81 | <0.05 | <0.05 | 1.63 |

| Sample Id | Borehole ID | Depth from | Depth to | Al2O3 | BaO | CaO | Cr2O3 | Fe (T) | Fe2O3 | K2O | MgO | MnO | Na2O | P2O5 | SO3 | TiO2 | SiO2 | SrO | V2O5 | LOI |
|------------|-------------|------------|----------|--------|-------|-------|-------|--------|-------|------|--------|-------|-------|-------|-------|------|-------|-------|-------|-------|
| DPS-BH2-2 | DPS/BH/02 | 3m | 4m | 2.3 | <0.05 | 0.13 | <0.05 | 1.54 | 2.21 | 0.89 | 0.24 | <0.05 | 0.08 | <0.05 | <0.05 | 0.16 | 92.55 | <0.05 | <0.05 | 1.32 |
| DPS-BH2-3 | DPS/BH/02 | 4m | 5m | 2.41 | <0.05 | 0.11 | <0.05 | 1.62 | 2.32 | 1.06 | 0.28 | <0.05 | 0.08 | <0.05 | <0.05 | 0.16 | 92.14 | <0.05 | <0.05 | 1.29 |
| DPS-BH2-4 | DPS/BH/02 | 5m | 6m | 3.04 | <0.05 | 0.12 | <0.05 | 1.98 | 2.83 | 1.17 | 0.32 | <0.05 | 0.26 | <0.05 | <0.05 | 0.2 | 90.23 | <0.05 | <0.05 | 1.65 |
| DPS-BH2-5 | DPS/BH/02 | 6m | 7m | 2.54 | <0.05 | 0.09 | <0.05 | 1.7 | 2.43 | 1.08 | 0.3 | <0.05 | 0.09 | <0.05 | <0.05 | 0.16 | 91.95 | <0.05 | <0.05 | 1.2 |
| DPS-BH2-5 | DPS/BH/02 | 6m | 7m | 2.59 | <0.05 | 0.08 | <0.05 | 1.67 | 2.39 | 1.06 | 0.32 | <0.05 | 0.08 | <0.05 | <0.05 | 0.16 | 91.92 | <0.05 | <0.05 | 1.28 |
| DPS-BH2-6 | DPS/BH/02 | 7m | 8m | 3.02 | <0.05 | 0.15 | 0.07 | 2.19 | 3.13 | 1.15 | 0.27 | <0.05 | 0.08 | <0.05 | <0.05 | 0.2 | 90.28 | <0.05 | <0.05 | 1.53 |
| DPS-BH2-7 | DPS/BH/02 | 8m | 9m | 2.84 | <0.05 | 0.13 | <0.05 | 2.07 | 2.96 | 0.97 | 0.29 | <0.05 | 0.08 | <0.05 | <0.05 | 0.18 | 90.88 | <0.05 | <0.05 | 1.53 |
| DPS-BH2-8 | DPS/BH/02 | 9.5m | 10.5m | 4.71 | <0.05 | 0.06 | 0.08 | 1.79 | 2.57 | 1.9 | 0.57 | <0.05 | 0.08 | <0.05 | <0.05 | 0.3 | 88.06 | <0.05 | <0.05 | 1.57 |
| DPS-BH2-9 | DPS/BH/02 | 10.5m | 11.5m | 9.59 | <0.05 | 0.18 | <0.05 | 2.58 | 3.69 | 3.39 | 1.22 | <0.05 | <0.08 | 0.06 | <0.05 | 0.63 | 77.6 | <0.05 | <0.05 | 3.38 |
| DPS-BH2-16 | DPS/BH/02 | 11.5m | 12m | 9.523 | <0.05 | 0.131 | 0.079 | 2.898 | 4.143 | 3.44 | 0.925 | <0.05 | <0.08 | 0.061 | 0.084 | 0.64 | 77.91 | <0.05 | <0.05 | 2.86 |
| DPS-BH2-10 | DPS/BH/02 | 12m | 13m | 7.93 | <0.05 | 12.73 | <0.05 | 4.44 | 6.35 | 2.67 | 8.22 | 0.15 | <0.08 | 0.09 | 0.64 | 0.53 | 39.61 | <0.05 | <0.05 | 20.93 |
| DPS-BH2-17 | DPS/BH/02 | 13m | 14m | 7.784 | <0.05 | 11.98 | <0.05 | 4.83 | 6.906 | 2.57 | 8.668 | 0.088 | <0.08 | 0.092 | 1.321 | 0.52 | 39.43 | <0.05 | <0.05 | 20.46 |
| DPS-BH2-18 | DPS/BH/02 | 14m | 15m | 5.073 | <0.05 | 19.03 | <0.05 | 3.697 | 5.285 | 1.74 | 12.128 | 0.186 | <0.08 | 0.053 | 1.141 | 0.34 | 25.19 | <0.05 | <0.05 | 29.72 |
| DPS-BH2-11 | DPS/BH/02 | 15m | 16m | 7.64 | <0.05 | 12.91 | <0.05 | 4.22 | 6.03 | 2.66 | 8.96 | 0.1 | <0.08 | 0.09 | 1.19 | 0.51 | 38.36 | <0.05 | <0.05 | 21.41 |
| DPS-BH2-19 | DPS/BH/02 | 16m | 16.5m | 10.127 | <0.05 | 9.171 | <0.05 | 3.526 | 5.041 | 3.87 | 6.885 | 0.067 | 0.148 | 0.11 | 0.724 | 0.66 | 47.17 | <0.05 | <0.05 | 15.9 |
| DPS-BH2-12 | DPS/BH/02 | 16.5m | 17.50m | 4.9 | <0.05 | 19.06 | <0.05 | 3.7 | 5.29 | 1.83 | 11.7 | 0.29 | 0.25 | <0.05 | 1.3 | 0.33 | 25.09 | <0.05 | <0.05 | 29.83 |
| DPS-BH2-20 | DPS/BH/02 | 17.5m | 18.5m | 5.741 | <0.05 | 15.04 | 0.053 | 3.308 | 4.73 | 2.11 | 9.632 | 0.156 | <0.08 | 0.058 | 1.342 | 0.34 | 36.7 | <0.05 | <0.05 | 23.99 |
| DPS-BH2-13 | DPS/BH/02 | 18.5m | 19.5m | 2.95 | <0.05 | 3.57 | 0.05 | 1.68 | 2.4 | 1.46 | 2.02 | <0.05 | <0.08 | <0.05 | 0.22 | 0.23 | 81.27 | <0.05 | <0.05 | 5.6 |
| DPS-BH2-14 | DPS/BH/02 | 19.5m | 20.5m | 4.91 | <0.05 | 0.16 | 0.07 | 1.05 | 1.5 | 2.26 | 0.48 | <0.05 | 0.13 | <0.05 | 0.08 | 0.41 | 88.55 | <0.05 | <0.05 | 1.27 |
| DPS-BH2-15 | DPS/BH/02 | 23m | 24m | 2.22 | <0.05 | 1.79 | 0.06 | 1.39 | 1.99 | 0.95 | 1.02 | <0.05 | 0.08 | <0.05 | 0.4 | 0.13 | 88.41 | <0.05 | <0.05 | 2.88 |
| DPS-BH2-15 | DPS/BH/02 | 23m | 24m | 2.2 | <0.05 | 1.76 | 0.05 | 1.37 | 1.96 | 0.99 | 1.01 | <0.05 | 0.09 | <0.05 | 0.43 | 0.13 | 88.37 | <0.05 | <0.05 | 2.92 |
| DPS-BH2-21 | DPS/BH/02 | 20.5m | 21.5m | 7.395 | <0.05 | 0.105 | 0.074 | 1.663 | 2.378 | 2.91 | 0.74 | <0.05 | 0.081 | 0.054 | 0.082 | 0.5 | 84.11 | <0.05 | <0.05 | 1.45 |
| DPS-BH2-22 | DPS/BH/02 | 21.5m | 22.5m | 7 | <0.05 | 0.397 | 0.083 | 1.393 | 1.991 | 2.73 | 0.806 | <0.05 | 0.08 | <0.05 | 0.118 | 0.49 | 84.25 | <0.05 | <0.05 | 1.9 |
| DPS-BH2-23 | DPS/BH/02 | 22.5m | 23m | 3.24 | <0.05 | 2.217 | 0.09 | 1.686 | 2.411 | 1.32 | 1.333 | <0.05 | <0.08 | <0.05 | 0.25 | 0.18 | 85.05 | <0.05 | <0.05 | 3.74 |
| DPS-BH2-23 | DPS/BH/02 | 22.5m | 23m | 3.259 | <0.05 | 2.236 | 0.109 | 1.671 | 2.389 | 1.3 | 1.303 | <0.05 | <0.08 | <0.05 | 0.289 | 0.16 | 85 | <0.05 | <0.05 | 3.77 |
| DPS-BH2-24 | DPS/BH/02 | 27m | 28m | 11.47 | <0.05 | 0.15 | <0.05 | 1.673 | 2.392 | 4.75 | 0.999 | <0.05 | 0.227 | 0.088 | 0.215 | 0.97 | 76.41 | <0.05 | <0.05 | 2.15 |
| DPS-BH2-25 | DPS/BH/02 | 28m | 29m | 9.411 | <0.05 | 0.176 | <0.05 | 1.702 | 2.434 | 3.91 | 0.854 | <0.05 | 0.217 | 0.061 | 0.096 | 0.84 | 80.02 | <0.05 | <0.05 | 1.77 |
| DPS-BH2-26 | DPS/BH/02 | 29m | 30m | 7.012 | <0.05 | 0.152 | 0.064 | 1.325 | 1.895 | 2.89 | 0.658 | <0.05 | 0.115 | <0.05 | 0.08 | 0.5 | 85.06 | <0.05 | <0.05 | 1.39 |

Annexure 6 Statement Showing analyses results for REE & Trace Elements (ICPMS analysis) of 36 Core samples

| Sample Id | Borehole ID | Depth from | Depth to | C u | Ni | P b | Sr | Zn | Zr | Li | Be | B | Sc | Co | G a | Ge | Se | Rb | Y | Nb | Mo | Cd | In | Sn | Sb | Te | Cs | La | Ce | Pr | Nd | S m | Eu | Gd | Tb | Dy | Ho | Er | Tm | Yb | Lu | Hf | Ta | W | Tl | Bi | Th | U |
|------------|-------------|------------|----------|-----|----|-----|-----|------|------|------|------|----|------|-----|-----|------|------|----|-----|------|------|------|------|------|------|------|------|------|------|-----|------|-----|------|-----|------|------|------|------|------|------|------|------|------|------|------|------|------|------|
| DPS-BH1-1 | DPS/BH/01 | 4m | 5m | 9 | 13 | 44 | 20 | 1289 | 29.7 | 29.1 | 1.1 | <5 | 5.3 | 9.5 | 7 | <0.5 | <0.5 | 63 | 11 | 3.1 | <0.5 | <0.5 | <0.5 | <0.5 | <0.5 | <0.5 | 3 | 17.4 | 35.9 | 4.3 | 16.5 | 3.9 | 0.7 | 2.9 | <0.5 | 2.3 | <0.5 | 1.4 | <0.5 | 1.1 | <0.5 | 3.5 | <0.5 | 0.5 | 1 | <0.5 | 2.2 | 1.1 |
| DPS-BH1-2 | DPS/BH/01 | 5m | 6m | 16 | 16 | 30 | 37 | 1416 | 164 | 26.4 | 1.3 | <5 | 11 | 13 | 12 | <0.5 | <0.5 | 12 | 16 | 11.1 | <0.5 | <0.5 | <0.5 | <0.5 | 0.7 | <0.5 | 7.1 | 30.1 | 63.2 | 6.6 | 25.4 | 3.5 | 0.9 | 3.7 | 0.5 | 3.2 | 0.8 | 1.9 | <0.5 | 2.3 | <0.5 | 2.7 | 3.1 | 3.8 | 1 | <0.5 | 12.3 | 2.2 |
| DPS-BH1-3 | DPS/BH/01 | 6m | 7m | 18 | 19 | 55 | 21 | 5511 | 112 | 28.2 | 0.9 | <5 | 5.4 | 14 | 7 | <0.5 | <0.5 | 61 | 12 | 5 | <0.5 | <0.5 | <0.5 | <0.5 | <0.5 | <0.5 | 3.7 | 16.6 | 40.5 | 4.1 | 19.1 | 4 | 0.8 | 3.4 | 0.5 | 2.8 | 0.5 | 1.3 | <0.5 | 1.2 | <0.5 | 4.6 | <0.5 | <0.5 | 1 | <0.5 | 8.1 | 1.2 |
| DPS-BH1-4 | DPS/BH/01 | 7m | 8m | 7 | 14 | 22 | 28 | 1310 | 109 | 29.8 | 1.5 | <5 | 8 | 8.9 | 9 | <0.5 | 0.5 | 87 | 11 | 8.4 | <0.5 | <0.5 | <0.5 | 1.5 | <0.5 | <0.5 | 5.1 | 21.6 | 46.8 | 5.1 | 20.5 | 4 | 0.6 | 3.6 | <0.5 | 2.9 | <0.5 | 1.3 | <0.5 | 1.2 | <0.5 | 4.1 | 0.9 | 0.9 | 1 | <0.5 | 7.3 | 1.4 |
| DPS-BH1-5 | DPS/BH/01 | 8m | 9m | 10 | 12 | 16 | 29 | 371 | 129 | 35.9 | 1.8 | <5 | 13 | 11 | 12 | <0.5 | 1.4 | 11 | 16 | 8.6 | 0.9 | <0.5 | <0.5 | <0.5 | <0.5 | <0.5 | 6.3 | 27.3 | 57.6 | 6.5 | 25.4 | 4.5 | 0.9 | 5.1 | 0.6 | 3.4 | 0.7 | 1.8 | <0.5 | 1.9 | <0.5 | 5.1 | 1 | 1.6 | 2 | <0.5 | 6.3 | 1.9 |
| DPS-BH1-6 | DPS/BH/01 | 9m | 10m | 8 | 15 | 21 | 37 | 91 | 131 | 25.9 | 0.9 | <5 | 6.5 | 8.8 | 9 | <0.5 | <0.5 | 82 | 12 | 3.3 | <0.5 | <0.5 | <0.5 | 1.3 | <0.5 | <0.5 | 4 | 19.2 | 41.7 | 4.5 | 20.5 | 3.8 | 0.7 | 3.7 | 0.5 | 2.4 | <0.5 | 1.7 | <0.5 | 1.2 | <0.5 | 2.1 | <0.5 | <0.5 | <0.5 | 7.9 | 1.4 | |
| DPS-BH1-7 | DPS/BH/01 | 10m | 11m | 7 | 12 | 14 | 41 | 99 | 120 | 36.9 | 0.9 | <5 | 9.2 | 6.4 | 8 | <0.5 | 2.1 | 82 | 17 | 5.8 | <0.5 | <0.5 | <0.5 | <0.5 | <0.5 | <0.5 | 4.2 | 21.7 | 45.1 | 5.1 | 23.5 | 4.7 | 0.9 | 4.5 | 0.6 | 3.4 | 0.6 | 2 | <0.5 | 1.8 | <0.5 | 6.1 | 0.6 | <0.5 | 2 | <0.5 | 9.9 | 1.7 |
| DPS-BH1-16 | DPS/BH/01 | 11m | 12m | 16 | 19 | 13 | 51 | 265 | 116 | 52.6 | 1 | <5 | 7.5 | 9.1 | 10 | <0.5 | 0.8 | 91 | 20 | 7.1 | <0.5 | <0.5 | <0.5 | <0.5 | <0.5 | <0.5 | 5.2 | 20.7 | 44.6 | 5.2 | 20.6 | 4.4 | 0.9 | 5.7 | 0.7 | 3.7 | 0.7 | 2.1 | <0.5 | 2 | <0.5 | 2.3 | 1.2 | 1.1 | <0.5 | <0.5 | 8.5 | 1.8 |
| DPS-BH1-17 | DPS/BH/01 | 12m | 13m | 14 | 15 | 24 | 59 | 4276 | 7625 | 25.8 | 0.8 | <5 | 5 | 10 | 7 | <0.5 | <0.5 | 66 | 15 | 3.7 | <0.5 | <0.5 | <0.5 | <0.5 | <0.5 | <0.5 | 4 | 14.2 | 30.8 | 3.6 | 13.7 | 3.2 | 0.7 | 4.1 | <0.5 | 2.7 | 0.5 | 1.6 | <0.5 | 1.3 | <0.5 | 1.4 | 0.9 | <0.5 | <0.5 | <0.5 | 5.1 | 1.5 |
| DPS-BH1-8 | DPS/BH/01 | 13.5m | 14.5m | 16 | 17 | 13 | 55 | 188 | 104 | 47.4 | 1.2 | <5 | 12 | 11 | 12 | <0.5 | <0.5 | 11 | 21 | 10.8 | <0.5 | <0.5 | <0.5 | <0.5 | 0.5 | <0.5 | 7.7 | 25.7 | 52.1 | 5.5 | 22.7 | 5 | 0.9 | 5.4 | 0.7 | 4.3 | 0.8 | 2.5 | <0.5 | 4.7 | <0.5 | 3.8 | 1.5 | 1.9 | 1 | <0.5 | 11.9 | 2.4 |
| DPS-BH1-18 | DPS/BH/01 | 14.5m | 15.5m | 16 | 15 | 18 | 56 | 6490 | 9032 | 32.1 | <5 | <5 | 6.2 | 9.4 | 8 | <0.5 | 1 | 87 | 16 | 5.8 | <0.5 | <0.5 | <0.5 | <0.5 | <0.5 | <0.5 | 5.9 | 17.2 | 36.3 | 4.3 | 16.4 | 3.4 | 0.8 | 4.3 | 0.6 | 3 | 0.5 | 1.8 | <0.5 | 1.4 | <0.5 | 2.4 | 1.2 | 1.1 | <0.5 | <0.5 | 7.1 | 1.9 |
| DPS-BH1-9 | DPS/BH/01 | 16.5m | 17.5m | 7 | 7 | 62 | 22 | <515 | 161 | 0.6 | <5 | <5 | 5.8 | 3.9 | 5 | <0.5 | <0.5 | 62 | 9.6 | 3.5 | 1 | <0.5 | <0.5 | 4.7 | 0.7 | <0.5 | 2.4 | 15.3 | 31.5 | 3.1 | 15.6 | 2.3 | 0.6 | 3.3 | <0.5 | 1.9 | <0.5 | 1.2 | <0.5 | 1.2 | <0.5 | 4.9 | <0.5 | 0.8 | 1 | <0.5 | 6.4 | 1.4 |
| DPS-BH1-10 | DPS/BH/01 | 18m | 19m | <5 | <5 | <5 | 10 | <522 | 5.7 | <0.5 | <5 | <5 | <0.5 | 0.9 | 2 | <0.5 | <0.5 | 20 | 2.5 | <0.5 | 2 | <0.5 | <0.5 | <0.5 | <0.5 | <0.5 | 0.5 | 7.9 | 15.2 | 1.6 | 6.6 | 1.1 | <0.5 | 0.7 | <0.5 | <0.5 | <0.5 | <0.5 | <0.5 | <0.5 | <0.5 | <0.5 | <0.5 | <0.5 | <0.5 | 0.5 | <0.5 | |
| DPS-BH1-10 | DPS/BH/01 | 18m | 19m | <5 | <5 | <5 | 9 | <521 | 5.3 | <0.5 | <5 | <5 | <0.5 | 0.7 | 2 | <0.5 | <0.5 | 19 | 2.3 | <0.5 | 2.1 | <0.5 | <0.5 | <0.5 | <0.5 | <0.5 | 0.7 | 7.2 | 14.6 | 1.5 | 6.9 | 0.9 | <0.5 | 0.8 | <0.5 | <0.5 | <0.5 | <0.5 | <0.5 | <0.5 | <0.5 | <0.5 | <0.5 | <0.5 | <0.5 | 0.6 | <0.5 | |
| DPS-BH1-11 | DPS/BH/01 | 19.5m | 20.5m | <5 | <5 | <5 | 10 | <524 | 5.5 | <0.5 | <5 | <5 | 1.2 | 0.7 | 2 | <0.5 | <0.5 | 24 | 2.9 | <0.5 | 1.5 | <0.5 | <0.5 | <0.5 | <0.5 | <0.5 | 0.5 | 7.5 | 15.6 | 1.3 | 6.4 | 1.4 | <0.5 | 0.9 | <0.5 | <0.5 | <0.5 | <0.5 | <0.5 | <0.5 | <0.5 | <0.5 | <0.5 | <0.5 | <0.5 | 0.9 | <0.5 | |
| DPS-BH1-12 | DPS/BH/01 | 21m | 22m | <5 | <5 | <5 | 9 | <530 | 3 | <0.5 | <5 | <5 | 1.8 | 0.9 | 2 | <0.5 | <0.5 | 22 | 3.2 | <0.5 | 1.1 | <0.5 | <0.5 | <0.5 | <0.5 | <0.5 | <0.5 | 7.9 | 15.4 | 1.5 | 6.3 | 1.3 | <0.5 | 1.2 | <0.5 | 0.7 | <0.5 | <0.5 | <0.5 | <0.5 | <0.5 | 2 | <0.5 | <0.5 | 1 | <0.5 | 0.6 | <0.5 |
| DPS-BH1-13 | DPS/BH/01 | 22.50m | 23.5m | <5 | 5 | <5 | 12 | <563 | 3.4 | <0.5 | <5 | <5 | <0.5 | 2 | 2 | <0.5 | <0.5 | 26 | 3.5 | <0.5 | 3.2 | <0.5 | <0.5 | <0.5 | <0.5 | <0.5 | 0.6 | 8.3 | 16.2 | 1.7 | 6.7 | 0.9 | <0.5 | 1 | <0.5 | 0.6 | <0.5 | <0.5 | <0.5 | <0.5 | <0.5 | <0.5 | <0.5 | <0.5 | <0.5 | 0.6 | 0.5 | |
| DPS-BH1-14 | DPS/BH/01 | 24m | 25m | <5 | <5 | <5 | 16 | <554 | 6.6 | <0.5 | <5 | <5 | 2.5 | 1.3 | 4 | <0.5 | <0.5 | 41 | 6.2 | 1 | 1.9 | <0.5 | <0.5 | <0.5 | <0.5 | <0.5 | 1.2 | 12.8 | 26.2 | 2.2 | 10.5 | 2 | <0.5 | 1.7 | <0.5 | 1.2 | <0.5 | 0.8 | <0.5 | 0.6 | <0.5 | 2.6 | <0.5 | <0.5 | 1 | <0.5 | 1.8 | 0.9 |
| DPS-BH1-15 | DPS/BH/01 | 27m | 28m | <5 | 6 | 63 | 3<5 | 2626 | 15.4 | 0.9 | <5 | <5 | 8.7 | 3.2 | 9 | <0.5 | <0.5 | 96 | 18 | 6 | <0.5 | <0.5 | <0.5 | 1.8 | <0.5 | <0.5 | 3.1 | 30.9 | 63.8 | 6.8 | 28.6 | 5.2 | 1 | 5.1 | 0.7 | 4 | 0.8 | 2.3 | <0.5 | 2.7 | <0.5 | 3.1 | <0.5 | 1 | 1 | <0.5 | 3.4 | 2.8 |
| DPS-BH2-1 | DPS/BH/02 | 2m | 3m | 13 | 16 | 26 | 137 | 706 | 20.6 | 0.7 | <5 | <5 | 5.5 | 6.5 | 5 | <0.5 | <0.5 | 36 | 6.4 | 3 | 1.6 | <0.5 | <0.5 | <0.5 | <0.5 | <0.5 | 1.6 | 13.3 | 27.8 | 2.9 | 12.1 | 2.2 | <0.5 | 1.8 | <0.5 | 1.6 | <0.5 | 0.8 | <0.5 | 0.7 | <0.5 | 2.2 | <0.5 | 10 | 1 | <0.5 | 9.3 | 0.7 |
| DPS-BH2-2 | DPS/BH/02 | 3m | 4m | 21 | 15 | 17 | 15 | 4134 | 347 | 18.7 | <0.5 | <5 | 2.8 | 6.7 | 4 | <0.5 | <0.5 | 32 | 5.7 | 1.2 | 0.5 | <0.5 | <0.5 | 2.2 | <0.5 | <0.5 | 1.4 | 12.8 | 25.8 | 2.6 | 10.1 | 1.9 | <0.5 | 1.5 | <0.5 | 1.5 | <0.5 | 0.8 | <0.5 | 0.5 | <0.5 | 2.9 | <0.5 | 9.6 | 1 | <0.5 | 1.7 | 0.6 |
| DPS-BH2-3 | DPS/BH/02 | 4m | 5m | 11 | 11 | 11 | 55 | 5039 | 398 | 21.8 | 0.7 | <5 | 3.4 | 4.4 | 4 | <0.5 | <0.5 | 32 | 5.5 | 1.7 | <0.5 | <0. | | | | | | | | | | | | | | | | | | | | | | | | | | |

| Sample Id | Borehole ID | Depth from | Depth to | C u | Ni | P b | Sr | Zn | Zr | Li | Be | B | Sc | Co | G a | Ge | Se | Rb | Y | Nb | Mo | Cd | In | Sn | Sb | Te | Cs | La | Ce | Pr | Nd | S m | Eu | Gd | Tb | Dy | Ho | Er | Tm | Yb | Lu | Hf | Ta | W | Tl | Bi | Th | U | |
|------------|-------------|------------|----------|-----|----|-----|----|----|-----|------|------|----|-----|-----|-----|------|------|----|-----|------|------|------|------|------|------|------|-----|------|------|-----|------|-----|------|-----|------|-----|------|-----|------|------|------|------|------|------|------|------|------|-----|-----|
| DPS-BH2-5 | DPS/BH/02 | 6m | 7m | 12 | 14 | 17 | 18 | 48 | 45 | 19.6 | 0.6 | <5 | 1.7 | 5.2 | 4 | <0.5 | <0.5 | 33 | 5.8 | <0.5 | 0.7 | <0.5 | <0.5 | <0.5 | <0.5 | <0.5 | 1.2 | 10.6 | 21.7 | 2.7 | 10.1 | 2.3 | <0.5 | 2.3 | <0.5 | 1.6 | <0.5 | 0.8 | <0.5 | <0.5 | 5 | <0.5 | 0.9 | <0.5 | 5.9 | <0.5 | <0.5 | 1.8 | 0.8 |
| DPS-BH2-6 | DPS/BH/02 | 7m | 8m | 16 | 17 | 12 | 7 | 26 | 64 | 19.5 | <0.5 | <5 | 4.3 | 6.9 | 4 | <0.5 | <0.5 | 38 | 6.4 | 1.6 | 1.5 | <0.5 | <0.5 | <0.5 | <0.5 | <0.5 | 1.5 | 11.9 | 24.9 | 2.5 | 11.4 | 2.3 | <0.5 | 2.3 | <0.5 | 1.7 | <0.5 | 0.9 | <0.5 | 0.8 | <0.5 | 2.4 | <0.5 | 12 | 1 | <0.5 | 1.7 | 0.8 | |
| DPS-BH2-7 | DPS/BH/02 | 8m | 9m | 15 | 15 | 17 | 6 | 27 | 43 | 19.1 | 0.6 | <5 | 4.3 | 6.6 | 5 | <0.5 | <0.5 | 35 | 5.9 | 1.1 | 1.7 | <0.5 | <0.5 | <0.5 | <0.5 | <0.5 | 1.3 | 11.9 | 26.1 | 2.6 | 11.9 | 2.3 | <0.5 | 1.9 | <0.5 | 1.4 | <0.5 | 0.7 | <0.5 | 0.7 | <0.5 | 3.7 | <0.5 | 14 | 1 | <0.5 | 1.9 | 0.5 | |
| DPS-BH2-8 | DPS/BH/02 | 9.5m | 10.5m | 8 | 10 | 8 | 19 | 68 | 83 | 18.9 | 0.8 | <5 | 6.6 | 4.4 | 7 | <0.5 | <0.5 | 64 | 8.4 | 3.6 | 4.4 | <0.5 | <0.5 | 0.9 | <0.5 | <0.5 | 3.1 | 17.5 | 37.8 | 4.1 | 17.9 | 2.5 | 0.6 | 2.2 | <0.5 | 1.7 | <0.5 | 1 | <0.5 | 0.9 | <0.5 | 3.7 | <0.5 | 1.8 | 1 | <0.5 | 3.6 | 1 | |
| DPS-BH2-9 | DPS/BH/02 | 10.5m | 11.5m | 5 | 15 | 14 | 1 | 22 | 147 | 27.8 | 1.1 | <5 | 12 | 8.1 | 12 | <0.5 | <0.5 | 12 | 15 | 11.7 | 0.5 | <0.5 | <0.5 | <0.5 | <0.5 | <0.5 | 7 | 32.9 | 68.6 | 7.3 | 27.6 | 3.8 | 0.7 | 4.4 | 0.5 | 3 | 0.7 | 2.2 | <0.5 | 1.9 | <0.5 | 4.6 | 3.2 | 3 | 1 | <0.5 | 5 | 2.1 | |
| DPS-BH2-10 | DPS/BH/02 | 12m | 13m | 10 | 14 | 19 | 1 | 10 | 103 | 32.4 | 1.3 | <5 | 9.1 | 7.4 | 11 | <0.5 | <0.5 | 99 | 20 | 10.8 | 0.7 | <0.5 | <0.5 | <0.5 | <0.5 | <0.5 | 6.3 | 23.7 | 52.9 | 5.4 | 25 | 5 | 0.8 | 5.4 | 0.8 | 4 | 0.8 | 2.1 | <0.5 | 2.3 | <0.5 | 3.3 | 0.9 | 1.4 | 1 | <0.5 | 7.8 | 2 | |
| DPS-BH2-11 | DPS/BH/02 | 15m | 16m | 12 | 15 | 26 | 2 | 18 | 95 | 42.1 | 1.1 | <5 | 10 | 8 | 9 | <0.5 | <0.5 | 96 | 17 | 7.6 | <0.5 | <0.5 | <0.5 | <0.5 | <0.5 | <0.5 | 6 | 19.1 | 41.8 | 4.8 | 21.7 | 4.5 | 1 | 3.9 | 0.5 | 3.3 | 0.6 | 2.3 | <0.5 | 1.5 | <0.5 | 6 | 1.2 | 1.1 | <0.5 | <0.5 | 5.4 | 2.1 | |
| DPS-BH2-12 | DPS/BH/02 | 16.5m | 17.50m | 8 | 13 | 24 | 5 | <5 | 63 | 17.4 | 0.8 | <5 | 5.4 | 7.9 | 6 | <0.5 | <0.5 | 64 | 13 | 7.8 | 5.9 | <0.5 | <0.5 | <0.5 | <0.5 | <0.5 | 4.5 | 12.9 | 29.2 | 3 | 13.7 | 3.4 | 0.7 | 3.1 | <0.5 | 2.6 | 0.5 | 1.5 | <0.5 | 1.2 | <0.5 | 2.9 | 0.7 | 0.6 | 1 | <0.5 | 2.8 | 1.7 | |
| DPS-BH2-13 | DPS/BH/02 | 18.5m | 19.5m | <5 | <5 | <5 | 18 | <5 | 91 | 8.8 | <0.5 | <5 | 2.3 | 1.2 | 3 | <0.5 | <0.5 | 44 | 8.5 | 0.9 | 0.9 | <0.5 | <0.5 | <0.5 | <0.5 | <0.5 | 1.4 | 11.1 | 22.1 | 2.2 | 10.6 | 2.4 | <0.5 | 2.2 | <0.5 | 1.6 | <0.5 | 1 | <0.5 | 1.3 | <0.5 | 0.9 | <0.5 | <0.5 | 1 | <0.5 | 3 | 1.3 | |
| DPS-BH2-14 | DPS/BH/02 | 19.5m | 20.5m | 13 | 6 | 7 | 24 | <5 | 30 | 15.3 | 0.6 | <5 | 5.5 | 1.5 | 6 | <0.5 | <0.5 | 70 | 11 | 6.4 | 1.4 | <0.5 | <0.5 | <0.5 | <0.5 | <0.5 | 2 | 18.7 | 37.5 | 3.6 | 15.6 | 2.6 | <0.5 | 2.5 | <0.5 | 1.8 | <0.5 | 1.3 | <0.5 | 1.7 | <0.5 | 2.5 | 0.6 | 0.7 | 1 | <0.5 | 2.6 | 1.8 | |
| DPS-BH2-15 | DPS/BH/02 | 23m | 24m | <5 | 8 | 12 | 1 | 62 | 38 | 5.3 | <0.5 | <5 | 2.3 | 4.8 | 3 | <0.5 | <0.5 | 30 | 4.6 | 1.7 | 2.9 | <0.5 | <0.5 | <0.5 | <0.5 | <0.5 | 1.2 | 10.1 | 20.9 | 2.2 | 9.6 | 1.9 | <0.5 | 1.5 | <0.5 | 1 | <0.5 | 0.6 | <0.5 | <0.5 | <0.5 | <0.5 | <0.5 | 2.8 | <0.5 | | | | |
| DPS-BH2-15 | DPS/BH/02 | 23m | 24m | <5 | 7 | 11 | 1 | 64 | 36 | 5.1 | <0.5 | <5 | 2.1 | 4.4 | 3 | <0.5 | <0.5 | 30 | 4.4 | 1.2 | 3.2 | <0.5 | <0.5 | <0.5 | <0.5 | <0.5 | 1.1 | 9.9 | 20.6 | 2.2 | 9 | 1.6 | <0.5 | 1.5 | <0.5 | 1.2 | <0.5 | 0.6 | <0.5 | <0.5 | <0.5 | 1.3 | <0.5 | <0.5 | <0.5 | 2.1 | <0.5 | | |
| DPS-BH2-24 | DPS/BH/02 | 27m | 28m | 8 | 13 | 8 | 47 | 34 | 343 | 23.4 | 1.8 | <5 | 9.3 | 6.8 | 13 | <0.5 | 0.6 | 14 | 24 | 10.3 | <0.5 | <0.5 | <0.5 | <0.5 | <0.5 | <0.5 | 5.6 | 36.7 | 74.7 | 8.7 | 31.6 | 6 | 1.1 | 7.7 | 0.9 | 4.2 | 0.8 | 2.6 | <0.5 | 2.6 | <0.5 | 6.6 | 1.7 | 2.4 | <0.5 | <0.5 | 14.8 | 3 | |
| DPS-BH2-25 | DPS/BH/02 | 28m | 29m | 21 | 11 | <5 | 42 | 27 | 407 | 23 | 1.7 | <5 | 8 | 5.1 | 12 | <0.5 | 0.7 | 12 | 22 | 10.3 | <0.5 | <0.5 | <0.5 | <0.5 | <0.5 | <0.5 | 4.7 | 35.3 | 71.7 | 8.2 | 29.5 | 5.7 | 1 | 7.1 | 0.8 | 4 | 0.8 | 2.4 | <0.5 | 2.5 | <0.5 | 7.3 | 1.4 | 1.9 | <0.5 | <0.5 | 13.7 | 2.9 | |
| DPS-BH2-26 | DPS/BH/02 | 29m | 30m | 16 | 11 | <5 | 32 | 19 | 340 | 19.4 | 1.3 | <5 | 5.1 | 4.9 | 9 | <0.5 | 0.8 | 89 | 14 | 5 | <0.5 | <0.5 | <0.5 | <0.5 | <0.5 | <0.5 | 3.5 | 22.5 | 46.3 | 5.1 | 18.2 | 3.2 | 0.6 | 4.6 | 0.5 | 2.5 | 0.5 | 1.6 | <0.5 | 1.7 | <0.5 | 5.1 | <0.5 | 0.9 | <0.5 | <0.5 | 8.5 | 2 | |

Annexure 6 Statement Showing co-ordinates & Comparison of analyses results for major oxides (XRF analysis) of 15 Bedrock External Check samples

Unit: %

| Primary sample analysis Results | | | | | | | | | | | | | | | | | | | | |
|---------------------------------|---------------------------------|----------|-----------|-------|-------|-------|-------|--------|-------|------|-------|-------|-------|-------|-------|-------|-------|-------|-------|-------|
| Primary sample ID | Corresponding Check sample Id | Latitude | Longitude | Al2O3 | BaO | CaO | Cr2O3 | Fe(T) | Fe2O3 | K2O | MgO | MnO | Na2O | P2O5 | SO3 | TiO2 | SiO2 | SrO | V2O5 | LOI |
| DPS-5 | CH/DS-01 | 25.88491 | 77.33413 | 4.94 | <0.05 | 6.11 | <0.05 | | 5.52 | 2.77 | 4.64 | 0.07 | <0.08 | <0.05 | 1.43 | 0.15 | 63.93 | <0.05 | <0.05 | 10.07 |
| DPS-7 | CH/DS-02 | 25.90357 | 77.39428 | 7.21 | <0.05 | 0.13 | <0.05 | | 1.62 | 3.24 | 0.49 | <0.05 | 0.08 | <0.05 | <0.05 | 0.6 | 84.56 | <0.05 | <0.05 | 1.86 |
| DPS-S-113 | CH/DS-03 | 25.88106 | 77.33981 | 4.55 | <0.05 | 0.26 | <0.05 | 2.16 | 3.09 | 1.93 | 0.83 | <0.05 | 0.08 | 0.15 | <0.05 | 0.17 | 87.08 | <0.05 | <0.05 | 1.75 |
| DPS-S-81 | CH/DS-04 | 25.96925 | 77.32939 | 1.12 | <0.05 | <0.05 | 0.07 | 0.71 | 1.02 | 0.62 | <0.05 | <0.05 | 0.08 | <0.05 | <0.05 | 0.07 | 96.61 | <0.05 | <0.05 | 0.3 |
| DPS-S-91 a | CH/DS-05 | 25.95889 | 77.39183 | 4.49 | <0.05 | 0.42 | <0.05 | 1.99 | 2.85 | 1.64 | 0.81 | <0.05 | 0.08 | 0.09 | <0.05 | 0.19 | 87.68 | <0.05 | <0.05 | 1.56 |
| DPS-S-94 | CH/DS-06 | 25.904 | 77.34189 | 1.89 | <0.05 | <0.05 | <0.05 | 1.25 | 1.78 | 0.73 | 0.3 | <0.05 | 0.08 | <0.05 | <0.05 | 0.07 | 94.52 | <0.05 | <0.05 | 0.51 |
| DPS-S-79 | CH/DS-07 | 25.96542 | 77.39794 | 0.89 | <0.05 | <0.05 | 0.05 | 0.54 | 0.77 | 0.36 | <0.05 | <0.05 | 0.08 | <0.05 | <0.05 | <0.05 | 97.32 | <0.05 | <0.05 | 0.39 |
| DPS-S-85 | CH/DS-08 | 25.92344 | 77.34394 | 2.58 | <0.05 | 10.1 | <0.05 | 2.47 | 3.53 | 1.21 | 1 | 0.11 | <0.08 | <0.05 | <0.05 | 0.09 | 71.48 | <0.05 | <0.05 | 9.63 |
| DPS-S-91 b | CH/DS-09 | 25.95889 | 77.39183 | 4.31 | <0.05 | 0.55 | <0.05 | 1.92 | 2.74 | 1.53 | 0.74 | <0.05 | 0.08 | 0.19 | <0.05 | 0.18 | 88.23 | <0.05 | <0.05 | 1.3 |
| DPS-S-114 | CH/DS-10 | 25.92403 | 77.34381 | 3.26 | <0.05 | 5.86 | 0.06 | 3.29 | 4.7 | 1.62 | 1.47 | <0.05 | <0.08 | <0.05 | <0.05 | 0.12 | 76.07 | <0.05 | <0.05 | 6.62 |
| DPS-S-115 | CH/DS-11 | 25.91006 | 77.41178 | 2.87 | <0.05 | <0.05 | 0.05 | 0.52 | 0.74 | 1.36 | 0.11 | <0.05 | 0.08 | <0.05 | <0.05 | 0.29 | 93.37 | <0.05 | <0.05 | 0.92 |
| DPS-S-127 | CH/DS-12 | 25.92175 | 77.39956 | 0.81 | <0.05 | 7.07 | 0.08 | 2.66 | 3.8 | 0.33 | 3.46 | 0.24 | <0.08 | <0.05 | 0.24 | <0.05 | 73.17 | <0.05 | <0.05 | 10.66 |
| DPS-S-133 | CH/DS-13 | 25.9595 | 77.37458 | 2.39 | <0.05 | 25.1 | <0.05 | 3.76 | 5.38 | 0.94 | 7.91 | 0.35 | <0.08 | <0.05 | 0.23 | 0.18 | 27.89 | <0.05 | <0.05 | 29.5 |
| DPS-S-147 | CH/DS-14 | 25.90133 | 77.36169 | 1.33 | <0.05 | <0.05 | <0.05 | 0.93 | 1.33 | 0.65 | 0.14 | <0.05 | 0.08 | <0.05 | 0.26 | 0.07 | 95.61 | <0.05 | <0.05 | 0.44 |
| DPS-54 | CH/DS-15 | 25.92731 | 77.38319 | 2.13 | <0.05 | <0.05 | <0.05 | 0.57 | 0.82 | 1.01 | 0.09 | <0.05 | 0.08 | <0.05 | <0.05 | 0.1 | 95.22 | <0.05 | <0.05 | 0.44 |
| Check Sample Analysis Results | | | | | | | | | | | | | | | | | | | | |
| Check Sample Id | Corresponding Primary Sample id | Latitude | Longitude | Al2O3 | BaO | CaO | Cr2O3 | Fe (T) | Fe2O3 | K2O | MgO | MnO | Na2O | P2O5 | SO3 | TiO2 | SiO2 | SrO | V2O5 | LOI |
| CH/DS-01 | DPS-5 | 25.88491 | 77.33413 | 4.74 | <0.05 | 6.03 | <0.05 | 3.78 | 5.41 | 2.78 | 4.71 | <0.05 | <0.08 | <0.05 | 1.39 | 0.14 | 63.88 | <0.05 | <0.05 | 10.53 |
| CH/DS-02 | DPS-7 | 25.90357 | 77.39428 | 7.22 | <0.05 | 0.11 | <0.05 | 1.10 | 1.57 | 3.21 | 0.48 | <0.05 | 0.08 | <0.05 | <0.05 | 0.60 | 84.46 | <0.05 | <0.05 | 2.06 |
| CH/DS-03 | DPS-S-113 | 25.88106 | 77.33981 | 4.55 | <0.05 | 0.26 | <0.05 | 2.11 | 3.02 | 1.92 | 0.87 | <0.05 | 0.08 | 0.15 | <0.05 | 0.16 | 86.67 | <0.05 | <0.05 | 2.22 |
| CH/DS-04 | DPS-S-81 | 25.96925 | 77.32939 | 1.24 | <0.05 | <0.05 | 0.07 | 0.64 | 0.91 | 0.61 | 0.06 | <0.05 | 0.08 | <0.05 | <0.05 | 0.07 | 96.61 | <0.05 | <0.05 | 0.27 |
| CH/DS-05 | DPS-S-91 a | 25.95889 | 77.39183 | 4.60 | <0.05 | 0.41 | <0.05 | 1.90 | 2.72 | 1.58 | 0.84 | <0.05 | 0.08 | 0.09 | <0.05 | 0.18 | 87.66 | <0.05 | <0.05 | 1.67 |
| CH/DS-06 | DPS-S-94 | 25.904 | 77.34189 | 1.83 | <0.05 | <0.05 | <0.05 | 1.20 | 1.71 | 0.71 | 0.31 | <0.05 | 0.08 | <0.05 | <0.05 | 0.08 | 94.38 | <0.05 | <0.05 | 0.79 |
| CH/DS-07 | DPS-S-79 | 25.96542 | 77.39794 | 0.97 | <0.05 | <0.05 | <0.05 | 0.56 | 0.80 | 0.37 | <0.05 | <0.05 | 0.08 | <0.05 | <0.05 | <0.05 | 97.03 | <0.05 | <0.05 | 0.57 |
| CH/DS-08 | DPS-S-85 | 25.92344 | 77.34394 | 2.51 | <0.05 | 9.97 | 0.06 | 2.42 | 3.46 | 1.19 | 1.05 | 0.10 | <0.08 | <0.05 | <0.05 | 0.09 | 71.72 | <0.05 | <0.05 | 9.65 |
| CH/DS-09 | DPS-S-91 b | 25.95889 | 77.39183 | 4.16 | <0.05 | 0.57 | <0.05 | 1.93 | 2.75 | 1.55 | 0.77 | <0.05 | 0.08 | 0.19 | <0.05 | 0.19 | 88.07 | <0.05 | <0.05 | 1.52 |
| CH/DS-10 | DPS-S-114 | 25.92403 | 77.34381 | 3.50 | <0.05 | 5.69 | 0.05 | 3.24 | 4.63 | 1.61 | 1.49 | <0.05 | <0.08 | <0.05 | <0.05 | 0.11 | 75.85 | <0.05 | <0.05 | 6.83 |
| CH/DS-11 | DPS-S-115 | 25.91006 | 77.41178 | 2.92 | <0.05 | <0.05 | 0.05 | 0.55 | 0.78 | 1.39 | 0.11 | <0.05 | 0.08 | <0.05 | <0.05 | 0.29 | 93.46 | <0.05 | <0.05 | 0.72 |
| CH/DS-12 | DPS-S-127 | 25.92175 | 77.39956 | 1.04 | <0.05 | 7.06 | 0.08 | 2.67 | 3.82 | 0.33 | 3.51 | 0.25 | <0.08 | <0.05 | 0.09 | <0.05 | 73.18 | <0.05 | <0.05 | 10.48 |
| CH/DS-13 | DPS-S-133 | 25.9595 | 77.37458 | 2.60 | <0.05 | 24.97 | <0.05 | 3.80 | 5.44 | 0.94 | 7.95 | 0.35 | <0.08 | <0.05 | 0.06 | 0.17 | 27.72 | <0.05 | <0.05 | 29.59 |
| CH/DS-14 | DPS-S-147 | 25.90133 | 77.36169 | 1.52 | <0.05 | <0.05 | <0.05 | 1.03 | 1.47 | 0.67 | 0.17 | <0.05 | 0.08 | <0.05 | <0.05 | 0.07 | 95.48 | <0.05 | <0.05 | 0.45 |
| CH/DS-15 | DPS-54 | 25.92731 | 77.38319 | 2.42 | <0.05 | <0.05 | <0.05 | 0.71 | 1.01 | 1.15 | 0.10 | <0.05 | 0.08 | <0.05 | <0.05 | 0.23 | 94.04 | <0.05 | <0.05 | 0.65 |

Note: The laboratory of analysis was *Shiva Analyticals India Limited*, Bangalore — a NABL-accredited facility. For the external check, a sample (with a changed Sample ID) prepared from the primary sample powder was sent for analysis.

Annexure 7 Statement Showing co-ordinates & Comparison of analyses results for REE & Trace Elements (ICPMS analysis) of 7 Bedrock External Check samples

Unit: ppm

| Primary sample Analysis Results | | | | | | | | | | | | | | | | | | | | | | | | | | | | | | | | | | | | | | | | | | | | |
|---------------------------------|---------------------------------|-----------|-----------|-------|------|------|------|------|------|------|------|-------|------|------|------|------|------|------|------|------|------|------|------|-----|------|-----|------|-----|------|-----|------|------|------|------|------|------|------|------|------|------|------|------|------|------|
| sample id | Corrsonding Check sample Id | Lattitude | Longitude | Li | Be | B | Sc | Co | Ga | Ge | Se | Rb | Y | Nb | Mo | Cd | In | Sn | Sb | Te | Cs | La | Ce | Pr | Nd | Sm | Eu | Gd | Tb | Dy | Ho | Er | Tm | Yb | Lu | Hf | Ta | W | Tl | Bi | Th | U | | |
| DPS-5 | CH/DS-01 | 25.884909 | 77.334128 | 350.8 | 3.5 | <5 | 3 | 21 | 16.8 | <0.5 | <0.5 | 101.2 | 9.9 | 0.7 | 0.6 | 1.3 | <0.5 | <0.5 | <0.5 | <0.5 | 4.8 | 5.8 | 15.5 | 2.2 | 10.4 | 2.7 | 0.9 | 2.7 | <0.5 | 2 | <0.5 | 0.9 | <0.5 | 0.8 | <0.5 | 1.7 | <0.5 | <0.5 | <0.5 | 3.2 | 2.5 | 0.6 | | |
| DPS-S-81 | CH/DS-04 | 25.96925 | 77.329389 | 7.6 | <0.5 | <5 | <0.5 | 1.2 | 2.1 | <0.5 | <0.5 | 23.0 | 3.7 | <0.5 | <0.5 | <0.5 | <0.5 | <0.5 | <0.5 | <0.5 | <0.5 | 9.1 | 18.8 | 2.2 | 7.9 | 1.1 | <0.5 | 1.2 | <0.5 | 0.7 | <0.5 | <0.5 | <0.5 | <0.5 | <0.5 | <0.5 | <0.5 | 1.2 | <0.5 | <0.5 | <0.5 | 0.9 | <0.5 | |
| DPS-S-94 | CH/DS-06 | 25.904 | 77.341889 | 32.3 | 0.6 | <5 | 0.5 | 2.2 | 3.9 | <0.5 | <0.5 | 26.1 | 5.6 | 1.6 | <0.5 | <0.5 | <0.5 | <0.5 | <0.5 | <0.5 | 0.8 | 13.0 | 18.8 | 3.2 | 12.5 | 2.3 | <0.5 | 2.2 | <0.5 | 1.2 | <0.5 | <0.5 | <0.5 | <0.5 | <0.5 | <0.5 | <0.5 | <0.5 | <0.5 | <0.5 | <0.5 | <0.5 | <0.5 | |
| DPS-S-91 b | CH/DS-09 | 25.958889 | 77.391833 | 23.7 | <0.5 | <5 | 2.2 | 4.6 | 5.1 | <0.5 | <0.5 | 50.7 | 13.7 | <0.5 | <0.5 | <0.5 | <0.5 | <0.5 | <0.5 | <0.5 | 1.0 | 10.4 | 21.5 | 2.8 | 12.2 | 5.2 | 1.2 | 6.9 | 0.7 | 3.2 | 0.5 | 1.3 | <0.5 | 1.1 | <0.5 | <0.5 | <0.5 | <0.5 | <0.5 | <0.5 | <0.5 | 1.8 | 0.8 | |
| DPS-S-115 | CH/DS-11 | 25.910056 | 77.411778 | 12.1 | <0.5 | <0.5 | 1.8 | 1.3 | 3.0 | <0.5 | <0.5 | 47.4 | 10.7 | 3.3 | <0.5 | <0.5 | <0.5 | <0.5 | <0.5 | <0.5 | 1.0 | 10.3 | 19.8 | 2.3 | 8.5 | 1.6 | 0.5 | 2.6 | <0.5 | 1.8 | <0.5 | 1.2 | <0.5 | 1.4 | <0.5 | 0.9 | <0.5 | 2.2 | <0.5 | <0.5 | 4.5 | 1.3 | | |
| DPS-S-147 | CH/DS-14 | 25.901333 | 77.361694 | 15.4 | <0.5 | <0.5 | 0.7 | 2.1 | 2.1 | <0.5 | <0.5 | 23.3 | 4.5 | 1.3 | <0.5 | <0.5 | <0.5 | <0.5 | <0.5 | <0.5 | 0.6 | 9.6 | 17.2 | 2.2 | 8.3 | 1.7 | <0.5 | 2.2 | <0.5 | 1.1 | <0.5 | 0.5 | <0.5 | <0.5 | <0.5 | <0.5 | <0.5 | <0.5 | 0.8 | <0.5 | <0.5 | 1.2 | <0.5 | |
| DPS-54 | CH/DS-15 | 25.927306 | 77.383194 | 13.7 | <0.5 | <5 | <0.5 | 2 | 1.9 | <0.5 | 0.8 | 32.4 | 3.5 | <0.5 | <0.5 | <0.5 | <0.5 | <0.5 | <0.5 | <0.5 | 0.6 | 8.8 | 18 | 2 | 7.1 | 1.3 | <0.5 | 1.1 | <0.5 | 0.7 | <0.5 | <0.5 | <0.5 | <0.5 | <0.5 | <0.5 | <0.5 | <0.5 | <0.5 | <0.5 | <0.5 | 1.4 | <0.5 | |
| Check Sample Analysis Result | | | | | | | | | | | | | | | | | | | | | | | | | | | | | | | | | | | | | | | | | | | | |
| sample id | Corresponding Primary Sample Id | Lattitude | Longitude | Li | Be | B | Sc | Co | Ga | Ge | Se | Rb | Y | Nb | Mo | Cd | In | Sn | Sb | Te | Cs | La | Ce | Pr | Nd | Sm | Eu | Gd | Tb | Dy | Ho | Er | Tm | Yb | Lu | Hf | Ta | W | Tl | Bi | Th | U | | |
| CH/DS-01 | DPS-5 | 25.884909 | 77.334128 | 311.5 | 2.6 | <5 | 1.7 | 21.3 | 16.3 | <0.5 | <0.5 | 108.1 | 10.9 | 1.7 | <0.5 | 0.8 | <0.5 | <0.5 | <0.5 | <0.5 | 4.9 | 6.0 | 16.8 | 2.4 | 10.8 | 3.0 | 0.9 | 3.0 | <0.5 | 2.0 | <0.5 | 0.9 | <0.5 | 0.7 | <0.5 | <0.5 | <0.5 | <0.5 | <0.5 | <0.5 | <0.5 | <0.5 | 2.5 | 0.5 |
| CH/DS-04 | DPS-S-81 | 25.96925 | 77.329389 | 7.6 | <0.5 | <5 | <0.5 | 1.0 | 1.9 | <0.5 | <0.5 | 21.8 | 3.8 | <0.5 | 3.5 | <0.5 | <0.5 | <0.5 | <0.5 | <0.5 | 0.6 | 9.0 | 19.4 | 2.1 | 7.7 | 1.1 | <0.5 | 1.2 | <0.5 | 0.7 | <0.5 | <0.5 | <0.5 | <0.5 | <0.5 | <0.5 | <0.5 | <0.5 | <0.5 | <0.5 | <0.5 | <0.5 | 1.9 | <0.5 |
| CH/DS-06 | DPS-S-94 | 25.904 | 77.341889 | 30.7 | 0.6 | <5 | <0.5 | 1.4 | 3.6 | <0.5 | <0.5 | 26.0 | 5.6 | <0.5 | <0.5 | <0.5 | <0.5 | <0.5 | <0.5 | <0.5 | 0.9 | 12.5 | 19.3 | 3.2 | 12.1 | 2.3 | <0.5 | 2.0 | <0.5 | 1.2 | <0.5 | 0.6 | <0.5 | <0.5 | <0.5 | <0.5 | <0.5 | <0.5 | <0.5 | <0.5 | <0.5 | 2.0 | <0.5 | |
| CH/DS-09 | DPS-S-91 b | 25.958889 | 77.391833 | 19.6 | <0.5 | <5 | 1.4 | 3.4 | 4.6 | <0.5 | <0.5 | 48.3 | 13.0 | 1.3 | <0.5 | <0.5 | <0.5 | <0.5 | <0.5 | <0.5 | 1.1 | 10.1 | 21.9 | 2.7 | 11.7 | 5.3 | 1.3 | 6.6 | 0.7 | 3.4 | <0.5 | 1.2 | <0.5 | 1.1 | <0.5 | 2.0 | <0.5 | <0.5 | <0.5 | <0.5 | <0.5 | 4.5 | 0.8 | |
| CH/DS-11 | DPS-S-115 | 25.910056 | 77.411778 | 11.3 | <0.5 | <5 | <0.5 | 0.7 | 2.8 | <0.5 | <0.5 | 46.9 | 10.4 | 3.3 | <0.5 | <0.5 | <0.5 | <0.5 | <0.5 | <0.5 | 1.0 | 10.8 | 20.3 | 2.4 | 8.7 | 1.9 | <0.5 | 1.8 | <0.5 | 1.8 | <0.5 | 1.2 | <0.5 | 1.2 | <0.5 | 8.2 | 1.1 | <0.5 | <0.5 | <0.5 | 5.2 | 1.2 | | |
| CH/DS-14 | DPS-S-147 | 25.901333 | 77.361694 | 13.3 | <0.5 | <5 | <0.5 | 1.4 | 1.9 | <0.5 | <0.5 | 22.2 | 4.4 | <0.5 | <0.5 | <0.5 | <0.5 | <0.5 | <0.5 | <0.5 | 0.6 | 9.3 | 16.6 | 2.1 | 8.3 | 1.6 | <0.5 | 1.6 | <0.5 | 1.0 | <0.5 | <0.5 | <0.5 | <0.5 | <0.5 | <0.5 | <0.5 | <0.5 | <0.5 | <0.5 | <0.5 | 2.0 | <0.5 | |
| CH/DS-15 | DPS 54 | 25.927306 | 77.383194 | 8.1 | <0.5 | <5 | <0.5 | 0.7 | 2.9 | <0.5 | <0.5 | 40.1 | 14.4 | 1.6 | <0.5 | <0.5 | <0.5 | <0.5 | <0.5 | <0.5 | 0.8 | 10.5 | 21.9 | 2.5 | 9.7 | 2.2 | 0.5 | 2.3 | <0.5 | 2.3 | <0.5 | 1.7 | <0.5 | 1.6 | <0.5 | 13.1 | <0.5 | <0.5 | <0.5 | <0.5 | 4.2 | 1.9 | | |

Annexure 8 Statement Showing co-ordinates & Comparison of analyses results for major oxides (XRF analysis) of 5 Pit External Check samples

Unit : %

| Pit Sample Primary Analysis Result | | | | | | | | | | | | | | | | | | | | |
|------------------------------------|---------------------------------|----------|----------|-------|-------|-------|-------|-------|-------|------|------|-------|-------|-------|-------|------|-------|-------|-------|-------|
| sample No | Check no | Lat | Long | Al2O3 | BaO | CaO | Cr2O3 | Fe(T) | Fe2O3 | K2O | MgO | MnO | Na2O | P2O5 | SO3 | TiO2 | SiO2 | SrO | V2O5 | LOI |
| DPS-P1(B) | DPS/PCH-1 | 25.93381 | 77.32366 | 2.54 | <0.05 | 0.14 | 0.08 | 1.67 | 2.38 | 1.27 | 0.44 | <0.05 | 0.08 | 0.05 | <0.05 | 0.1 | 91.79 | <0.05 | <0.05 | 1.04 |
| DPS-P3(A) | DPS/PCH-2 | 25.90419 | 77.34182 | 2.65 | <0.05 | <0.05 | <0.05 | 1.4 | 2 | 1.32 | 0.19 | <0.05 | 0.08 | <0.05 | <0.05 | 0.15 | 92.41 | <0.05 | <0.05 | 1.09 |
| DPS-P11(B) | DPS/PCH-3 | 25.92275 | 77.34331 | 4.03 | <0.05 | 30.77 | <0.05 | 1.85 | 2.65 | 1.53 | 1.06 | 0.19 | <0.08 | <0.05 | <0.05 | 0.28 | 33.68 | <0.05 | <0.05 | 25.61 |
| DPS-P-16 | DPS/PCH-4 | 25.92669 | 77.33158 | 1.48 | <0.05 | <0.05 | <0.05 | 0.92 | 1.31 | 0.72 | 0.1 | <0.05 | 0.08 | <0.05 | <0.05 | 0.08 | 95.68 | <0.05 | <0.05 | 0.42 |
| DPS-P-21 | DPS/PCH-5 | 25.89469 | 77.33383 | 2.13 | <0.05 | <0.05 | 0.06 | 1.01 | 1.45 | 0.92 | 0.19 | <0.05 | 0.08 | <0.05 | <0.05 | 0.08 | 94.32 | <0.05 | <0.05 | 0.68 |
| Pit Sample Check Result | | | | | | | | | | | | | | | | | | | | |
| Check sample Id | Corresponding Primary Sample iD | Lat | Long | Al2O3 | BaO | CaO | Cr2O3 | Fe(T) | Fe2O3 | K2O | MgO | MnO | Na2O | P2O5 | SO3 | TiO2 | SiO2 | SrO | V2O5 | LOI |
| DPS/PCH-1 | DPS-P1(B) | 25.93381 | 77.32366 | 2.61 | <0.05 | 0.13 | 0.07 | 1.64 | 2.34 | 1.24 | 0.46 | <0.05 | 0.08 | <0.05 | <0.05 | 0.10 | 91.61 | <0.05 | <0.05 | 1.22 |
| DPS/PCH-2 | DPS-P3(A) | 25.90419 | 77.34182 | 2.75 | <0.05 | <0.05 | <0.05 | 1.40 | 2.01 | 1.30 | 0.21 | <0.05 | 0.08 | <0.05 | <0.05 | 0.16 | 92.31 | <0.05 | <0.05 | 1.05 |
| DPS/PCH-3 | DPS-P11(B) | 25.92275 | 77.34331 | 3.90 | <0.05 | 30.55 | <0.05 | 1.85 | 2.65 | 1.52 | 1.06 | 0.21 | <0.08 | <0.05 | <0.05 | 0.29 | 33.73 | <0.05 | <0.05 | 25.88 |
| DPS/PCH-4 | DPS-P-16 | 25.92669 | 77.33158 | 1.43 | <0.05 | <0.05 | <0.05 | 0.94 | 1.35 | 0.72 | 0.10 | <0.05 | 0.08 | <0.05 | <0.05 | 0.08 | 95.58 | <0.05 | <0.05 | 0.52 |
| DPS/PCH-5 | DPS-P-21 | 25.89469 | 77.33383 | 2.06 | <0.05 | <0.05 | 0.06 | 1.00 | 1.42 | 0.97 | 0.18 | <0.05 | 0.08 | <0.05 | <0.05 | 0.09 | 94.37 | <0.05 | <0.05 | 0.67 |

Annexure 9 Statement Showing co-ordinates & Comparison of analyses results for major oxides (XRF analysis) of 5 Core Check samples

Unit: %



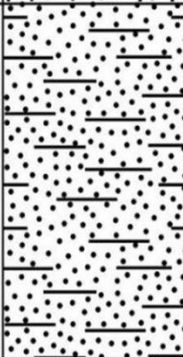
| Primary Results XRF | | | | | | | | | | | | | | | | | | |
|---------------------|---------------------------------|-------|-------|-------|-------|--------|-------|------|------|-------|-------|-------|-------|------|-------|-------|-------|-------|
| Primary sample Id | Corresponding check sample ID | Al2O3 | BaO | CaO | Cr2O3 | Fe (T) | Fe2O3 | K2O | MgO | MnO | Na2O | P2O5 | SO3 | TiO2 | SiO2 | SrO | V2O5 | LOI |
| DPS-BH1-3 | DPS-BCH-1 | 4.98 | <0.05 | 0.12 | <0.05 | 2.5 | 3.57 | 1.8 | 0.59 | <0.05 | 0.08 | <0.05 | <0.05 | 0.34 | 85.86 | <0.05 | <0.05 | 2.47 |
| DPS-BH1-15 | DPS-BCH-2 | 6.89 | <0.05 | 0.52 | <0.05 | 1.19 | 1.7 | 3.18 | 0.75 | <0.05 | 0.22 | 0.05 | 0.07 | 0.7 | 83.65 | <0.05 | <0.05 | 2.07 |
| DPS-BH1-5 | DPS-BCH-3 | 7.73 | <0.05 | 0.23 | <0.05 | 2.25 | 3.22 | 2.95 | 0.93 | <0.05 | <0.08 | 0.07 | <0.05 | 0.53 | 81.09 | <0.05 | <0.05 | 3.05 |
| DPS-BH2-8 | DPS-BCH-4 | 4.71 | <0.05 | 0.06 | 0.08 | 1.79 | 2.57 | 1.9 | 0.57 | <0.05 | 0.08 | <0.05 | <0.05 | 0.3 | 88.06 | <0.05 | <0.05 | 1.57 |
| DPS-BH2-11 | DPS-BCH-5 | 7.64 | <0.05 | 12.91 | <0.05 | 4.22 | 6.03 | 2.66 | 8.96 | 0.1 | <0.08 | 0.09 | 1.19 | 0.51 | 38.36 | <0.05 | <0.05 | 21.41 |
| Check results XRF | | | | | | | | | | | | | | | | | | |
| Check Sample Id | Corresponding Primary Sample Id | Al2O3 | BaO | CaO | Cr2O3 | Fe (T) | Fe2O3 | K2O | MgO | MnO | Na2O | P2O5 | SO3 | TiO2 | SiO2 | SrO | V2O5 | LOI |
| DPS-BCH-1 | DPS-BH1-3 | 5.13 | <0.05 | 0.12 | <0.05 | 2.51 | 3.59 | 1.80 | 0.61 | <0.05 | 0.08 | <0.05 | <0.05 | 0.34 | 85.89 | <0.05 | <0.05 | 2.25 |
| DPS-BCH-2 | DPS-BH1-15 | 7.02 | <0.05 | 0.52 | <0.05 | 1.19 | 1.70 | 3.17 | 0.76 | <0.05 | 0.21 | <0.05 | 0.07 | 0.69 | 83.65 | <0.05 | <0.05 | 2.00 |
| DPS-BCH-3 | DPS-BH1-5 | 7.49 | <0.05 | 0.23 | <0.05 | 2.26 | 3.23 | 2.96 | 0.91 | <0.05 | <0.08 | 0.07 | <0.05 | 0.52 | 81.27 | <0.05 | <0.05 | 3.11 |
| DPS-BCH-4 | DPS-BH2-8 | 4.64 | <0.05 | 0.06 | 0.08 | 1.81 | 2.59 | 1.90 | 0.55 | <0.05 | 0.08 | <0.05 | <0.05 | 0.30 | 88.14 | <0.05 | <0.05 | 1.53 |
| DPS-BCH-5 | DPS-BH2-11 | 7.49 | <0.05 | 12.91 | <0.05 | 4.27 | 6.10 | 2.68 | 8.92 | 0.11 | <0.08 | 0.09 | 1.17 | 0.51 | 37.85 | <0.05 | <0.05 | 22.03 |

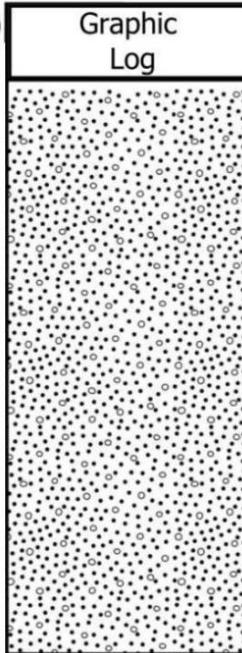

Annexure 10 Statement Showing co-ordinates & Comparison of analyses results for REE & Trace Elements (ICPMS analysis) of 3 Core External Check samples

Unit: ppm

| Primary Sample Analysis result | | | | | | | | | | | | | | | | | | | | | | | | | | | | | | | | | | | | | | | | |
|--------------------------------|--------------------------------|------|-----|------|------|------|------|------|------|-------|------|-----|------|------|------|------|------|------|-----|------|------|------|------|-----|-----|-----|------|-----|------|-----|------|-----|------|-----|------|------|------|------|------|-----|
| Primary Sample Id | Corresponding Check Sample Id | Li | Be | B | Sc | Co | Ga | Ge | Se | Rb | Y | Nb | Mo | Cd | In | Sn | Sb | Te | Cs | La | Ce | Pr | Nd | Sm | Eu | Gd | Tb | Dy | Ho | Er | Tm | Yb | Lu | Hf | Ta | W | Tl | Bi | Th | U |
| DPS-BH1-3 | DPS/BCH-1 | 28.2 | 0.9 | <5 | 5.4 | 13.7 | 6.7 | <0.5 | <0.5 | 61.1 | 11.5 | 5 | <0.5 | <0.5 | <0.5 | <0.5 | <0.5 | <0.5 | 3.7 | 16.6 | 40.5 | 4 | 19.1 | 4 | 0.8 | 3.4 | 0.5 | 2.8 | 0.5 | 1.3 | <0.5 | 1.2 | <0.5 | 4.6 | <0.5 | <0.5 | 0.5 | <0.5 | 8.1 | 1.2 |
| DPS-BH1-5 | DPS/BCH-3 | 35.9 | 1.8 | <5 | 13.3 | 11.3 | 11.6 | <0.5 | 1.4 | 112.4 | 15.5 | 8.6 | 0.9 | <0.5 | <0.5 | <0.5 | <0.5 | <0.5 | 6.3 | 27.3 | 57.6 | 6.5 | 25.4 | 4.5 | 0.9 | 5.1 | 0.6 | 3.4 | 0.7 | 1.8 | <0.5 | 1.9 | <0.5 | 5.1 | 1 | 1.6 | 1.6 | <0.5 | 6.3 | 1.9 |
| DPS-BH2-11 | DPS/BCH-5 | 42.1 | 1.1 | <5 | 10.4 | 8 | 9.1 | <0.5 | <0.5 | 95.9 | 17 | 7.6 | <0.5 | <0.5 | <0.5 | <0.5 | <0.5 | <0.5 | 6 | 19.1 | 41.8 | 4.8 | 21.7 | 4.5 | 1 | 3.9 | 0.5 | 3.3 | 0.6 | 2.3 | <0.5 | 1.5 | <0.5 | 6 | 1.2 | 1.1 | <0.5 | <0.5 | 5.4 | 2.1 |
| Check sample Analysis Result | | | | | | | | | | | | | | | | | | | | | | | | | | | | | | | | | | | | | | | | |
| Check Sample Id | Corresponding PrimarySample Id | Li | Be | B | Sc | Co | Ga | Ge | Se | Rb | Y | Nb | Mo | Cd | In | Sn | Sb | Te | Cs | La | Ce | Pr | Nd | Sm | Eu | Gd | Tb | Dy | Ho | Er | Tm | Yb | Lu | Hf | Ta | W | Tl | Bi | Th | U |
| DPS/BCH-1 | DPS-BH1-3 | 29.5 | 0.9 | <0.5 | 3.3 | 14.9 | 6.0 | <0.5 | <0.5 | 60.4 | 10.6 | 1.5 | 1.8 | <0.5 | <0.5 | <0.5 | <0.5 | <0.5 | 3.2 | 16.4 | 40.7 | 7.3 | 32.7 | 3.9 | 0.8 | 4.4 | <0.5 | 2.6 | <0.5 | 1.4 | <0.5 | 1.3 | <0.5 | 1.9 | 1.5 | 1.7 | <0.5 | <0.5 | 5.4 | 1.1 |
| DPS/BCH-3 | DPS-BH1-5 | 35.2 | 1.5 | <0.5 | 5.9 | 11.5 | 9.9 | <0.5 | 0.5 | 103.3 | 14.3 | 5.4 | 2.0 | <0.5 | <0.5 | <0.5 | <0.5 | <0.5 | 5.0 | 25.0 | 56.1 | 10.8 | 48.1 | 4.6 | 0.9 | 5.6 | 0.5 | 3.3 | 0.5 | 2.0 | <0.5 | 1.9 | <0.5 | 4.1 | 3.2 | 2.0 | <0.5 | <0.5 | 10.2 | 1.6 |
| DPS/BCH-5 | DPS-BH2-11 | 46.9 | 0.9 | <0.5 | 5.1 | 9.0 | 8.4 | <0.5 | 0.5 | 91.3 | 15.8 | 5.2 | 0.8 | <0.5 | <0.5 | <0.5 | <0.5 | <0.5 | 5.1 | 18.2 | 42.1 | 9.0 | 40.4 | 4.1 | 0.9 | 5.4 | 0.5 | 3.6 | 0.6 | 2.1 | <0.5 | 2.1 | <0.5 | 3.3 | 3.2 | 1.8 | <0.5 | <0.5 | 8.9 | 1.9 |

Annexure 13 Statement showing Run-wise Litholog of exploratory boreholes drilled by MMPL in the block

| Graphic Litholog with Potash Intersection Zones DPS/BH/01 | | | | | | | | | | | | | | | | |
|--|------------------|---|-------------------------------|----------|-----------------------------------|-------------------------------------|----------------|---------|--|------------------------------------|--|--|--|--|--|--|
| Block: Reconnaissance Survey (G4) for Glauconite and associated mineralization in Dhamni-Piparwasi Simliya area, Sheopur district, Mad | | | | | | | | | | | | | | | | |
| Agency | Date of Commence | Date of Closing | Easting | Northing | RL | Lattitude | Longitude | BH NC | | | | | | | | |
| Maheshwari Mining Pvt Ltd. | 04-05-2025 | 08-05-2025 | 734452.9 | 2864576 | 297.7743 | 25:52:50.94191 | 77:20:23.81120 | DPS/BH- | | | | | | | | |
| Depth(m) | RL (m) | Graphic Litholog | Potash Intersection Zones | | | Lithology | | | | | | | | | | |
| 0 | 298 |  | K2O%, Thickness Average K2O % | | | Loose Material | | | | | | | | | | |
| 1 | 297 | | | | | | | | | | | | | | | |
| 2 | 296 | | | | | | | | | | | | | | | |
| 3 | 295 | | | | | | | | | | | | | | | |
| 4 | 294 | | | | | | | | | | | | | | | |
| 5 | 293 |  | 1.74 | | | Shale with sandstone intercalations | | | | | | | | | | |
| 6 | 292 | | 3.25 | | | | | | | | | | | | | |
| 7 | 291 | | 1.8 | | | | | | | | | | | | | |
| 8 | 290 | | 2.43 | | | | | | | Sandstone with shale intercalation | | | | | | |
| 9 | 289 | | 2.95 | | | | | | | | | | | | | |
| 10 | 288 | | 2.78 | | | | | | | | | | | | | |
| 11 | 287 | | 2.3 | 12.5 | 2.43% | | | | | Calcareous Shale | | | | | | |
| 12 | 286 | | 2.521 | | | | | | | | | | | | | |
| 13 | 285 | | 1.807 | | | | | | | | | | | | | |
| 14 | 284 | | 2.87 | | | | | | | | | | | | | |
| 15 | 283 | | 2.376 | | | | | | | | | | | | | |
| 16 | 282 | | 2.115 | | | | | | | | | | | | | |
| 17 | 281 | 1.98 | | | | | | | | | | | | | | |
| 18 | 280 | | | | | | | | | | | | | | | |
| 19 | 279 | 0.73 | | | Glauconite Bearing Lithic Arenite | | | | | | | | | | | |
| 20 | 278 | 0.84 | | | | | | | | | | | | | | |
| 21 | 277 | 0.74 | | | | | | | | | | | | | | |
| 22 | 276 | 1.08 | | | | | | | | | | | | | | |
| 23 | 275 | 1.42 | | | | | | | | | | | | | | |
| 24 | 274 |  | 4.399 | 9 | 3.07% | | | | | Shale and sandstone intercalations | | | | | | |
| 25 | 273 | | | | | | | | | | | | | | | |
| 26 | 272 | | 1.991 | | | | | | | | | | | | | |
| 27 | 271 | | 3.18 | | | | | | | | | | | | | |
| 28 | 270 | | 2.696 | | | | | | | | | | | | | |
| 29 | 269 | 3.932 | | | Shale | | | | | | | | | | | |
| 30 | 268 | | | | | | | | | | | | | | | |
| 31 | 267 | 3.551 | | | | | | | | | | | | | | |
| 32 | 266 | 2.185 | | | | | | | | | | | | | | |
| 33 | 265 | 2.481 | | | | | | | | | | | | | | |
| 34 | 264 | | | | | | | | | | | | | | | |

| Graphic Litholog with Potash intersection zones DPS/BH/02 | | | | | | | | | |
|---|------------------|---|------------|----------------|-----------------------------------|-----------------------------------|----------------|-----------|-----------|
| Block: Reconnaissance Survey (G4) for Glauconite and associated mineralization in Dhamni-Piparwasi Simliya area, Sheopur district, Madhya Prade | | | | | | | | | |
| Agency | Date of Commence | Date of Closing | Easting | Northing | RL | Lattitude | Longitude | BH NO | Inclinati |
| Maheshwari Mining Pvt Ltd | 09-05-2025 | 13-05-2025 | 733524.788 | 2866738.401 | 282.1039 | 25:54:01.72442 | 77:19:51.86654 | DPS/BH-02 | 0 |
| DEPTH (M) | RL(M) | Graphic Log | K2O % | Zone Thickness | Zone Average K2O % | Lithology | | | |
| 0 | 283 |  | | | | Loose Material | | | |
| 1 | 282 | | | | | | | | |
| 2 | 281 | | | | | | | | |
| 3 | 280 | | 1.04 | | | | | | |
| 4 | 279 | | 0.89 | | | | | | |
| 5 | 278 | | 1.06 | | | | | | |
| 6 | 277 | | 1.17 | | | | | | |
| 7 | 276 | | 1.08 | | | | | | |
| 8 | 275 | | 1.15 | | | | | | |
| 9 | 274 | 0.97 | | | Sandstone with intercalated Shale | | | | |
| 10 | 273 | | | | | | | | |
| 11 | 272 | 1.9 | | | | | | | |
| 12 | 271 | 3.39 | | | | | | | |
| 13 | 270 | 3.444 | | | | | | | |
| 14 | 269 | 2.67 | | | Calcareous Shale | | | | |
| 15 | 268 | 2.572 | | | | | | | |
| 16 | 267 | 1.744 | | | | | | | |
| 17 | 266 | 2.66 | 13 | 2.34 | | | | | |
| 18 | 265 | 3.865 | | | | | | | |
| 19 | 264 | 1.83 | | | Sandstone | | | | |
| 20 | 263 | 2.107 | | | | | | | |
| 21 | 262 | 1.46 | | | | | | | |
| 22 | 261 | 2.26 | | | Shale | | | | |
| 23 | 260 | 2.912 | | | | | | | |
| 24 | 259 | 2.734 | | | | | | | |
| 25 | 258 | 1.319 | | | Sandstone | | | | |
| 26 | 257 | 0.99 | | | | | | | |
| 27 | 256 | | | | | | | | |
| 28 | 255 |  | 4.746 | 3 | 3.847 | Shale intercalated with sandstone | | | |
| 29 | 254 | | 3.908 | | | | | | |
| 30 | 253 | | 2.888 | | | | | | |
| | 252 | | | | | | | | |

Annexure 14 Statement Showing Borehole-wise intersection of Potassic Zone Reconnaissance Survey (G4) for Glauconite and associated mineralization in Dhamni-Piparwasi Simliya area, Sheopur district, Madhya Pradesh

| Borehole ID | Zone | Depth From (m) | Depth To (m) | Thickness (m) | Bulk Density t/m3 | Zone of influence m2 | Average K ₂ O (%) | Resource metric tonne |
|-------------|-------|----------------|--------------|---------------|-------------------|----------------------|------------------------------|-----------------------|
| DPS/BH/01 | BH1/A | 5 | 17.5 | 12.5 | 2.545 | 1,60,000 | 2.43 | 5090000 |
| DPS/BH/01 | BH1/B | 25 | 34 | 9 | 2.545 | 1,60,000 | 3.07% | 3664800 |
| Total BH01 | | | | 21.5 | | | | |
| DPS/BH/02 | BH2/A | 9 | 22 | 13 | 2.545 | 1,60,000 | 2.39 | 5293600 |
| DPS/BH/02 | BH2/B | 27 | 30 | 3 | 2.545 | 1,60,000 | 3.85 | 1221600 |
| Total BH02 | | | | 16 | | | | 1,52,70,000 |

Resource (Inferred, UNFC 334):

Annexure 15 Statement Showing drillhole wise resource for K₂O ≥ 2% in Reconnaissance Survey (G4) for Glauconite and associated mineralization in Dhamni-Piparwasi Simliya area, Sheopur district, Madhya Pradesh

| Borehole ID | Zone | Depth From (m) | Depth To (m) | Thickness (m) | Average K ₂ O (%) | Description |
|-------------|-------|----------------|--------------|---------------|------------------------------|--|
| DPS/BH/01 | BH1/A | 5.0 | 17.5 | 12.5 | 2.43 | Glauconite bearing quartz arenite, Glauconite bearing lithic arenite, Calcareous Shale are the lithologies showing elevated K ₂ O content, lithologies are generally intercalated but calcareous shale dominates 10.5m depth to 16.50m depth. |
| DPS/BH/01 | BH1/B | 25 | 34.0 | 9.0 | 3.07% | This zone is black shale dominated and in upper part shale intercalated with sandstone, most values are above 3 percent irrespective of lithology. |
| DPS/BH/02 | BH2/A | 9.0 | 22.0 | 13.0 | 2.39 | This zone is dominated by shale but intercalations of sandstone in upper and lower portions common, K ₂ O values are above 2 % in most samples and above 3% in some portion irrespective of lithologies. |
| DPS/BH/02 | BH2/B | 27.0 | 30.0 | 3.0 | 3.85 | This zone has peak value of 4.7% K ₂ O in glauconite bearing sandstone and values are from shale and sandstone intercalation. |

Annexure 16 Statement showing X-Ray Diffraction studies carried out in Reconnaissance Survey (G4) for Glauconite and associated mineralization in Dhamni-Piparwasi Simliya area, Sheopur district, Madhya Pradesh

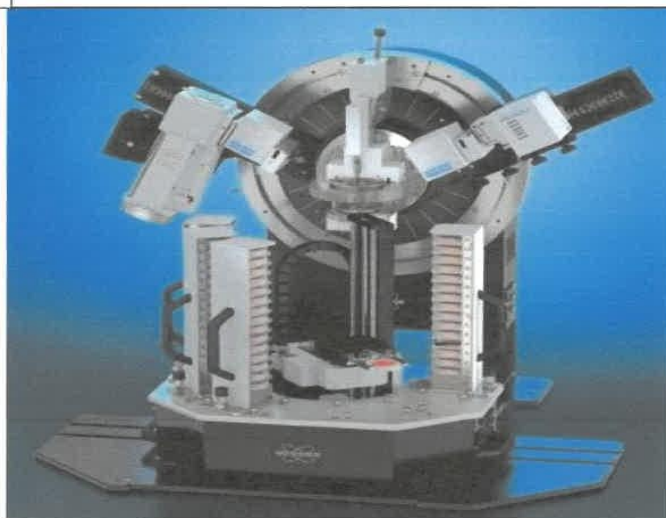


SHIVA ANALYTICALS INDIA PRIVATE LIMITED

Customer Name: Maheshwari Mining Private Limited
Customer Address: Maheshwari Mining Private Limited
 Qtr No UCM/3, near Syndicate Bank, Ukwa Parawada,
 Madhya Pradesh – 481105
Customer Ref: DPS-XRD-1
Lab ID : G3420-1
Date of Sample Analysis : 11/12/2025
Date of Reporting : 12/12/2025

MINERALOGY TEST REPORT

1.60 KW POWDER X RAY DIFRACTOMETER METHOD



INTRODUCTION

X-ray diffraction (XRD) and petrology studies are both valuable techniques used in geology and materials science for analysing minerals and rocks, but they serve different purposes and offer unique advantages. Here's how XRD is superior to petrology studies in certain aspects. XRD excels in identifying crystalline minerals present in a sample. It provides precise information about the crystal structure and lattice parameters of minerals, which can be challenging to ascertain solely through petrological observations. XRD allows for quantitative analysis of mineral phases present in a sample, providing accurate estimates of mineral composition based on peak intensities. Petrology studies, while descriptive, may not always provide quantitative data on mineral abundance. XRD is highly sensitive and can detect trace amounts of minerals present in a sample, even at concentrations as low as a few percent. Powder Diffraction (XRD) Database, contains a comprehensive collection of more than 6000 diffraction patterns for various materials. Researchers use this resource for identifying unknown substances, confirming crystal structures, and conducting material characterization. Shiva Analyticals team has decades of experience on XRD studies. Accurate chemical assay coupled with reliable mineralogy information is vital in resource characterisation.

Prepared by: Nagaraj Singh
 Verified by: Satyanarayana



Page 1 of 7



SHIVA ANALYTICALS INDIA PRIVATE LIMITED

Sample Code: G3420-1(DPS-XRD-1)

Instruments: WDXRF – Bruker S8 Tiger Series 2 (4 kW); XRD – Bruker D8 Advance (1.6 kW).

2θ Scan Range: 5–80° | Crystallinity: 77.40% | Amorphous: 22.60% |

Bulk Oxides by WDXRF:

| Oxides | Wt% |
|--------------------------------|-------|
| Al ₂ O ₃ | 4.71 |
| BaO | <0.05 |
| CaO | 6.04 |
| Cr ₂ O ₃ | <0.05 |
| Fe ₂ O ₃ | 5.22 |
| K ₂ O | 2.72 |
| MgO | 4.44 |
| MnO | 0.06 |
| Na ₂ O | 0.07 |
| P ₂ O ₅ | <0.05 |
| SiO ₂ | 64.21 |
| SO ₃ | 1.43 |
| SrO | <0.05 |
| TiO ₂ | 0.20 |
| V ₂ O ₅ | <0.05 |
| ZrO ₂ | <0.05 |
| HfO ₂ | <0.05 |
| CuO | <0.05 |
| NiO | <0.05 |
| PbO | <0.05 |
| ZnO | <0.05 |
| LOI | 0.19 |
| | 10.62 |

Mineral Phases by XRD:

| Sl. No. | Mineral Name | Chemical Formula | XRD Wt. % | XRD Crystallinity (Wt%*0.774) | Molecular Weight (g/mol) |
|---------|-------------------|---|------------|----------------------------------|-----------------------------|
| 1 | Glaucanite/illite | KAl ₂ (AlSi ₃ O ₁₀)(OH) ₂ | 34.45 | 26.66 | 375-422 |
| 2 | Quartz | SiO ₂ | 39.38 | 30.48 | 60.08 |
| 3 | Dolomite | CaMg(CO ₃) ₂ | 7.96 | 6.16 | 184.4 |
| 4 | Biotite | K(Mg,Fe) ₃ AlSi ₃ O ₁₀ (OH) ₂ | 12.57 | 9.73 | 425 |
| 5 | Calcite | CaCO ₃ | 4.91 | 3.80 | 100.09 |
| 6 | Pyrite | FeS ₂ | 0.73 | 0.57 | 119.98 |
| | Total | | 100 | 77.40 | |

Prepared by: Nagaraj Singh
 Verified by: Satyanarayana



Stoichiometric Comparison Table:

| Oxides | XRF (wt%) | XRD crystallinity (wt%) | Amorphous (wt%) |
|--------------------------------|-----------|-------------------------|-----------------|
| Al ₂ O ₃ | 4.71 | 4.24 | 0.47 |
| CaO | 6.04 | 4.00 | 2.04 |
| Fe ₂ O ₃ | 5.22 | 2.63 | 2.59 |
| K ₂ O | 2.72 | 2.11 | 0.61 |
| MgO | 4.44 | 2.58 | 1.86 |
| SiO ₂ | 64.21 | 53.26 | 10.95 |
| SO ₃ | 1.43 | 0.38 | 1.05 |
| TiO ₂ | 0.20 | 0.00 | 0.20 |
| LOI | 10.62 | 0.00 | 10.62 |
| CO ₂ | 0.00 | 4.61 | - |
| H ₂ O | 0.00 | 3.58 | - |
| Trace | 0.41 | 0.00 | 0.41 |

Interpretation

- Quartz dominates the mineralogy with 53.26 wt% of silica is crystalline. Additionally 10.95 wt% corresponds to amorphous, indicating the presence of opaline silica, microcrystalline quartz, or silica cement not detected by XRD.
- Carbonates are significant, with crystalline calcite/dolomite (CaO 4.00 wt%, CO₂ 4.61 wt %) plus an additional 2.04 wt% amorphous Ca-bearing phases, showing mixed crystalline and poorly crystalline carbonate components.
- Clay/mica minerals (illite–glaucanite–biotite) account for most of the Al₂O₃, K₂O, MgO, and structural H₂O, confirming a silicate-rich, moderately altered sedimentary source.
- Iron (Fe²⁺ and Fe³⁺) traces are responsible for the green colour of the sample that is split among the crystalline and amorphous phases. The amorphous phase contain 50% of total Fe₂O₃ (2.59 wt % as Fe oxyhydroxides, indicating weathering or diagenetic alteration.
- High LOI (10.62 wt%) reveals substantial volatile-bearing components—structural water, hydroxyls, organics, and amorphous carbonates—together contributing to the overall 22.60wt% amorphous fraction, which strongly influences the material reactivity and physical behaviour.

Secondary/Amorphous Phases

- Silica from non-crystalline Si-rich material.
- Carbonates from poorly crystalline Ca–Mg phases.
- Fe–Mg–Al silicates from altered clay/mica and Fe-oxyhydroxides.

Prepared by: Nagaraj Singh
Verified by: Satyanarayana





SHIVA ANALYTICALS INDIA PRIVATE LIMITED

Stoichiometric Oxide Table:

| Sl.No | Mineral (wt %) | Chemical Formula | Mineral wt% | SiO ₂ | Al ₂ O ₃ | K ₂ O | MgO | CaO | Fe ₂ O ₃ | CO ₂ | H ₂ O | SO ₃ |
|-------|-------------------|---|-------------|------------------|--------------------------------|------------------|------|------|--------------------------------|-----------------|------------------|-----------------|
| 1 | Glauconite/illite | KAl ₂ (AlSi ₃ O ₁₀)(OH) ₂ | 26.66 | 19.10 | 3.20 | 1.15 | 0.00 | 0.00 | 0.00 | 0.00 | 3.21 | 0.00 |
| 2 | Quartz | SiO ₂ | 30.48 | 30.48 | 0.00 | 0.00 | 0.00 | 0.00 | 0.00 | 0.00 | 0.00 | 0.00 |
| 3 | Dolomite | CaMg(CO ₃) ₂ | 6.16 | 0.00 | 0.00 | 0.00 | 1.35 | 1.87 | 0.00 | 2.94 | 0.00 | 0.00 |
| 4 | Biotite | K(Mg,Fe) ₃ AlSi ₃ O ₁₀ (OH) ₂ | 9.73 | 3.68 | 1.04 | 0.96 | 1.23 | 0.00 | 2.44 | 0.00 | 0.37 | 0.00 |
| 5 | Calcite | CaCO ₃ | 3.80 | 0.00 | 0.00 | 0.00 | 0.00 | 2.13 | 0.00 | 1.67 | 0.00 | 0.00 |
| 6 | Pyrite | FeS ₂ | 0.57 | 0.00 | 0.00 | 0.00 | 0.00 | 0.00 | 0.19 | 0.00 | 0.00 | 0.38 |
| Total | | | 77.40 | 53.26 | 4.24 | 2.11 | 2.58 | 4.00 | 2.63 | 4.61 | 3.58 | 0.38 |

Prepared by: Nagaraj Singh
 Verified by: Satyanarayana

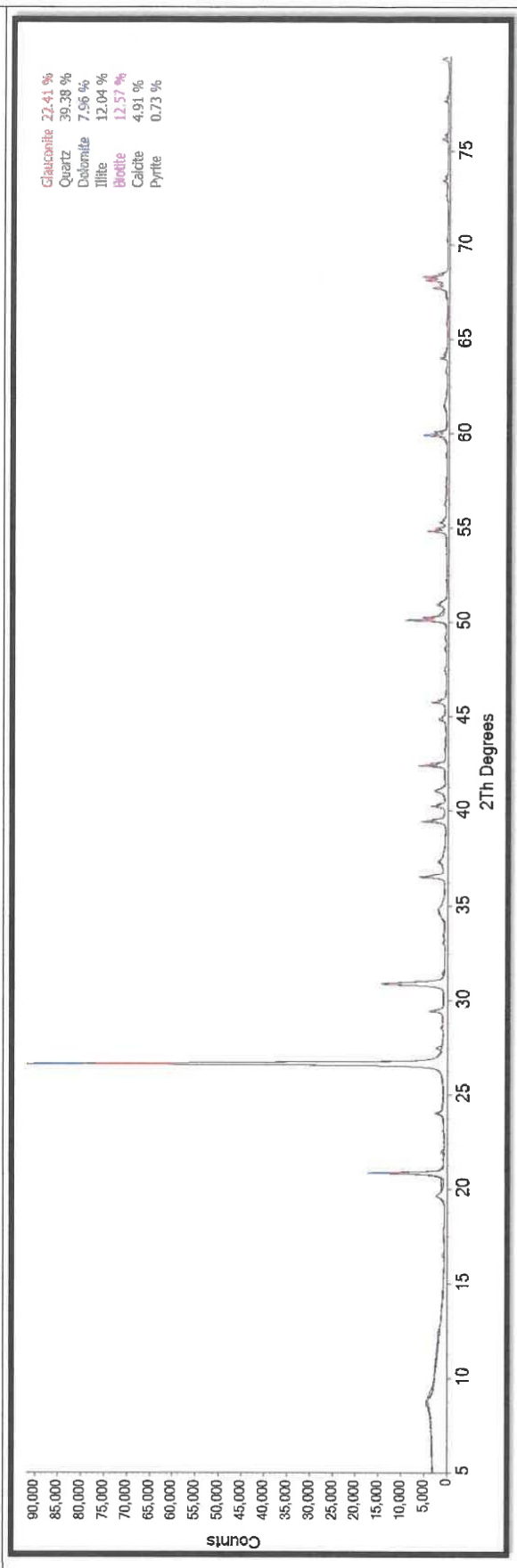


SHIVA SHIVA ANALYTICALS INDIA PRIVATE LIMITED
Part of the Cotecna Group

G3420-1

DPS-XRD-1

XRD Scan Report_2 of 2



Prepared by: Nagaraj Singh
Verified by: Satyanarayana



Page 7 of 7

Annexure 17 Statement showing Bulk Density Determination of sample



SHIVA ANALYTICALS INDIA PRIVATE LIMITED

Plot No. 24D [P] & 34 D, KIADB Industrial Area, Hoskote,
Bangalore – 562 114. Phone No: 080 -2801 -5333,
Website: www.shivaanalytics.com

Shiva Assay(Bulk)_G1482

| TEST REPORT | |
|---------------|---|
| Customer Name | Maheshwari Mining Pvt Limited -Madhya Pradesh QTR No UCM/3 Near Syndicate Bank Ukwa, Paraswara-481105 |

Discipline & Group Chemical & Ores and Minerals.

Customer Ref. MMPL/SHIVA/2024/WO-02

Commodity Geological Rock Samples

Lab ID G1482

Sample Receipt Date 28-May-25

Analysis Completion Date 16-Jun-25

Date of Reporting 16-Jun-25

Sample Count 3

| Sl. No. | Customer Code | Sample Description | Method | SOP/OM/094 |
|---------|---------------|--------------------|----------|--------------|
| | | | Units | gm/cm3 |
| | | | Lab ID | Bulk Density |
| | | | | |
| 1 | DPS-BH1-10 | Rock | G1482-10 | 2.60 |
| 2 | DPS-BH1-14 | Rock | G1482-14 | 2.50 |
| 3 | DPS-BH2-9 | Rock | G1482-24 | 2.59 |
| | | | | |



Mr. SATYANARAYANA - Head - ORES & MINERALS - AUTHORIZED SIGNATORY.

**** END OF THE REPORT ****

1. The results listed above pertain only to the tested samples and applicable parameters. 2. Samples which are degradable will be disposed immediately after testing and others will be disposed after one month from the date of issue of test certificate unless otherwise specified. 3. Total liability of our laboratory is limited to the invoiced amount. 4. This report is not to be reproduced either wholly or in part and cannot be used as an evidence in the Court of Law and should not be used in any advertising media without prior written permission. 5. In case any reconfirmation of contents of this test certificate is required, please contact our office. 6. Sampling is not done by us unless otherwise specified. 7. Any discrepancy in the Test Certificate should be notified within 30 days.

Prepared by: Naveen

Verified by: Satyanarayana

Page No 1 Of 1

Annexure 18 Minutes of 10th meeting of Technical-cum-Cost Committee - II (TCC - II) held on 23rd, 24th & 25th June 2025, the committee recommended to carry out the modal analysis of potash minerals and a certain mineral phase for potash content. The committee approved time extension of 3 months up to 20th November 2025 for submission of final geological report.

Ministry of Mines National Mineral Exploration Trust

Minutes of 10th meeting of Technical-cum-Cost Committee - II (TCC - II) held on 23rd, 24th & 25th June 2025

The 10th meeting of Technical-cum-Cost Committee – II (TCC - II) of National Mineral Exploration Trust (NMET) was held through video conferencing under the Chairmanship of Shri Pradeep Singh, Deputy Director General (DDG), Geological Survey of India (GSI) and Chairman, TCC-II, NMET on 23rd, 24th & 25th June 2025.

Agenda 10.2.15 Reconnaissance Survey (G4) for Glaucinite in Dhamni-Piparwasi-Simliya Area, Sheopur, Madhya Pradesh

[Implementing Agency: M/s Maheshwari Mining Pvt. Ltd. (MMPL)]

- a) M/s Maheshwari Mining Pvt. Ltd. (MMPL) informed that the project was approved in the 66th TCC Meeting held on 24th, 25th and 26th June, 2024. The OM was issued on 21st August, 2024 with timeline of 12 months (up to 20.08.2025) and approved cost was ₹1,06,22,030/-.
- b) MMPL also informed that final geological report has been prepared, it will be submitted for peer review soon. The agency requested for time extension of 3 months up to 20th November 2025 for submission of final geological report.
- c) The committee suggested to carry out the modal analysis of potash minerals and ascertain mineral phase for potash content. It was also suggested to mention the maturity of glaucinite and the stratigraphic horizon.
- d) MMPL presented the lithium concentrations ranged from 10 ppm to 60 ppm in most samples, with a few isolated values reaching up to 383.9 ppm. The committee advised to identify the mineral containing lithium.
- e) The TCC-II agreed for time extension of 3 months up to 20th November 2025 for submission of final geological report.

Recommendations of TCC-II

The committee recommended to carry out the modal analysis of potash minerals and ascertain mineral phase for potash content. The committee approves time extension of 3 months up to 20th November 2025 for submission of final geological report.

Annexure 19 Minutes of 66th TCC Meeting held on 24th, 25th and 26th June, 2024,

The committee recommends the proposal for the approval of EC for “Reconnaissance Survey (G4) for Glauconite and associated mineralisation in Dhamni-Piparwasi Simliya area, Sheopur district, Madhya Pradesh” with an estimated cost of Rs. 106.22 lakh (including GST) within time schedule of 12 months and submission of report as per Annexures 7A & 7B. The item will be reviewed after 05 months.

Ministry of Mines, National Mineral Exploration Trust

Minutes of the 66th Technical-cum-Cost Committee (TCC) meeting held on 24th, 25th & 26th June, 2024 through video conferencing

Agenda 66.3.6. Reconnaissance Survey (G4) for Glauconite and associated mineralization in and around Dhamni, Piparwasi, Simliya area, Sheopur District, Madhya Pradesh.

[Implementing Agency: Maheshwari Mining Private Ltd]

- a) The proposed area belongs to Vindhyan Supergroup and falls in part of SOI toposheet no. 54F/8.
- b) Sandstone is found in the nala sections west of Basantpura, in Kapeli Nadi south of Kapel Hor, and along Dham Nadi southeast of Damni. This sandstone is fine-grained, light green, thinly bedded, and moderately sorted, containing about 5-10% glauconite (visual estimate).
- c) During the field season of 1989-90, GSI reported glauconite-bearing Rewa sandstone exposed from Dhodha-Burera in the east (toposheet No. 54 G/9) to Bagwani-Piparwas-Surad-Magarda-Dubera in the west (toposheet No. 54 G/5).
- d) National Geochemical Mapping in parts of Shivpuri and Morena districts, M.P., reported K₂O values ranging from 1.45% to 3.30%.
- e) Geologists from Maheshwari Mining Pvt. Ltd. conducted two visits to the area to collect samples from glauconitic sandstone. In the first phase, five samples were analyzed, revealing K₂O values of 1.31% and 2.81% in two of the samples. In the second phase, seven samples were analyzed, with four samples showing K₂O values of 1.15%, 1.59%, 1.30%, and 1.33%.
- f) Expanding upon the above findings and the favorable geological setup, the G4 stage exploration item has been proposed.

Recommendation of TCC:

The committee recommends the proposal for the approval of EC for “Reconnaissance Survey (G4) for Glauconite and associated mineralisation in Dhamni-Piparwasi Simliya area, Sheopur district, Madhya Pradesh” with an estimated cost of Rs. 106.22 lakh (including GST) within time schedule of 12 months and submission of report as per Annexures 7A & 7B. The item will be reviewed after 05 months

Annexure 20- Modal Analysis report of Glauconite-Bearing Samples

Project: *Reconnaissance Survey (G4) for Glauconite and Associated Mineralization in Dhamni–Piparwasi–Simliya Area, Sheopur District, M.P.*

As part of the ongoing reconnaissance program, selected samples were subjected to petrographic examination to assess the presence of glauconite and associated mineral phases. Based on initial petrographic study, three representative samples (two surface samples and one drill core sample) were identified as glauconite-bearing and were recommended for modal analysis. The objective of this exercise was to quantify mineral proportions in the thin section and validate petrographic observations and evaluate the significance of glauconite mineralization in both surface and subsurface lithologies.

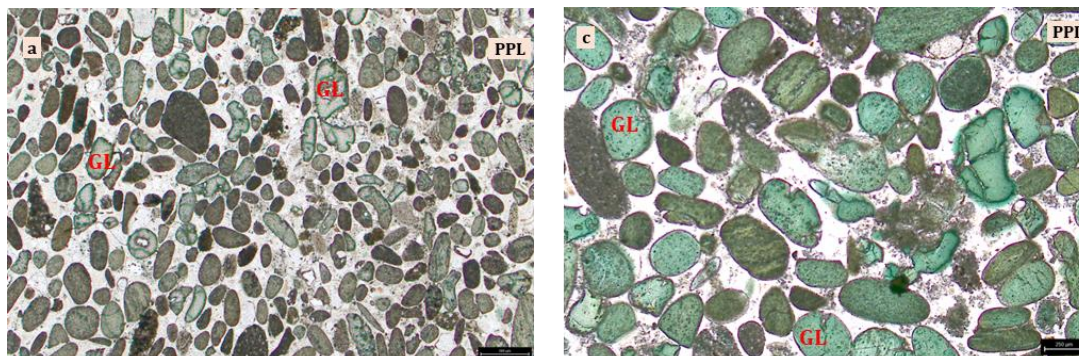
The modal analysis was conducted using the **point counting method**, with **1,000 counts per thin section under 20× magnification**. This method provides statistically reliable estimates of modal mineralogy, ensuring accurate representation of the mineral assemblage.

Observations: Sample DPS01 (Surface Sample)

The modal study of DPS01 reveals **glauconite as the dominant constituent (80.6%)**, accompanied by a subordinate quartz-rich matrix (11.6%) and lithic fragments (7.7%). The exceptionally high glauconite proportion establishes this sample as a glauconite-rich lithounit of considerable significance. The results confirm earlier petrographic. The quartz present in the thin section occurs as grains finer than typical sand size, forming part of a very fine-grained matrix.

| SAMPLE ID: DPS01 | |
|--|---------------|
| Minerals | Modal% |
| Glauconite | 80.6 |
| Matrix (with very fine-grained Quartz) | 11.6 |
| Lithic Fragments | 7.7 |

Photomicrographs are as follows:

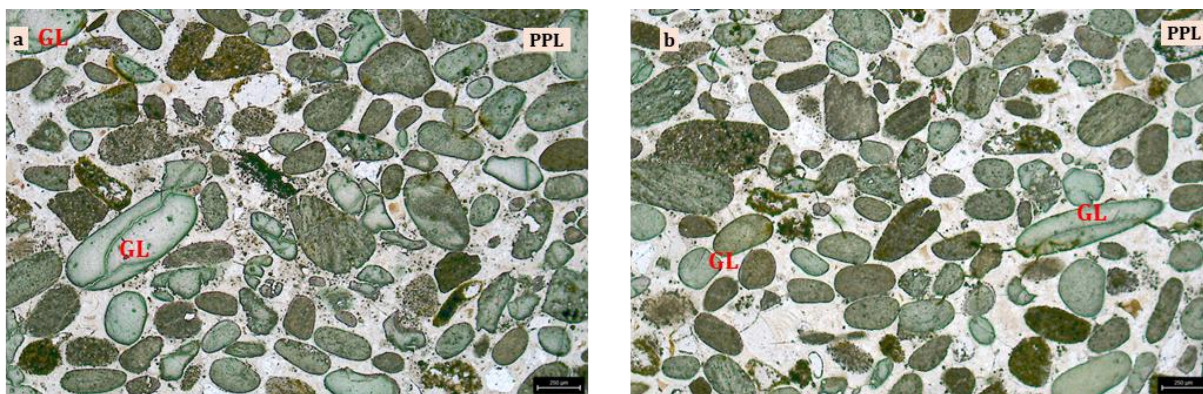


Sample DPS04 (Surface Sample)

In DPS04, modal analysis indicates **glauconite (72.2%)** as the principal constituent, with quartz in the fine-grained matrix (18.4%) and lithic fragments (9.4%) forming secondary components. However, the quartz grains observed in the thin section are predominantly finer than sand size, indicated by a very fine-grained matrix.

| SAMPLE ID: DPS04 | |
|--|--------|
| Minerals | Modal% |
| Glauconite | 72.2 |
| Matrix (with very fine-grained Quartz) | 18.4 |
| Lithic Fragments | 9.4 |

The photomicrographs are as follows:

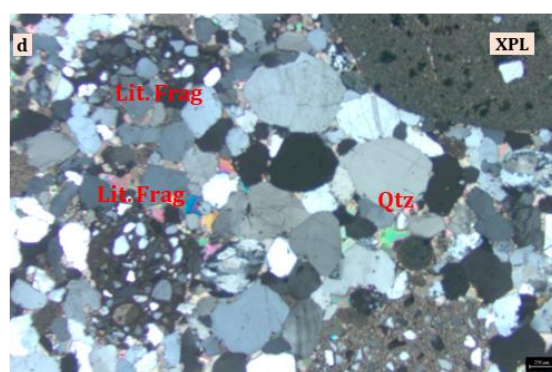
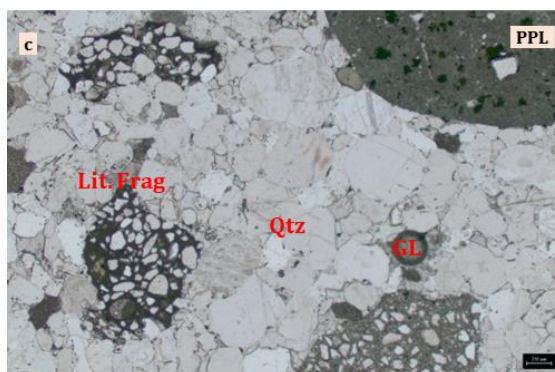
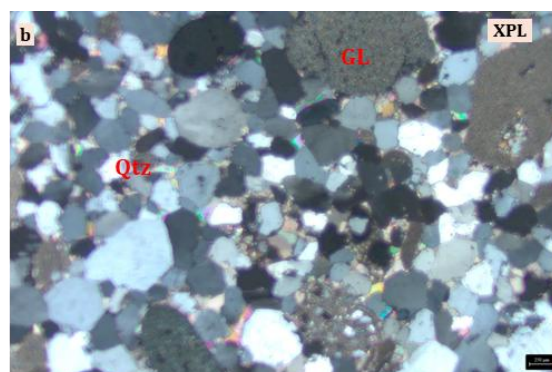
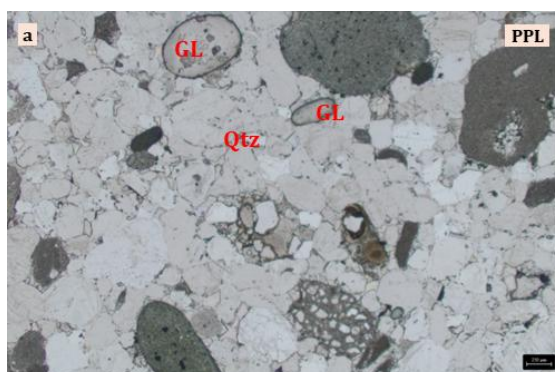


Sample DPS-BH1-PG2 (Drill Core, DPS-BH01)

The drill core sample DPS-BH1-PG2 presents a **quartz-dominated composition (73.4%)**, with significant lithic fragments (19.4%), minor glauconite (6.2%), and a very low concentration of matrix (0.8%) and feldspar (0.2%).

| SAMPLE ID: DPS-BH1-PG2 | |
|------------------------|--------|
| Minerals | Modal% |
| Quartz | 73.4 |
| Lithic Fragments | 19.4 |
| Glauconite | 6.2 |
| Matrix | 0.8 |
| Felspar | 0.2 |

The photomicrographs are as follows:



Conclusion

The modal analysis of three representative samples—DPS01, DPS04, and DPS-BH1-PG2 were done, and results confirms the observations during petrography. The surface samples selected for thin section shows significant occurrence of glauconite, with concentrations reaching over 70% in surface samples and a measurable presence in drill core. The detailed logs of modal analysis are attached as annexures for reference.

*Annexure 21 Petrography report of Dhamini Piparwasi Simliya glauconite block***PETROGRAPHY:****GENERAL:**

Petrographic examination of thin sections was carried out on 5 bedrock samples and 5 Borehole core samples from Dhamni Piparwasi Shimliya Glauconite block to characterize their mineralogical constituents, grain textures, and diagenetic features. The objective of the study was to understand the provenance, depositional environment, and diagenetic history of the glauconite-bearing sedimentary unit.

PETROGRAPHIC OBSERVATIONS:

The thin section analysis reveals that the rocks are predominantly composed of quartz, with very limited glauconite presence—restricted to isolated grains in only a few samples. Most thin sections exhibit moderate to good sorting and sub-rounded quartz grains, indicative of a mature quartz arenite. Minor amounts of feldspar, lithic fragments, and occasional mica are present in some samples. The scarcity of glauconite across the sections suggests restricted formation conditions, supporting the inference of localized glauconite development rather than widespread enrichment.

Glauconite is the dominant accessory mineral, occurring as sub-rounded to elliptical grains of variable sizes. Under plane-polarized light (PPL), glauconite exhibits a range of colours from pale green to bluish dark green. In some altered zones, glauconite shows signs of oxidation, presenting brownish yellow to reddish-brown hues. Under crossed polars (XPL), the mineral displays a very dark grey interference colour and is characterized by mottled extinction.

Glauconite shows different shapes viz. ellipsoidal, circular, elongated, and fragmented. Quartz grains are mostly monocrystalline, with occasional undulatory extinction, suggesting mild deformation signatures either pre or post deposition. The feldspar grains are sparse and relatively fresh, without significant signs of alteration. Lithic fragments, though limited in abundance, show sub angular and appear compositionally diverse.

BEDROCK SAMPLES

Sample: DPS01

Rock type: Glauconitic sandstone

The thin section reveals a matrix-supported sandstone composed primarily of rounded grains. The rock exhibits a high glauconite concentration, forming approximately 80% of the modal composition. Glauconite grains are rounded and exhibit a distinct green colour under plane-polarized light (PPL). Fine grained quartz and feldspar are present in subordinate amounts, with the matrix comprising fine siliceous material. The abundance and rounding of glauconite grains suggest considerable sediment reworking prior to final deposition. However, the quartz grains observed in the thin section are predominantly finer than sand size, indicated by a very fine-grained matrix.

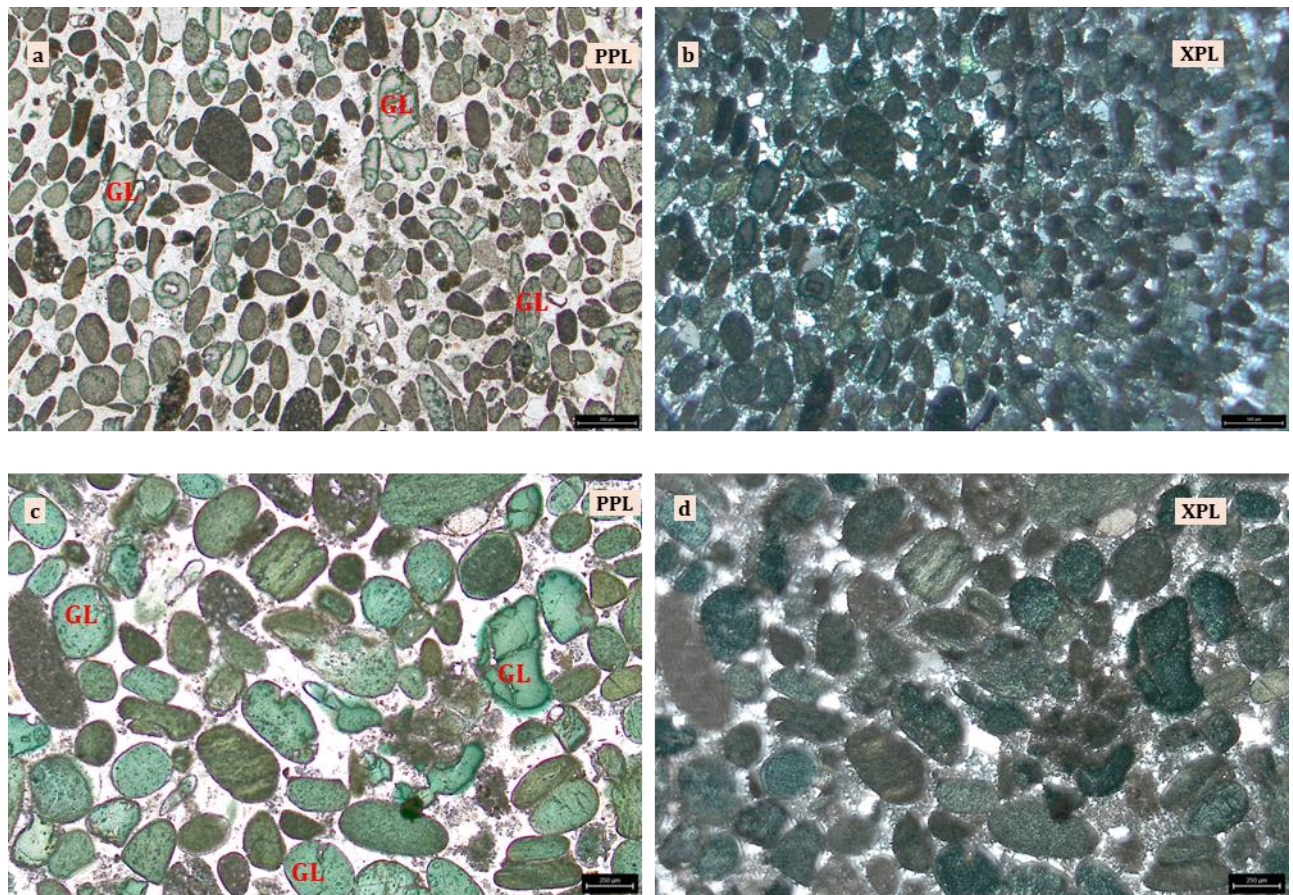


Fig. 1. Microphotographs of thin section DPS01 show (a, c) rounded glauconite grains forming a significant portion of the rock under PPL, with green coloration and fine siliceous matrix, (b, d) quartz and glauconite under XPL exhibiting moderate sorting and rounded grains.

Modal analysis results: Modal analysis was performed using the **point counting method**, based on **1,000 counts per thin section under 20× magnification**. The results show **glauconite as the**

dominant phase (80.6%), accompanied by a subordinate quartz-rich matrix (11.6%) and lithic fragments (7.7%). The exceptionally high glauconite proportion establishes DPS01 as a strongly glauconite-rich lithounit. The results confirm earlier petrographic. However, the grain size of quartz grains indicate that the sample might be glauconitic shale.

Sample: DPS04

Rock Type: Glauconite bearing lithic sandstone

This sample is texturally similar to DPS01 but exhibits a higher abundance of lithic fragments. Glauconite remains a prominent component, constituting approximately 70% of the modal composition, and appears sub-rounded with a greenish hue in PPL. The lithic fragments are angular to sub-angular and suggest a multi-source sediment provenance. Fine grained quartz and feldspar grains are present in minor quantities within a fine matrix. The quartz present in the thin section occurs as grains finer than typical sand size, forming part of a very fine-grained matrix. The overall fabric indicates moderate sorting and deposition under relatively low-energy conditions with mixed input, consistent with field observations of interbedded sandstone and mudstone.

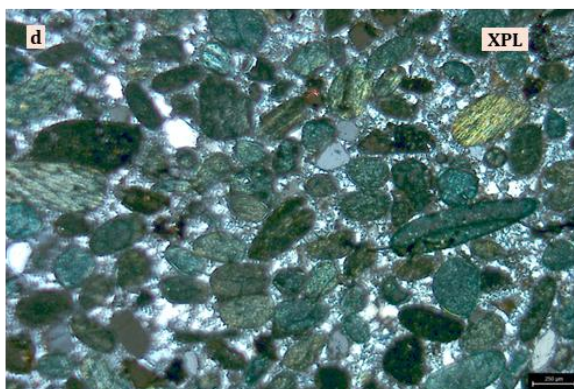
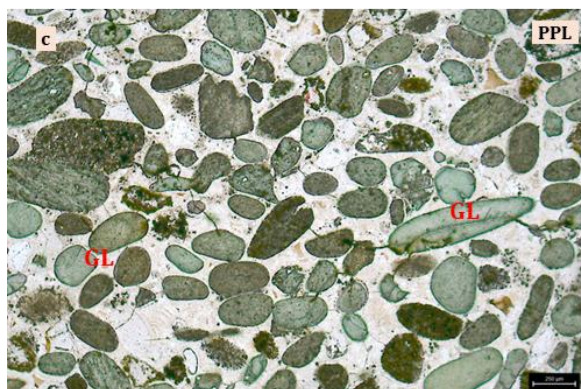
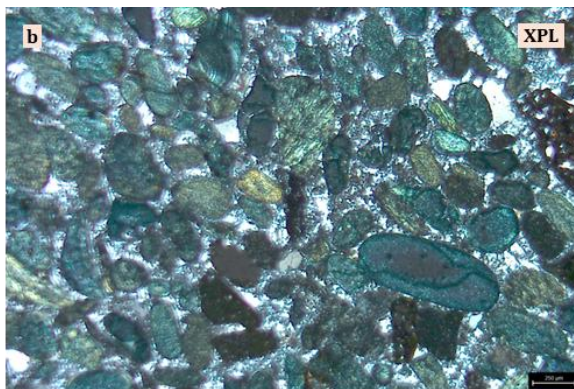
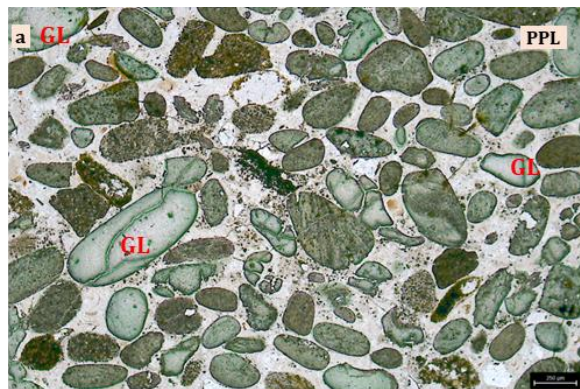


Fig. 2. Microphotographs of thin section DPS04 show (a, c) abundant glauconite and lithic fragments under PPL; glauconite appears sub-rounded and green, while lithic fragments are sub-angular, (b, d) under XPL, reflecting moderate sorting.

Modal analysis results: Using the **point counting method** (1,000 counts; 20× magnification), modal analysis shows a high proportion of **glauconite (72.2%)**, with matrix of fine-grained quartz (18.4%) and lithic fragments (9.4%). The relatively high glauconite content, coupled with good preservation, indicates an enriched glauconite-bearing lithology.

Sample: DPS11

Rock Type: Fine grained sandstone with localized glauconite bearing zones

This thin section is dominated by fine-grained anhedral quartz grains. Glauconite is sporadically present, concentrated mainly in small, localized zones associated with coarser quartz grains. The finer-grained portions of the rock are nearly devoid of glauconite, highlighting heterogeneous distribution. The glauconitic pockets show pale green grains under PPL, whereas the rest of the section is composed of tightly packed fine quartz grains. This textural variation suggests fluctuating depositional energy and selective glauconite settling.

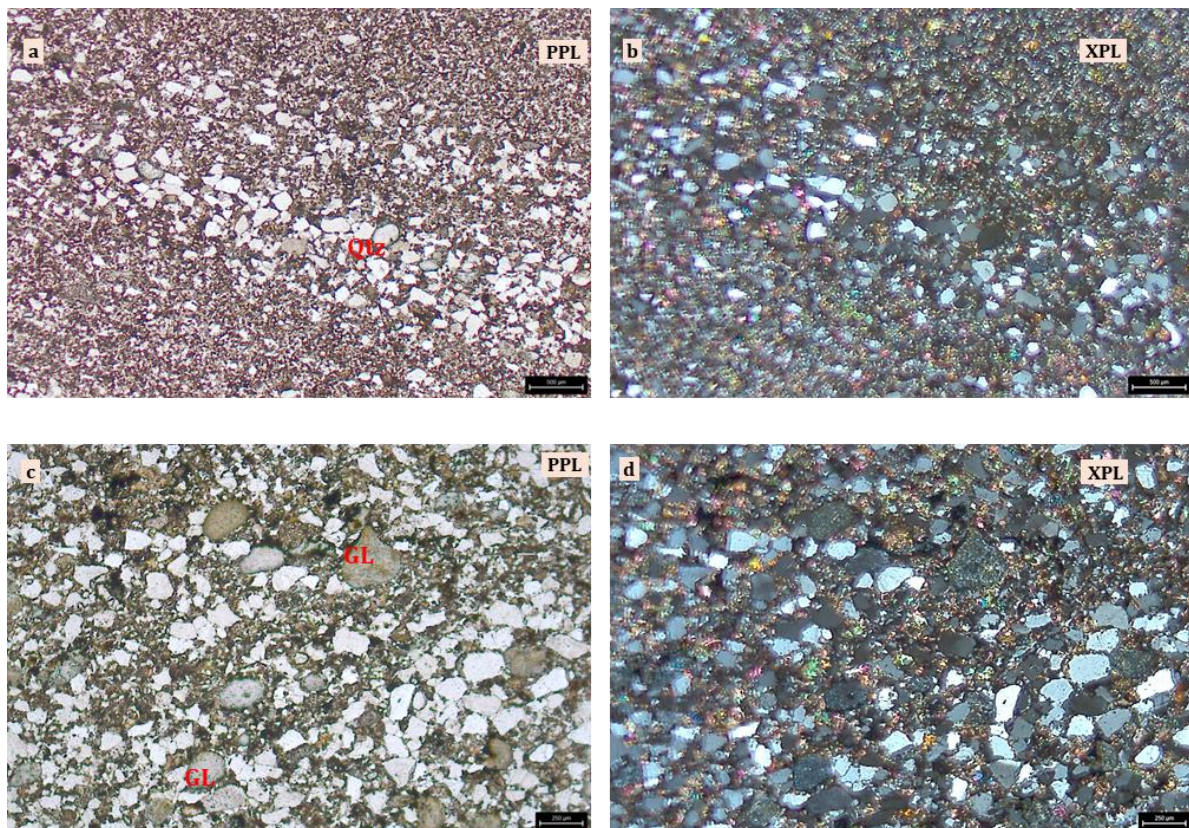


Fig. 3. Microphotographs of thin section DPS11 show (a, c) fine-grained anhedral quartz grains with localized glauconite zones under PPL; glauconite appears pale green and concentrated near coarser quartz grains, (b, d) interlocking textures of quartz under XPL, illustrating heterogeneous glauconite distribution.

Sample: DPS25**Rock Type: Quartz arenite**

The sample is composed entirely of anhedral quartz grains, exhibiting no evidence of glauconite. The grains are tightly packed, showing interlocking textures and well-developed triple junctions—clear indicators of advanced diagenetic recrystallization and compaction under elevated pressure. The absence of glauconite, coupled with the high degree of grain contact and lack of rounding, suggests that the rock has undergone significant burial diagenesis. These petrographic features align with field observations of fine-grained quartz arenite, likely representing high-energy fluvial or reworked sediments subjected to deep burial conditions, resulting in the loss of primary porosity.

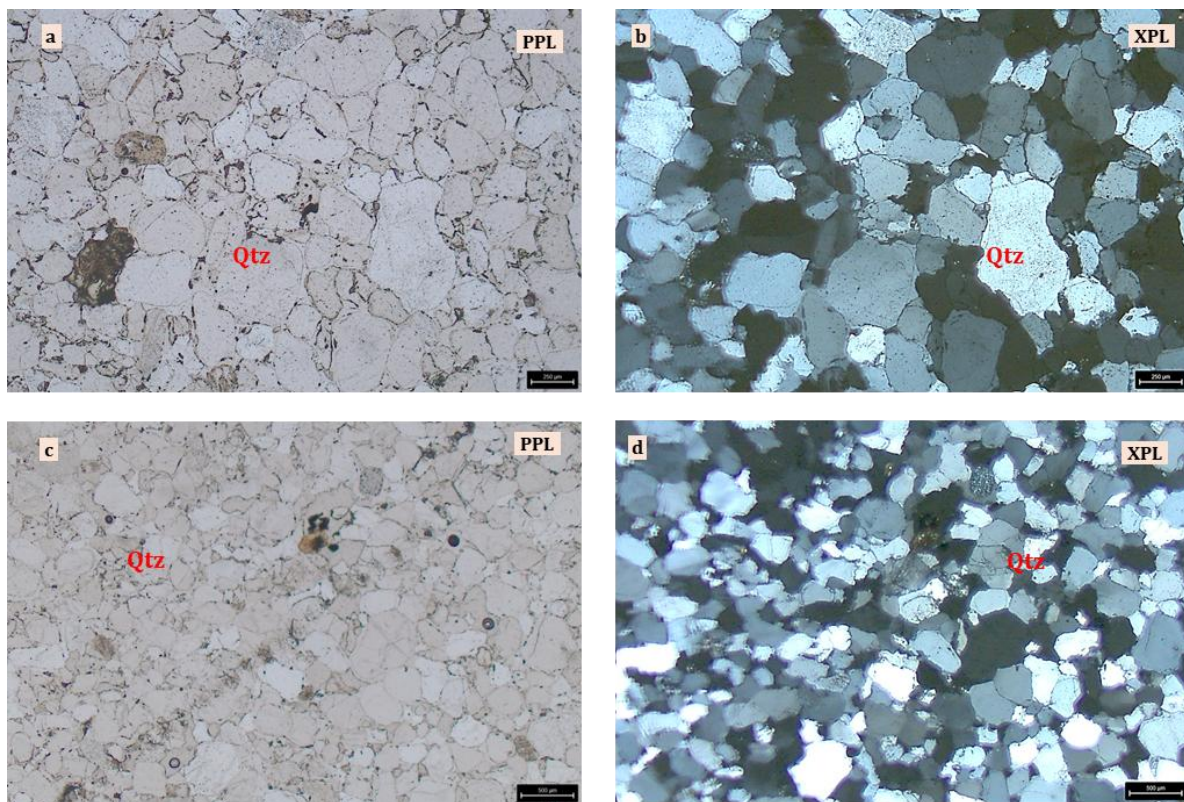


Fig. 4. Microphotographs of thin section DPS25 show (a, c) tightly packed anhedral quartz grains lacking glauconite under PPL, with evidence of triple junctions, (b, d) strong interlocking textures under XPL, indicative of diagenetic recrystallization.

Sample: DPS41**Rock Type:** Glauconite bearing sandstone

This section displays medium-grained quartz with sub-rounded morphology, interspersed with rounded glauconite grains comprising about 10% of the modal composition. Glauconite grains appear distinctly green under PPL. These glauconite grains seem to be oriented along a preferred direction, maybe along a weak plane within the host sandstone. The quartz framework is moderately sorted, and the overall fabric suggests deposition in a shallow marine setting with limited glauconitic enrichment. The presence of both quartz and glauconite, with moderate maturity, points toward mixed sedimentary dynamics.

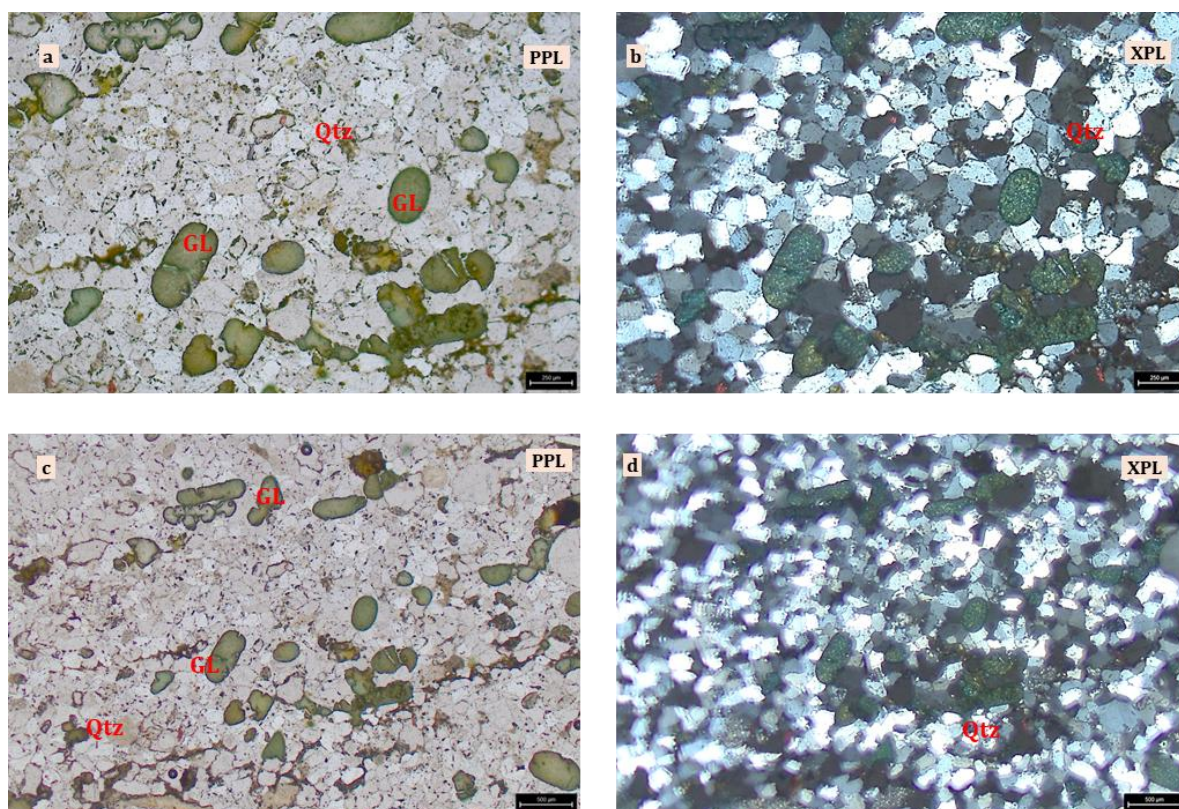


Fig. 5. Microphotographs of thin section DPS41 show (a, c) medium-grained quartz with sub-rounded grains and oriented glauconite grains under PPL; glauconite appears distinct green and rounded, (b, d) quartz framework under XPL showing moderate sorting.

Although samples were selected based on visual identification, significant glauconite content (70–80%) was confirmed in only two (DPS01 and DPS04), while others showed sparse or no presence. Thus, the petrographic analysis reveals a heterogeneous and localized distribution of glauconite. This indicates that glauconite is confined to specific stratigraphic pockets rather than being pervasive, reflecting a complex depositional environment with localized geochemical conditions favourable for glauconite formation.

BOREHOLE CORE SAMPLES

Sample: DPS-BH1-PG1

Rock Type: Calcareous shale

The thin section reveals a very fine-grained, laminated shale. Distinct calcite-rich bands are present, where coarse micritic to microsparry calcite grains are concentrated. These carbonate-rich layers interrupt the dominant clay-rich matrix, consistent with field observations of effervescence. The fabric is compact with occasional silt-sized detrital quartz grains. Under PPL, the calcite appears with low relief and distinct 3rd order colours under XPL, suggesting secondary carbonate enrichment during early diagenesis. Some Opaque minerals are seen within these layers.

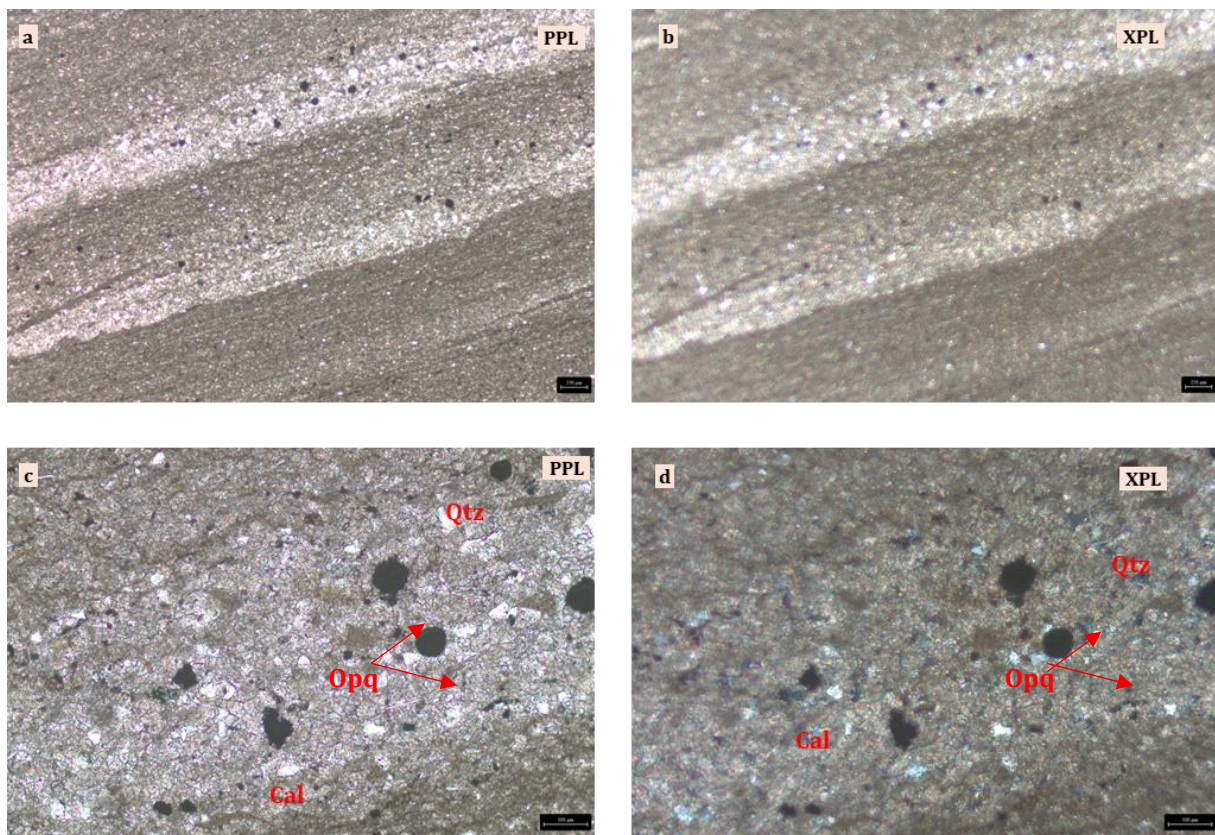


Fig. 6. Microphotographs of thin section **DPS-BH1-PG1** show (a, c) fine laminations and alternating calcite-rich bands under PPL, with micritic to microsparry calcite grains concentrated in discrete zones, and (b, d) under XPL, supporting field evidence of carbonate enrichment.

Sample: DPS-BH1-PG2**Rock Type:** Glauconite bearing lithic arenite

The thin section displays a sandstone composed of medium-grained, sub-rounded quartz grains with scattered, well-rounded glauconite pellets showing characteristic green coloration under PPL. Numerous lithic fragments are present, varying in composition and texture, contributing to the immature character of the rock. The matrix is sparse, and the grains are in close contact, indicating a grain-supported framework. Few plagioclase felspar grains observed in the thin section. The texture suggests moderate sorting with low matrix support and limited post-depositional compaction.

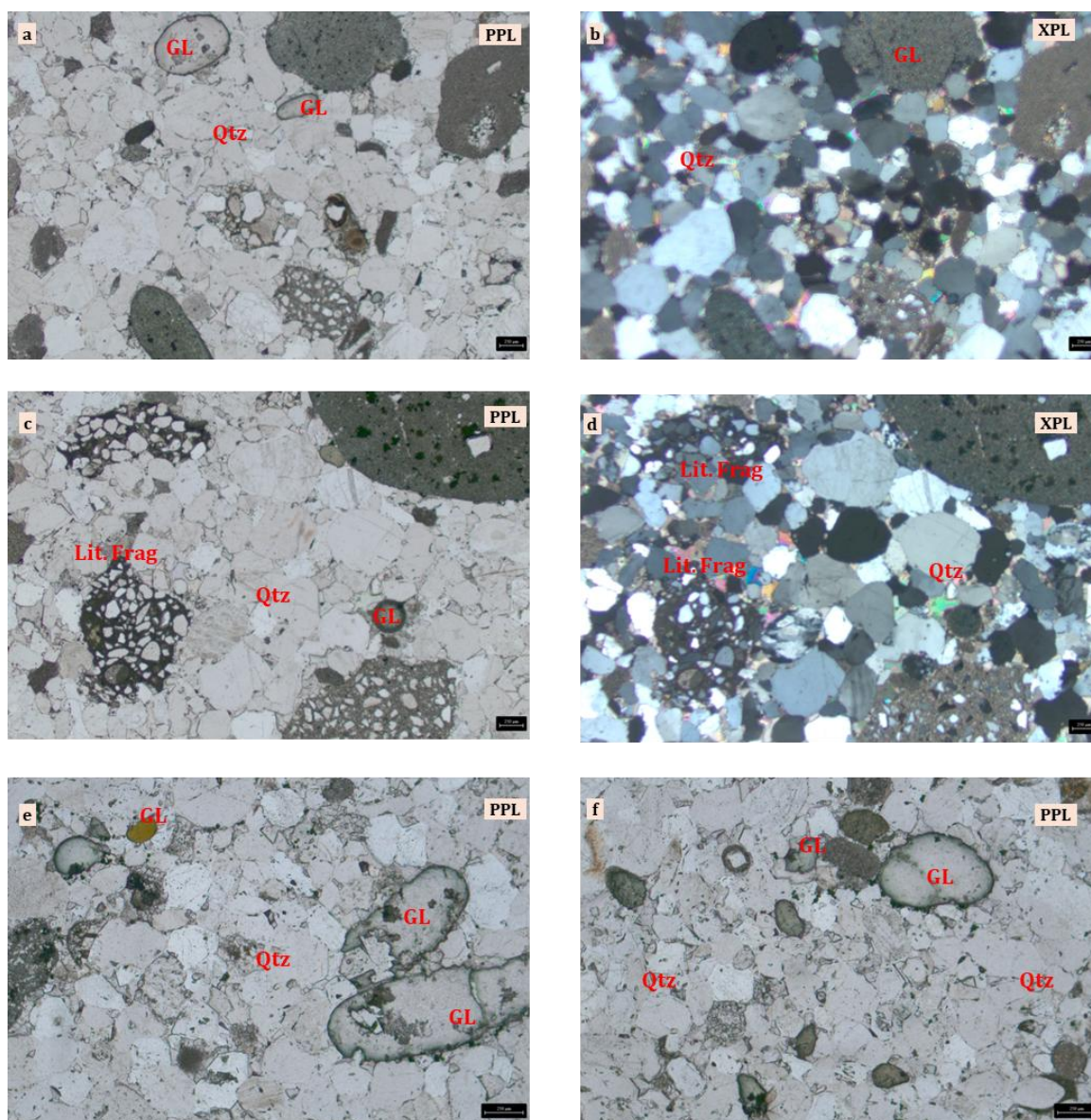


Fig. 7. Microphotographs of thin section **DPS-BH1-PG2** show (a, c) medium-grained quartz with well-rounded glauconite pellets and numerous lithic fragments under PPL, (b, d) quartz and lithics in a grain-supported framework with minimal matrix under XPL, reflecting

moderate sorting and immature texture. Photomicrographs in (e,f) shows glauconite grains in PPL within sandstone.

Modal analysis results: The modal study, carried out by the point counting method (1,000 counts; 20× magnification), reveals quartz as the dominant phase (73.4%), followed by lithic fragments (19.4%), glauconite (6.2%), and a very low matrix (0.8%) and 0.2% of feldspar grains.

Sample: DPS-BH1-PG3

Rock Type: Glauconite bearing quartz arenite

The thin section shows a quartz arenite composed almost entirely of medium- to fine-grained, sub-rounded quartz grains with well-developed point and long grain contacts. Quartz grains exhibit weak roundness and minimal alteration. One to two glauconite grains are present, appearing as rounded greenish grains under PPL. Minor feldspar grains and small lithic fragments are scattered throughout the section. The rock is cemented by overgrowth silica, with little to no matrix, indicating a mature, well-washed sandstone.

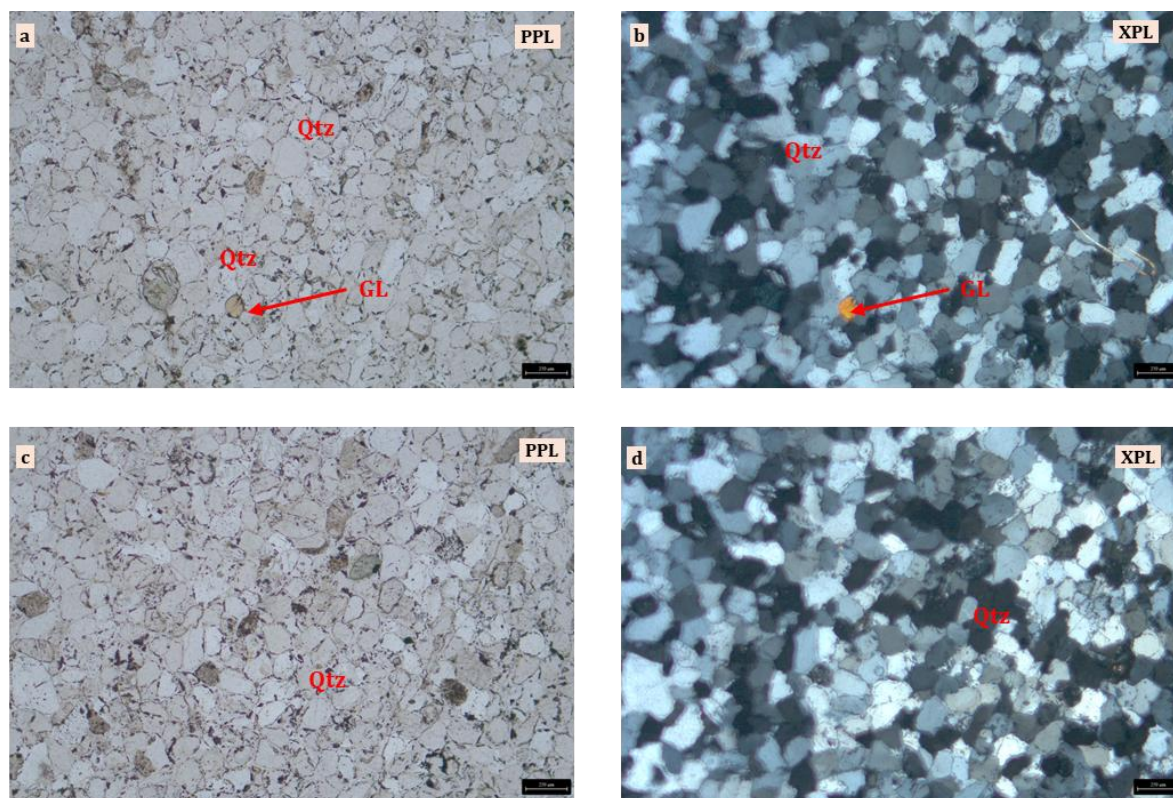


Fig. 8. Microphotographs of thin section **DPS-BH1-PG3** show (a, c) sub-rounded medium- to fine-grained quartz grains with isolated glauconite pellets and occasional feldspar and lithic fragments under PPL, (b, d) well-developed quartz grain contacts and overgrowths under XPL, indicative of a mature quartz arenite.

Sample: DPS-BH2-PG4

Rock Type: Glauconite bearing quartz arenite

The thin section comprises a quartz arenite with tightly packed medium- to fine-grained quartz grains. Quartz shows sub-rounded boundaries and displays uniform extinction under XPL. One to two glauconite grains are visible, appearing as isolated rounded green grains under PPL. The framework is grain-supported with silica cement, and no significant feldspar or lithic grains are present. The texture indicates high compositional and textural maturity, consistent with reworking and prolonged transport.

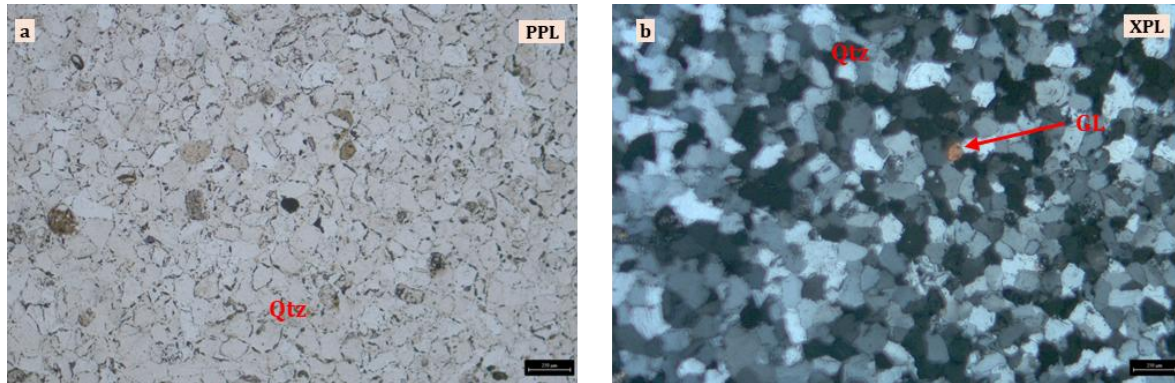


Fig. 9. Microphotographs of thin section **DPS-BH2-PG4** show medium- to fine-grained quartz grains with sub-rounded grain boundaries and isolated glauconite grains under PPL in (a) and XPL in (b).

Sample: DPS-BH2-PG5**Rock Type:** Glauconite bearing Quartz arenite

This thin section is a quartz arenite composed of medium- to fine-grained quartz grains exhibiting sub-rounded boundaries and point contacts. One to two glauconite grains are present and show characteristic green color and rounded shape under PPL. Muscovite or other micaceous minerals are occasionally observed intergrown with the quartz framework. Minor feldspar grains and small lithic fragments are also present, reflecting a slightly less mature composition than PG4. The rock is silica-cemented with minimal matrix.

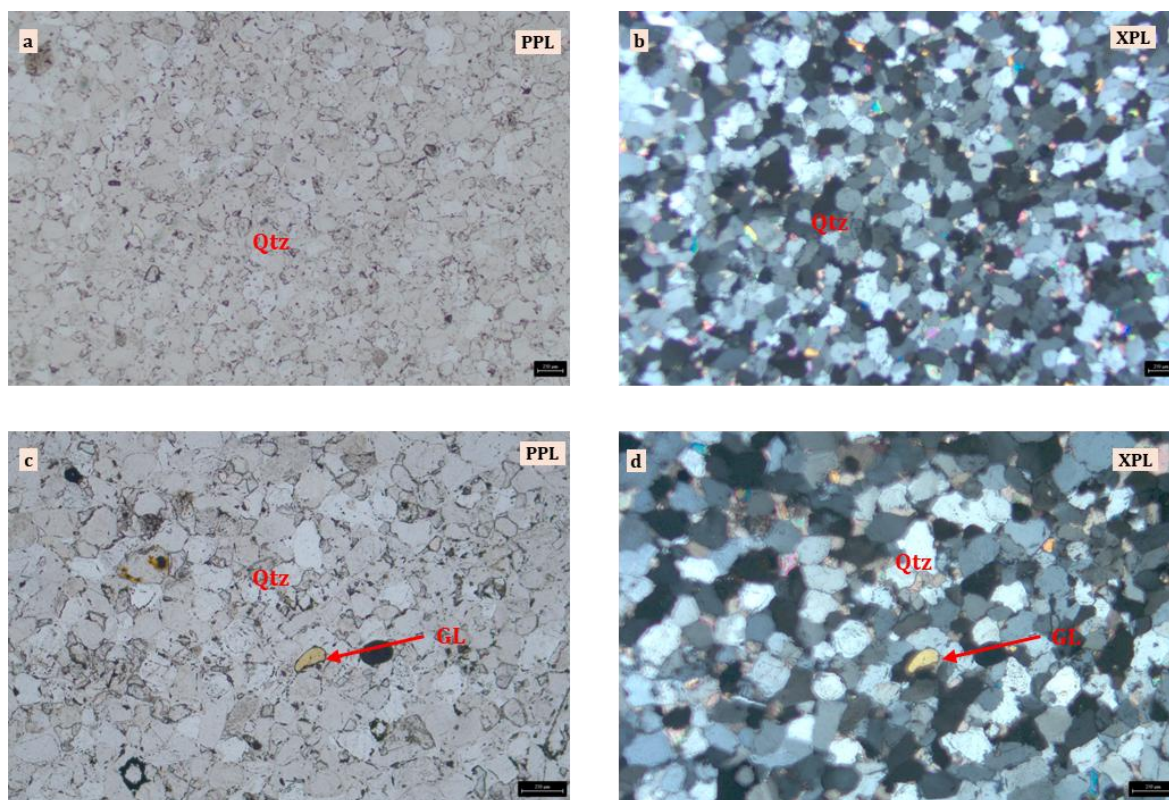


Fig. 10. Microphotographs of thin section **DPS-BH2-PG5** show (a, c) quartz grains with minor glauconite, feldspar, and micaceous minerals under PPL, (b, d) quartz with sub-rounded contacts and occasional lithic fragments under XPL, indicating a mature framework with slightly more compositional variation.

CONCLUSION

Petrographic analysis of samples from the Dhamni Piparwasi Shimliya Glauconite Block reveals that glauconite bearing sandstones are not encountered everywhere and does not show much lateral or vertical continuity. Significant glauconite content was observed only in two surface samples, DPS01 and DPS04 where glauconite comprises about ~80% and ~70% of the modal composition respectively as analysed using modal point counting analysis. These samples show well-rounded glauconite grains within a fine siliceous matrix, consistent with a low-energy marine depositional environment.

Other surface samples, DPS11, DPS41, and DPS25 show minimal to no glauconite. DPS11 has patchy glauconite, DPS41 contains only about 10%, and DPS25 is entirely barren of glauconite, composed mainly of tightly interlocked quartz grains, indicating mature quartz arenite.

Subsurface borehole samples reflect a similar trend. Only DPS-BH1-PG2 showed notable presence of glauconite of about 6% using modal point counting analysis. The rest thin sections

are dominated by quartz with at the most 1–2 glauconite grains per field, suggesting glauconite is not sustained in these samples.

These findings indicate that glauconite enrichment is confined to specific beds or lenses formed under favourable conditions at limited locations, and it does not persist across the block or at depth. Targeted exploration guided by stratigraphy and detailed petrography is essential, as glauconite occurrence is unpredictable and restricted.

Annexure 22 Report of Phase Identification using XRD carried out by GSI

Mineral Physics Laboratory
Geological Survey of India, Central Region, Nagpur

Report of **X-Ray Diffraction** Submitted By **M/S MMPL PVT. LTD**

<Director TCS Division >

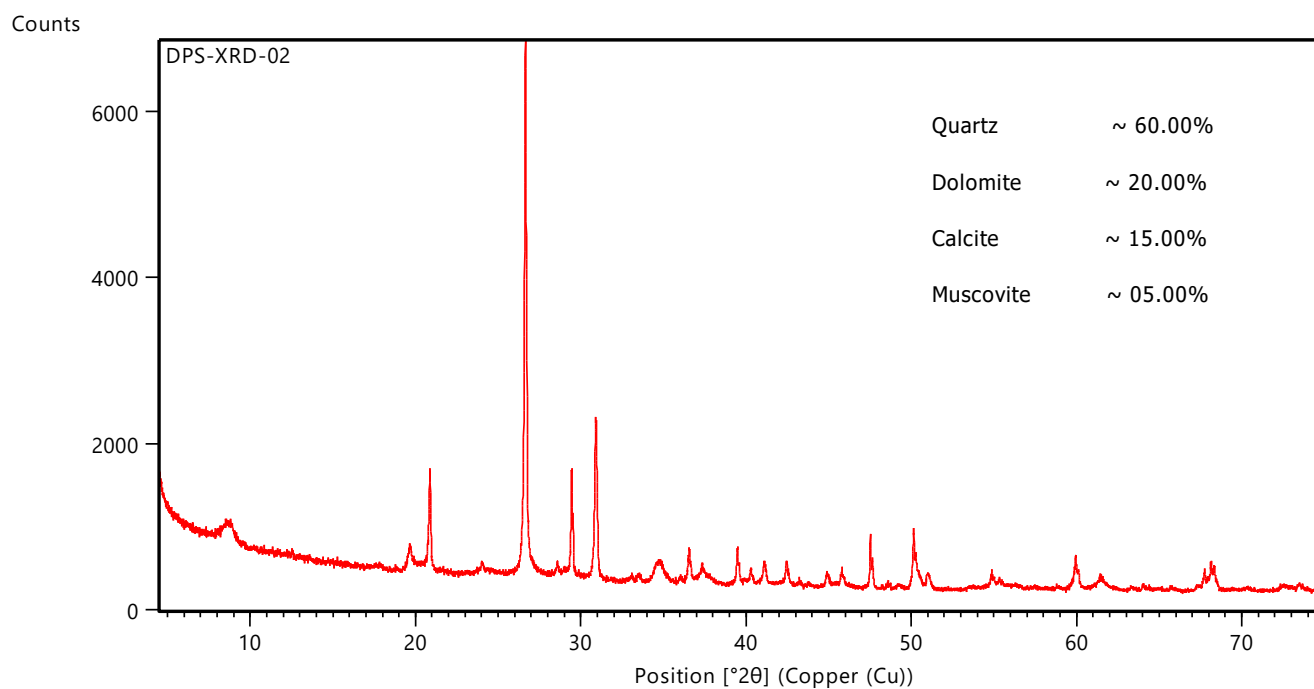
Number of Samples -03

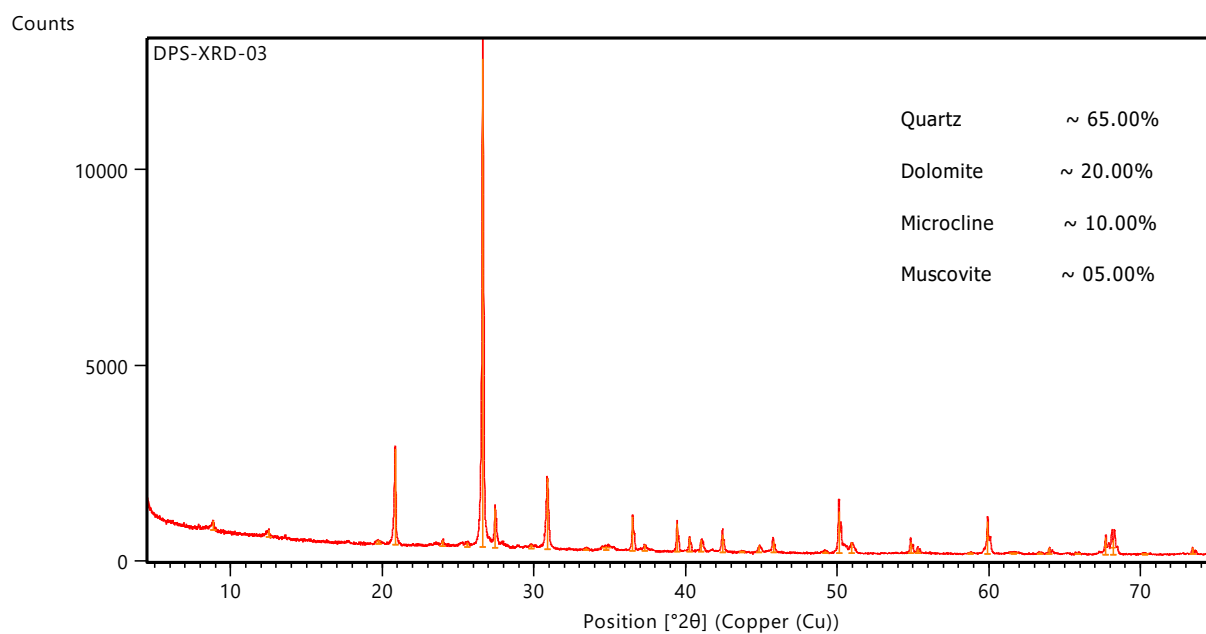
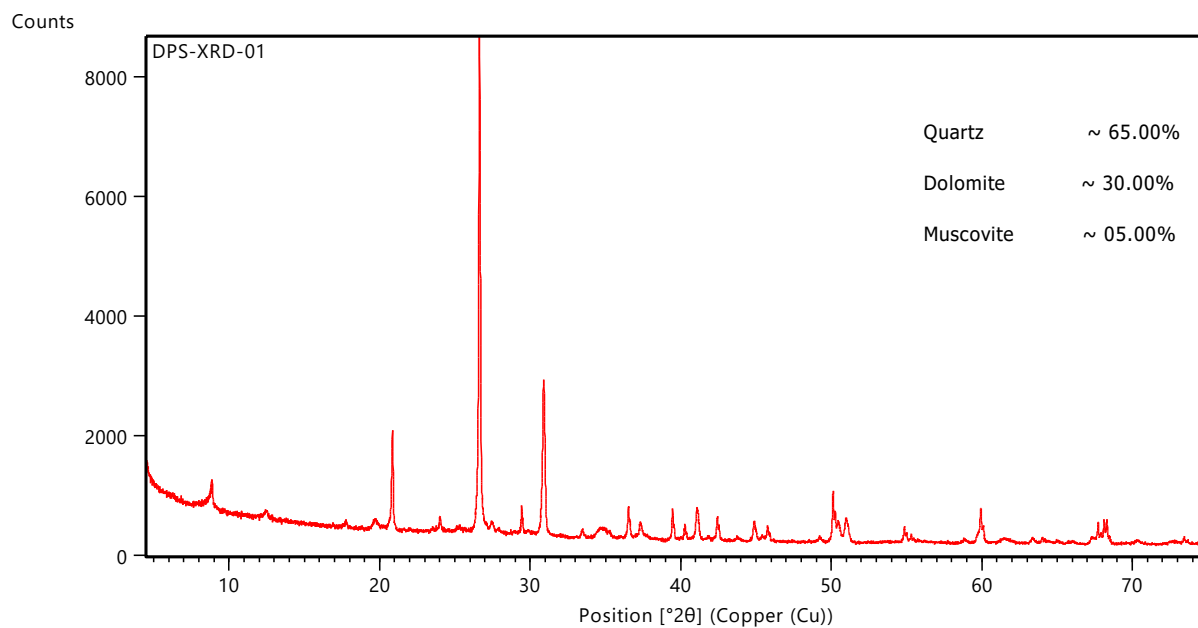
Date of Sample Submission: 29/09/2025

Analysed By: Lovelesh Kumar Soni

Supervised By: R. S. Wasnik, Director

Date of Report Preparation: 03.11.2025





Annexure 23 Compliance to Peer Review Comments

The comments received during the peer review of the Geological Report have been carefully examined and addressed in the revised report. The detailed responses to the comments are given below.

Comment-1: Under the MEMC Amendment rule 2021, there is a specific format laid down for resource estimation and reporting which must be followed whenever mineral resources are reported. As resources of 334 category are reported here, the geological report should be submitted in the 2021 format.

Response: The Geological Report has been revised and organized in accordance with the **Mineral (Evidence of Mineral Contents) Amendment Rules, 2021**. The mineral resource estimation for **Category 334 (Inferred Resources)** has been presented following the prescribed reporting format under the UNFC classification system.

Comment-2: A geological map may be included in the text itself where local geology is discussed.

Response: Incorporated at **page no 51 and 52** of geological report.

Comment-3: Based on mineralogical evidence from XRD and petrography, positive correlations between K_2O and Fe_2O_3 and Al_2O_3 , along with an inverse correlation with SiO_2 , are anticipated where potassium is structurally bound within glauconite-illite phases. It is recommended that these relationships be verified through statistical correlation analysis, similar to the correlation study already carried out for Fe_2O_3 .

Response: Incorporated at **page no 45** of geological report.

Comment-4 RQD values recorded in the borehole logs have not been interpreted in the main text. Rock mass quality classification based on standard RQD ranges may be presented. Further, a correlation analysis between RQD, core recovery, lithology, assay values (K_2O), and depth should be examined to assess structural control, degree of fracturing, and potential influence on mining conditions, and the findings incorporated in the relevant sections of the report

Response: incorporated at **page no 96** of geological report.

Comment-5 A fence diagram integrating borehole data is recommended to depict the three-dimensional geometry, lateral continuity, and thickness variation of glauconite-bearing sandstone horizons across the block

Response: Only **two scout boreholes** have been drilled in the block during the present stage of investigation. The strata encountered are **nearly horizontal with gentle rolling dips**, and both boreholes lie approximately along the **strike direction** at a distance of about **2.39 km from each other**. Due to the limited number of boreholes and their spatial disposition, preparation of a meaningful fence diagram is not feasible at this stage. However, for the purpose of stratigraphic correlation, a **correlation diagram incorporating RL (Reduced Level) and lateral scale** has been prepared and included in the report to illustrate the continuity and relative position of the glauconite-bearing horizons between the boreholes.

Comment-6: Plates showing borehole cross-sections (besides Annexure 13) and borehole-wise resource blocks prepared for resource estimation should be included in the report to substantiate the geological interpretation and resource calculation methodology

Response: Incorporated at **page no 110-111** of geological report.

Comment-7: The resources estimated using the polygonal method should be cross-checked using an independent alternative estimation method to evaluate the robustness and sensitivity of the primary estimates. A comparative table summarizing tonnage, grade, and percentage variation between the two methods should be prepared to assess the reliability and stability of the primary resource estimation.

Response: During the present stage of investigation, only **two scout boreholes** have been drilled within the block, located approximately **2.39 km apart**. Due to the **limited borehole density and wide spacing**, application of alternative resource estimation methods such as **cross-sectional or geostatistical approaches** is not considered feasible at this stage. Therefore, the **polygonal (zone of influence) method** has been adopted for resource estimation, which is considered appropriate for **widely spaced reconnaissance-level drilling data** corresponding to **G4 level of exploration**. The reliability and robustness of the resource estimates are expected to improve with **additional drilling during the G3 stage of exploration**, when sufficient borehole data will allow the application of alternative estimation methods for cross-verification.

Comment-8: Considering that the present investigation indicates 5–7 m of overburden over ~15 million tonnes of Category 334 glauconite resources recommended for G3.

Response: Incorporated at **page no 132**.

Comment-9: The 334-resource figure estimated by this investigation may be shown in Executive summary, Resource chapter, and Conclusions.

Response: Incorporated at **page no 9, 13 and 134**.

Comment-10: Borehole deviation test has not been done for the two holes drilled. Justification may be given for the same. However, for improved confidence in resource estimations and upgradation of exploration stage, deviation measurements may be followed in subsequent drilling programmes, even in shallow holes.

Response: Borehole deviation tests were not carried out as the drilled boreholes are **shallow vertical scout holes in relatively undeformed, horizontally bedded sedimentary strata**, where the likelihood of significant deviation is minimal. However, borehole deviation measurements are recommended during **future drilling programmes in the G-3 exploration stage**

Annexure 24 Official Memorandum of NMET approval of Reconnaissance Survey (G4) in Dhamini Piparwasi Simliya area for glauconite and associated mineralization, Sheopur District Madhya Pradesh

**Government of India
Ministry of Mines
National Mineral Exploration Trust**

File No. 23/492/2024-NMET/ 283

New Delhi, 21st Aug, 2024

OFFICE MEMORANDUM

Subject: Approval of mineral exploration project (Reconnaissance Survey (G4) for Glauconite and associated mineralization in Dhamni-Piparwasi Simliya area, Sheopur district, Madhya Pradesh) through NMET fund.

Agency: M/s Maheshwari Mining Pvt. Ltd.

On the recommendation of the Technical-cum-Cost Committee (TCC) in its 66th meeting held on 24th, 25th and 26th June, 2024, the Secretary, Mines and Chairman, Executive Committee (EC) of NMET approved the mineral exploration project of M/s Maheshwari Mining Pvt. Ltd. through NMET fund as per following details:

| S. No | Project/Block Name | Agency | Duration (Months) | Approved Cost (₹ Including GST) |
|--|---|---------------------------------|-----------------------|---------------------------------|
| 1 | Reconnaissance Survey (G4) for Glauconite and associated mineralization in Dhamni-Piparwasi Simliya area, Sheopur district, Madhya Pradesh. | M/s Maheshwari Mining Pvt. Ltd. | 12 (Up to 20.08.2025) | 1,06,22,030/- |
| Total (Rupees One crore six lakh twenty two thousand thirty only) | | | | ₹1,06,22,030/- |

2. M/s Maheshwari Mining Pvt. Ltd. shall submit progress on monthly basis to NMET Secretariat. The TCC, NMET shall review the progress of project and provide update to the Executive Committee enclosed in **Annexure**, as summarized below:-

- **Field Mobilization** : 1st month (up to 20.09.2024).
- **Exploration** : 1st to 10th month (up to 20.06.2025).
(Mapping, Sampling, Survey, Camp Setting, Survey, Drilling Geophysical Survey, Core Sampling, Chemical analysis)
- **Laboratory Studies** : 4th month to 12th month (up to 20.08.2025)
- **Report Writing with Peer Review and submission to NMET** : 10th month to 12th (up to 20.08.2025)

3. M/s Maheshwari Mining Pvt. Ltd. shall complete the project as per the above terms.

4. Further, as per clause 3.2(viii) of the Office Memorandum no. 6/3/2015-NMET/380 dated 12th December 2023 regarding Mode of engagement of Notified Private Exploration Agencies and funding by NMET for exploration of Critical and Strategic Minerals, NPEA may avail mobilization advance (up to 30% of the approved project cost) upon submission of Bank Guarantee (BG, including e-bank guarantee) of equal value of advance to NMET.

Yours faithfully,



(Geetika Sharma)

Deputy Secretary & HoD, NMET

Copy for information and further necessary action

1. M/s Maheshwari Mining Pvt. Ltd., FR07, Shilpangan, Plot LB1, Sector 3, Salt Lake, Kolkata – 700098.
2. Dr. S. Ravi, Dy. Director General and Chairman ,TCC-NMET, Geological Survey of India, SU: Karnataka & Goa, Bangalore-560078.
3. I.F. Division, Ministry of Mines, Shastri Bhawan, New Delhi.
4. Executive Committee (EC) Meeting file (F.No.6/2/2015-NMET)
5. Grant-in aid Sanction order file.